



Facultad de Ciencias

Departamento de Química Orgánica

Novel Applications of Diboron Reagents through Graphene-based Cu(I) Catalysis and Lewis Base Activation

Mario Franco Fernández

Doctoral Thesis

Supervised by:

Prof. M^a Belen Cid de la Plata

Prof. Mariola Tortosa Manzanares

Madrid, 2022



Facultad de Ciencias

Departamento de Química Orgánica

*Novel Applications of Diboron Reagents through
Graphene-based Cu(I) Catalysis and Lewis Base Activation*

Memoria presentada por

Mario Franco Fernández

Tesis para la obtención del grado de

DOCTOR EN QUÍMICA ORGÁNICA

(RD 99/2011)

Madrid, 2022

This Doctoral Thesis was carried out at the Organic Chemistry Department of the Universidad Autónoma de Madrid, under the supervision of Prof. M^a Belén Cid de la Plata and Prof. Mariola Tortosa Manzanares.

The financial support for this work has been obtained from the Spanish government (CTQ2016-78779-R, PID2019-107380GB-100) and the European Research Council (ERC-337776).

Esta Tesis Doctoral ha sido realizada en el Departamento de Química Orgánica de la Universidad Autónoma de Madrid bajo la dirección de la Profesora M^a Belén Cid de la Plata y la Profesora Mariola Tortosa Manzanares.

La financiación ha provenido del Ministerio de Economía y Competitividad (CTQ2016-78779-R, PID2019-107380GB-100) y del European Research Council (ERC-337776).

Agradecimientos

En primer lugar, quiero empezar agradeciendo a mis directoras Belén y Mariola por haberme dado la oportunidad de realizar esta tesis doctoral bajo su guía y tutela. A Belén en concreto agradecerle su cercanía, con la que ha conseguido llegar a hacer de nuestro trato más de amistad que profesional.

Sin duda agradecer a esos compañeros de laboratorio que acabaron siendo amigos para siempre: Emily, Luis, Sonia y Laura. Con ellos he compartido no sólo el trabajo diario, sino una buena cantidad de experiencias (y desayunos) que espero no dejemos de acumular en el futuro.

A Edu, mi amigo en Alemania, que pese a los años y la distancia nunca ha dejado de ser un apoyo y un referente, alguien con quien tener una larga conversación.

Al resto de mis compañeros y compañeras que han pasado por el grupo de investigación: Cecilia, Valentina, Ramiro, Alejandro, Óscar, Juanfran, Víctor, César, Javi, Irene, los cuales han hecho cada año único y diferente.

A mis colegas del L-408 Naiara, Víctor, Javi, con los que he compartido mi última etapa en la universidad y me han dejado un bonito recuerdo del laboratorio de “enfrente”.

También quiero agradecer a mis amigos de siempre, Ramos, Moreno, Chelle, Chipy, Marta A., así como a mis amigos de la carrera, Dabo, Kike, Maca, Merino, Kelly, por haber estado escuchando mis batallitas de la tesis durante cuatro largos años y haber estado ahí siempre que les he necesitado. Que no perdamos la amistad nunca.

Agradecimientos

Por supuesto a Marta, mi compañera de viaje, por ser mi ejemplo de superación y motivación, por ser la que más ha soportado mis altibajos y siempre ha sabido levantarme, por estar siempre a mi lado.

A mis abuelos Roque y Celandia, porque si había alguien en este mundo con más ganas que yo de que me sacara la tesis, esos eran ellos.

Por último, quiero agradecer a mis padres, Jesús y Elena, por siempre alentarme, por siempre tener las palabras correctas, por ser padres, amigos y psicólogos, por ser ellos.

A todos os agradezco vuestra inestimable ayuda y compañía, sin las cuales no habría sido posible superar esta etapa de mi vida. Una etapa que ha tenido momentos muy buenos y menos buenos, pero que sobre todo me ha ayudado a crecer como persona y profesional, dejando una huella imborrable para el resto de mi vida. Sin la tesis, no sería la persona que soy hoy.

Table of contents	Page
Preface	1
Summary in English	2
Resumen en español	7
Part I. Graphene-based Cu(I) catalysts in borylation	13
<u>Chapter 1. Evaluation of the Role of Graphene-based Cu(I) Catalysts in Borylation Reactions</u>	15
1. Introduction	15
1.1. Graphene and its derivatives	16
1.2. Graphene derivatives as carbocatalysts	22
1.3. Graphene derivatives in metallic catalysis	24
1.4. Group's experience in heterogeneous catalysis	32
1.5. Organoboron compounds	38
1.6. Borylation of alkyl and aryl halides	45
1.7. Heterogeneous catalyzed borylation of halides	49
2. Objectives	54
3. Results and discussion	56
3.1. Preparation and characterization of material A	56
3.2. Optimization of the borylation reaction using material A	58
3.3. Preparation of Graphene-based Cu(I) Catalysts using MWI and analysis of the catalytic activity	61
3.4. Scope of the Borylation of Aliphatic Halides	66
3.5. Optimization and scope of the Borylation of Aromatic Halides	68
3.6. Study of the Active Catalytic Species	73
3.7. Study of the mechanism of the Borylation Reaction	76
3.8. Study of the Recyclability	82
3.9. Study the effect of the graphenic surface on the catalytic performance of the materials.	85
3.10. Additional insights into the graphenic support role as macromolecular ligand	89
4. Conclusions	91
5. Experimental section of Part I	95

Table of contents **Page**

Part II. Diboron reagents in C-S bond formation, deoxygenation of N-O bonds, and C=N activation **129**

1. Introduction	131
1.1. Pyridine mediated B-B bond activation and application in organic synthesis	133
1.1.1. Pyridine-boryl radicals and their application	133
1.1.2. Diboron derivatives in deoxygenation of N-O bonds	143
1.1.3. Super electron donors based on pyridine-boryl complexes	149
2. Objectives	158

Chapter 2. Coupling of Thiols and Aromatic Halides Catalyzed by Pyridine-Boryl Super Electron Donors **161**

2.1 Introduction	163
2.1.1. The interest of aromatic thioethers	163
2.1.2. Methods to prepare diaryl thioethers	164
2.2. Results and discussion	176
2.2.1. Optimization of the reaction	176
2.2.2. Substrate scope	182
2.2.3. Comparative study with other methods	188
2.2.4. Catalytic version of the method	190
2.2.5. Mechanistic insights	191
2.3. Conclusions	198

Chapter 3. Evaluation of nitrones reactivity mediated by diboron compounds **201**

3.1. Introduction	203
3.1.1. The nitron functionality	203
3.1.2. Deoxygenation of nitrones	205
3.1.3. Nitrones in reactions involving radicals	208
3.2. Results and discussion	212
3.2.1. Reactivity with diboron reagents	212
3.2.2. Reactivity with base-activated diborons	220
3.2.3. Reactivity with pyridine-boryl radicals	223
3.2.4. Reactivity with super electron donors	228
3.3. Conclusions	230

4. Experimental section of Part II	235
------------------------------------	-----

List of Abbreviations and Acronyms

AC	Activated Carbon
bcp	Bond Critical Points
B ₂ cat ₂	Bis(catecholato)diboron
B ₂ eg ₂	Bis(ethylene glycolato)diboron
B ₂ nep ₂	Bis(neopentyl glycolato)diboron
B ₂ pin ₂	Bis(pinacolato)diboron
Boc	<i>tert</i> -Butyloxycarbonyl
CB	Carbon Black
°C	Celsius degree
CCG	Chemically Converted Graphene
conv.	Conversion
CuAAC	Copper catalyzed Azide-Alkyne Cycloaddition
CVD	Chemical Vapor Deposition
DBU	1,8-Diazabicyclo[5.4.0]undec-7-ene
DFT	Density Functional Theory
DMA	Dimethylacetamide
DME	1,2-Dimethoxyethane
DMF	Dimethylformamide
DMPO	5,5-Dimethyl-1-pyrroline <i>N</i> -oxide
DMSO	Dimethyl sulfoxide
EDG	Electron Donating Group
equiv.	Equivalents
EPR	Electron Paramagnetic Resonance
EtOAc	Ethyl acetate
EWG	Electron Withdrawing Group
G _d	Graphene derivative

List of Abbreviations and Acronyms

GNPs	Graphene Nanoplatelets
GO	Graphene Oxide
h	Hours
HFIP	Hexafluoroisopropanol
HRMS	High Resolution Mass Spectrometry
<i>m</i> -CPBA	<i>m</i> -Chloroperbenzoic acid
min	Minute/s
MNPs	Metal Nanoparticles
MS	Mass Spectrometry
MTBE	<i>tert</i> -Butyl Methyl Ether
MW	Microwave
MWI	Microwave Irradiated
n.d.	not determined
NMP	<i>N</i> -Methyl-2-pyrrolidone
NMR	Nuclear Magnetic Resonance
NPs	Nanoparticles
OAc	Acetate
OTf	Trifluoromethanesulfonate
OTs	<i>p</i> -Toluenesulfonate
PBC	Periodic Boundary Conditions
ppm	Parts per million
QTAIM	Quantum Theory of Atoms in Molecules
rGO	Reduced Graphene Oxide
SED	Super Electron Donor
SET	Single Electron Transfer
S _{RN} 1	Unimolecular Nucleophilic Radical Substitution

List of Abbreviations and Acronyms

SV	Single Vacancy
TBAI	Tetrabutylammonium iodide
TEM	Transmission Electron Microscopy
TM	Transition Metal
THF	Tetrahydrofuran
TS	Transition State
TXRF	Total Reflection X-Ray Fluorescence
US	Ultrasound
UV	Ultraviolet
wt.	Weight
XPS	X-Ray Photoelectron Spectroscopy
XRD	X-Ray Diffraction

Preface

The present doctoral thesis is divided in two different parts, having each part independent numeration of compounds, schemes, figures and tables. For the sake of clarity, the numeration of the pages and references is uninterrupted during the whole document.

Although every section addresses different subjects and transformations, they have in common the use of diboronic esters as versatile and powerful reagents.

The **first part** includes one chapter related to the study of graphene-supported heterogenous copper catalysts in the borylation of halides (**Chapter 1**). The **second part** englobes two chapters (**Chapter 2 and Chapter 3**) dealing with the use of diboron containing systems promoting valuable transformations different from borylations.

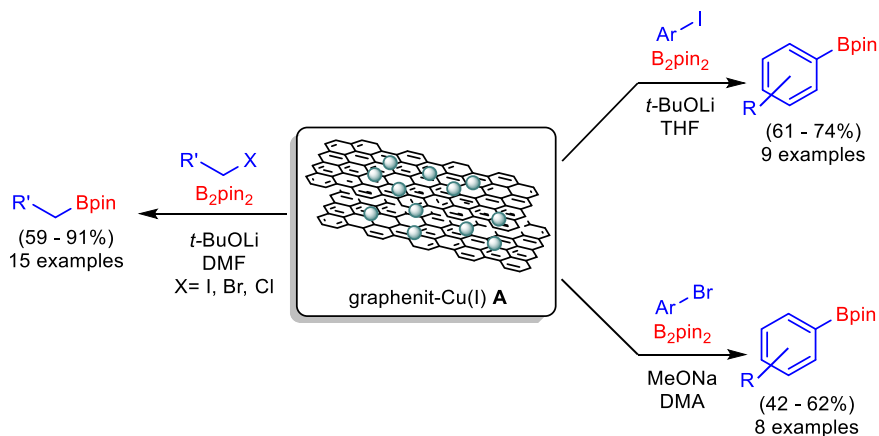
The experimental section of the different chapters contained in the thesis is located at the end of each part.

Summary in English

Diboron compounds are non-toxic, easily available, and valuable reagents for a wide variety of organic transformations. Proof of their utility is the exponential growth of scientific publications reported in this area, especially with B_2pin_2 appearing as either reactant or reagent.

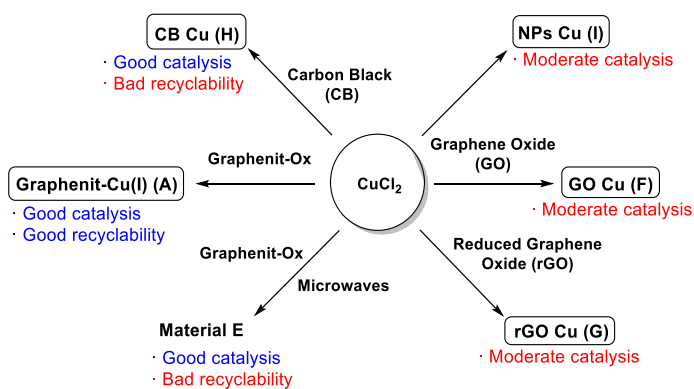
The most common use of diboron compounds is the introduction of **boronic ester** moieties in different functional groups such as alkenes, alkynes, or aliphatic and aromatic halides. The introduction of boronic esters is usually catalyzed by transition metals, and among all of them, copper is of especial importance due to its low cost and toxicity. The use of homogenous copper catalysts in this field has been largely studied. However, the employment of **graphene-derived heterogenous copper catalysts** in borylation reactions has been recently developed, but a deep analysis of the role of the graphenic support in the catalysis is still missing.

According to this scenario, **Part I** of this doctoral thesis details the **development and study of new heterogeneous copper catalysts supported on graphene surfaces in the borylation of aliphatic and aromatic halides**. Recent advances in our research group led to the preparation of a new graphene-supported heterogenous Cu_2O catalyst (**A**) prepared from inexpensive and sustainable nanoplatelets (graphenit-Ox), which previously demonstrated a good catalytic performance in some organic transformations such as click cycloadditions. Using this catalyst as model, we have found reaction conditions in which we could borylate both aliphatic and aromatic substrates (Scheme I), something unprecedented using other heterogenous copper catalysts.



Scheme I. Material A as catalyst in borylation of halides.

The preparation and study of different materials under microwave radiation revealed that these catalysts have a stronger copper anchorage, but a lower catalytic performance due to the Cu(0) present on their structure. Additional catalysts were prepared using commonly employed graphenic materials (GO, rGO, CB) as well as unsupported Cu(I) nanoparticles (NPs), and we carried out a deep study of their structure and catalytic performance in order to understand the role of the support in the reaction (Scheme II).



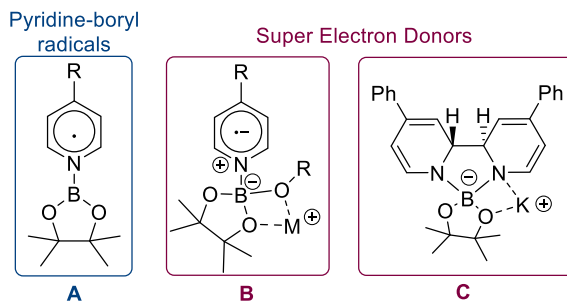
Scheme II. Comparative study of different materials.

Although all the prepared materials catalyzed the borylation reaction to some extent, they demonstrated to be less general, recyclable, and efficient than material **A**.

Along with the structure analysis of the materials, we carried out some theoretical calculations to understand the effect of the graphenic surface in the reaction. Through these investigations we could conclude that does exist a synergistic effect between the graphene surface and the Cu₂O nanoparticles that enhances the catalytic activity of this copper species, especially when radicals are involved.

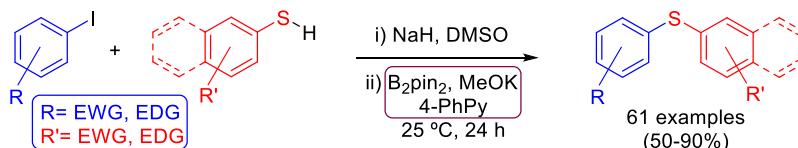
The importance of diboron compounds is not limited to the introduction of boron containing moieties. Recently, many interesting contributions can be found in the literature using these products as promoters of different transformations apart from borylations. **Part II** of this doctoral thesis relates different applications of diboron compounds, and it is divided in two chapters.

The activation of diboron compounds with different additives have extended their field of application during the last decades. The use of bases as additives of diboron reagents is well-known, but the addition of pyridines to activate diborons is more recent and leads to the formation of pyridine-boryl radicals (**A**). These pyridine-boryl radicals have demonstrated a great performance promoting reduction, pyridine functionalization, and C-H activation reactions. On the other hand, the combination of B₂pin₂, a pyridine, and an alkoxide, lead to the formation of highly reducing intermediates (**B**, **C**) known as super electron donors (SED). These systems have been recently developed and, despite their great potential, they have been basically employed in metal-free borylation reactions (Scheme III).



Scheme III. Activated diboron containing systems.

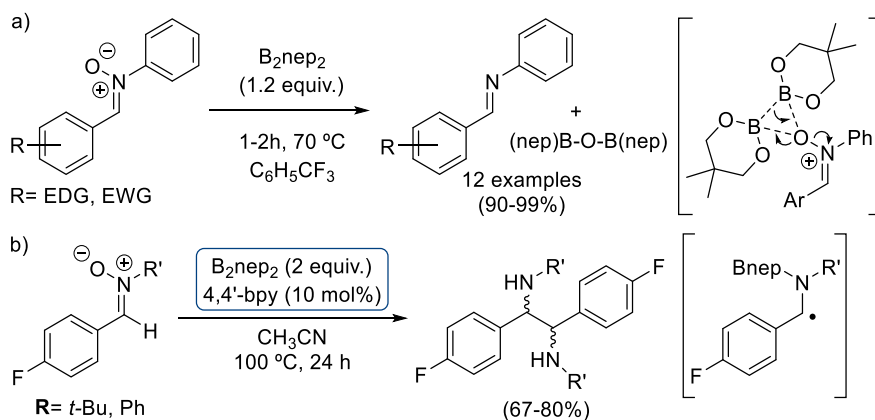
Chapter 2 of the thesis deals with the use of diboron based super electron donors (SED) to catalyze the radical coupling of aromatic thiols and halides (Scheme IV). The method demonstrated to be general for a wide number of coupling counterparts, representing a general and mild alternative to the previously reported procedures. Moreover, the approach exemplifies the latent potential of the use of SEDs in transformations via $S_{RN}1$ mechanisms different than the previously described borylations.



Scheme IV. SED catalyzed C-S bond formation.

Attending to some intriguing results obtained during the C-S coupling reaction study, we decided to explore the reactivity of nitrones in presence of unactivated and activated diborons. In the literature, the use of boron containing systems has been previously studied with different nitrogenated groups such as imines or *N*-oxides, but an analysis of the reactivity of these systems in presence of nitrones has not been reported.

Chapter 3 describes the reactivity of nitrones with diboronic esters, pyridine-boryl radicals and boron based super electron donors. Through this study, we determined that diboronic esters are able to promote the deoxygenation of nitrones to imines in high yields and short reaction times (Scheme Va). The analysis of the products revealed the presence of a $(RO)_2B-O-B(OR)_2$ species which is in accordance with a plausible concerted mechanism supported by preliminary theoretical calculations. The activation of diboron through the formation of pyridine-boryl radicals afforded the formation of diamines (Scheme Vb). These diamines could come from the coupling of two α -amino radicals. If this is true, the capture of the radical intermediate could open new synthetic possibilities in the future.



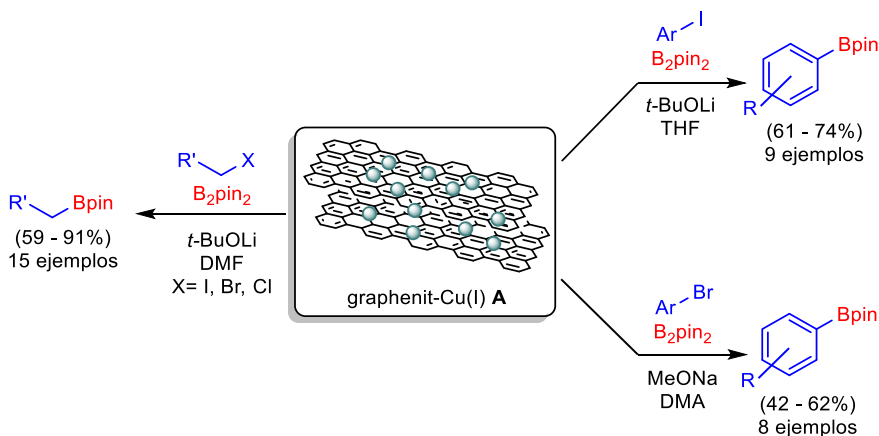
Scheme V. Diboron mediated nitron reactivity.

Resumen en español

Los **compuestos de diboro** son reactivos no tóxicos, accesibles, y valiosos para una gran variedad de transformaciones orgánicas. Prueba de su utilidad es el crecimiento exponencial de publicaciones científicas en esta área, especialmente en las que el B_2pin_2 aparece tanto como reactivo como sustrato.

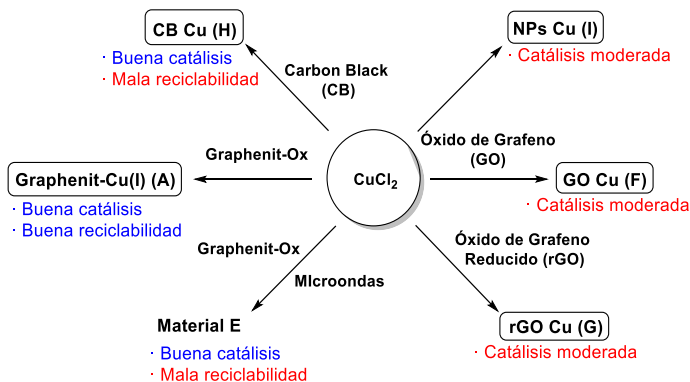
El uso más común de los reactivos de diboro es la introducción de fragmentos de ésteres borónicos en diferentes grupos funcionales como alquenos, alquinos, o haluros alifáticos y aromáticos. La introducción de ésteres borónicos está normalmente catalizada por metales de transición, entre los cuales destaca el cobre por su reducido coste y toxicidad. El uso de catalizadores homogéneos de cobre en este campo ha sido ampliamente estudiado. No obstante, el **empleo de catalizadores heterogéneos de cobre soportados en grafeno** para reacciones de borilación ha sido desarrollado recientemente, pero aún falta un análisis profundo del papel del soporte grafénico en la catálisis.

De acuerdo con este escenario, la **parte I** de esta tesis doctoral detalla el **desarrollo y estudio de nuevos catalizadores de cobre heterogéneos soportados en superficies grafénicas en la borilación de haluros alifáticos y aromáticos**. Avances recientes en nuestro grupo de investigación llevaron a la preparación de un nuevo catalizador heterogéneo de Cu_2O soportado en grafeno (**A**), preparado a partir de nanoplaquetas baratas y sostenibles (graphenit-Ox), el cual previamente demostró buena actividad catalítica en otras reacciones químicas como las cicloadiciones tipo click. Usando este catalizador como modelo, hemos encontrado condiciones de reacción con las que borilar tanto sustratos alifáticos como aromáticos (Esquema I), algo sin precedentes usando catalizadores de cobre heterogéneos.



Esquema I. Material A como catalizador de la borilación de haluros.

La preparación y el estudio de diferentes materiales usando radiación microondas reveló que estos catalizadores tienen el cobre más fuertemente anclado, pero una menor actividad catalítica debido al Cu(0) presente en su estructura. Catalizadores adicionales fueron preparados usando materiales gráfenicos comúnmente empleados (GO, rGO, CB), así como nanopartículas de Cu(I) sin soportar (NPs). Además, llevamos a cabo un profundo estudio de su estructura y actividad catalítica con el fin de entender el papel del soporte en la reacción (Esquema II).



Esquema II. Estudio comparativo de los materiales.

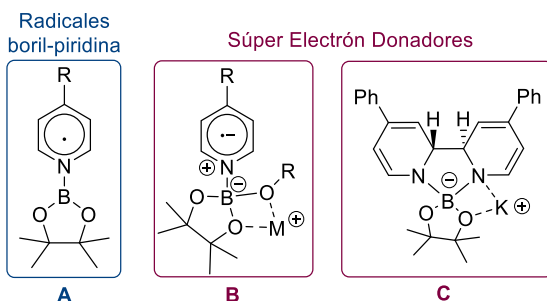
Aunque los materiales preparados catalizan la reacción de borilación en cierta medida, demostraron ser menos generales, reciclables, y eficientes que el material **A**.

Junto con el análisis estructural de los materiales, llevamos a cabo cálculos teóricos para entender el efecto de la superficie grafénica en la reacción. Con este estudio pudimos concluir que existe un efecto sinérgico entre la superficie de grafeno y las nanopartículas de Cu_2O que mejora la actividad catalítica de esta especie de cobre, especialmente cuando hay radicales involucrados en la reacción como es el caso.

La importancia de los compuestos de diboro no se limita a la introducción de fragmentos borilados. Recientemente se han publicado numerosas contribuciones interesantes donde se usan estos productos como promotores de diferentes transformaciones aparte de las borilaciones. La **parte II** de esta tesis doctoral relata diferentes aplicaciones de los compuestos de diboro y está dividida en dos capítulos.

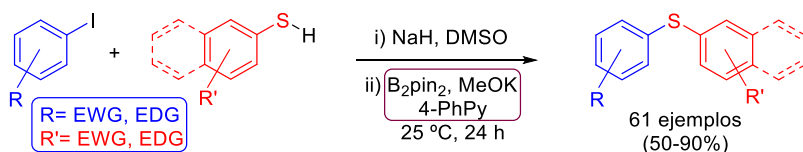
Durante las últimas décadas la activación de los compuestos de diboro con diferentes aditivos ha extendido su campo de aplicación. El uso de bases como aditivos de diboros es bien conocida, pero la adición de piridinas para activar estos compuestos es más reciente y lleva a la formación de radicales boril-piridina (**A**). Estos radicales han mostrado grandes resultados promoviendo reacciones de reducción, funcionalización de piridinas, y activación C-H. Por otro lado, la combinación de B_2pin_2 , una piridina, y un alcóxido lleva a la formación de intermedios altamente reductores (**B**, **C**) conocidos como súper electrón donadores (SED). Estos sistemas han sido desarrollados recientemente y pese a su gran potencial, han sido básicamente

utilizados en reacciones de borilación libres de metales de transición (Esquema III).



Esquema III. Activación de ésteres diborónicos usando piridinas.

El primer capítulo de esta segunda parte de la tesis (**capítulo 2**) trata el uso de súper electrón donadores (SED) basados en compuestos de diboro como catalizadores del acoplamiento radicalario de tioles y haluros aromáticos (Esquema IV). El método demostró ser general para un amplio número de sustratos, representando una alternativa suave y general con respecto a los procedimientos previamente publicados. Además, el método ejemplifica el potencial latente del uso de “SEDs” en transformaciones vía mecanismos $S_{RN}1$ distintas de las borilaciones previamente descritas.

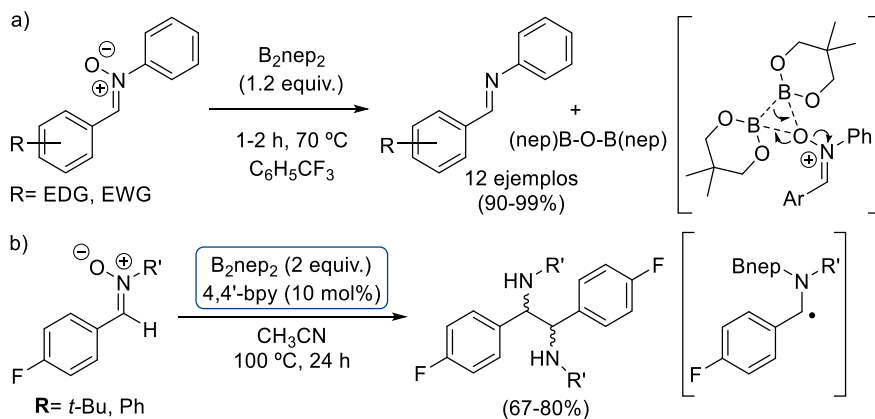


Esquema IV. Formación de enlaces C-S catalizadas por SED.

De acuerdo con algunos resultados interesantes obtenidos durante el estudio de la reacción de acoplamiento C-S, decidimos explorar la reactividad de las nitronas en presencia de diboros activados y desactivados. En la bibliografía, el uso de sistemas que contienen

diboros ha sido previamente estudiado en reacciones con diferentes grupos nitrogenados como iminas o *N*-óxidos, pero un análisis de la reactividad de estos sistemas con nitronas no ha sido publicado.

El **capítulo 3** describe la reactividad de las nitronas con ésteres diborónicos, radicales boril-piridina, y súper electrón donadores basados en diboro. Mediante este estudio, determinamos que **los ésteres diborónicos son capaces de capaces de desoxigenar nitronas para proporcionar iminas** con elevados rendimientos y cortos tiempos de reacción (Esquema Va). El análisis de los productos reveló la presencia de una especie $(RO)_2B-O-B(OR)_2$ la cual concuerda con un mecanismo concertado apoyado por unos cálculos teóricos preliminares. **La activación de los diboros mediante la formación de radicales boril-piridina llevó a la formación de diaminas** (Esquema Vb). Estas diaminas podrían proceder del acoplamiento de dos α -amino radicales. De ser así, la captura de uno de estos radicales intermedios podría abrir nuevas posibilidades sintéticas en el futuro.



Esquema V. Reactividad de nitronas en presencia de diboros.

Part I. Graphene-based Cu(I) Catalysts in Borylation Reactions

Chapter 1. Graphene-based Cu(I) Catalysts in Borylation Reactions

1. Introduction

This introduction will summarize the most relevant information about graphene derivatives as supports in heterogeneous catalysis and Cu-mediated borylation reactions.

A brief discussion of graphene and its derivatives' history is going to be presented. We will describe the types of graphenic materials paying special attention to the most commonly employed: graphene (**G**), graphene oxide (**GO**) and reduced graphene oxide (**rGO**).

We will also mention some of the applications of carbonaceous materials, being their main uses as **heterogeneous supports** with different purposes. The volume of references regarding the use of graphenic supports in heterocatalysis is tremendous, and therefore several reviews have been published collecting all this information. Some heterogeneous carbon materials like **GO** have been used to promote some chemical transformations giving rise to the area of catalysis known as **carbocatalysis**. The use of graphene derivatives to support organocatalysts has been scarcely explored.

Therefore, we will mention some examples related to the use of these materials as **carbocatalysts**, and the development of **heterogeneous metallic catalysts**, paying attention to those aspects related to graphene derivatives that we have considered to be closely related to our research, including the methods of preparation that use microwave radiation. To contextualize the work presented in this thesis we will describe our experience in the area.

Following this, we will present a second section depicting the properties and preparation methods of **borylated products** mainly employing copper catalysts, area in which we also have experience thanks to Professor Tortosa's investigations. To conclude, we will describe the existing reported borylation methods using **heterogeneous copper catalysts** supported on graphene derivatives.

1.1. Graphene and its derivatives

Carbon is after oxygen the most abundant element on earth, coming homogeneously distributed in the biosphere.¹ The union of these two atoms along with hydrogen compose the basis of living beings, biochemistry, and renewable energy storage (*e.g.* carbohydrates). Due to the importance of the structures composing these atoms, chemistry around them have been extensively studied over the years. A specific field where these premises have made a great impact is the materials chemistry.

The development of sustainable materials has become extremely important due to the challenges presented by the global energy demand, as well as the environmental necessities of the planet.² Thus, carbon-based systems are increasingly acquiring a major role in renewable energy conversion and modern ecofriendly technologies (Figure 1).

¹ a) Abbasi, T.; Abbasi, A. *Renewable Sustainable Energy Rev.* **2011**, *15*, 1828. b) Titirici, M. M.; White, R. J.; Brun, N.; Budarin, V. L.; Sun, D. S.; Del Monte, F.; Clark, J. H.; Maclachlan, M. J. *Chem. Soc. Rev.* **2015**, *44*, 250.

² Zhang, Q.; Uchaker, E.; Candelaria, S. L.; Cao, G. *Chem. Soc. Rev.* **2013**, *42*, 3127.

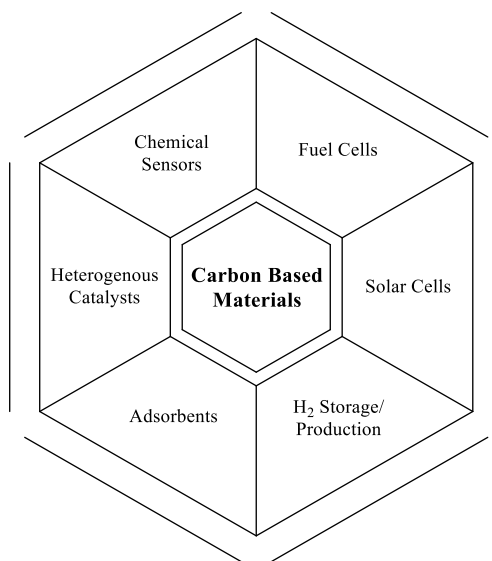


Figure 1. Carbon based materials applications.

Examples are the development of electrodes in energy storage devices,^{3,4} H₂ storage and production,⁵ adsorbents,⁶ heterogeneous catalysts,^{7,8,9,10,11} biofuels, etc.¹² In addition, carbon-based materials should also be low cost, scalable and based on renewable and highly abundant resources to be industrially and economically attractive.

The first material used for some of these applications, especially as adsorbent, was the activated carbon (AC).¹³ Although its origin is

³ Linares, N.; Silvestre-Albero, A. M.; Serrano, A.; Silvestre-Albero, J.; García-Martínez, J. *Chem. Soc. Rev.* **2014**, *43*, 7681.

⁴ Xu, C.; Xu, B.; Gu, Y.; Xiong, Z.; Sun, J.; Zhao, X.S. *Energy Environ. Sci.* **2013**, *6*, 1388.

⁵ Wu, C. D.; Fang, T. H.; Lo, J. Y. *Int. J. Hydrog. Energy.* **2012**, *37*, 14211.

⁶ Chen, Y.; Chen, L.; Bai, H.; Li, L. *J. Mater. Chem. A*, **2013**, *1*, 1992.

⁷ Dreyer, D. R.; Bielawski, C. W. *Chem. Sci.* **2011**, *2*, 1233.

⁸ Machado, B. F.; Serp, P. *Catal. Sci. Technol.* **2012**, *2*, 54.

⁹ Hu, M.; Yao, Z.; Wang, X. *Ind. Eng. Chem. Res.* **2017**, *56*, 3477.

¹⁰ Descorme, C.; Gallezot, P.; Geantet, C.; George, C. *Chem. Cat. Chem.* **2012**, *4*, 1897.

¹¹ Hebnner, S.; de Vries, J. G.; Farina, V. *Adv. Synth. Catal.* **2016**, *358*, 3.

¹² Wang, H.; Yuan, X.; Zeng, G.; Wu, Y.; Liu, Y.; Jiang, Q.; Gu, S. *Adv. Journal of Colloid and Interface Science.* **2015**, *221*, 41.

¹³ Heidarinejad, Z.; Dehghani, M. H.; Heidari, M.; Javedan, G.; Ali, I.; Sillanpää, M. *Environ. Chem. Lett.* **2020**, *18*, 393.

associated with the Ancient Egypt (1500 BC), when it truly experienced its maximum growth was in the 20th Century. During the 1930's decade, **AC** gained huge popularity in industrial sectors, for both gaseous and aqueous phase adsorption applications.¹⁴ Nevertheless, the starring material in this field changed since the innovative experiments carried out by Novoselov and Geim in 2004, where they described the preparation of graphene.¹⁵

This revolutionary material consisted of a single atom carbon monolayer with outstanding physical and electronic properties. It exhibits a great measured surface area (400–700 m²/g), high electron mobility, lack of a band gap, robustness, and flexibility, making graphene desirable for many commercial purposes.¹⁶ These unique features have attracted the interest in the scientific and engineering communities over the past two decades, meaning a significant growth of the scope of applications that graphene has been used for.¹⁷

Nowadays, graphene production is divided in two approaches: bottom-up and top-down (Scheme 1).^{18,19} The bottom-up approach is based on building graphene sheets starting from simple carbon molecules such as methane and ethanol, utilizing techniques like

¹⁴ Allen, S. J.; Whitten, L.; McKay, G. *Dev. Chem. Eng. Min. Process.* **1998**, *6*, 231.

¹⁵ Novoselov, K. S.; Geim, A. K.; Morozov, S. V.; Jiang, D.; Zhang, Y.; Dubonos, S. V.; Grigorieva, I. V.; Firsov, A. A. *Science*. **2004**, *306*, 666.

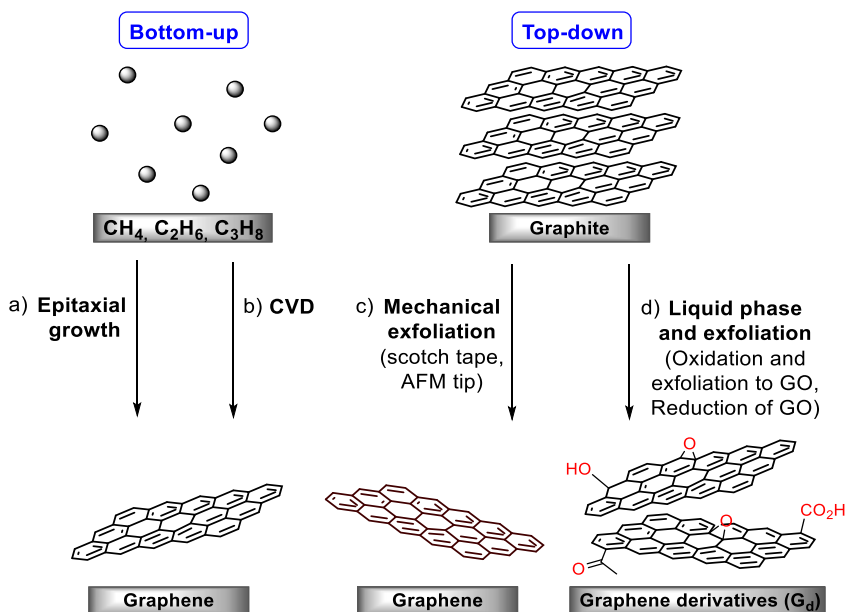
¹⁶ Dreyer, D. R.; Ruoff, R. S.; Bielawski, C. W. *Angew. Chem. Int. Ed.* **2010**, *49*, 9336.

¹⁷ Zhu, Y.; Murali, S.; Cai, W.; Li, X.; Suk, J. W.; Potts, J. R.; Ruoff, R. S. *Adv. Mater.* **2010**, *22*, **3906**.

¹⁸ Mahmoudi, T.; Wang, Y.; Hahn, Y. B. *Nano Cell.* **2018**, *47*, 51.

¹⁹ Choi, W.; Lee, J. *Graphene: Synthesis and Applications*. Ed.; Taylor & Francis Group, Boca Raton, 2012.

epitaxial growth (Scheme 1a),²⁰ or chemical vapor deposition (CVD) (Scheme 1b),²¹



Scheme 1. Different approaches to graphene preparation.

On the other hand, the top-down approach relies on the idea of extracting graphene layers from graphite by exfoliation, which can be achieved through mechanical (Scheme 1c) or chemical ways (Scheme 1d). Although mechanical exfoliation provides graphene of better quality, the top-down approach via chemical oxidation of graphite to graphene oxide (**GO**) and reduction is the most convenient method due to the higher yields and lower cost to prepare graphene derivatives (**G_d**). It is important to note that, although in many reports authors refer to their materials as graphene, this is a simplification, and they are in fact graphene derivatives with variable oxygen content.

²⁰ Bae, S.; Kim, H.; Lee, Y.; Xu, X.; Park, J. S.; Zheng, Y.; Balakrishnan, J.; Lei, Y.; Kim, H. R.; Song, Y. I.; Kim, Y. J.; Kim, K. S.; Özyilmaz, B.; Ahn, J. H.; Hong, B. H.; Iijima, S. *Nat. Nano.* **2010**, *5*, 574.

²¹ Bonaccorso, F.; Sun, Z.; Hasan, T.; Ferrari, A. C. *Nat. Photonics.* **2010**, *4*, 611.

Moreover, pristine graphene obtained by mechanical exfoliation has the additional drawback of being more difficult to functionalize due to its lack of defects.²²

For these reasons, graphene derivatives (**G_d**) obtained through chemical treatment are important for researchers who use these materials in applications such as composites, coatings, paints, conductive layers, catalysts, bioapplications, and energy storage.²³ Thus, one of the materials that has played a significant role in the development of graphene applications is graphene oxide (**GO**).²⁴ This graphene derivative characterizes on having a carbon structure containing a variety of oxygenated functional groups (alcohols, epoxides, ketones and carboxylic acids). This functionalization and high degree of sp³ hybridization creates multiple defects and anchor points that makes **GO** easy to functionalize compared to graphene. The classical preparation of **GO** goes through exfoliation of graphite oxide, whose layers are easier to separate than graphite due to their less packing.

The first approach to obtain graphite oxide was described by Brodie in 1859,²⁵ but this methodology implied the addition of potassium chlorate to graphite in fuming nitric acid. After many years of research and development of this synthesis, Hummers and Offeman published a safer method to get graphite oxide.²⁶ In this case, they dissolved KMnO₄

²² Dreyer, D. R.; Todd, A. D.; Bielawski, C. W. *Chem. Soc. Rev.* **2014**, *43*, 5288.

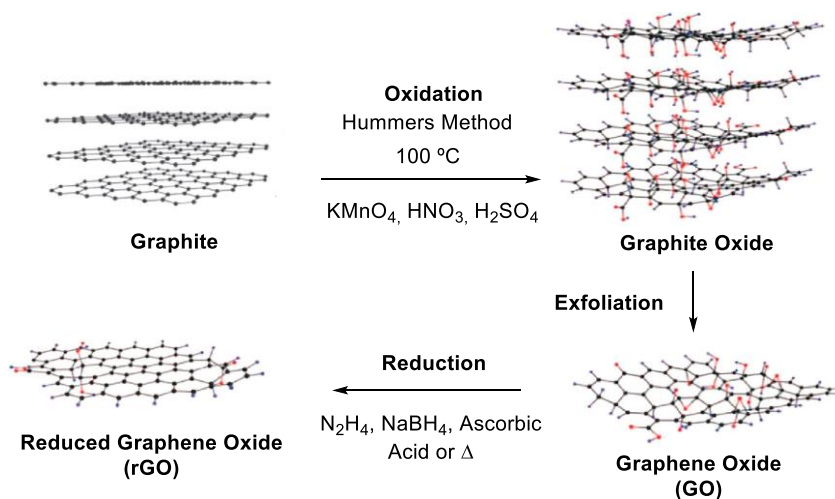
²³ Huang, X.; Qi, X.; Boey, F.; Zhang, H. *Chem. Soc. Rev.* **2012**, *41*, 666.

²⁴ Dreyer, D. R.; Park, S.; Bielawski, C. W.; Ruoff, R. S. *Chem. Soc. Rev.* **2010**, *39*, 228.

²⁵ Brodie, B. C. On the Atomic Weight of Graphite. *Philos Trans R Soc London.* 1859, *14*, 249–259.

²⁶ Hummers, W. S.; Offeman, R. E. *J. Am. Chem. Soc.* **1958**, *80*, 1339.

and NaNO_3 in concentrated H_2SO_4 to oxidize graphite within a few hours (Scheme 2).



Scheme 2. Classic preparation of GO and rGO from graphite.

Thanks to the easy execution and short reaction times, Hummers' method has been widely adopted to afford **GO** during many years.²⁷ However, the toxicity of the reagents and gases generated during this procedure have driven researchers to find alternatives, developing modifications to this method.^{28,29,30}

The high degree of functionalization present in **GO** could become a problem for some purposes. To overcome this limitation, **GO** can be reduced under several conditions to obtain a material with still a measurable oxygen percentage but with much less degree of sp^3 hybridization known as reduced graphene oxide (**rGO**) (Scheme 2).³¹ Synthesis of **rGO** has been extensively studied, finding many methods

²⁷ Eigler, S.; Hirsch, A. *Angew. Chem. Int. Ed.* **2014**, *53*, 2.

²⁸ Yu, H.; Zhang, B.; Bulin, C.; Li, R.; Xing, R. *Sci. Rep.* **2016**, *6*, 36143.

²⁹ Eigler, S. *Chem. Eur. J.* **2016**, *22*, 7012.

³⁰ Singh, R. K.; Kumar, R.; Singh, D. P. *RSC Adv.* **2016**, *6*, 64993.

³¹ Chua, C. K.; Pumera, M. *Chem. Soc. Rev.* **2014**, *43*, 291.

to its preparation from **GO** using different reducing agents such as hydrazine,³² NaBH₄,³³ LiAlH₄,³⁴ or ascorbic acid.³⁵ The C/O ratio found in the materials under the different reaction conditions is always between 4 and 14, indicating a good degree of functionalization remaining in the obtained **rGO**.³¹

A final family of carbonaceous materials which is worth to mention are the carbon blacks (**CB**). These materials have been also employed as supports for a variety of purposes such as sensors, catalysts, or energy storage.³⁶ However, as these materials are obtained as industrial waste from different manufacturing processes, carbon blacks are structurally less well defined than graphene derivatives,³⁷ limiting their study.

1.2. Graphene derivatives as carbocatalysts

Graphene structures functionalized with oxygen-containing groups have been widely used as catalysts.^{38,39,40} The oxygenated functional groups present in **GO** and **rGO** can be directly used to catalyze reactions (carbocatalysis) or as substrates to introduce different heteroatoms to the materials.^{41,42} Although there are many contributions existing in the literature about this field, in order to show

³² Chua, C. K.; Pumera, M. *Chem. Commun.* **2016**, 52, 72.

³³ Muszynski, R.; Seger, B.; Kamat, P. V. *J. Phys. Chem. C* **2008**, 112, 5263.

³⁴ Ambrosi, A.; Chua, C. K.; Bonanni, A.; Pumera, M. *Chem. Mater.* **2012**, 24, 2292.

³⁵ Gao, J.; Liu, F.; Liu, Y.; Ma, N.; Wang, Z.; Zhang, X. *Chem. Mater.* **2010**, 22, 2213.

³⁶ Lawrence, K.; Baker, C. L.; James, T. D.; Bull, S. D.; Lawrence, R.; Mitchels, J. R.; Opallo, M.; Arotiba, O. A.; Ozoemena, K. I.; Marken, F. *Chem. Asian J.* **2014**, 9, 1226.

³⁷ Donnet, J. B.; Bansal, R. C.; Wang, M. J. *Carbon Black*; Marcel Dekker: New York, NY, USA, 1993.

³⁸ Tang, P.; Hu, G.; Li, M.; Ma, D. *ACS Catal.* **2016**, 6, 6948

³⁹ Navalon, S.; Dhakshinamoorthy, A.; Alvaro, M.; Garcia, H. *Coord. Chem. Rev.* **2016**, 312, 99.

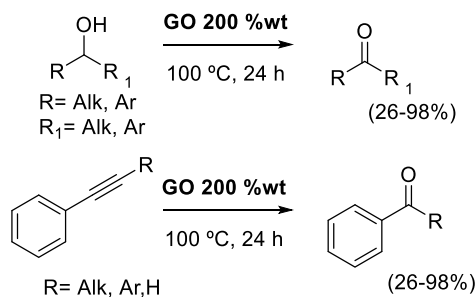
⁴⁰ Navalon, S.; Dhakshinamoorthy, A.; Alvaro, M.; Garcia, H. *Chem. Rev.* **2014**, 114, 6179.

⁴¹ Deng, D.; Novoselov, K. S.; Fu, Q.; Zheng, N.; Tian, Z.; Bao, X. *Nat. Nanotechnol.* **2016**, 11, 218.

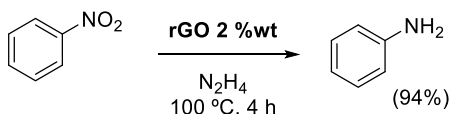
⁴² Satheesh, D.; Shanmugam, S.; Ravichandran, K. *Mat. Lett.* **2014**, 137, 153.

a general view of the utility of these materials some representative examples are depicted in scheme 3.

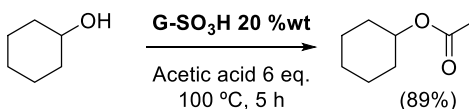
a) Bielawski et al, 2010



b) Gao et al, 2011



c) Xiao et al, 2012



Scheme 3. Application of carbon-based materials in catalysis.

A seminal example using carbon-based materials in carbocatalysis was published in 2010 by Bielawski and coworkers.⁴³ In this work, authors reported that **GO** was able to promote the oxidation of different alcohols, as well as the hydration of phenyl acetylenes to get to the corresponding carbonyl products with good yields (Scheme 3a).

Later, the group of Gao published the effective reduction of nitrobenzene catalyzed by **rGO** in presence of hydrazine (Scheme 3b).⁴⁴ This report explores again the potential of graphene derivatives

⁴³ Dreyer, D. R.; Jia, H. P.; Bielawski, C. W. *Angew. Chem. Int. Ed.* **2010**, *49*, 6813.

⁴⁴ Gao, Y.; Ma, D.; Wang, C.; Guan, J.; Bao, X. *Chem. Commun.* **2011**, *47*, 2432.

as carbocatalysts, where the material is able to promote the reaction with no need of further functionalize the surface.

As an example of the utility of functionalized **GO** in acid catalysis, it is worth to mention the work by Xiao and coworkers.⁴⁵ In this publication, they reported the synthesis of sulfated graphene oxide (G-SO₃H) from a facile hydrothermal sulfonation of reduced graphene oxide with fuming sulfuric acid at 180 °C, and its utilization as an efficient solid acid in the esterification of alcohols (Scheme 3c).

As shown in these examples, the potential of graphene derived materials as catalysts in different processes is a growing and promising area, which nowadays is still being studied to expand their scope of application.^{46,47}

1.3. Graphene derivatives in metallic catalysis

The advantages of the different graphene-based materials in catalysis have also been explored using metal nanoparticles (MNPs) supported over these materials.^{48,49,50} Many studies suggest that the unique electronic properties of the graphene-based surfaces can affect the characteristics of the metal when it is attached to the carbonaceous material.^{51,52}

⁴⁵ Liu, F.; Sun, J.; Zhu, L.; Meng, X.; Qi, C.; Xiao, F. S. *J. Mater. Chem.* **2012**, *22*, 5495.

⁴⁶ For selected reviews see: a) Carbocatalytic Activity of Graphene Oxide in Organic Synthesis. Majumdar, B.; Sarma, D.; Sarma, T. K. *InTechOpen.* **2018**, b) Navalon, S.; Dhakshinamoorthy, A.; Alvaro, M.; Antonietti, M.; Garcia, H. *Chem. Soc. Rev.* **2017**, *46*, 4501. c) Ahmad, M. S.; Nishina, Y. *Nanoscale.* **2020**, *12*, 12210. d) Lombardi, L.; Bandini, M. *Angew. Chem. Int. Ed.* **2020**, *59*, 20767.

⁴⁷ Meng, G.; Patel, M.; Luo, F.; Li, Q.; Flach, C.; Mendelsohn, R.; Garfunkel, E.; He, H.; Szostak, M. *Chem. Commun.* **2019**, *55*, 5379.

⁴⁸ Liu, L.; Corma, A. *Chem. Rev.* **2018**, *118*, 4981

⁴⁹ Pérez-Mayoral, E.; Calvino-Casilda, V.; Soriano, E. *Catal. Sci. Technol.* **2016**, *6*, 1265.

⁵⁰ Zhang, G.; Zhang, F.; Fan, X. *Chem. Soc. Rev.* **2015**, *44*, 3023.

⁵¹ Ding, M.; Tang, Y.; Star, A. J. *Phys. Chem. Lett.* **2013**, *4*, 147.

⁵² Cheng, Y.; Fan, Y.; Pei, Y.; Qiao, M. *Catal. Sci. Technol.* **2015**, *5*, 3903.

In the literature, the support-metal nanoparticle interaction is explained by the overlapping between the π orbitals of graphene derivatives with the d orbitals of transition metal (TM) atoms.³⁹ Additionally, the sp^2 hybridization of carbon atoms and the extended molecular π orbital makes graphene able to even interact with certain reagents not only by van der Waals forces, but also by stronger π - π interactions (Figure 2).⁵³

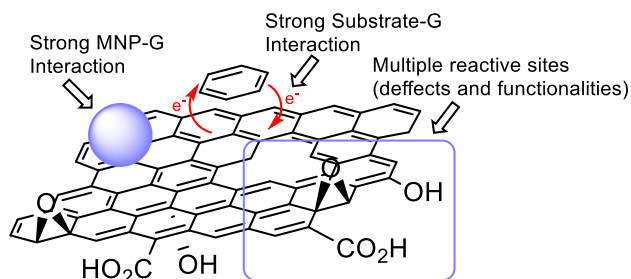


Figure 2. Different interactions and anchor points of graphene derivatives.

Thus, surface chemical properties of the graphene derivatives are crucial for catalyst anchoring as well as, in some cases, for explaining the catalytic behavior of a graphene-supported catalyst. Moreover, the possible modification of the anchored atom electron density has been studied through theoretical calculations,⁵⁴ observing a tendency of this modulation depending on the atom's electronegativity. For nonmetallic atoms, the charge transfer is postulated to occur from graphene to the atoms. However, for metals is the opposite, finding that this charge transfer is stronger for early TM and milder for late TM due to the electronegativity increase.⁵⁵ The modification of the electron density of the reaction substrates and intermediates has also been

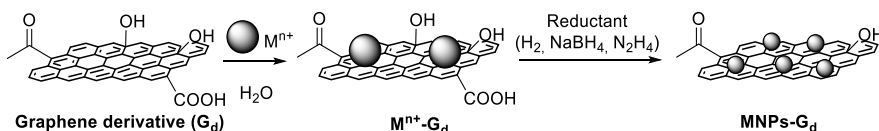
⁵³ Martinez Laguna, J.; Caballero, A.; Perez, P. J. *Chem. Rev.* **2021**, *363*, 1740.

⁵⁴ Nakada, K. I., Akira In Graphene Simulation; Gong, J. R., Ed.; IntechOpen, 2011.

⁵⁵ Gerber, I. C.; Serp, P. *Chem. Rev.* **2020**, *120*, 1250.

speculated.⁴⁰ This effect is associated to adsorption phenomena and could favor some reaction steps.

The typical preparation procedure to get these heterogenous catalysts involve the so-called deposition-precipitation method (Scheme 4).^{56,57}



Scheme 4. Typical procedure for MNPs supported on graphene derivatives.

This reaction comprises a first step where the graphenic surface associates with the metal salts by Coulombic forces and via formation of covalent bonds. This deposition process requires a long contact time between the material and the metal ions, normally taking hours or days. The second step involves the treatment of the obtained material with a reductant, which could be a hydrogen stream or another reducing agent. This step leads to a final material (**MNPs-G_d**) with a substantial less oxygen content than the original and reduced MNPs supported on it. Other reported preparation methods employ the solvothermal anchorage of the metal nanoparticles in ethylene glycol at high temperatures,⁵⁸ or the use of organic linkers as interphase between the support and the MNPs.⁵⁹

The use of **MNP-G_d** materials can give access to additional transformations unreachable for non-metallic G materials, being the cross-coupling reactions the most representative.⁶⁰ Among all

⁵⁶ Haruta, M.; Tsubota, S.; Kobayashi, T.; Kageyama, T.; Genet, M. *J. Catal.* **1993**, *144*, 175.

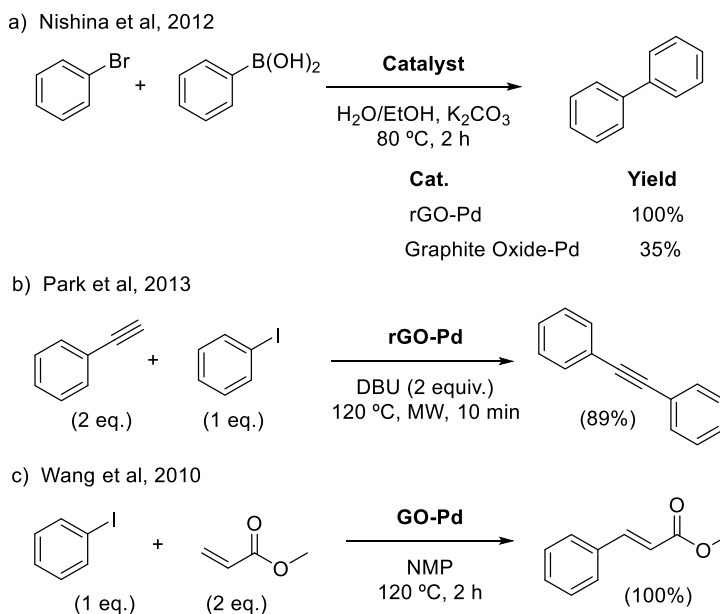
⁵⁷ Haruta, M. *Catal. Today.* **1997**, *36*, 153.

⁵⁸ Xu, C.; Wang X.; Zhu J. *J. Phys. Chem. C.* **2008**, *112*, 19841.

⁵⁹ Shaabani, A.; Mahyari, M. *J. Mater. Chem. A.* **2013**, *1*, 9303.

⁶⁰ Scheuermann, G. M.; Rumi, L.; Steurer, P.; Bannwarth, W.; Mulhaupt, R. *J. Am. Chem. Soc.* **2009**, *131*, 8262.

transition metals, palladium is the most studied, and many contributions using these catalysts have been published over the years. In scheme 5 are depicted some relevant examples of graphene-supported palladium materials in catalysis. Although a systematic study analyzing the effect of the different graphenic supports on the MNPs is still lacking, in the selected examples the effect of the surface over the metal can be glimpsed.



Scheme 5. Examples of MNPs-G catalyzed reactions.

In 2012 Nishina and coworkers published the preparation and catalytic activity of a rGO-Pd catalyst in the Suzuki-Miyaura coupling reaction (Scheme 5a).⁶¹ The prepared heterogenous catalyst was able to be recycled until the third run, after which the reaction yield dropped to a 58%. In their report, they also studied the performance of the graphite oxide-Pd material (precursor in the synthesis of rGO-

⁶¹ Nishina, Y.; Miyata, J.; Kawai, R.; Gotoh, K. *RSC Adv.* **2012**, *2*, 9380.

Pd), and they got a pronounced reduction in the product yield, meaning a great influence of the surface structure on the catalysis.

Another reaction where metallic graphenic materials have been widely employed is the Sonogashira cross-coupling. Park reported in 2013 that rGO-Pd materials can efficiently catalyze the Sonogashira reaction (Scheme 5b).⁶² Herein, through a systematic study employing characterization techniques such as XRD, XPS and TEM, authors demonstrated that small and well-dispersed MNPs have a beneficial effect on the reaction yield. In this paper authors demonstrated again the better performance of the rGO-Pd material compared to the graphite oxide precursor. Additionally, their material was able to catalyze the reaction until the third cycle with no erosion of the yield.

A final example highlighting the applicability of these materials in metal catalysis was reported by Wang's group, where they developed a GO-Pd material able to catalyze the Heck cross-coupling reaction with full regioselectivity (Scheme 5c).⁶³

The catalytic applications of graphene based heterogeneous metallic catalysts have been largely demonstrated over the years. Some of these studies, mainly using single atom metals, have also led to the conclusion that the support structure is important to the reactivity as well. However, this hypothesis has not been demonstrated through a deeper study, as well as tested in other materials wearing different metals.

An interesting publication focused on the study of the modulating effects of the surface to supported metals and reagents was published

⁶² Lee, K. H.; Han, S. W.; Kwon, K. Y.; Park, J. B. *J. Colloid Interface. Sci.* **2013**, 403, 127.

⁶³ Tang, Z.; Shen, S.; Zhuang, J.; Wang, X. *Angew. Chem. Int. Ed.* **2010**, 49, 4603.

in 2017 by Zhang and coworkers.⁶⁴ Herein, authors analyzed the synergistic effect between rGO and Cu₂O in the photocatalytic degradation of methylene orange, a common dye (Figure 3). The main features of this study are the employment of a metal salt, much less studied than other single atom metals such as palladium, as well as being the first deep evaluation of a copper supported graphene material in catalysis. Through this study they suggested that support provides the octahedral Cu₂O particles enhanced photocatalytic properties such as a narrower band gap, that improve the catalytic performance of the metal in the degradation of methylene orange dyes.

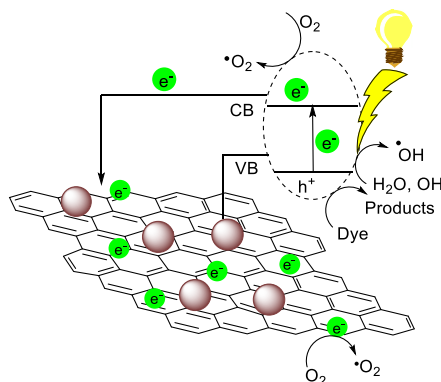


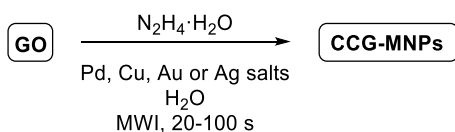
Figure 3. Zhang's rGO-Cu₂O charge transfer under visible light proposal.

A different approach to graphene supported metal catalysts is the utilization of microwave irradiation (MWI) during their preparation. The microwave assisted synthesis of metal nanoparticles has been known since the early 2000s thanks to the works of Strouse and El-

⁶⁴ Zhang, W.; Ma, Y.; Yang, Z.; Tang, X.; Li, X.; He, G.; Cheng, Y.; Fang, Z.; He, R.; Zhang, Y. *J. Alloys Compd.* **2017**, 712, 704.

Shall groups, who were able to efficiently synthesize different metal nanoparticles, nanorods and nanoplates.^{65,66}

The advances in the use of microwaves to synthesize metal nanoparticles led the group of El-Shall to publish in 2009 the preparation of graphene supported metal nanoparticles using this methodology.⁶⁷ In their publication, authors used single atom metals to obtain different MNPs supported over chemically converted graphene (CCG) sheets starting from GO and using hydrazine as reducing agent (Scheme 6).



Scheme 6. Microwave irradiated Graphene supported MNPs synthesis method by El-Shall.

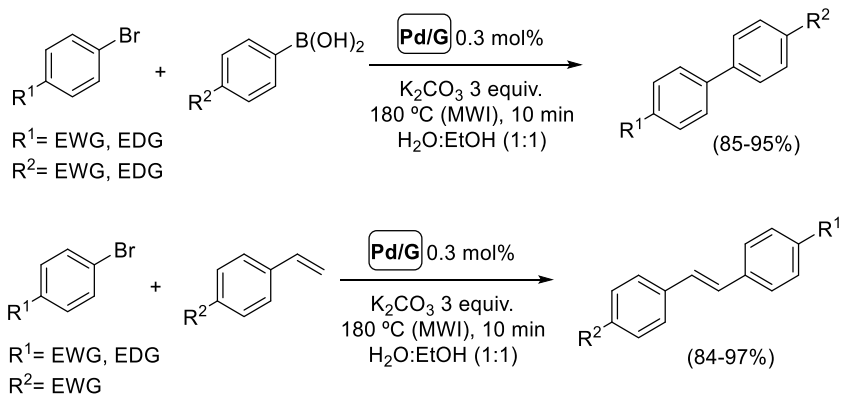
The simplicity of the method developed by El-Shall to get supported metal materials allowed their application in catalysis. In 2011, the same research group in collaboration with Gupton and coworkers published the utilization of the recently developed CCG-Pd material as catalyst (Scheme 7).⁶⁸

⁶⁵ Gerbec, J. A.; Magana, D.; Washington, A.; Strouse, G. F. *J. Am. Chem. Soc.* **2005**, *127*, 15791.

⁶⁶ a) Panda, A. B.; Glaspell, G.; El-Shall, M. S. *J. Am. Chem. Soc.* **2006**, *128*, 2790. b) Panda, A. B.; Glaspell, G.; El-Shall, M. S. *J. Phys. Chem. C* **2007**, *111*, 1861.

⁶⁷ Hassan, H. M.; Abdelsayed, V.; Abd El Rahman, S. K.; AbouZeid, K. M.; Turner, J.; El-Shall, M. S.; Al-Resayes, S. I.; El-Azhary, A. A. *J. Mater. Chem.* **2009**, *19*, 3832.

⁶⁸ Siamaki, A. R.; Khder, A. E. R. S.; Abdelsayed, V.; El-Shall, M. S.; Gupton, B. F. *J. Catal.* **2011**, *279*, 1.



Scheme 7. El-Shall and Gupton's method for the heterogeneous cross-coupling reactions.

Particularly, they reported the Suzuki and Heck cross-coupling products under the same reaction conditions, using a 0.3 mol% of the heterogeneous catalyst during 10 minutes at 180 °C into a microwave apparatus.

The following years, Gupton's group kept studying the microwave irradiated heterogeneous palladium catalysts to improve their preparation methods and understand the relationship between the Pd nanoparticles and the supports.^{69,70,71,72} Through DFT studies they have suggested that the beneficial effect of microwaves to the catalysis in cross coupling reactions resides in the generation of defects on the materials structure.⁶⁹ This not only provides a stronger anchorage of

⁶⁹ Yang, Y.; Reber, A. C.; Gilliland III, S. E.; Castano, C. E.; Gupton, B. F.; Khanna, S. N. *J. Catal.* **2018**, *360*, 20.

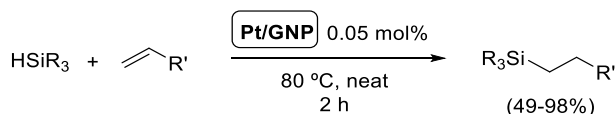
⁷⁰ Gilliland III, S. E.; Meynard, J.; Tengcob, M.; Yanga, Y.; Regalbutob, J. R.; Castano, C. E.; Gupton, B. F. *Appl. Catal. A*, **2018**,

⁷¹ Yang, Y.; Reber, A. C.; Gilliland III, S. E.; Castano, C. E.; Gupton, B. F.; Khanna, S. N. *J. Phys. Chem. C* **2018**, *122*, 25396.

⁷² Ghobadi, S.; Burkholder, M. B.; Smith, S. E.; Gupton, F. B.; Castano, C. E. *Chem. Eng. J.* **2020**, *381*, 122598.

the MNPs on the support, but also lowers the activation energy of some reaction steps.

The understanding gathered of the materials led his group to even extend this preparation methodology to other metals such as platinum, proving to be useful in the hydrosilylation of olefins under batch and flow conditions using inexpensive graphene nanoplatelets (GNP) as support (Scheme 8).⁷³



Scheme 8. Gupton's approach to heterogenous catalyzed hydrosilylation of olefines.

1.4. Our previous experience in the use of graphene derivatives in heterogeneous organocatalysis

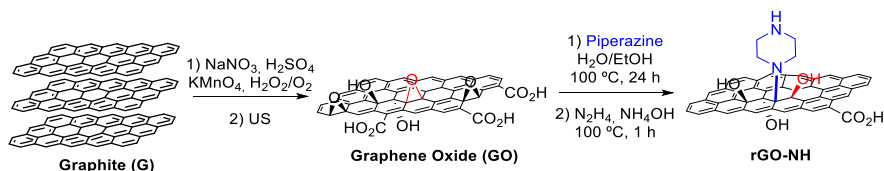
As previously mentioned, the study of functionalized graphene derivatives as organocatalysts has been poorly studied compared to the carbocatalyzed and metal catalyzed methods. However, as mentioned in the outline of the chapter, Dr. Cid's research group has explored the use of graphene derivatives as supports of organocatalysts. The first example, published in 2014, implied the formation of nitrogen functionalized reduced graphene oxide (rGO-NH) which was able to act as heterogeneous multifunctional aminocatalyst in various organic reactions.⁷⁴ The material **rGO-NH** was prepared in collaboration with Nanoinnova Technologies⁷⁵ as represented in Scheme 9.

⁷³ Kong, C. J.; Gilliland III, S. E.; Clark, B. R.; Gupton, F. B. *Chem. Commun.* **2018**, 54, 13343.

⁷⁴ Rodrigo, E.; García, B.; Sainz, R.; García-Fierro, J. L.; Ferritto, R.; Cid, M. B. *Chem. Commun.*, **2014**, 50, 6270.

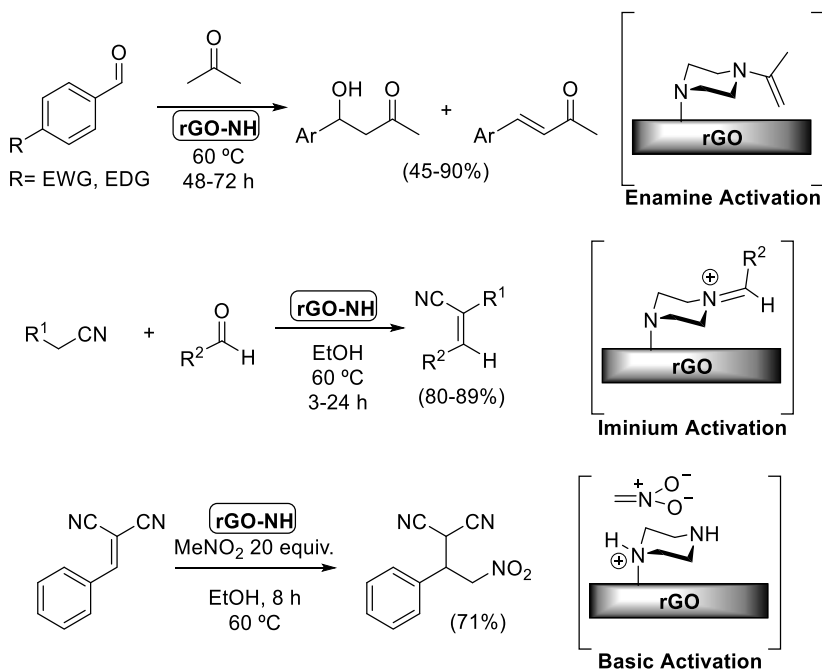
⁷⁵ <https://www.nanoinnova.com/>

The introduction of piperazine was performed by the simple opening of the epoxide groups of **GO** (prepared using Hummer's method). Further reduction with hydrazine under basic conditions afforded material **rGO-NH**.



Scheme 9. rGO-NH preparation method described by Cid and coworkers.

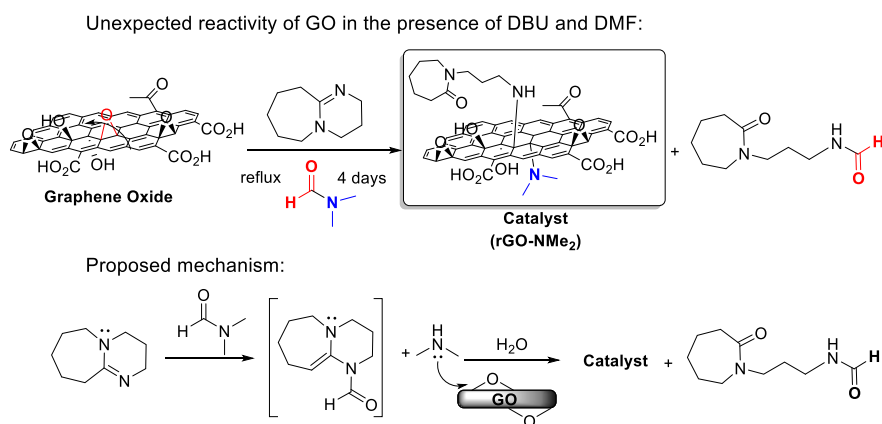
The catalyst showed a good catalytic activity towards aldol condensation, Knoevenagel condensation, and Michael addition reactions (Scheme 10). These processes follow three different activation pathways: through enamine, iminium, and basic activation. Thus, demonstrating the multifunctional character of the material.



Scheme 10. Piperazine functionalized rGO as catalyst in organic reactions.

Additionally, the comparison of the catalytic activity of the **rGO-NH** with some precursors suggests an effect of the surface stabilizing positively charged intermediates.⁷⁶ These results also suggest that the material is not a mere carrier of the piperazine, but also plays a key role on the catalysis.

Another example that shows the potential of the graphene-based materials as precursors of functionalized surfaces as well as the limited knowledge in this area, was published later in 2018.⁷⁷ In the context of some studies oriented to functionalize **GO** surfaces by epoxide opening using alcohols instead of amines, it was found that the reaction of DBU and DMF in presence of **GO** leads to the unexpected hydrolysis of DBU, generating the corresponding acyclic amine along with HNMe_2 . These amines can undergo either the reaction of both of them with DMF to afford the transamidation product, or the attachment to the GO through the epoxides present on its surface (Scheme 11 above).

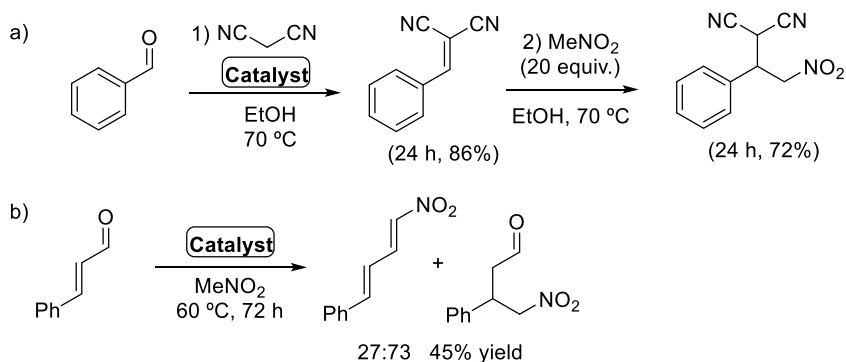


Scheme 11. DBU/DMF reaction in presence of GO and mechanistic proposal.

⁷⁶ Pan, Y.; Wang, S.; Kee, C. W.; Duibson, E.; Yang, Y.; Loh, K. P.; Tan, C. H. *Green Chem.* **2011**, *13*, 3341.

⁷⁷ Ramírez-Jiménez, R.; Franco, M.; Rodrigo, E.; Sainz, R.; Ferritto, R.; Lamsabhi, A. M.; Aceña, J. L.; Cid, M. B. *J. Mater. Chem. A*, **2018**, *6*, 12637.

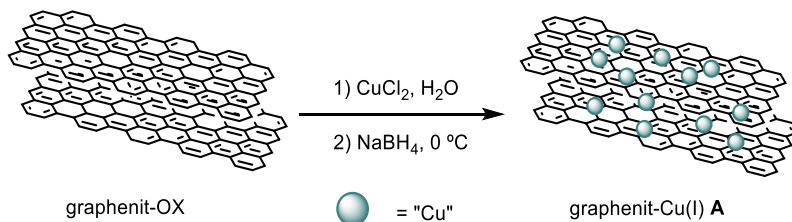
A plausible mechanism was proposed based on DFT where DBU hydrolyzes in presence of DMF to afford a new amide product and a functionalized material bearing the dimethylamine coming from the DMF and the amine coming from the DBU (Scheme 11 below). Material **rGO-NMe₂** was able to catalyze some processes such as the Knoevenagel-Michael (Scheme 12a) and Henry/Michael reactions (Scheme 12b).



Scheme 12. Synthetic applications of the heterogeneous organocatalyst.

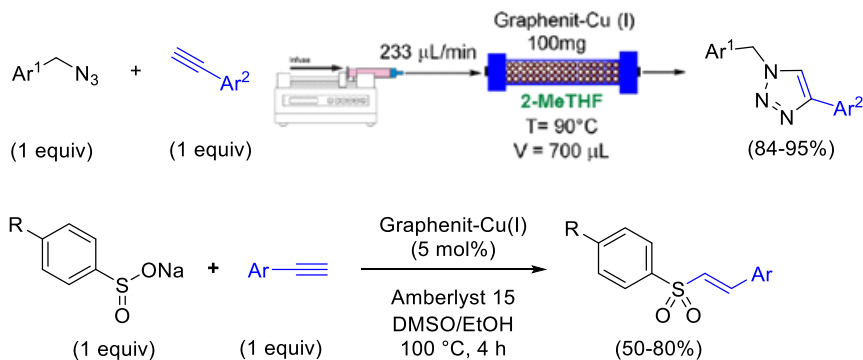
As mentioned above, previously reported metallic catalysts supported on graphene derivatives exhibited a great potential. Nevertheless, some points needed to be addressed. For example, it would be desirable to use inexpensive and abundant metal salts instead of the most extended expensive transition metal complexes. Another issue to be improved was the sustainability of the support and stability and recyclability of the prepared materials.

In order to overcome these limitations among others, a new robust material called graphenit-Cu(I) (**A**), was prepared anchoring Cu over graphene nanoplatelets commercialized as **graphenit-Ox** by Nanoinnova Technologies⁷⁵ (Scheme 13). This material was prepared from graphite in the absence of acids and oxidants required for the preparation of **GO** from graphite, being a more sustainable support.



Scheme 13. Graphenit-Cu(I) catalyst representation and its preparation method.

In collaboration with the professor Luisi's group (Università degli Studi di Bari Aldo Moro) the efficiency under batch and flow conditions of the heterogenous catalyst graphenit-Cu(I) (A) was analyzed in the copper(I) catalyzed azide-alkyne cycloaddition (CuAAC) as well as in the alkyne sulfonylation (Scheme 14).⁷⁸



Scheme 14. Graphenit-Cu(I) catalyzed CuAAC and alkyne sulfonylation reactions.

Interestingly, apart from the catalytic performance exhibited by the new material, it was observed that the commonly air unstable Cu(I) salts, when anchored to the graphenic surface, remained un-oxidized for at least one year at open air. Moreover, the catalyst showed a

⁷⁸ De Angelis, S.; Franco, M.; Trimini, A.; González, A.; Sáinz, R.; Degennaro, L.; Romanazzi, G.; Carlucci, C.; Petrelli, V.; De la Esperanza, A.; Goñi, A.; Ferritto, R.; Aceña, J. L.; Luisi, R.; Cid, M. B. *Chem. Asian J.* **2019**, *14*, 3011.

remarkable performance in terms of recyclability, demonstrating no erosion of the reaction yield after 5 cycles of reutilization. These promising results laid the foundations for its application in other types of reactions.

To summarize the antecedents depicted above, we can affirm that the utilization of heterogeneous catalysts in organic chemistry has attracted some attention during the last decades. The functionalization of graphene derivatives with organic moieties or with metal nanoparticles has led to the development of many alternative methods to the previously reported homogeneous procedures but with the advantages of the heterogeneous materials. However, despite the great synthetic achievements and a few efforts to study the role of the heterogeneous surface in the catalyzed reactions, a deep understanding is still lacking, making difficult the analysis of the role of the different materials in a catalytic process.

Therefore, it would be interesting to study the performance of different supported catalysts in a useful reaction and comprehend their role through additional studies such as theoretical calculations and structure analysis. For that, taking advantage of our experience in boron chemistry, we considered that a borylation reaction could be an excellent candidate to both reaffirm the value of Graphene-Cu(I) (**A**) developing a robust and general method to prepare organoboranes, and also to deeply analyze some other factors that remain unclear in the heterogeneous metal catalyzed processes such as the role of the support.

1.5. Organoboron compounds

The importance and interest of the borylated products are reflected in the copious number of publications including these compounds day by day throughout the different scientific journals. The organoboron compounds have found since the 1960's a great variety of uses. They have been employed in many organic synthesis transformations, mostly the hydroboration and the Suzuki-Miyaura cross-coupling reactions among others.⁷⁹

Furthermore, thanks to their low toxicity and stability, these compounds have been employed in a wide range of chemistry fields, such as material chemistry,⁸⁰ medicinal chemistry,⁸¹ and as delivery agents for neutron capture therapy.⁸²

Boron can be found being part of a variety of functional groups. These can be boranes, boronic acids, boronic esters, borohydrides, trifluoroborates... etc. However, among all of them we could highlight the boronic acids and esters, especially the ones derived from pinacol (Bpin).

⁷⁹ a) Matteson, D. S. *Chem. Rev.* **1989**, *89*, 1535. b) DeFrancesco, H.; Dudley, J.; Coca, A. *ACS Symposium Series* Vol. 1236. **2016**. c) Magano, J.; Dunetz, J. R. *Chem. Rev.* **2011**, *111*, 2177 d) Leonori D.; Aggarwal, V. K. *Acc. Chem. Res.* 2014, *47*, 3174 e) Leonori, D.; Aggarwal, V. K. *Synthesis and Application of Organoboron Compounds*, ed.; Fernández, E. and Whiting, A. Springer International Publishing, Cham, **2015**, pp. 271–295. f) Crudden, C. M.; Edwards, D. *Eur. J. Org. Chem.* **2003**, 4695. g) Carroll, A-M.; O'Sullivan, T. P.; Guiry, P. J. *Adv. Synth. Catal.* **2005**, *347*, 609. h) Schiffner, J. A.; Mütter, K.; Oestreich, M. *Angew. Chem. Int. Ed.* **2010**, *49*, 1194.

⁸⁰ Brooks, W. L. A.; Sumerlin, B. S. *Chem. Rev.* **2016**, *116*, 1375.

⁸¹ a) Beenen, M. A.; An, C.; Ellman, J. A. *J. Am. Chem. Soc.* **2008**, *130*, 6910. b) Milo Jr., L. J.; Lai, J. H.; Wu, W.; Liu, Y.; Maw, H.; Li, Y.; Jin, Z.; Shu, Y.; Poplawski, S. E.; Wu, Y.; Sanford, D. G.; Sudmeier, J. L.; Bachovchin, W. W. *J. Med. Chem.* **2011**, *54*, 4365. c) Ban, Y. S.; Nakamura, H. *Chem. Rec.* **2015**, *15*, 616.

⁸² a) Barth, R. F.; Vicente, M. G. H.; Harling, O. K.; Kiger W. S.; Riley, K. J.; Binns, P. J.; Wagner, F. M.; Suzuki, M.; Aihara, T.; Kato, I.; Kawabata, S. *Radiat. Oncol. J.* **2012**, *7*, 146. b) Yang, W.; Mi, P.; Barth, R. F. *Cancer Commun.* **2018**, *38*:35.

Boronic acids and esters have become a very interesting tool due to their easy interconversion, versatility, and their moderate moisture, air, and reaction conditions stability.⁸³ These properties, along with their low toxicity are the reason why these moieties are inserted in different commercial pharmaceutical drugs existing nowadays (Figure 4).

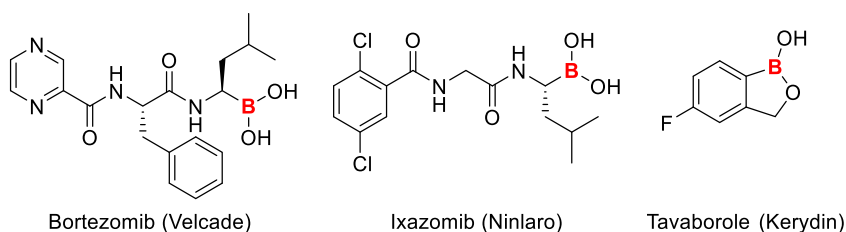


Figure 4. Commercial pharmaceutical drugs including borylated groups in their structure.

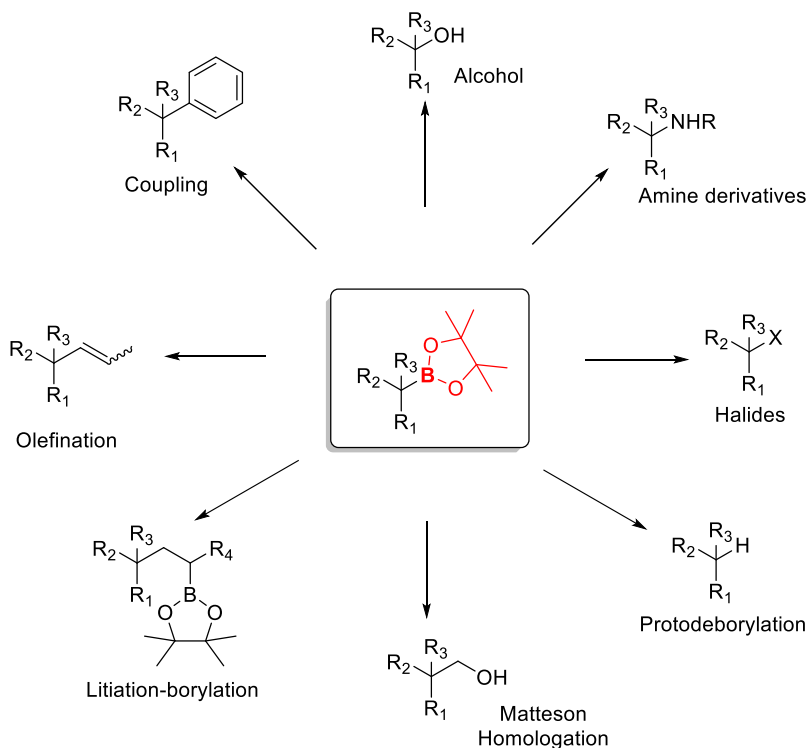
The easy transformation of the carbon-boron bond into a wide range of different carbon-carbon or carbon-heteroatom bonds makes these groups versatile precursors to have in many molecules.⁸⁴ A plethora of well-known reactions can be applied to transform this bond, such as cross-coupling,⁸⁵ or homologation reactions (Scheme 15).⁸⁶

⁸³ a) Matteson, D. S. *J. Organomet. Chem.* **1999**, *581*, 51. b) Scott H. K.; Aggarwal, V. K. *Chem. Eur. J.* **2011**, *17*, 13124. c) Chinnusamy, T.; Feeney, K.; Watson, C. G.; Leonori, D.; Aggarwal, V. K. *Comprehensive Organic Synthesis*, ed. G. A. Molander and P. Knochel, Elsevier, Oxford, 2nd edn, 2014, vol. 7, pp. 692–718. d) Lennox, A. J. J.; Lloyd-Jones, G. C. *Chem. Soc. Rev.* **2014**, *43*, 412. e) Meng, F.; McGrath, K. P.; Hoveyda, A. H. *Nature*, **2014**, *513*, 367. f) António, J. P. M.; Russo, R.; Carvalho, C. P.; Cal, P. M. S. D.; Gois, P. M. P. *Chem. Soc. Rev.* **2019**, *48*, 3513. g) Wang, M.; Shi, Z. *Chem. Rev.* **2020**, *120*, 7348.

⁸⁴ a) Brown, H. C.; Singaram, B. *Acc. Chem. Res.* **1988**, *21*, 287. b) Neeve, E. C.; Geier, S. J.; Mkhilaid, I. A. I.; Westcott, S. A.; Marder, T. B. *Chem. Rev.* **2016**, *116*, 9091. c) Cuenca A. B.; Shishido, R.; Ito, H.; Fernández, E. *Chem. Soc. Rev.* **2017**, *46*, 415. d) Sandford, C.; Aggarwal, V. K. *Chem. Commun.* **2017**, *53*, 5481.

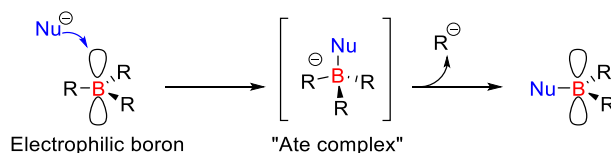
⁸⁵ Kotha, S.; Lahiri, K.; Kashinath, D. *Tetrahedron.* **2002**, *58*, 9633.

⁸⁶ a) Matteson, D. S.; Mah, R. W. H. *J. Am. Chem. Soc.* **1963**, *85*, 2599. b) Matteson, D. S.; Majumdar, D. J. *J. Am. Chem. Soc.* **1980**, *102*, 7588. c) Stymiest, J. L.; Dutheuil, G.; Mahmood, A.; Aggarwal, V. K. *Angew. Chem. Int. Ed.* **2007**, *46*, 7491.



Scheme 15. Boronic esters reactivity.

Normally, the boron atom in boronic acid and ester structures acts as an electrophile. Due to the empty p orbital on the boron in these compounds, the presence of nucleophilic species leads to their addition to the boron.⁸⁷ The final product would be the result of the elimination of one of the substituents of the boron, through an anionic intermediate known as “ate complex” (Scheme 16).

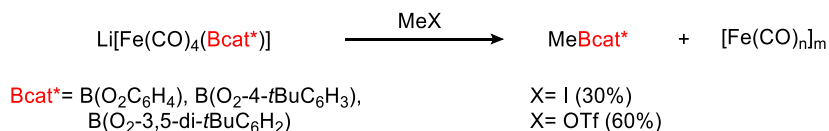


Scheme 16. Boron center as an electrophile.

⁸⁷ Gulyás, H.; Bonet, A.; Pubill-Ulldemolins, C.; Solé, C.; Cid, J.; Fernández, E. *Pure Appl. Chem.* **2012**, *84*, 2219.

Nevertheless, the electronic properties of the boron center in these tricoordinated species can switch from electrophilic to nucleophilic depending on the boron source and conditions. Diboron reagents react with some transition metals, main group metals, or even rare earth metals, to form species that have a strong tendency to react with electrophilic centers of organic molecules.⁸⁸

The first approach to this concept was described by Hartwig and He in 1996, where they got to the synthesis of the first anionic iron complexes including boron species (Scheme 17).⁸⁹ When these complexes reacted with methyl triflate or iodide, they got the substitution of the halide or pseudohalide with the borylated fragment.



Scheme 17. Hartwig's approach to the nucleophilic boronic esters formation.

In addition to Hartwig's input, another two publications very relevant to this chemistry were given by the groups of Hosomi and Miyaura.^{90,91} Hosomi and coworkers described in 2000 the first borylation of α,β -unsaturated ketones with a copper(I) salt and B_2pin_2 as boron source (Scheme 18). In this publication, they also found that the addition of phosphine ligands improved drastically the product

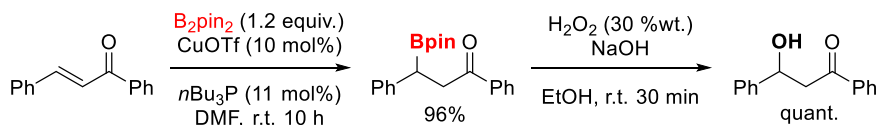
⁸⁸ a) Cid, J.; Gulyás, H.; Carbó, J. J.; Fernández, E. *Chem. Soc. Rev.* **2012**, *41*, 3558. b) Pécharman, A. L.; Colebatch, A. L.; Hill, M. S.; McMullin, C. L.; Mahon, M. F.; Weetman, C. *Nat. Commun.* **2017**, *8*, 15022. c) Pietsch, S.; Neeve, E. C.; Apperley, D. C.; Bertermann, R.; Mo, F.; Qiu, D.; Cheung, M. S.; Dang, L.; Wang, G.; Radius, U.; Lin, Z.; Kleeberg, C.; Marder, T. B. *Chem. Eur. J.* **2015**, *21*, 7082.

⁸⁹ He, X.; Hartwig, J. F. *Organometallics.* **1996**, *15*, 400.

⁹⁰ Ito, H.; Yamanaka, H.; Tateiwa, J.; Hosomi, A. *Tetrahedron Lett.* **2000**, *41*, 6821.

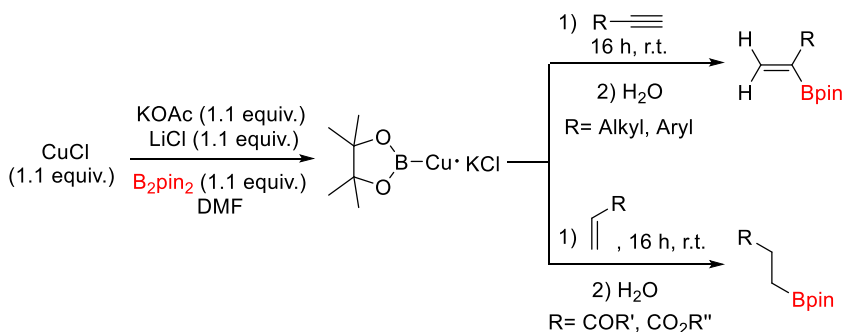
⁹¹ K. Takahashi, T. Isiyama, N. Miyaura. *J. Organomet. Chem.* **2001**, *47*, 625.

yields. The further oxidation of the C-B bond to the corresponding β -hydroxy ketones exemplifies the utility of the boronic ester moiety.



Scheme 18. Hosomi's copper catalyzed borylation of α,β -unsaturated ketones.

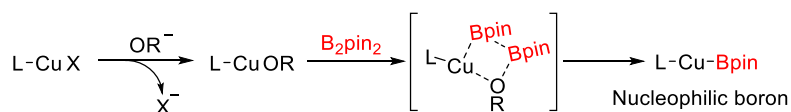
In 2001, Miyaura described the formation of a copper-boryl complex from bis(pinacolato)diboron (B_2pin_2), a copper salt, and a Lewis base, able to act as a nucleophilic boron donor (Scheme 19).



Scheme 19. Miyaura's seminal work in the formation of boryl copper species.

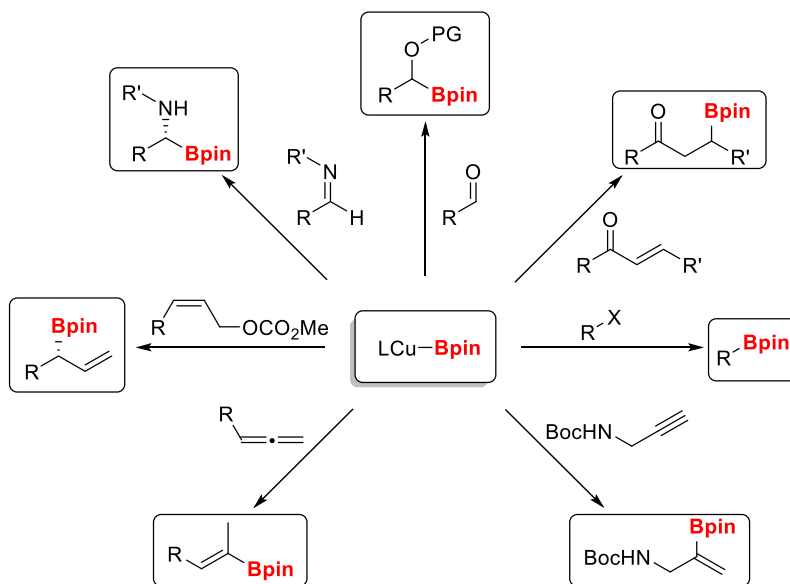
The use of a stoichiometric amount of $CuCl$ in presence of $KOAc$, B_2pin_2 and $LiCl$ was able to afford the regioselective hydroboration of terminal alkynes as well as the conjugate addition of $Bpin$ to Michael acceptors. Thank to these seminal works, Hosomi and Miyaura's became pioneers in the boryl copper chemistry.

The formation of these nucleophilic boron species typically follows the steps depicted in scheme 20, where the copper alkoxide, commonly formed *in situ* by the reaction of free alkoxides with a copper salt, undergoes a σ -bond metathesis reaction with B_2pin_2 to render the boryl copper species.



Scheme 20. Formation of nucleophilic boron species.

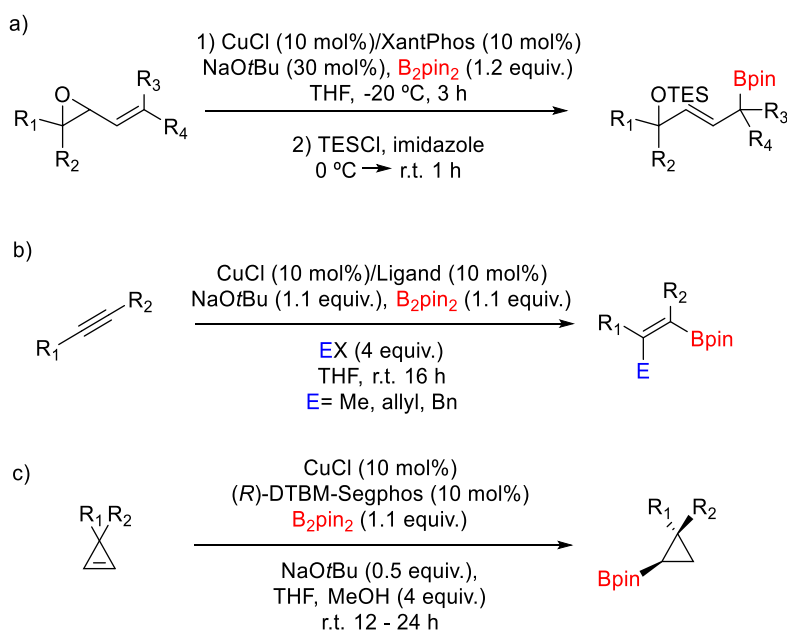
The discovery of these nucleophilic boron species coming from the simple mixture of copper complexes with inexpensive diboronic esters and Lewis bases, led to the development of many borylation reactions (Scheme 21).⁹²



Scheme 21. Copper-boryl complexes in organic synthesis.

⁹² Hemming, D.; Fritzemeier, R.; Westcott, S. A.; Santos, W. L.; Steel, P. G. *Chem. Soc. Rev.* **2018**, *47*, 7477.

In this area, Dr. Tortosa's group have an extensive experience using boryl copper species. They have reported the borylation of several versatile intermediates through unconventional approaches.⁹³ Among their publications we could highlight the diastereoselective borylation of allylic epoxides (Scheme 22a),⁹⁴ the carboboration of alkynes to afford tri and tetrasubstituted alkenes (Scheme 22b),⁹⁵ or the diastereo- and enantioselective synthesis of cyclopropylboronates (Scheme 22c).⁹⁶



Scheme 22. Group's experience in C-B bond formation reactions.

⁹³ Selected articles: a) Jarava-Barrera, C.; Parra, A.; Lopez, A.; Cruz-Acosta, F.; Collado-Sanz, D.; Cárdenas, D. J.; Tortosa, M. *ACS Catal.* **2016**, *6*, 442. b) Guisan-Ceinós, M.; Parra, A.; Martín-Heras, V.; Tortosa, M. *Angew. Chem. Int. Ed.* **2016**, *55*, 6969. c) Lopez, A.; Clark, T. B.; Parra, A.; Tortosa, M. *Org. Lett.* **2017**, *19*, 6272. d) Aménos, L.; Trulli, L.; Novoa, L.; Parra, A.; Tortosa, M. *Angew. Chem. Int. Ed.* **2019**, *58*, 1. e) Novoa, L.; Trulli, L.; Fernández, I.; Parra, A.; Tortosa, M. *Org. Lett.* **2021**, *23*, 7434.

⁹⁴ Tortosa, M. *Angew. Chem. Int. Ed.* **2011**, *50*, 3950.

⁹⁵ Alfaro, R.; Parra, A.; Alemán, J.; García Ruano, J. L.; Tortosa, M. *J. Am. Chem. Soc.* **2012**, *134*, 15165.

⁹⁶ Parra, A.; Aménos, L.; Guisán-Ceinós, M.; López, A.; García Ruano, J. L.; Tortosa, M. *J. Am. Chem. Soc.* **2014**, *136*, 15833.

1.6. Borylation reactions of alkyl and aryl halides

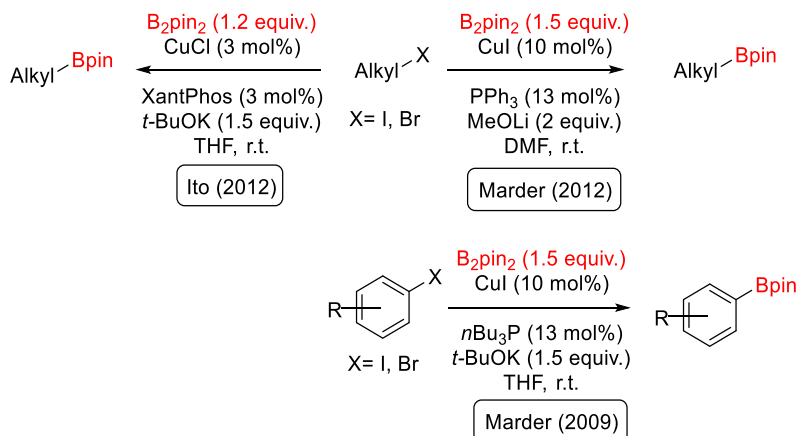
One of the interesting transformations mediated by these copper-boryl complexes is the borylation of halide derivatives. They are important due to their simplicity and the utility of the generated products.⁹⁷ In this aspect, are of special importance the works from Marder and Ito, being the first groups developing the borylation of aliphatic and aromatic halides using an in situ generated copper-boryl complex (Scheme 23).^{98,99}

The importance of these studies resides on the easy access to a vast spectrum of valuable borylated products due to the wide variety of commercially available halogenated organic compounds using inexpensive copper salts.

⁹⁷ Kubota, K.; Iwamoto, H.; Ito, H. *Org. Biomol. Chem.* **2017**, *15*, 285.

⁹⁸ For a selection of papers published by Marder see: a) Kleeberg, C.; Dang, L.; Lin, Z.; Marder, T. B. *Angew. Chem. Int. Ed.* **2009**, *48*, 5350. b) Yang, C. T.; Zhang, Z. Q.; Tajuddin, H.; Wu, C. C.; Liang, J.; Liu, J. H.; Fu, Y.; Czyzewska, M.; Steel, P. G.; Marder, T. B. *Angew. Chem. Int. Ed.* **2012**, *124*, 543. c) Bose, S. K.; Brand, M.; Omoregie, H. O.; Haehnel, M.; Maier, J.; Bringmann, G.; Marder, T. B. *ACS Catal.* **2016**, *6*, 8332. d) Eck, M.; Würtemberger-Pietsch, S.; Eichhorn, A.; Berthel, J. H. J.; Bertermnn, R.; Paul, U. S. D.; Schneider, H.; Friedrich, A.; Kleeberg, C.; Radius, U.; Marder, T. B. *Dalton Trans.* **2017**, *46*, 3661.

⁹⁹ For a selection of papers published by Ito see: a) Kubota, K.; Ito, H. *Org. Lett.* **2012**, *14*, 890. b) Kubota, K.; Yamamoto, E.; Ito, H.; *J. Am. Chem. Soc.* **2013**, *135*, 2635. c) Iwamoto, H.; Kubota, k.; Yamamoto, E.; Ito, H. *Chem. Commun.* **2015**, *51*, 9655. d) Iwamoto, H.; Akiyama, S.; Hayama, K.; Ito, H. *Org. Lett.* **2017**, *19*, 2614.

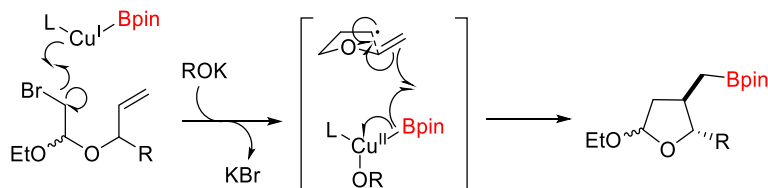


Scheme 23. Initial approaches to the borylation of halides by Ito and Marder.

Due to the interest of pinacol boronic esters, since Marder and Ito developed their methods, many research groups kept studying and improving these processes to get to the borylated products. Apart from the copper catalysts, the use of other metals has been explored, like iron or cobalt.¹⁰⁰

Since the seminal publications by Ito and Marder, the presence of radical intermediates in these reactions has been speculated. These suspicions have been confirmed over the years by several authors, finding mechanisms and methods involving radical species. A clear example of this is the radical borylative cyclization described by Ito, where they generate an alkyl radical using a copper-boryl complex as catalyst (Scheme 24).^{99d}

¹⁰⁰ a) Yang, M.; Yu, J.; Yan, G. *Lett. Org. Chem.* **2012**, *9*, 71. b) Takemoto, Y.; Kamio, S.; Osaka, I.; Takaki, K.; Yoshida, H. *Org. Chem. Front.* **2017**, *4*, 1215. c) Yoshida, T.; Ilies, L.; Nakamura, E. *ACS Catal.* **2017**, *7*, 3199. d) Verma, P. K.; Mandal, S.; Geetharani, K. *ACS Catal.* **2018**, *8*, 4049. e) Verma, P. K.; Prasad, K. S.; Varghese, D.; Geetharani, K. *Org. Lett.* **2020**, *22*, 1431.



Scheme 24. Ito's example of radical borylative cyclization.

In this publication, the authors demonstrated that the generated aliphatic radical reacts intramolecularly with a double bond to finally get to the cyclized borylated product.

In the same way Ito's example shows the ability of these copper-boryl complexes to generate alkyl radicals, many other publications have extended the generation of aliphatic and aromatic radicals through different approaches using copper,¹⁰¹ or alternative metal catalysts.¹⁰²

On the other hand, a methodology that keeps getting attention is the metal free approach to the halide borylation. The growth of this strategy during the last years reflects the importance of green chemistry and the need of adapting the previous methods to get more sustainable synthetic options. In this field, the first works were published by the groups of Ito and Zhang.^{103,104} In the case of Ito's method, it is based on the use of silylboronic esters as boron sources. These reagents in presence of an organic base can give the borylation

¹⁰¹ a) Iwamoto, H.; Endo, K.; Ozawa, Y.; Watanabe, Y.; Kubota, K.; Imamoto, T.; Ito, H. *Angew. Chem. Int. Ed.* **2019**, *131*, 11229. b) Nitelet, A.; Thevenet, D.; Schiavi, B.; Hardouin, C.; Fournier, J.; Tamion, R.; Pannecoucke, X.; Jubault, P.; Poisson, T. *Chem. Eur. J.* **2019**, *25*, 3262.

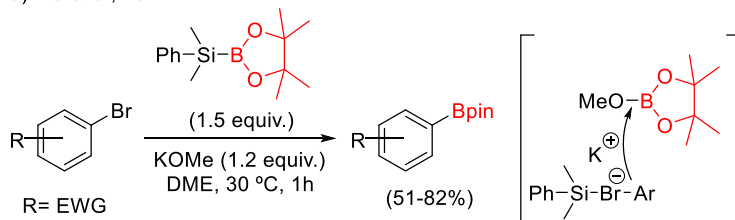
¹⁰² a) Friese, F. W.; Studer, A. *Angew. Chem. Int. Ed.* **2019**, *58*, 9561. b) Friese, F. W.; Studer, A. *Chem. Sci.* **2019**, *10*, 8503.

¹⁰³ Yamamoto, E.; Izumi, K.; Horita, Y.; Ito, H. *J. Am. Chem. Soc.* **2012**, *134*, 19997.

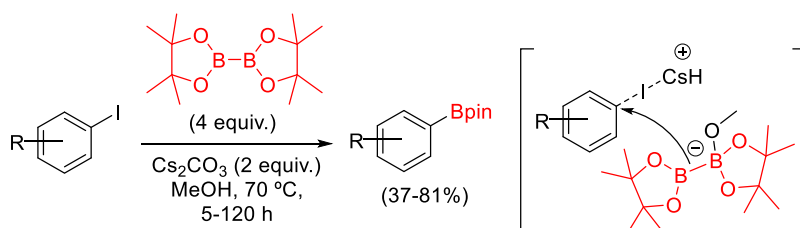
¹⁰⁴ Zhang, J.; Wu, H. H.; Zhang, J. *Eur. J. Org. Chem.* **2013**, *28*, 6263.

of aromatic bromides substituted with electron withdrawing groups (EWG) (Scheme 25a).

a) Ito et al, 2012



b) Zhang et al, 2013



Scheme 25. First metal free approaches described by Ito and Zhang.

Zhang's approach employs B_2pin_2 as boron source and an inorganic base to borylate aromatic iodides with a better functional group tolerance, but under harsher reaction conditions than Ito's method (Scheme 25b). Although the mechanism is unclear, authors proposed a cesium promoted cleavage of the C-I bond followed by the borylation through a boron ate complex.

The metal free borylation of these compounds have become a powerful tool thanks to the many contributions published to this day in this area using either aliphatic or aromatic substrates.^{105,106}

¹⁰⁵ For a selection of articles related to aromatic halide borylation see: a) Chen, K.; Zhang, S.; He, P.; Li, P. *Chem. Sci.* **2016**, *7*, 3676. b) Mfuh, A. M.; Doyle, J. D.; Chhetri, B.; Arman, H. D.; Larionov, O. V. *J. Am. Chem. Soc.* **2016**, *138*, 2985. c) Zhang, L.; Jiao, L. *J. Am. Chem. Soc.* **2017**, *139*, 607. d) Cheng, Y.; Lichtenfeld, C. M.; Studer, A. *Angew. Chem. Int. Ed.* **2018**, *57*, 16832.

¹⁰⁶ For a selection of articles related to aliphatic halide borylation see: a) Zhang, L.; Wu, Z. Q.; Jiao, L. *Angew. Chem. Int. Ed.* **2019**, *58*, 1. b) Liu, Q.; Hong, J.; Sun, B.; Bai, G.; Li, F.; Liu,

1.7. Heterogenous catalyzed borylation of halide derivatives

An underdeveloped strategy compared to the previous, perhaps due to the lack of detailed studies, is the use of heterogenous catalysts for the borylation of halide derivatives.¹⁰⁷ As described above, developing more sustainable processes is a topic of great interest in all chemistry fields. In the case of the halide borylation, in order to decrease the environmental impact of using metal catalysts there are two different strategies nowadays: the transition metal-free methodologies, and the use of heterogenous catalysis. This second strategy clearly reduces the metal traces in the process as well as avoids the use of ligands in most cases. Among all heterogeneous catalysts, the use of carbonaceous materials as supports, and especially those derived from graphene, represents an interesting tool due to the unique electronic properties of these materials.¹⁰⁸

In the context of the borylation of aliphatic halides, the first example in the literature using an heterogenous copper catalyst was described by Chung in 2014 (Scheme 26a).¹⁰⁹ In this publication, authors developed the use of commercial copper nanoparticles to get to the borylation of primary and secondary aliphatic bromides with

G.; Yang, Y.; Mo, F. *Org. Lett.* **2019**, *21*, 6597. c) Mazzarella, D.; Magagnano, G.; Schweitzer-Chaput, B.; Melchiorre, P. *ACS Catal.* **2019**, *9*, 5876.

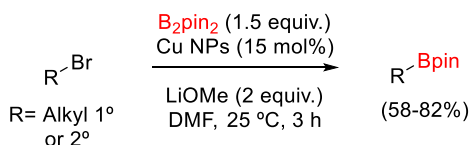
¹⁰⁷ Verma, P. K.; Shegavi, M. L.; Bose, S. K.; Geetharani, K. *Org. Biomol. Chem.* **2018**, *16*, 857.

¹⁰⁸ For a selection of reviews about heterogeneous catalysts based on graphenic surfaces see: a) Blanita, G.; Lazar, M. D. *Micro Nano Syst.* **2013**, *5*, 138. b) Gawande, M. B.; Goswami, A.; Felpin, F. X.; Asefa, T.; Huang, X.; Silva, R.; Zou, X.; Zboril, R.; Varma, R. S. *Chem. Rev.* **2016**, *116*, 3722. c) Deng, D.; Novoselov, K. S.; Fu, Q.; Zheng, N.; Tian, Z.; Bao, X. *Nat. Nanotechnol.* **2016**, *11*, 218. d) Fan, X.; Zhang, G.; Zhang, F. *Chem. Soc. Rev.* **2015**, *44*, 3023. e) Georgakilas, V.; Tiwari, J. N.; Kemp, K. C.; Perman, J. A.; Bourlinos, A. B.; Kim, K. S.; Zboril, R. *Chem. Rev.* **2016**, *116*, 5464. f) Descorme, C.; Gallezot, P.; Geantet, C.; George, C. *Chem Cat Chem.* **2012**, *4*, 1897.

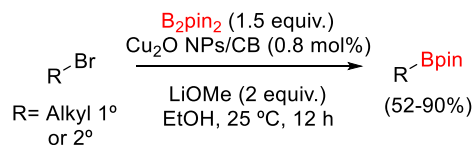
¹⁰⁹ Kim, J. H.; Chung, Y. K. *RSC Adv.* **2014**, *4*, 39755.

moderate to good yields. Although the method presents a reasonable functional group tolerance, the authors could not recycle the catalyst.

a) Chung et al, 2014



b) Xu et al, 2015



Scheme 26. Chung and Xu's works in the heterogeneous copper catalyzed borylation of aliphatic halides.

A year later, Xu and coworkers presented a method using Cu₂O nanoparticles as catalyst supported over a carbonaceous material (Scheme 26b).¹¹⁰ In this work authors employed carbon black (CB) as support, an amorphous material obtained as industrial waste.¹¹¹ This publication involved two main differences regarding the previous: the complete preparation and characterization of the catalyst, and the possibility to recycle it. Nevertheless, even with these improvements, the reaction scope was still limited to primary and secondary aliphatic bromides, and the recyclability of the catalyst did not overcome the third cycle.

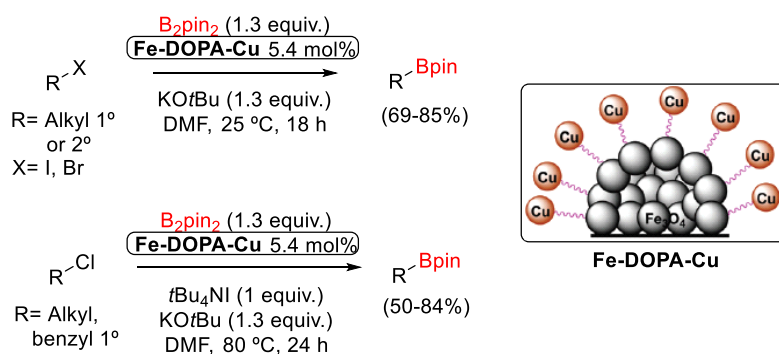
During the course of our investigations in this area, a good contribution in terms of recyclability and substrate scope was reported by the group of Bose in 2020.¹¹² Within their publication, they

¹¹⁰ Zhou, X. F.; Wu, Y. D.; Dai, J. J.; Li, Y. J.; Huang, Y.; Xu, H. J. *RSC Adv.* **2015**, *5*, 46672.

¹¹¹ <https://www.sciencedirect.com/topics/chemistry/carbon-black/>

¹¹² Shegavi, M. L.; Agarwal, A.; Bose, S. K. *Green Chem.* **2020**, *22*, 2799.

developed a Cu(I) catalyst supported over magnetite (Fe_2O_3) able to catalyze the borylation of primary and secondary alkyl iodides and bromides, as well as the borylation of alkyl and benzyl chlorides using $t\text{-Bu}_4\text{NI}$ as additive (Scheme 27). Despite the substrate scope, the utility of this publication relies on the use of magnetite as support of the copper catalyst using a hydrocarbon chain as linker (dopamine-DOPA). This magnetite support makes the catalyst easy to handle due to its magnetic properties and provides the process a great recyclability (up to 10 times).

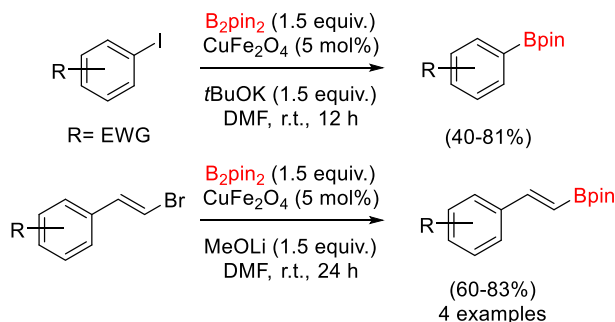


Scheme 27. Bose's approach to alkyl halides borylation using a Cu/ Fe_2O_3 catalyst.

Being the aliphatic halides the most extended substrates for the heterogenous catalyzed borylation, the group of Park published in 2016 the only method to get to the borylation of vinyl and aromatic halides using a heterogeneous catalyst so far (Scheme 28).¹¹³ In this case, they employed non-supported metal nanoparticles as catalyst. Instead, they got to the borylation of β -bromo substituted styrenes and aromatic iodides using copper ferrite nanoparticles (CuFe_2O_4). In this example the reaction scope is quite limited again, finding only

¹¹³ Mohan, B.; Kang, H.; Park, K. H. *Catal. Commun.* **2016**, *85*, 61.

examples of electron withdrawing groups in the aromatic ring. Moreover, no recyclability of the catalysts was reported.



Scheme 28. Park's method for the vinyl and aromatic halides borylation.

Despite their limitations, these methods conformed the development of the halide borylation under heterogenous catalysis conditions. Improving the reaction conditions to afford the borylation of both aromatic and aliphatic substrates could be useful to facilitate the translation of this methodology to industry and flow chemistry.

The following years since the first works described by Chung and Xu, the heterogeneous catalysis using supported and non-supported metal nanoparticles to get different borylated products kept under development.^{114,115} Finding new examples in the literature of heterogenous copper-catalyzed transformations such as Sonogashira cross-coupling,¹¹⁶ hydroboration of carbonyl compounds,¹¹⁷ or alkyne hydroboration.¹¹⁸ Nevertheless, in the halide borylation area the

¹¹⁴ Ohja, N. K.; Zyryanov, G. V.; Majee, A.; Charushiin, V. N.; Chupakhin, O. N.; Santra, S. *Coord. Chem. Rev.* **2017**, *353*, 1.

¹¹⁵ Gawande, M. B.; Goswami, A.; Felpin, F. X.; Asefa, T.; Huang, X.; Silva, R.; Zou, X.; Zboril, R.; Varma, R. S. *Chem. Rev.* **2016**, *116*, 3722.

¹¹⁶ Bing, W. Y.; Wang, X.; Guo, Z.; Jiao, G.; Jin, X. G. *Catal. Commun.* **2017**, *101*, 36.

¹¹⁷ Shegavi, M. L.; Baishya, A.; Geetharani, K.; Bose, S. K. *Org. Chem. Front.* **2018**, *5*, 3520.

¹¹⁸ Tsai, H. Y.; Madasu, M.; Huang, M. H. *Chem. Eur. J.* **2019**, *25*, 1300.

remaining limitation is **the absence of a general methodology that allows the borylation of both aliphatic and aromatic halides.**

Moreover, a better understanding of the catalyst role in the reaction is still lacking. According to the radical mechanism proposed for the halide borylation reactions, the use of graphene supports as ligands in metal catalysis could modify the reaction mechanism.¹¹⁹

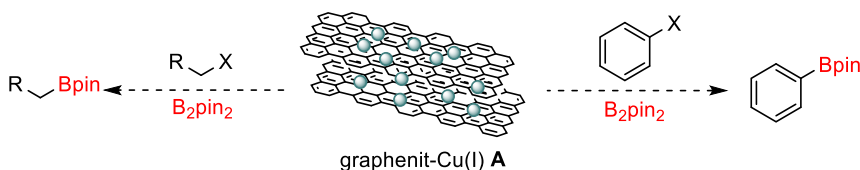
To this end, **a deep study of the possible determinant role of the different supports in the reactivity** would be useful. This study could explain the behavior of the supported nanoparticles, helping the improvement of the existing methods, and even the development of unprecedented methodologies using copper catalysis.

¹¹⁹ Stathi, P.; Gournis, D.; Deligiannakis, Y.; Rudolf, P. *Langmuir*. **2015**, *31*, 10508.

2. Objectives

According to the precedents, the development of new heterogenous catalysts able to borylate both aromatic and aliphatic halides under mild conditions with good recyclability properties would be an excellent scenario to improve the scope of graphenic materials. Also, this could give us a chance of progressing in the knowledge of the role of graphene supports in catalysis. Thus, the objective of the current chapter is to **deeply analyze the catalytic activity of graphene-based Cu(I) materials in borylation reactions**. The different points evaluated, and steps followed to reach this end are depicted below.

- As described in the previous section, one of the main gaps in heterogenous copper catalyzed halide borylation procedures is the absence of a **general method able to borylate both aliphatic and aromatic substrates**. Therefore, our first aim has been testing the catalytic activity of our previously synthesized graphenit-Cu(I) material in both transformations (Scheme 29).



Scheme 29. Borylation of aliphatic and aromatic substrates employing material **A**.

- Moreover, we also consider of interest to prepare **different materials under MW radiation** in order to understand the effect of this preparation method in their structure and catalytic performance of the materials using inexpensive copper salts.

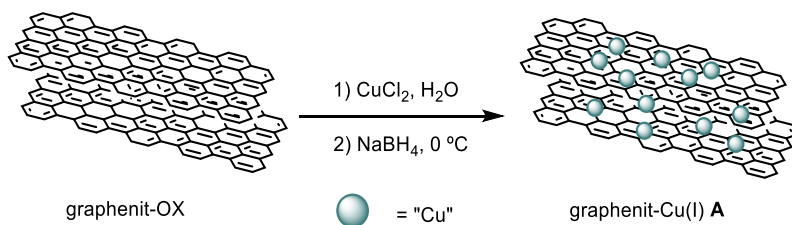
- Through this study we will also take into consideration important aspects such as the **evaluation of the catalytically active species** as well as **recyclability of the materials and their structure** after catalysis.
- To contribute to cover the lack of knowledge about the **role of the graphenic heterogenous support in the catalysis** we consider essential to prepare, under the same reaction conditions, a series of graphene-based copper catalysts and compare their behaviour in the borylation of both aliphatic and aromatic substrates.
 - We will pay special attention to **understand the mechanism** and particularly the role of the support in the catalysis analyzing through a **set of experiments and theoretical calculations** the interactions between support, metal, and reagents.

3. Results and discussion

The present section is divided according to the different stages of the study. First, although the graphenit-Cu(I) material was described in our previous publication, we considered appropriate to explain here its preparation. After this, we are going to discuss the optimization of the borylation of aliphatic substrates, as well as the preparation of microwave irradiated (MWI) materials and the reaction scope. Later, we are going to summarize the optimization and scope of the reaction using aromatic substrates. Finally, we will show the mechanistic study based on theoretical calculations and the evaluation of catalytically active species, followed by the recyclability and the studies comparing materials using different supports.

3.1. Preparation and characterization of material A

Material **A**, as described in the antecedents, was prepared in our research group in collaboration with Nanoinnova technologies and was first tested in the CuAAC reaction.⁷⁸ The material was prepared following the well-known deposition-precipitation method, which is composed by two steps (Scheme 30).



Scheme 30. Graphenit-Cu(I) (**A**) catalyst preparation method.

The first step implies the reaction of the graphenic surface with a metal salt in water. In our case, we employed graphene nanoplatelets as surface, which are stacks of around 15 layers of graphene, and CuCl_2

as metal source. After 24 h of reaction time, NaBH_4 is added to the mixture to afford a material with well dispersed Cu(I) nanoparticles supported on it (Figure 5). A low temperature and slow addition rate of the reductant are crucial to obtain small nanoparticles instead of aggregates.

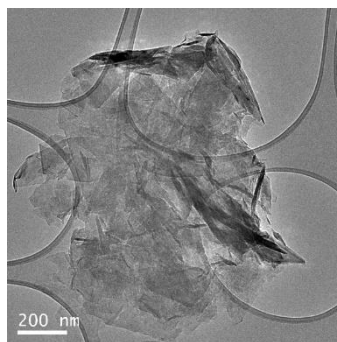


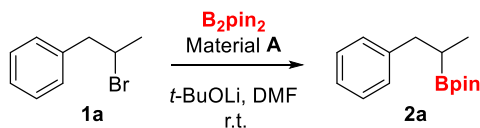
Figure 5. TEM image of material Graphenit-Cu(I) (A).

TXRF (Total Reflection X-Ray Fluorescence) analysis of different batches showed a reproducible synthesis of the material, having a consistent copper amount around 7% anchored on it. Moreover, the XRD (X-Ray Diffraction) experiments also revealed that the Cu species present in the catalyst was exclusively Cu_2O . A deeper study of the material through XPS (X-ray Photoelectron Spectroscopy) showed the presence of chlorine atoms in the material (0.03 wt%), so a very small presence of copper chloride species could not be discarded.

3.2. Optimization of the borylation reaction with material A

In order to perform our wide, deep and systematic study, we first needed to test the catalytic activity of material **A** in the borylation reaction, our target transformation. So, with this robust and reproducible catalytic material in hand, we optimized the borylation conditions using **1a** as model secondary alkyl bromide and bis(pinacolato)diboron (B_2pin_2) as boron source. We chose this substrate at first due to the higher difficulty observed in the borylation of alkyl halides when the substitution of substrates increases.¹¹⁰ We started our study employing typical borylation conditions,^{98b} in presence of 2 equiv. of *t*-BuOLi as base, 2 equiv. of B_2pin_2 as boron source, and 10 mol% of material **A** as catalyst in DMF. Prior to the addition of the bromide to the reagents' mixture, the solution is subjected to US (ultrasounds) during 5 minutes in order to homogenize the heterogenous catalyst suspension. We were delighted to observe full conversion of the starting material **1a** to the desired borylated product **2a** at room temperature after 1 h with no need of using inert atmosphere (Table 1, entry 1).

Attending to this first result, we then moved to lower the catalyst loading of the reaction (entries 2-4). When we added 2 mol% of material **A** the product **2a** could be isolated with a 60% yield after 15 h of reaction (entry 4).

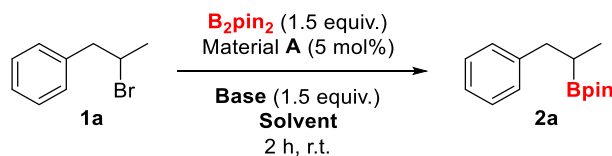
Table 1. First experiments and reagents ratio optimization.

Entry	Catalyst (%)	B_2pin_2 (equiv.)	$t-BuOLi$ (equiv.)	t (h)	Conv ^a (%)
1	10	2	2	1	100
2	5	2	2	2	100
3	2	2	2	4	60
4	2	2	2	15	100(60)
5	10	1.5	2	2	100
6	5	1.5	2	2	100
7	5	1.5	1.5	2	100(90)
8	5	1.2	1.2	2	50
9	1	1.5	1.5	24	0

^aConversions determined by 1H -NMR as starting material disappearance. Results in parenthesis correspond to the yields of the isolated products.

To make the process more efficient we also explored the use of lower amount of boron reagent and base (entries 5-9). In this case, the best balance yield/ratio of reagents and catalyst was using 1.5 equiv. of both the boron reagent and base, and 5 mol% of heterocatalyst. Under these conditions, **2a** could be isolated with a 90% yield (entry 7). Lowering the reagents ratio down to 1.2 equiv. or the catalyst loading to 1% led to poorer results (entries 8 and 9).

Then, we moved to check the influence of the solvent and the base in the reaction (Table 2). As we suspected, among all the different solvents we employed (entries 1-5), the best result in terms of conversion was obtained using DMF (entry 1).

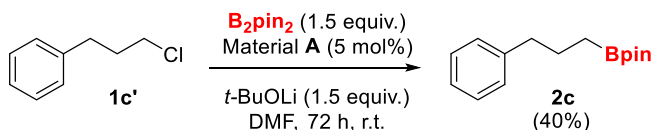
Table 2. Aliphatic bromide: solvent and base optimization.

Entry	Solvent	Base	Conv. ^a (%)
1	DMF	<i>t</i> -BuOLi	100
2	Toluene	<i>t</i> -BuOLi	20
3	THF	<i>t</i> -BuOLi	75
4	CH ₃ CN	<i>t</i> -BuOLi	35
5	EtOH	<i>t</i> -BuOLi	50
6	DMF	<i>t</i> -BuOK	90
7	DMF	<i>t</i> -BuONa	50
8	DMF	MeOLi	50
9	DMF	MeOK	0
10	DMF	MeONa	0

^aConversions determined by ¹H-NMR as starting material disappearance.

In the case of the base screening (entries 6-10), we found again that the most convenient base was the *t*-BuOLi (entry 1), although we observed a similar result when we used *t*-BuOK (entry 6). This was a feasible result as this base has also been commonly employed in copper catalyzed borylation reactions.⁹⁹

The good results obtained in terms of catalytic activity of the material for the aliphatic bromide borylation made us wonder if under the optimized conditions aliphatic chlorides could also work (Scheme 31).

**Scheme 31.** Aliphatic chloride **1c'** borylation.

Using the primary aliphatic chloride **1c'** as model substrate, we found that under the optimized conditions the reaction works with a 40% conversion but needing longer reactions times. Nevertheless, all the attempts to increase this conversion using different organic and inorganic bases, higher catalyst loadings, and higher temperatures led to poorer results (for more details see annex in experimental section).

3.3. Preparation of Graphene-based Cu(I) Catalysts using MWI and analysis of the catalytic activity

Having established that our graphenit-Cu(I) **A** was able to efficiently catalyze the borylation of aliphatic bromides, we then moved to explore new materials using MWI and analyze the catalytic properties of the materials.

As mentioned in the antecedents section, it is known that the interaction between metal and graphene surface can significantly affect the electron transfer properties of the metal and therefore its catalytic activity.⁶⁹ Gupton and coworkers demonstrated that graphenic materials of Pd and Pd-Ni prepared using microwaves irradiation display more strongly anchored metal nanoparticles and lower activation energy in several steps of Suzuki reactions.⁶⁸ This behavior has been explained on the base of the formation of defects on the surface of graphene that favor interaction with the metal, allowing the support to act as both a charge donor and a charge acceptor enhancing the different steps of the catalytic cycle. Due to the lack of reports studying this effect using inexpensive copper salts over sustainable graphitic supports such as nanoplateles, we decided to study the impact of MW irradiation in Cu₂O/graphene based materials. We anticipated that MW irradiation would help to create defects that

could favor the interactions between the Cu_2O nanoparticles and the graphenic surface.

In order to check this hypothesis, in collaboration with Dr. Díaz we studied first the effect of the possible defects in the graphene surface over the Cu_2O nanoparticles from a theoretical point of view. Theoretical calculations based on DFT in periodic boundary conditions (DFT-PBC) showed that the copper atoms of Cu_2O and the graphene layer exchange electronic density, and consequently, the MNPs get more strongly adsorbed on the surface (Figure 6). As can be observed from the comparison between pristine and single defect graphene (Figure 6b and 6d), a single vacancy (SV) induces an increase of the electronic density exchanged. This variation is reflected in the adsorption energy, that increases by 398 kJ mol^{-1} from pristine (Figure 6a and 6b) to SV-graphene (Figure 6c and 6d). Interestingly, these results do not depend on the number of graphene layers considered in the calculation, so the neighboring layers present in the nanoplatelets seem to be not interfering in the copper-graphene interactions.

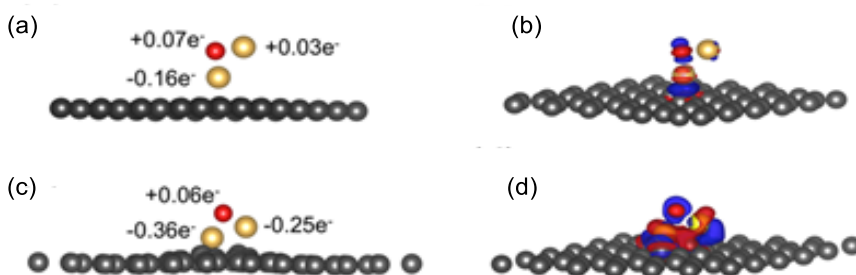


Figure 6. Optimized structure and electronic density redistribution upon adsorption of Cu_2O on pristine graphene (a) & (b), and single-vacancy graphene (c) & (d).

According to the calculations, the presence of defects on the graphene surface could favor the metal-graphene interactions, and

therefore, the microwave assisted catalyst preparation developed by Gupton could lead to new and interesting heterogenous copper materials.

With these premises in hand, we prepared a series of catalysts (**B_{MW}**-**E_{MW}**) using different MW radiation times and different on/off cycles (Table 3). For the sake of clarity, all materials prepared following this method have been identified with the MW subscript. In the table, the MW treatment of the materials is represented by the number of cycles (2 – 12), the duration of each MW pulse (10 – 30 s), and the total radiation time (60 – 120 s).

Table 3. MW catalysts preparation and characterization.

Entry	MW ^a Cycles/t (s) Materials (A-E)	Cu (%) ^b	Crystallite size(nm) ^c Cu (I) / Cu(0)
1	A	6.4	19 / --
2	6 /10 s (60 s) B_{MW}	6.8	4 / 12
3	3 /20 s (60 s) C_{MW}	8.7	4 / 17
4	12/10 s (120s) D_{MW}	7.5	11 / 14
5	2 /30 s (60 s) E_{MW}	6.9	14 / 7
6	3 /20 s (60 s) F_{MW}	0.3	--

^a Number of cycles and time per cycle, total time in brackets.

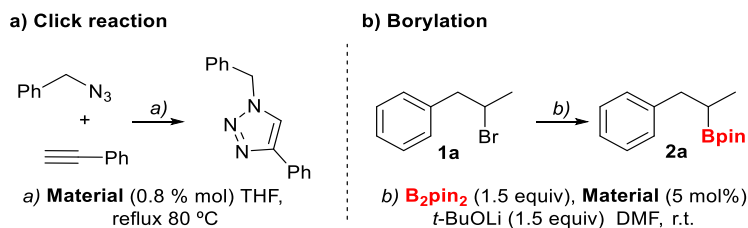
^b Determined by Total reflection X-Ray Fluorescence (TXRF).

^c Estimated from the peak width of the (111) Bragg reflection by using the Scherrer's equation. ^d No NaBH₄ addition.

Materials **B_{MW}**-**E_{MW}** were formed using MW irradiation in different cycles (entries 2-5) following similar conditions to the ones used in the preparation of other materials prepared in the literature.⁶⁸ These brand-new materials were subjected to structural analysis before the

catalytic study. In all the cases the content of copper (determined by TXRF) was around 7-8 %, similar to graphenit-Cu(I) (**A**) prepared using an analogous method in the absence of microwaves (entry 1).⁷⁸ Interestingly, the total reaction time under MW irradiation and the duration of each cycle did not correlate with the final copper amount anchored to the materials (compare entries 2-5). Unlike the copper amount, which was comparable in the MW materials and the model catalyst **A** (6.4 – 8.7 Cu%), the XRD analysis reflects a big difference in the copper species they wear. Material **A** prepared using Cu(II) salts and NaBH₄ in the absence of microwaves only evolves towards Cu(I) (entry 1). However, the combination of both MW and a reductant afforded in all cases mixtures of Cu(I) and Cu(0) (entries 2-5). Additionally, when we employed the same conditions (3 cycles of 20 s MW irradiation) in absence of NaBH₄, the material obtained contained only 0.3% of Cu (entry 6).

To compare the catalytic performance of material **A** and the new materials we chose two different model transformations, the click and borylation reactions, both represented in table 4.

Table 4. Catalytic activity of the graphene-derived materials.

Entry	Mat	Click Reaction (conv.) ^a		Borylation (conv.) ^b 30 min	Cu (%) after borylation / % loss ^c	
		(3 h)	(1 h)			
1	A	100	64	100	5.9	7.8
2	B_{MW}	39	37	61	6.0	11.8
3	C_{MW}	59	37	64	7.0	19.5
4	D_{MW}	46	33	56	7.4	1.3
5	E_{MW}	61	39	61	6.8	1.45

^a Conversion determined by ¹H NMR under conditions (a) **Material** (0.8 % mol) THF, reflux 80 °C, ^b Conversion determined by ¹H-NMR under conditions (b) B₂pin₂ (1.5 equiv.) Graphenit-Cu(I) (5 mol%) t-BuOLi (1.5 equiv.), DMF, r.t. ^c Percentage of Cu loss in recovered materials.

We tested the click reaction using phenyl acetylene and benzyl azide, along with a 0.8 mol% of supported copper catalyst (Table 4a). In the case of material **A** we observed a 64% conversion after 1 h of reaction, and full conversion after 3 h (entry 1). Nevertheless, for the MW materials we observed lower conversions towards the triazole product (compare entry 1 with 2-5). Moreover, the reaction slows down after 1 h, obtaining in some cases almost the same conversion after 3 h (entry 2). We hypothesized that this fact could be a consequence of the Cu(I) and Cu(0) mixture present in the MW materials (as it was determined by XRD). This implies a lower amount of Cu(I) available for the reaction which, according to the literature, is the only copper species catalytically active for this transformation.¹²⁰

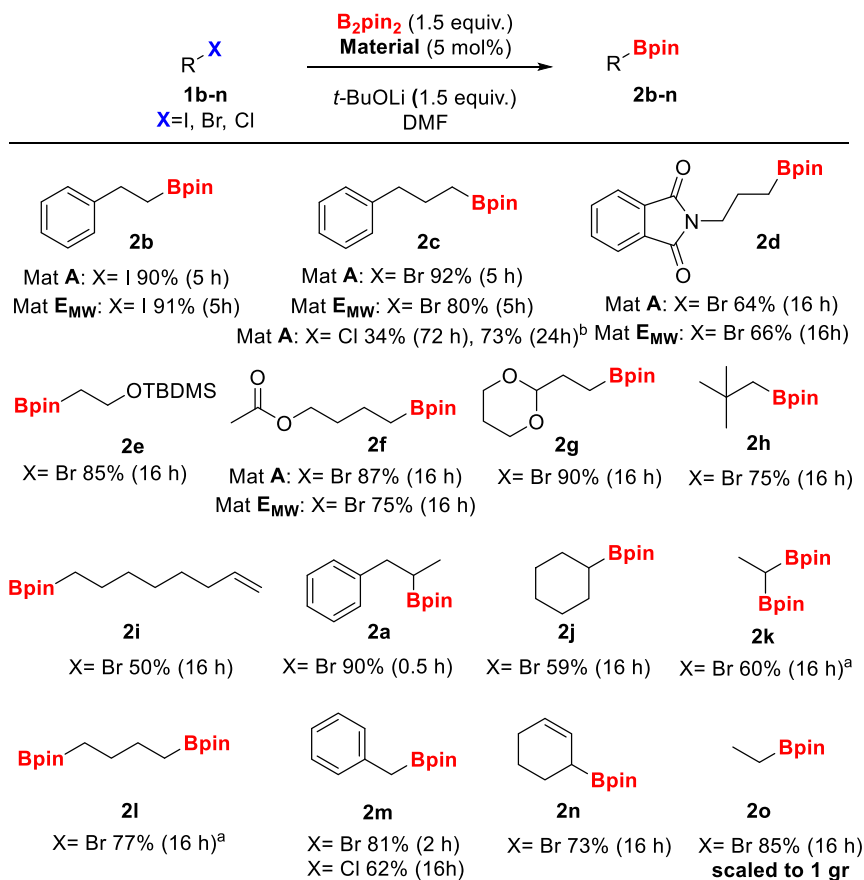
¹²⁰ Liang, L.; Astruc, D. *Coord. Chem. Rev.* **2011**, 255, 2933.

Then, we moved to study the performance of materials **B_{MW}**-**E_{MW}** in the borylation reaction. For that, we used **1a** as model bromide and conditions optimized in table 1. All MW materials were able to catalyze the reaction, although in a less efficient manner than material **A** (Table 4b, entries 2-5). After 30 minutes only around 60 % of conversion was obtained in the case of MW materials. However, complete conversions were obtained after 2 h. Interestingly, when we recovered the materials after the borylation reaction and analyzed their copper content by TXRF, we observed that materials **D_{MW}** and **E_{MW}** lost a very small amount of copper (around 1.4%). This could be explained due to the larger number of MW cycles in material **D_{MW}**, and the longer cycles in material **E_{MW}** (see table 3, entries 4 and 5). Therefore, longer reaction times under microwaves irradiation do not increase the amount of copper but it fixes it in a more efficient way.

According to these results, we decided to choose material **E_{MW}** as the optimal of the MW materials prepared to be analyzed in the rest of our study because of its better catalytic activity and lower copper leaching.

3.4. Scope in the Borylation Reaction of Aliphatic Halides using Graphene-based Cu(I) Catalysts

Once optimized the reaction conditions, we moved to study the scope of the borylation using material **A** as reference catalyst, but also studying the performance of material **E_{MW}** in some examples (Table 5). Through this study, we were delighted to find out that the conditions were also compatible with primary iodides (**2b**) and bromides (**2c**) as substrates. Additionally, the yield of the more challenging chlorides could be improved by the addition of TBAI (see note b).¹¹² For a more detailed aliphatic chloride borylation optimization see experimental part.

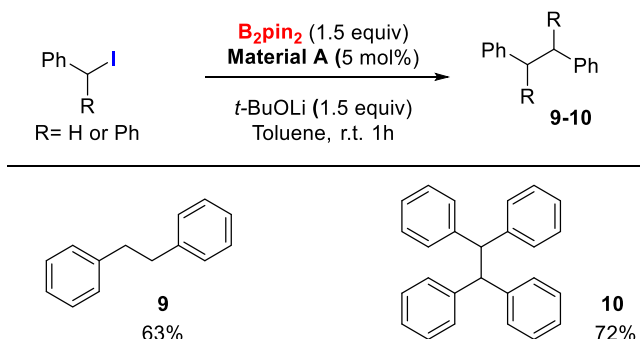
Table 5. Scope of borylation reactions of aliphatic halides.

Reactions were carried out at 25 °C using 5 mol% Material **A**/**E_{MW}**, 1 mL DMF, 0.38 mmol B_2pin_2 , 0.38 mmol $t\text{-BuOLi}$, and 0.25 mmol alkyl bromide unless otherwise stated. Yields showed are those for purified, isolated products. ^a 0.5 mmol B_2pin_2 . ^b TBAI (1 equiv.), 80 °C.

Throughout the scope we could find a remarkable functional group tolerance, with examples bearing phthalimides (**2d**), silylated alcohols (**2e**), esters (**2f**), or ketals (**2g**) in their structure. Also, bulky substrates (**2h**), or even terminal alkenes (**2i**) gave the corresponding borylated products with good yields. Apart from the model substrate (**2a**), we found out that other secondary bromides worked as well (**2j**), and with the addition of a larger excess of B_2pin_2 we could get to bis-borylated products in different positions (**2k**, **2l**). As a proof of the possible utility

of the method in industry, we carried out the borylation of the bromoethane in gram scale, getting a good 85% yield (**2o**). Material **E_{MW}** also provided the borylated products **2b**, **2c**, **2d** and **2f** in similar yields under the same conditions.

Finally, we tested the method with activated halides such as benzylic (**2m**) and allylic (**2n**) bromides, which have been reported to be prone to the homocoupling reaction under copper catalyzed conditions.^{98b} However, under our optimized conditions, we obtained selectively the borylated products with good yields (Table 5). It is important to note, that in the case of these benzylic and dibenzylic substrates, when we switched the solvent from DMF to toluene, the homocoupled products were selectively obtained (Scheme 32).



Scheme 32. Homocoupling reaction of benzylic substrates.

3.5. Optimization and scope of the Borylation Reaction of Aromatic Halides using Graphene-based Cu(I) Catalysts

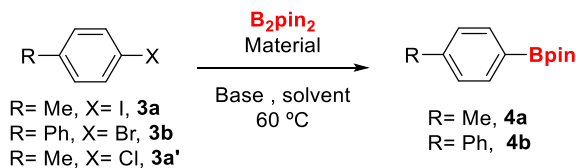
Given the good results obtained in the borylation of aliphatic halides, we moved to study the performance of materials **A** and **E_{MW}** in the borylation of aromatic substrates. We paid special attention to find conditions where our graphene-based Cu(I) materials could catalyze both alkyl and aryl halides. As mentioned in the introduction, there was

no previous report of heterogeneous Cu-catalysts able to promote both transformations.

The optimization process to attain the optimal conditions to afford the borylation of aromatic halides was long and tedious, needing some variations depending on the halide substituent. In order to facilitate the comprehension of the whole process, only the most representative results are shown in this section. Detailed optimization tables for each halide model substrate varying catalyst loading, reagents ratio, solvents and bases are depicted in the experimental section of the chapter.

As shown in table 6, we examined the catalytic activity of materials **A** and **E_{MW}** in the borylation of aromatic iodides, bromides and chlorides. First, we chose *p*-iodotoluene (**3a**) as model substrate to test the borylation, but under the optimized conditions used for alkyl halides, the borylated product **4a** was obtained in low yield, with either catalyst **A** or **E_{MW}** (Table 6, entries 1 and 2). We postulated that the low yield observed was mainly due to the formation of toluene in an amount difficult to quantify due to its volatility. Toluene could be formed through a proto dehalogenation of **3a** or protodeboronation of **4a**. To understand the origin of the formation of toluene, we set up the reaction in the absence of B₂pin₂ and with 15 mol% of catalyst **E_{MW}** (entry 3).

Table 6. Optimization of the borylation conditions using materials **A** and **E_{MW}** as catalysts.



Entry	Halide	mol% Catalyst	Solvent	B ₂ pin ₂ (equiv.)	Base (equiv.)	t (h)	Conv (Yield 6) ^b
1	3a	5 (A)	DMF	2	<i>t</i> -BuOLi (1.5)	16	100 (35)
2	3a	5 (E_{MW})	DMF	2	<i>t</i> -BuOLi (1.5)	16	100 (40)
3	3a	15 (E_{MW})	DMF	-	<i>t</i> -BuOLi (2.5)	16	70 (0)
4	4a	15 (E_{MW})	DMF	2.5	<i>t</i> -BuOLi (1.5)	24	20 (80)
5	3a	15 (E_{MW})	DMF	2.5	-	16	60 (0)
6	3a	15 (E_{MW})	DMF	2.5	<i>t</i> -BuOLi (2.5)	16	100 (38)
7	3a	2.5 (E_{MW})	DMF	2.5	<i>t</i> -BuOLi (1.5)	16	80 (50)
8	3a	2.5 (E_{MW})	THF	2.5	<i>t</i> -BuOLi (1.5)	24	100 (75)
9	3a	2.5 (A)	THF	2.5	<i>t</i> -BuOLi (1.5)	24	100 (75)
10	3a	2.5 (E_{MW}) ^c	THF	2.5	<i>t</i> -BuOLi (1.5)	24	66 (53)
11	3a	2.5 (E_{MW}) ^d	THF	2.5	<i>t</i> -BuOLi (1.5)	24	76 (13)
12	3b	5 (E_{MW})	DMF	2.5	<i>t</i> -BuOLi (1.5)	6	100 (40)
13	3b	5 (E_{MW})	DMA	2.5	<i>t</i> -BuOLi (1.5)	6	100 (50)
14	3b	5 (E_{MW})	DMA	2.5	MeONa (1.5)	6	100 (60)
15	3a'	15 (A) ^e	Tol	2.5	<i>t</i> -BuOLi (2.5)	18	25 (25)

Aryl halide (0.25 mmol). ^aAll the solvents were deoxygenated using the freeze-pump-thaw protocol. ^bDetermined by ¹H-NMR using nitromethane as internal standard. ^c2 equiv. of H₂O were added. ^dReaction performed under air ^eReaction performed at 110 °C using material **A**.

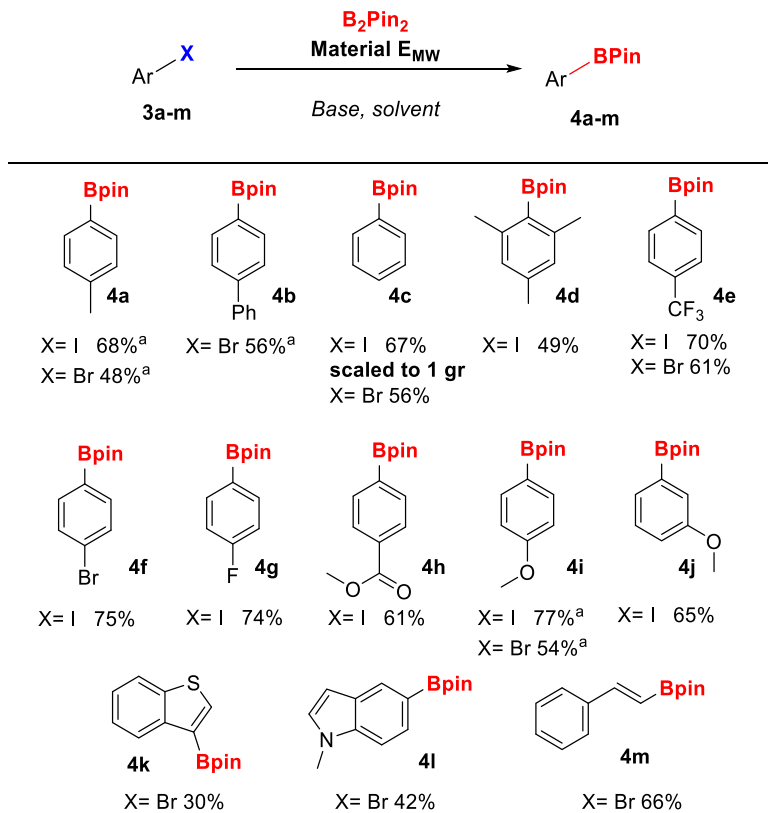
Under these conditions, a significant disappearance of aryl iodide **3a** was observed. Additionally, when borylated product **4a** was heated under the same reaction conditions, only a small

percentage was lost (entry 4). These results suggest that the formation of toluene is due to proto dehalogenation reaction of **3a** under the reaction conditions.

We demonstrated that the reaction did not take place in absence of base (entry 5). Reducing the catalyst loading to 2.5 mol% and the base amount to 1.5 equivalents, a better borylation/dehalogenation ratio was observed (compare entries 6 and 7). Among all the solvents tested, the use of THF (entry 8) instead of DMF significantly improved the yield. With these optimized conditions, catalyst **A** showed similar results than **E_{MW}** (entry 9). Moreover, the reaction seems more sensitive to oxygen than to water (compare entries 10 and 11). The borylation reaction of bromide **3b** did not work under the reaction conditions optimized for the iodide **3a**. In this case, MeONa turned out to be a more efficient base, and the reaction only worked when DMF or DMA were used as solvent (entries 12-14). These amide-based solvents have previously demonstrated a key role in some borylation processes.¹²¹ Finally, we tested the reaction employing a chloride derivative as substrate (**3a'**), which underwent borylation reaction to some extent using material **A** and toluene as solvent (entry 15).

Since materials **A** and **E_{MW}** provided similar results in borylation of aromatic halides, but **E_{MW}** showed lower leaching of Cu than material **A** (Table 4), we decided to study the scope of the aromatic halides using mostly material **E_{MW}** (Table 7). As can be seen in table 7, the reaction tolerates differently substituted arenes, including bulky substrates such as mesitylene derivatives (**4d**), or iodobenzene (**4c**), which was scaled up to 1 gram with no erosion of the yield.

¹²¹ Fawcett, A.; Pradeilles, J.; Wang, Y.; Mutsuga, T.; Myers, E. L.; Aggarwal, V. K. *Science*. **2017**, 357, 283.

Table 7. Aromatic halide borylation substrate scope.

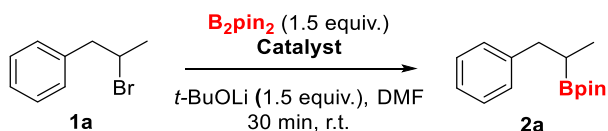
X= I, Conditions B: B₂pin₂ (2.5 equiv.), t-BuOLi (1.5 equiv.), Material E_{MW} (2.5 mol%), THF (1mL), 60 °C, 24 h. X=Br, Conditions C: B₂pin₂ (2.5 equiv.), MeONa (1.5 equiv.), Material E_{MW} (5 mol%), DMA (1 mL), 60 °C, 6 h. ^aReactions performed using material A gave the same results.

The reaction also works in the presence of deactivating functional groups like CF₃ (**4e**) or methyl esters (**4h**), as well as other halides such as bromides (**4f**) or fluorides (**4g**). Aromatic compounds with electron-donating groups are also tolerated (**4i**, **4j**), and even some interesting heteroaromatic compounds like benzothiophenes (**4k**) and indoles (**4l**) showed moderate reactivity. As an extension of the aromatic compounds, we could also borylate olefinic bromides with good yield (**4m**). Selected examples using material **A** as catalyst led to the same yields as material E_{MW} (notes *a*, table 7).

3.6. Study of the Active Catalytic Species in Graphene-based Cu(I) Catalysts after Borylation Reactions

Once demonstrated the potential of these catalysts in the borylation reaction of a plethora of aromatic and aliphatic halides, we focused on understanding the mechanism ruling the reactions. First, in order to get more insight into the catalytically active species in the reaction media and the role of the support, we carried out the model borylation reaction using different Cu species in the presence and in the absence of the support itself (Table 8).

Table 8. Control experiments of the catalytic species in borylation of **1a**.



Entry	Catalyst	Conversion
1	Graphenit-Cu (A)	100
2	-	0
3	Cu ₂ O	0
4	Graphenit	0
5	Cu ₂ O+Graphenit	0
6	CuO	0
7	CuO+Graphenit	0
8	CuCl (2.9%) ^a	57
9	CuCl+Graphenit ^a	51
10	CuCl ₂ (3.5%) ^a	52
11	CuCl ₂ +Graphenit ^a	70

^aAround 100-fold more catalyst than the traces of chloride detected.

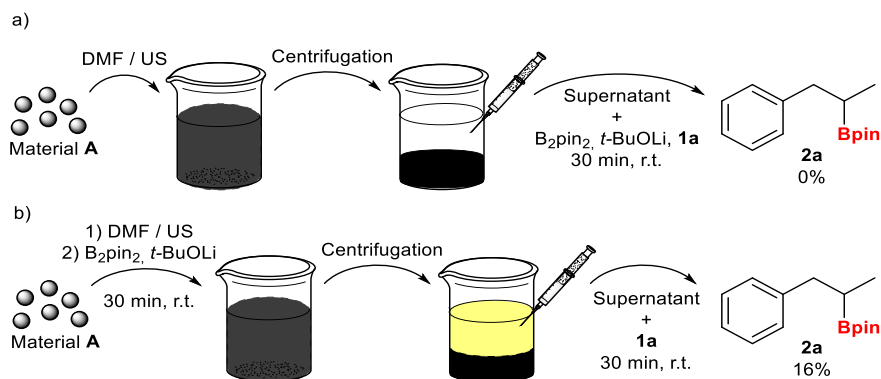
As shown in table 8, we first discarded the existence of background reaction as we obtained no product **2a** when we performed the blank experiment in absence of catalyst (entry 2). According to the characterization of material **A**, the copper species present is almost exclusively Cu₂O (according to XRD diffractogram). So, we carried out

a control experiment adding Cu_2O as the sole catalyst to the borylation reaction of **1a** under the standard conditions (entry 3). The addition of commercial non-supported Cu_2O turned out to be ineffective, obtaining null conversion of the borylated product. To study the possible role of the graphenit surface in the catalysis, we also carried out the reaction just with the addition of graphenit-Ox, as well as the addition of a mixture of both graphenit-Ox and Cu_2O (entries 4 and 5). Again, we observed no evolution from the starting material in both cases, indicating that only the anchorage of the copper nanoparticles over the graphenic surface triggers the catalysis. We also checked that Cu in oxidation state (II) is not active in the reaction with or without graphene (entries 6 and 7).

On the other hand, according to XPS and TXRF analysis, some traces of chlorides (0.03 wt%) are also present in material **A**. This is reasonable, as we prepared the material adding CuCl_2 and then reducing it. In order to discard any input of these species to the catalysis we carried out the same control experiments using CuCl and CuCl_2 (entries 8-11). Is important to note that, due to the impossibility to add such low amount detected in the material, we carried out the reactions with around 100-fold higher catalyst amount than the traces of chloride detected. Under these conditions, all the reactions showed lower conversions towards **2a** compared to the reference reaction (entry 1). Although we cannot rule out a possible catalytic effect of these species in the process, it should be insignificant according to the conversions obtained with much higher catalyst loading.

Finally, we carried out some experiments to study the possible species in solution and ensure that the catalysis comes from the Cu NPs

anchored to the graphene and not from the Cu leaching after the ultrasound (US) treatment or during the reaction (Scheme 33).



Scheme 33. Study of possible catalytic species in solution.

In the first experiment, we kept material **A** in a US bath during 5 min, centrifugated the solution, and then performed the reaction adding the supernatant to the reagents' mixture (Scheme 33a). Under these conditions we got null conversion towards product **2a**.

For the second assay, we pretreated again material **A** in a US bath for 5 min, then we added B_2pin_2 and $t-BuOLi$, and the slurry was stirred for 30 min in DMF. After that, the supernatant was recovered and added to 1 equiv. of **1a**, and we carried out the reaction under standard conditions (Scheme 33b). In this case, a 16% of conversion was determined, meaning that maybe a small fraction of the yield could be attributed to the species in solution.

According to this deep analysis, we could conclude that the catalytic performance of Cu_2O is remarkably higher when is attached to the graphenic surface. Following this study, we also carried out some control experiments with the borylation of aromatic substrates (Table 9).

Table 9. Control experiments of the catalytic species in borylation of aromatic halides.

Entry	Catalyst	3a Conditions B ^a conversion 24 h	3b Conditions C ^a conversion 6 h
1	Graph-Cu (A)	100	100
2	-	2	6
3	Cu ₂ O	4	8
4	Graphenit	6	5

^a X=I; Conditions B: B₂pin₂ (2.5 equiv.), *t*-BuOLi (1.5 equiv.), Material A (2.5 mol%), THF (1 mL), 60 °C, 6 h. X=Br, Conditions C: B₂pin₂ (2.5 equiv.), MeONa (1.5 equiv.), Material A (5 mol%), DMA (1 mL), 60 °C, 6 h.

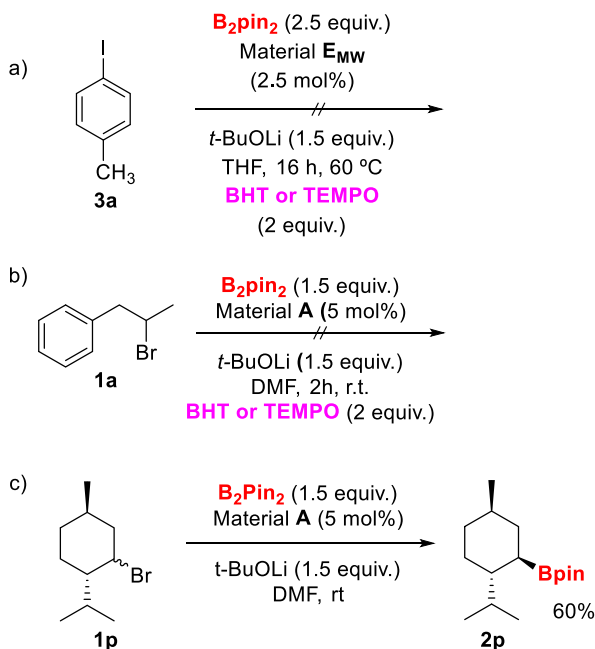
Through these assays we could confirm that material **A** is crucial to the catalysis, finding no reaction in the absence of catalyst (entry 2), and only traces of the borylated products when performing the reactions with Cu₂O and graphenit-Ox separately (entries 3 and 4).

Therefore, these control experiments seem to indicate that the catalysis is mainly due to a synergetic effect of graphenic support with the attached Cu₂O.

3.7. Study of the Borylation Mechanism using Graphene-based Cu(I) Catalysts

After analyzing the role of possible species present in solution during the reaction and confirming that the anchored Cu₂O is the major catalytically active species, we continued our study of the reaction mechanism with additional experiments and theoretical calculations. According to the precedents, a radical mechanism would be expected.^{98b,99a,110,106b}

For that purpose, we designed some mechanistic assays to understand both processes, aromatic and aliphatic borylation (Scheme 34).

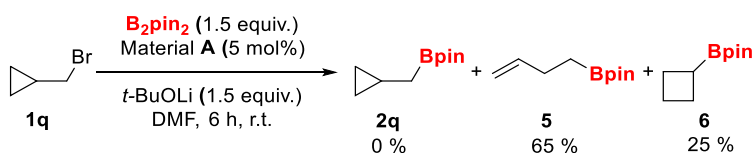


Scheme 34. Additional mechanistic assays of the borylation reaction.

First, we carried out the borylation reaction of the model aryl iodide **3a** in presence of BHT and TEMPO separately (Scheme 34a). These compounds are well-known radical scavengers, which in presence of radical intermediates they quench the reaction by trapping them. As shown in the scheme, when we performed the reactions with these additives, we observed no product formation, indicating that a radical mechanism could be ruling the reaction. In the same way, when we replicated these conditions with the aliphatic bromide **1a** we did not get to the borylated product (Scheme 34b). However, attempts to isolate or identify the intermediates generated did not lead to conclusive results. In order to unravel this unconclusive results, we decided to carry out an additional experiment. Therefore, we

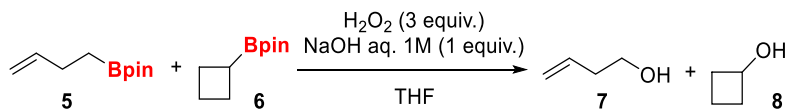
performed the borylation reaction of the brominated menthol derivative **1p** (Scheme 34c). Starting from the diastereomeric mixture, we obtained selectively the diastereomer **2p**. This result reinforces the theory of a radical mechanism since the formation of this isomer can be explained by the formation of a flat radical intermediate and the subsequent entrance of the Bpin moiety from the less hindered face of the molecule.^{99a}

Finally, an interesting result was obtained when we performed the “radical clock” reaction and deserves special attention (Scheme 35).



Scheme 35. Radical clock reaction of (bromomethyl)cyclopropane.

Using the (bromomethyl)cyclopropane **1q** as substrate, we did not observe the product **2q** coming from the direct borylation of the bromide. Instead, we obtained the ring opening product **5** as the major product as expected for a reaction ruled by a radical mechanism.^{99a} Nevertheless, we were surprised by the appearance of new unidentified NMR signals in the reaction crude belonging to another compound apart from **5**. After thorough analysis of the NMR spectra, we hypothesized that these signals could come from the formation of product **6**. This was a very interesting result, because as far as we know, it is unprecedented in the borylation reaction of **1q**. Attempts to isolate the product from the mixture were unsuccessful, so we designed an oxidation experiment of the borylated product mixture to confirm our hypothesis (Scheme 36).



Scheme 36. Oxidation of the borylated products mixture experiment.

Through the derivatization of the borylated products mixture into their corresponding alcohols using H_2O_2 in basic medium, we could successfully detect through NMR the characteristic quintuplet at 4 ppm of the CH attached to the alcohol in compound **8** (for detailed NMR spectra see experimental section). The formation of product **6** could suggest that the methyl cyclopropyl radical generated could be stabilized by the graphene surface time enough to evolve towards a cyclobutyl radical, which is then borylated. At this point, we considered that a theoretical calculation could confirm this hypothesis, enhancing the potential of this kind of material, which could be used in the future for non-available transformations under conventional conditions. To confirm these premises, in collaboration with Dr. Lamsabhi we explored the potential energy surface of the formation of both **5** and **6** products.

The main objective of these calculations was to estimate if the energy obtained from the interaction between graphene, Cu_2O and **1q**, would be enough to get the unexpected product **6**. Effectively, the results of the calculations (based on the ONIOM method) sustained such a hypothesis (Figure 7).

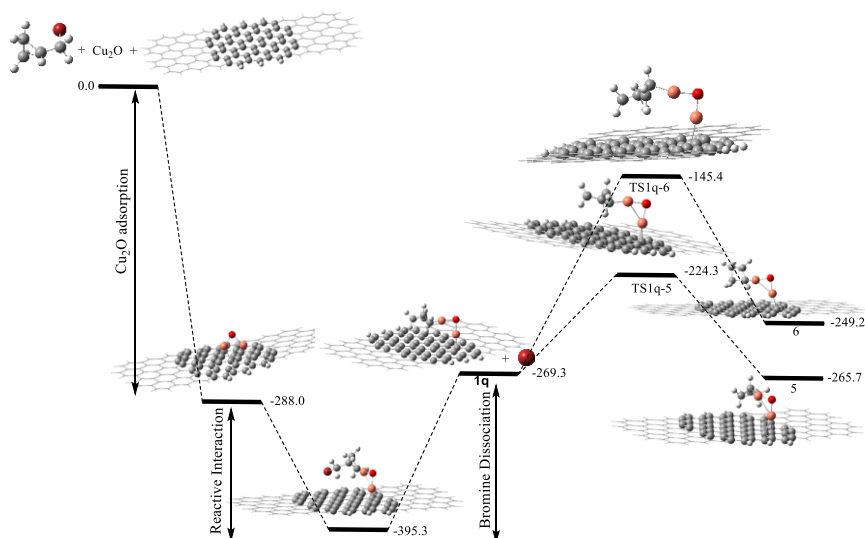


Figure 7. Energy profile of the catalytic process of **1q** to attain **5** and **6** products (values in $\text{kJ}\cdot\text{mol}^{-1}$), obtained by means of the ONIOM method.

In fact, the chemisorption of Cu_2O on graphene reports an energy gain of about $-288 \text{ kJ}\cdot\text{mol}^{-1}$. If we add the interaction of **1q** with this material (about $107 \text{ kJ}\cdot\text{mol}^{-1}$), the energy increases to about $-395.3 \text{ kJ}\cdot\text{mol}^{-1}$. The radical dissociation of bromine is then ensured, and consequently the evolution to the radical precursors of products **5** and **6** through transition states **TS1q-5** and **TS1q-6**. The activation energy required for each product is in line with the yields observed experimentally. In fact, to get the most abundant product **5** the reactant needs to surpass about $45 \text{ kJ}\cdot\text{mol}^{-1}$, whereas to reach product **6** the process requires about three times this activation energy, around $124 \text{ kJ}\cdot\text{mol}^{-1}$ (Figure 7).

We also explored, at the same level of theory, the energy profile for the formation of products **5** and **6** in the absence of graphene (Figure 8).

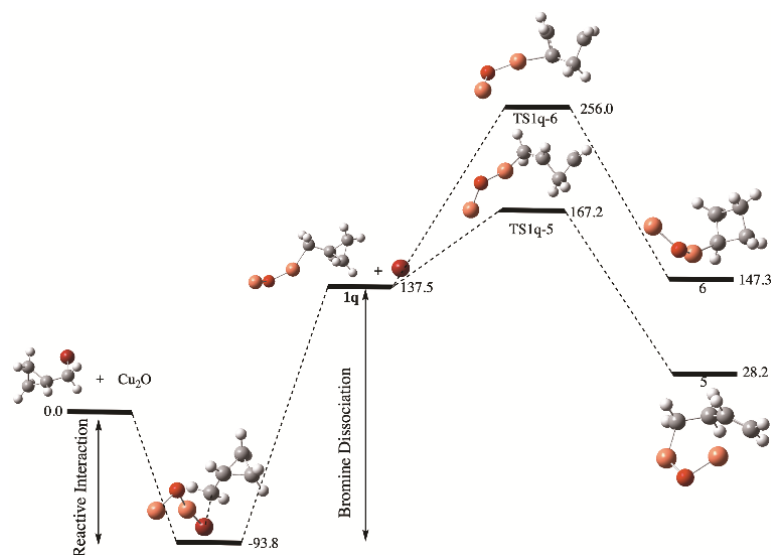


Figure 8. Energy profile, at the B3LYP/6-311+G(d,p) level of theory, of the catalytic process of **1q** to attain the radical precursors of products **5** and **6** by complexation of Cu_2O (values are in kJ mol^{-1}).

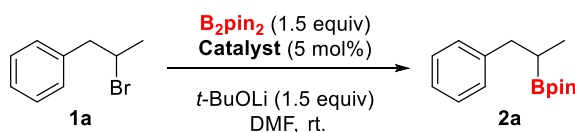
The results pointed out that after the bromine radical departure, the process to attain **5** is exothermic, in agreement with the experimental results. However, the mechanism to get product **6** is revealed to be endothermic, which disfavors the thermodynamic obtention of this compound. We should recall that the activation energy to attain **5** is much smaller than the energy barrier needed to reach **6**. Comparing both pathways presented in figures 7 and 8, the importance of the adsorption of Cu_2O on the graphene derivative as a catalyst for borylation seems to be clear.

These calculations seem to indicate that the mechanism of the reaction in presence of the graphene surface could be different from the homogeneous mechanism described by Marder,^{98a} where the copper first reacts with the diboron and then with the halide. However, a deeper study would be necessary to validate this hypothesis.

3.8. Study of the Recyclability of Graphene-based Cu(I) Catalysts after Borylation Reactions

According to the antecedents depicted in the previous section, one of the main goals of the heterogenous catalysis resides in the capability of these catalysts to be recycled after the reaction. So, after studying the performance and generality of material **A** and **E_{MW}** in the halide borylation reaction, we focused our attention on the study of their recyclability. To this end, we carried out the consecutive borylation of model substrate **1a** employing the same material recovered by filtration after each reaction (Table 10).

Table 10. Recyclability of materials **A** and **E_{MW}** in the borylation reaction.



Cycle	Material A ^a yield (%)	Material E_{MW} ^a yield (%)	Material A ^b yield (%)
1	85	86	90
2	87	87	87
3	90	85	87
4	87	61	86
5	88	37	84
6	84	-	22
7	85	-	-
8	66	-	-

^a Before the addition of the reagents, the mixture of solvent and heterogenous material was kept for 5 minutes in an ultrasound bath. ^b The mixture was kept for 5 minutes under vortex stirring.

As shown in the table, both materials exhibited a good recyclability until the 3rd cycle. After this, the catalytic activity of material **E_{MW}** decreased to a 61% yield in the 4th run, and completely vanished after the 5th cycle. In contrast, material **A** showed a much better performance in terms of recyclability, getting to the product **2a** with no erosion of the yield until the 8th run. Moreover, we also checked if the selected

dispersion method of the material (US in the standard conditions) was comparable with another method such as vortex stirring (Table 10, right column). Applying the same dispersion time (5 min), we observed a remarkable yield drop in the 5th cycle when using vortex, meaning a beneficial effect of the ultrasound to the catalysis. This behavior could be explained by a better exfoliation of the graphene sheets thanks to the ultrasound, exposing the catalytically active Cu(I) nanoparticles supported on them.

The different behavior between both materials could be explained at first by the presence of inactive Cu(0) on material **E_{MW}**, which is absent in material **A**. However, a deeper study of the materials would reveal more details about the reason of such a difference in recyclability. To afford it, we carried out the XPS (x-ray photoelectron spectroscopy) and XRD analysis of the original and recycled materials, which in addition to the previous TXRF experiments gave us a better understanding of the catalysts structure (Table 11).

Table 11. Structural analysis of the materials.

Technique		Material				
		Graphenit	A	Ar	E _{MW}	E _{MW} r
TXRF	wt% Cu	--	6.4	5.9	6.9	6.8
XPS	HR regions wt %					
	C 1s	C (98.6)	C (88.3)	C (93.2)	C (95.5)	C (96.1)
	O 1s	O (1.4)	O (10.4)	O (6.6)	O (4.0)	O (3.6)
	Cu 2p		Cu (1.3)	Cu (0.2)	Cu (0.4)	Cu (0.3)
	Species of Cu (%) Cu(0) and Cu(I) /Cu(II)	-	15.6/ 84.4	28.9/ 71.1	21.0/ 79.0	29.0/ 71.0
XRD	Species of Cu	-	Cu(I)	Cu(I)	Cu(I) and Cu(0)	Cu(I) and Cu(0)

The first difference observed when we compared the composition of the materials in terms of global copper content (detected by TXRF) and superficial copper content (detected by XPS) is that there is much more copper located inside the graphene layered structure than on the external surface of the material. In the case of material **A**, only a 1.3% of the overall 6.4% is on the surface. Moreover, analysis of the recycled material **Ar** shows that after one run the material loses 1.5% overall copper, of which 1.1% departs from the surface. These results suggest that most of the copper present in material **A** is mainly located between the graphitic layers, and is also more strongly anchored, being more resistant to leaching. This result correlates with the fact that ultrasound exfoliation affects positively to the reaction yield (see results in table 10). In contrast, the analysis of material **E_{MW}** and **E_{MW}r** showed a more constant copper content in both overall (6.9 to 6.8) and surface (0.4 to 0.3). These values are in accordance with the proposed stronger anchorage of the Cu NPs in graphenit-Ox obtained by the creation of defects through microwave irradiation.

There is also a clear difference in the oxidation state of Cu detected by XRD and XPS on the surface. In the case of materials **A** and **Ar**, only Cu₂O species are detected by XRD, whereas this technique detects Cu₂O and Cu(0) species for materials **E_{MW}** and **E_{MW}r**. However, Cu(II) is also detected in all cases but exclusively on the surface (using XPS). This result is reasonable due to the higher tendency to oxidation of the Cu(I) in the external layer, due to the exposure to oxygen. Presumably, the reason why this Cu(II) is not detected by XRD is the small size of these particles, which is lower than the detection limit of the apparatus. Therefore, anchoring of the copper between internal layers would prevent oxidation and would explain the necessity for a previous

exfoliation treatment of the heterogeneous materials, so that they are effective as catalysts.

In addition, we studied the morphology of the materials through their TEM (transmission electron microscopy) images (Figure 9). In the case of material **A**, we observed very well dispersed small particles of 2 nm average diameter (light grey in figure 9), which suffer some aggregation after the reaction in material **Ar** as observed in the zoomed image (dark grey in figure 9). On the other hand, material **E_{MW}** shows much more aggregation and low dispersity in the starting material, which aggravates after catalysis. For additional TEM images see experimental part.

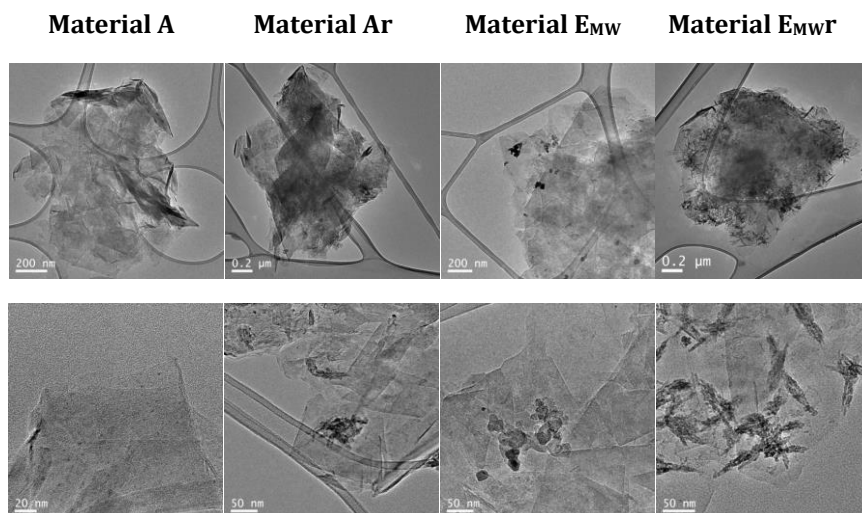
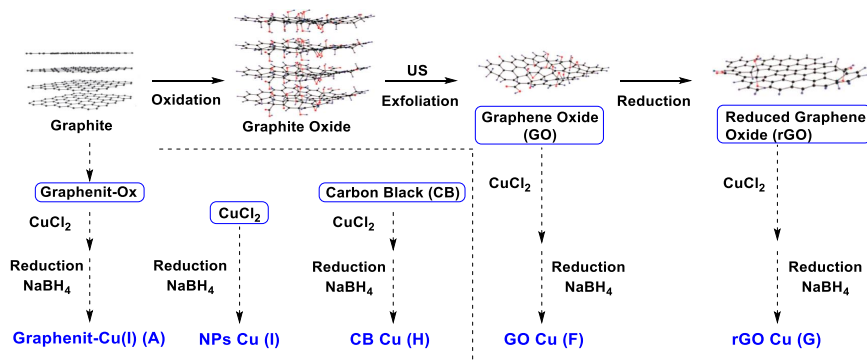


Figure 9. TEM images of the materials.

3.9. Study the effect of the graphenic surface on the catalytic performance of the materials.

Finally, we decided to further study the effect of the graphenic surface nature on the catalytic performance of the materials. To that end, we prepared a series of catalysts starting from different

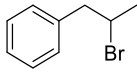
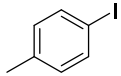
commonly employed graphene derivatives using the same preparation conditions as material **A** (Scheme 37).



Scheme 37. Preparation of Cu(I)-materials employing different graphenic supports.

Within this study, we utilized materials such as GO (**F**), rGO (**G**), Carbon Black (**H**), and unsupported copper nanoparticles (**I**), and we performed the model alkyl and aryl halide borylations to test their efficiency (Table 12). In the case of aromatic substrates, we employed also shorter reaction times along with the standard 24 h.

Table 12. Comparison of copper catalysts with different graphenic supports.

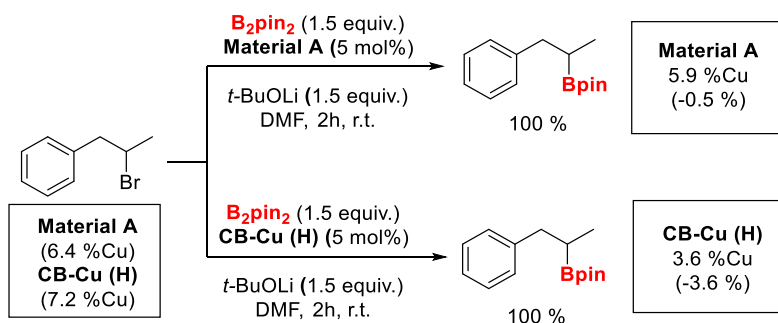
		$\text{R-X} \xrightarrow[\text{Base, solvent}]{\text{B}_2\text{Pin}_2 \text{ Material}} \text{R-BPin}$		
		R= Aliphatic 1a	Conditions A	2a
		R= Aromatic 3a	Conditions B	4a
Entry	Material			
		1a^a	3a^a	
		Conversion	Conversion	
		0.5 h	24 h	8h
1	A	100	100	75
2	GO (F)	10	72	n.d.
3	rGO (G)	80	100	31
4	CB (H)	100	100	30
5	NPs (I)	0	73	n.d.
6	EMW	61	100	72

^a Conversion determined by ¹H NMR. Conditions A: **1a**, Catalyst (5 mol%), B₂pin₂ (1.5 equiv.), t-BuOLi (1.5 equiv.), DMF (1 mL), r.t., 0.5h. Conditions B: **3a** B₂pin₂ (2.5 equiv.), t-BuOLi (1.5 equiv.), catalyst (2.5 mol%), THF (1 mL), 60 °C, 24h.

As might be expected, the support nature of the catalysts has a great impact on the reaction, observing big differences between the supports employed. In the case of the graphene oxide catalyst (**F**), a material with much higher oxygen content and functional groups than the graphene nanoplatelets employed in material **A**, we observed a clear decrease in the alkyl and aryl halide borylation yields (entry 2). On the other hand, when we tested the reaction using reduced graphene oxide as support (**G**), we got to a slightly lower yield in the alkyl borylation and full conversion of the halide in the aromatic substitution (entry 3). The reaction yield at intermediate times (8 hours) revealed a worse performance than material **A**. The same behavior observed with the rGO catalyst was also observed when we used carbon black (**H**), obtaining very good results in both borylation reactions, only inferior

to material **A** at partial times of the aryl iodide borylation (entry 4). This amorphous material comes from industrial waste and relates to the rGO and material **A** in terms of oxygen content present on its structure. These results could suggest that the lower oxygen content in the material's structure the better catalytic performance in the borylation reaction. Material **I** on the other hand was prepared following the same preparation method parting from CuCl_2 but in absence of support, getting to copper nanoparticles of CuO and CuO_2 . This material exemplified the need of copper oxide to be attached to graphene to be active in the borylation reaction of alkyl bromide **1a**, leading to no product formation (entry 5). Surprisingly, this non-supported copper catalyst afforded **3a** with a remarkable 73% conversion.

Due to the similar catalytic efficiency exhibited by materials **A** and **H**, we analysed them in terms of stability and recyclability, measuring the copper content in both materials after one run of the reaction (Scheme 38).



Scheme 38. Recyclability comparison between material **A** and material **H**.

As can be seen, carbon black (**H**) loses half of the copper content (only a 3,6% of copper remains in the material) whereas material **A** is recovered with a 5,9% of Cu. Therefore, a clear superiority of material

A has been determined compared to material **H** probably due to a weaker metal-support interaction in the case of the carbon black.

3.10. Additional insights into the graphenic support role as macromolecular ligand

As we have been able to demonstrate through all these studies, the catalytic performance of Cu_2O drastically increases when attached to the graphenic surface. Thus, we considered interesting to study theoretically this apparent synergistic effect between metal and support to disclose the changes exerted by the graphene to the Cu_2O that enhances its catalytic performance in this reaction.

For this purpose, we analyzed the energy profiles and the electronic population of Cu_2O free and anchored on graphene in their interaction with alkyl halide **1q** (Figure 10).

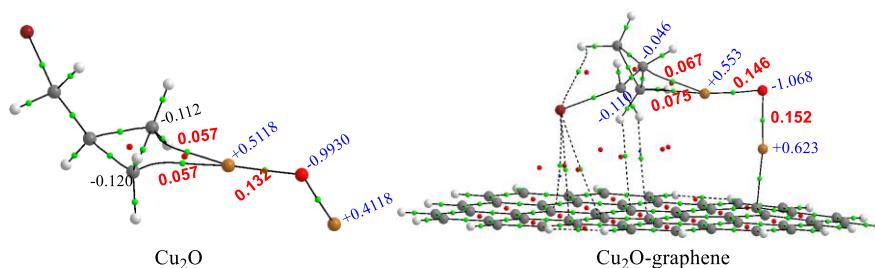


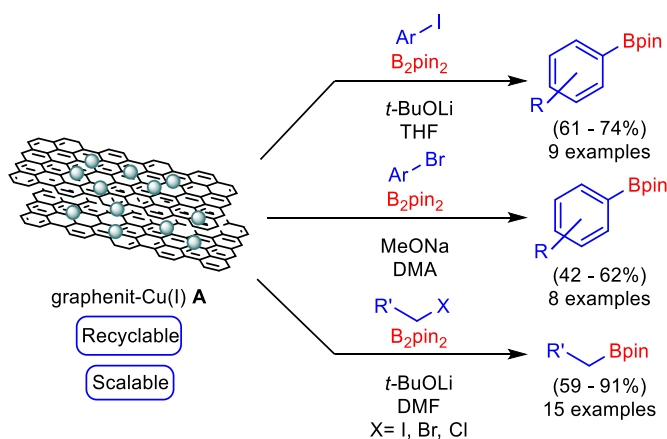
Figure 10. Molecular graphs of the complexes of Cu_2O and $\text{Cu}_2\text{O-graphene}$ with (bromomethyl)cyclopropane (**1q**). Green dots are the bond critical points, and the red dots are the ring critical points. The red values are the electronic density in a.u. and the blue values are the atomic charges

The analysis of the electronic density in the bond critical points (bcp) of the metal with halide **1q** clearly show a difference between Cu_2O supported on graphene, and isolated copper oxide. In fact, the QTAIM population analysis of the complexes resulting from the interaction of Cu_2O and $\text{Cu}_2\text{O-graphene}$ with (bromomethyl)cyclopropane (**1q**) stand out the differences in the electronic density

estimated for the most important bcps (Figure 7). The electrostatic binding of the metal in free Cu_2O , the bcp depicted between the metal and cyclopropane presents a lower charge density (about 0.05 a.u) than in Cu_2O -graphene (0.070 a.u.). This means that the metal presents a weaker affinity to the halide in **1q** when it is free than when it is supported on graphene. The role played by the support, acting indeed as a macromolecular ligand, is then crucial in the borylation process since it increases the interaction capability of the metal and so the catalytic efficiency of the whole material.

4. Conclusions

In conclusion, we have found that the graphenit-Cu(I) material (**A**), prepared from cheap and sustainable nanoplatelets and Cu(II) salts, is **able to catalyze the borylation reaction of both aliphatic and aromatic halides** in good to moderate yields (Scheme 39). The material is not only a general and efficient catalyst, but it is also easily recyclable, and the reactions are scalable.

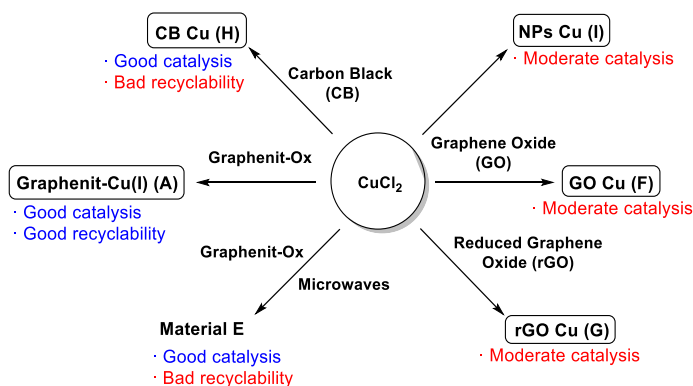


Scheme 39. Catalytic performance of material **A**.

Encouraged by the works by Gupton and El-Shall groups, we prepared a series of novel heterogeneous copper catalysts under MW irradiation. Through materials characterization and computational studies, we observed that the use of **microwaves provided strongly supported metal nanoparticles**. However, these materials exhibited lower generality and recyclability towards the borylation reaction, presumably due to inactive Cu(0) and the formation of aggregates.

As a continuation of the **graphenic support comparative study**, we also prepared different materials using other classical graphenic supports (GO, rGO, Carbon Black), as well as unsupported Cu(I) nanoparticles (NPs). Although with a variable behavior, all of them

provided poorer results in terms of efficiency and/or recyclability than material A (Scheme 40).



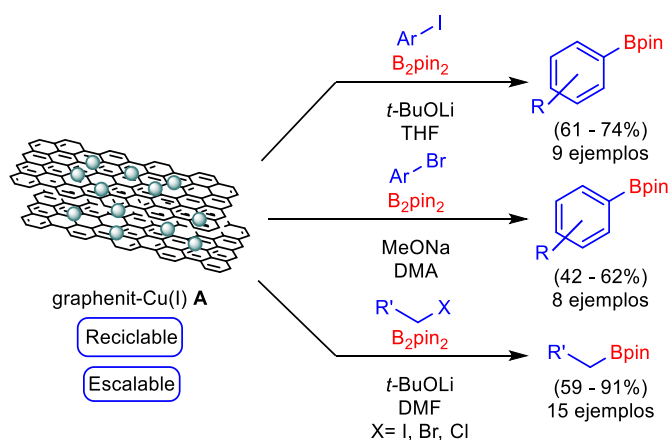
Scheme 40. Prepared materials for the comparative studies.

A detailed study of all the possible catalytic species revealed an interesting **synergetic performance of Cu_2O when anchored to a graphenic support**, which was corroborated by calculations at a high level of theory. The presence of graphene reinforces the electrostatic interaction between copper oxide and halide derivatives which enables a radical departure of the halogen. The exploration of the potential energy surface of (bromomethyl)cyclopropane transformation with free and supported Cu_2O exemplifies the catalytic effect triggered by the presence of the graphene derivative. The surface promotes the electronic exchange between the species under study, stabilizing radical intermediates and favoring processes not described for typical Cu(I) homogeneous catalysis.

This means that the metal presents a weaker affinity to the halide when it is free than when it is supported on graphene. Understanding the modulation of cheap, accessible, and sustainable salts such as Cu_2O by graphenic supports is a valuable strategy to study other transformations that are not viable under conventional conditions or require the presence of expensive noble metals and/or ligands.

4. Conclusiones

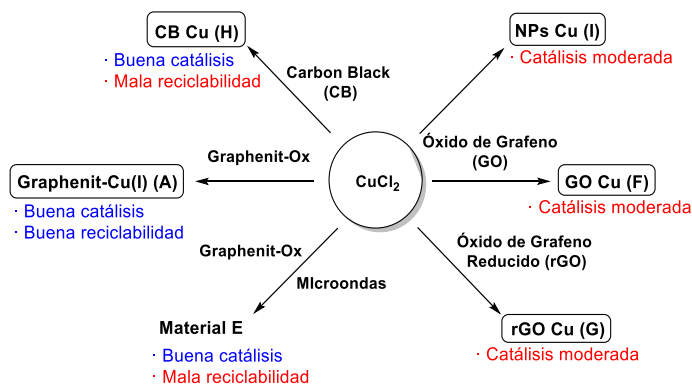
En conclusión, hemos encontrado que el material graphenit-Cu(I) (A), preparado a partir de nanoplaquetas de grafeno baratas y sostenibles, es **capaz de catalizar la borilación de haluros alifáticos y aromáticos** en rendimientos de moderados a buenos (esquema 39). El material no solo es un catalizador general y eficiente, sino que es también reciclable, y las reacciones son escalables.



Esquema 39. Eficiencia del material A como catalizador.

Inspirados por los trabajos de los grupos de Gupton y El Shall, preparamos una serie de novedosos catalizadores heterogéneos de cobre utilizando radiación microondas. A través de la caracterización de los materiales y de estudios computacionales, observamos que **el uso de microondas proporcionaba nanopartículas metálicas fuertemente ancladas**. Sin embargo, estos materiales exhibieron menor generalidad y reciclabilidad en la reacción de borilación, presumiblemente debido a que poseían Cu(0) inactivo y agregados. Continuando con el **estudio comparativo de soportes gráfenicos**, también preparamos diferentes materiales usando otros soportes clásicamente utilizados (GO, rGO, Carbon Black), así como

nanopartículas de Cu(I) sin soportar (NPs). Aunque con un comportamiento variable, todos dieron peores resultados que el material **A** en términos de eficiencia y/o reciclabilidad (esquema 40).



Esquema 40. Materiales preparados para el estudio comparativo.

Un estudio detallado de todas las posibles especies catalíticas reveló un interesante **efecto sinérgico entre las partículas de Cu_2O y el soporte grafénico**, el cual fue corroborado mediante cálculos DFT. La presencia de grafeno refuerza las interacciones electrostáticas entre el óxido de cobre y los derivados halogenados que produce la salida radicalaria del halógeno. El estudio de la superficie de energía potencial de la reacción del (bromoetil)ciclopropano con Cu_2O libre y anclado ejemplifica el efecto sobre la catálisis de la presencia del derivado de grafeno. La superficie promueve el intercambio electrónico entre las especies bajo estudio, estabilizando los radicales intermedios y favoreciendo procesos no descritos en catálisis de Cu(I) homogénea. Esto significa que el metal presenta una menor afinidad por el haluro cuando está libre que cuando está soportado. Conocer la modulación de sales baratas y sostenibles como el Cu_2O por los soportes grafénicos es una estrategia valiosa para estudiar otras transformaciones no accesibles mediante condiciones convencionales, o que requieren el uso de metales nobles y/o ligandos caros.

Part I. Chapter 1. Experimental Section

General methods and materials

Nuclear Magnetic Resonance (NMR)

NMR spectra were acquired using CDCl_3 as solvent, running at 300 and 75 MHz for ^1H and ^{13}C , respectively. Chemical shifts (δ) are reported in ppm relative to residual solvent signals (CDCl_3 , 7.26 ppm for ^1H NMR, and 77.0 ppm for ^{13}C NMR). In all ^1H NMR spectra, multiplicity is indicated as follows: bs (broad singlet), s (singlet), d (doublet), t (triplet), q (quartet) or m (multiplet). Coupling constant values (in Hertz) and number of protons for each signal are also indicated.

Mass spectrometry

Mass spectra (MS) were obtained in a *VG AutoSpec Spectrometer* in positive electrospray ionisation (ESI) or electron impact ionisation (EI). Obtained data are expressed in mass/charge (m/z) units.

Chromatography

For thin layer chromatography (TLC) was performed using pre-coated aluminium backed plates (Merck Kieselgel 60 F254) and visualized by ultraviolet irradiation (254 nm) by treatment with a solution of KMnO_4 (1.5 g), K_2CO_3 (10 g), and 10% NaOH (1.25 mL) in H_2O (200 mL) or a solution of phosphomolybdic acid (12 g), in EtOH (250 mL) followed by heating. Flash column chromatography (FCC) was performed using Merck pore 60 Å, 40-63 μm silica gel and compressed air.

Analysis of the materials

TXRF analysis were carried out in a Bruker TXRF S2 PicoFox spectrometer. SEM images were acquired in a Hitachi Tabletop Microscope TM-1000-151. For XPS analysis a XPS Spectrometer Kratos

AXIS Supra apparatus was used. The copper amount added to each experiment was calculated based on the %wt Cu determined through TXRF for each material. A 200 KV JEOL 2100 transmission electron microscope was employed for the TEM analysis. Samples were prepared by adding a drop of each material dispersion in ethanol on a lacey carbon-coated copper grid 200 Mesh and then let to dry.

Miscellaneous

Cyclohexane and EtOAc were supplied by *Carlo Erba* and were used without previous purification. THF, DMF and DMA were purchased dry and with no stabilizers in *Acros Organics*. All reagents were acquired from commercial sources and were used without further purification. For all described synthesized products, spectroscopic data are consistent with the references indicated next to the name of each compound. For separation of materials, we used a mini centrifuge LBX MC7000 working at 7000 rpm.

Graphenit-OX, graphene oxide (GO, synthesized using a modified Hummers' method),²⁶ reduced graphene oxide (rGO, prepared from GO and reduced using hydrazine in basic media), and Carbon Black were supplied by NanoInnova Technologies SL. For the synthesis of the microwave irradiated materials, we used an *Orbegozo MI-2014 conventional microwave at approximately 560 W* (measured by heating 1 L of D.I. water at full power and measuring the temperature difference before and after the radiation).

Part A. Preparation and characterization of the materials

A.1. Preparation of the materials

Preparation of material A

A suspension of graphenit-Ox (1.75 g) in deionized H₂O (175 mL) was sonicated for 1 h. Then, CuCl₂ (381 mg, 2.83 mmol) was added, and the mixture was vigorously stirred at room temperature for 16 h. After that, the mixture was cooled down to 0 °C and a solution of NaBH₄ (227 mg, 6.00 mmol) in deionized H₂O (175 mL) was added dropwise over 30 min. After stirring at room temperature for 24 h, the material was filtered, washed with deionized water (4 x 50 mL) and acetone (3 x 50 mL), and finally dried under vacuum for 4 h to afford 1.98 g of graphenit-Cu(I).

Preparation of materials B-E_{MW}

To a suspension of graphenit-Ox (500 mg) in deionized H₂O (100 mL), CuCl₂ (100 mg) is added, and the mixture is sonicated for 1 h. Then, the NaBH₄ (65 mg) diluted in 25 mL of D.I. water is added dropwise to the suspension vigorously stirred at 0 °C. Once the addition of the reductant was complete, the flask was placed into a conventional microwave and was irradiated during the corresponding time (see Table 3) at 560 Watts. Passed this time the flask is stirred manually outside the microwave for 40 seconds and the process is repeated the corresponding number of times (see Table 3). Once the microwave cycles are finished and the mixture reaches r.t., the material is filtered, and washed with D.I. water and acetone. Finally, the material is dried in a vacuum tube at 60 °C overnight.

Preparation of material F

Material F was prepared following the standard method described for graphenit-Cu(I) (procedure A) but using GO (500 mg) as starting material, CuCl_2 (109 mg, 0.8 mmol) and NaBH_4 (650 mg, 17.5 mmol) as reducing agent.

Preparation of material G

Material G was prepared following the standard method described for graphenit-Cu(I) (procedure A) but using rGO (500 mg) as starting material, CuCl_2 (109 mg, 0.8 mmol) and NaBH_4 (650 mg, 17.5 mmol) as reducing agent.

Preparation of material H

Material H was prepared following the standard method described for graphenit-Cu(I) (procedure A) but using carbon black (500 mg) as starting material, CuCl_2 (109 mg, 0.8 mmol) and NaBH_4 (650 mg, 17.5 mmol) as reducing agent.

Preparation of material I

Material I was prepared following the standard method described for graphenit-Cu(I) (procedure A), but using CuCl_2 (109 mg, 0.8 mmol) and NaBH_4 (65 mg, 1.75 mmol) as reducing agent.

A.2. XRD Analysis

XRD patterns of GNPs and materials A, B_{MW} , C_{MW} , D_{MW} and E_{MW} are shown in figure S1. Characteristic peaks for Cu_2O (36.6° and 42.6°), Cu (43.5° , 50.4°) and GNPs (26.2° , 43.8° , 54.6° , 77.6°) are observed in different proportions in the materials studied. CuO peaks at 35.7° and 39° are absent in all materials.

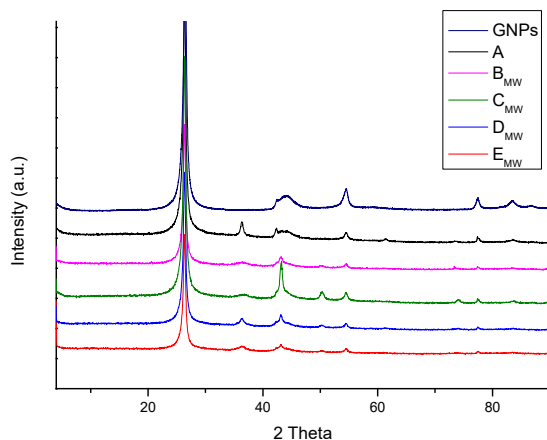


Figure S1. XRD pattern comparison of the materials.

The ratio between Cu(I) and Cu(0) for each material has been approximated by fitting the XRD peaks at 36.6 and 50.4 degrees (Table S1). Table S1 shows for each material the areas under the Cu(I) peak at 36.6 and the Cu (0) peak at 50°, and also the ratio between both areas. Material **A** only contains Cu₂O as no peak is observed at 50°. For microwave materials **E** is the one with higher ratio of Cu(I)/Cu(0) and material **C** is the one with lower ratio.

Table S1. Calculated Cu(I) and Cu(0) areas from XRD patterns of the materials.

Material	Cu(I) area	Cu(0) area	Area ratio (I)/(0)
Material A	976.58434	--	--
Material B_{MW}	943.84039	178.95673	5.27
Material C_{MW}	891.03331	750.07325	1.19
Material D_{MW}	798.19892	230.8028	3.46
Material E_{MW}	806.86873	122.75404	6.57

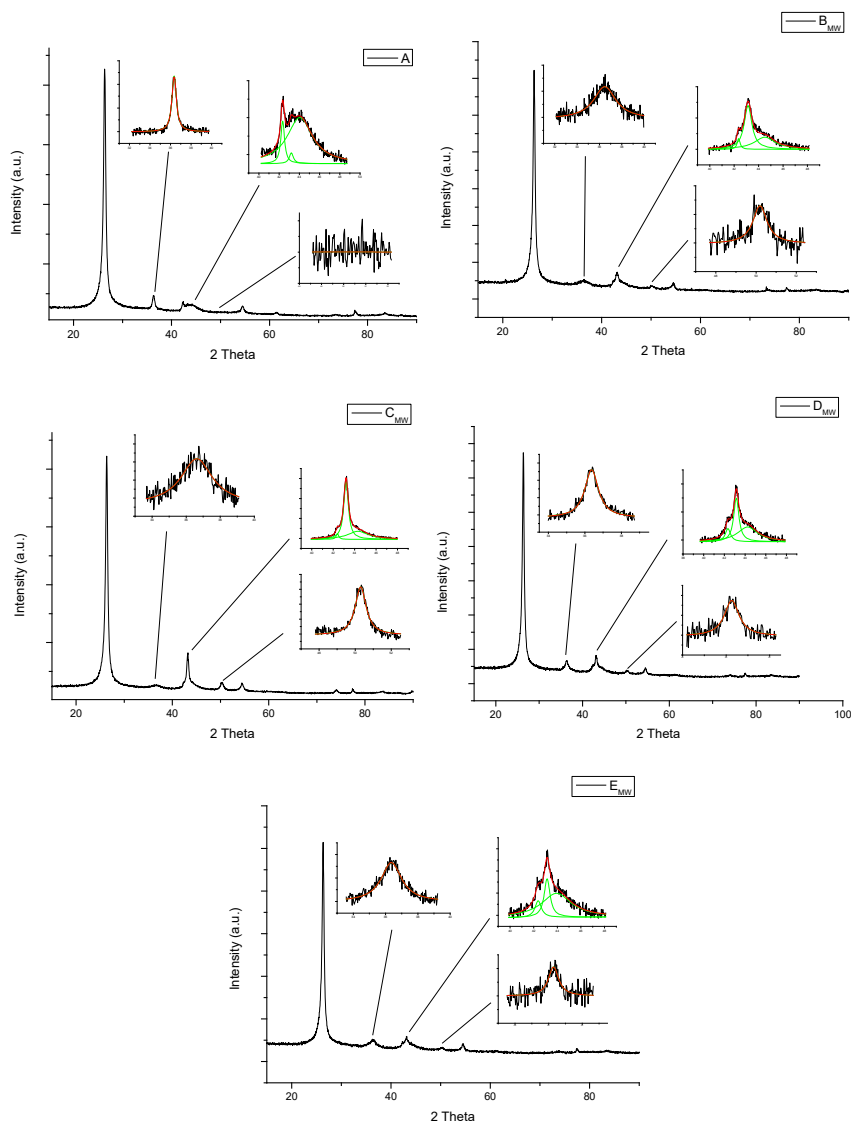


Figure S2. Zoomed peak areas of the XRD patterns.

Comparison between initial and used materials are shown in figures S3 (A and Ar) and S4 (E and Er). In both cases the oxidation state of Cu does not change after using the catalysts, but the amount of Cu seems to be lower in used materials and especially for material A (Table S2).

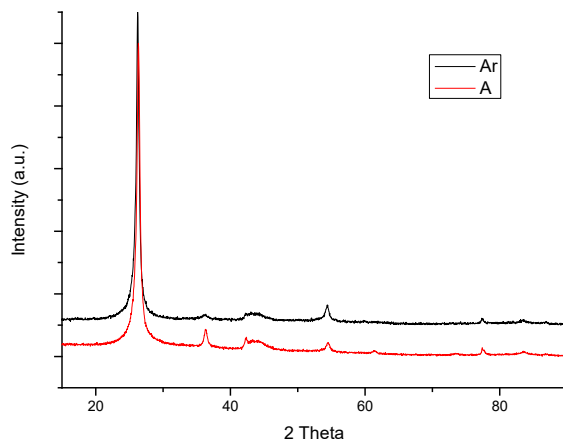


Figure S3. XRD pattern of the initial and recycled material A.

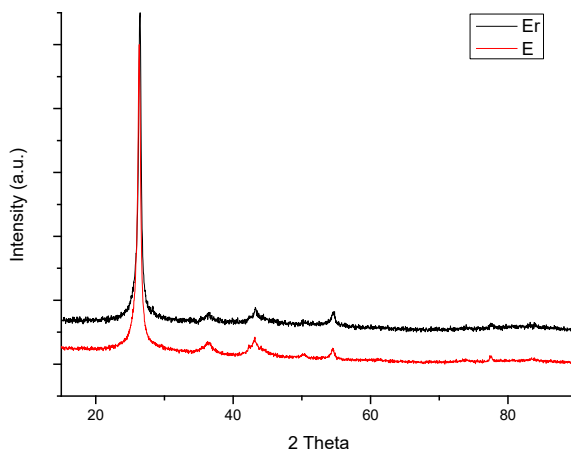


Figure S4. XRD pattern of the initial and recycled material E.

Table S2. Calculated Cu(I) and Cu(0) areas from XRD patterns of the materials.

Material	Cu(I) area 36.4°	Cu(0) area 50°	Area ratio (I)/(0)
Material A	976.58	0	--
Material Ar	236.34	0	--
Material E _{MW}	806.87	122.75	6.57
Material E _{MW} r	233.43	37.83	6.17

A.3. XPS Analysis

Figure S5 shows the XPS survey spectra of GNPs and materials **A**, **Ar**, **E_{MW}**, **E_{MW}r**.

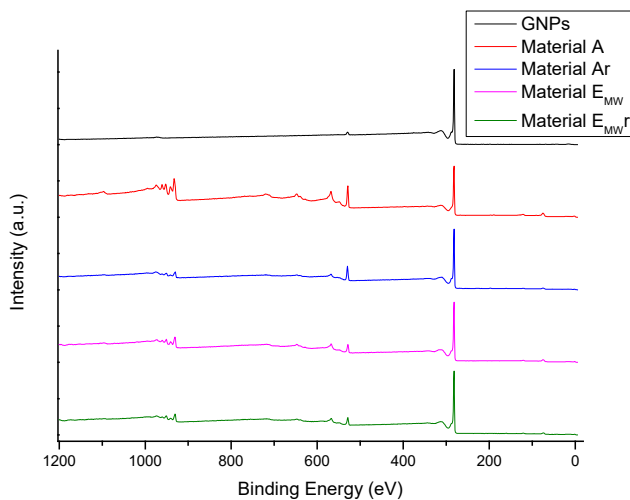


Figure S5. XPS spectra of the support and prepared materials.

Table S3 shows the atomic % for C, O and Cu obtained from the survey spectra of the different materials.

Table S3. Atomic percentage of C, O and Cu in the materials.

Sample	C 1s %	O 1s %	Cu 2p %
GNPs	98.2	1.8	--
Material A	81.0	12.8	6.3
Material Ar	90.8	8.0	6.3
Material E_{MW}	92.9	4.9	2.2
Material E_{MW}r	93.9	4.6	1.5

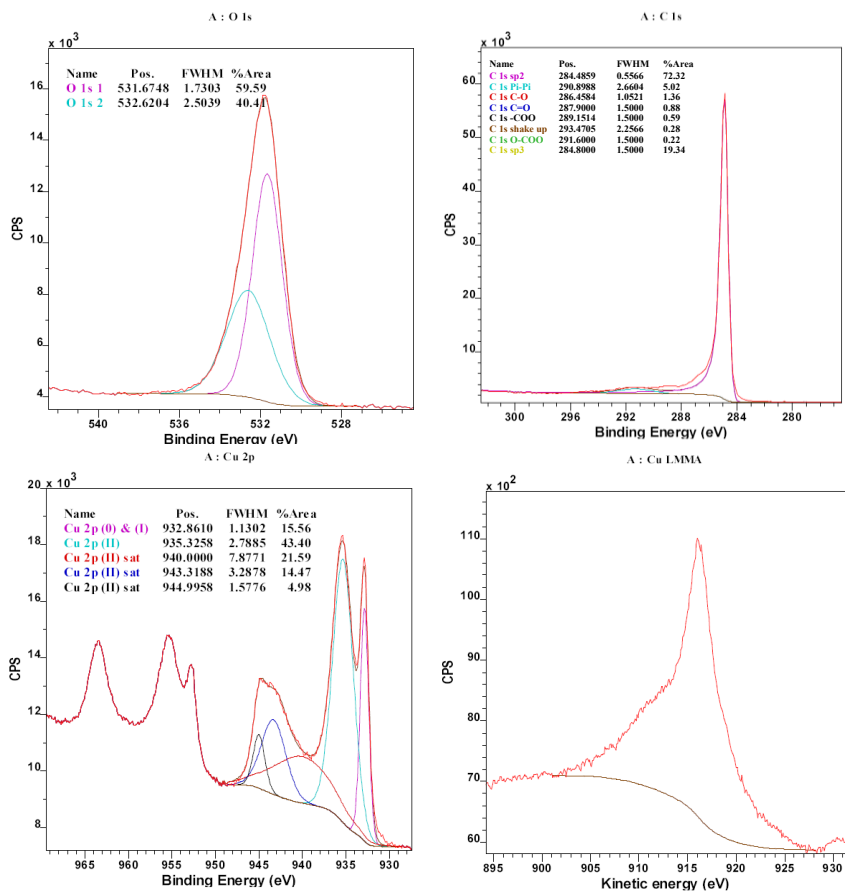


Figure S6. De-convoluted high resolution XPS C1s, O1s, Cu2p region spectra and Cu Auger LMM kinetic energy spectra of Material A.

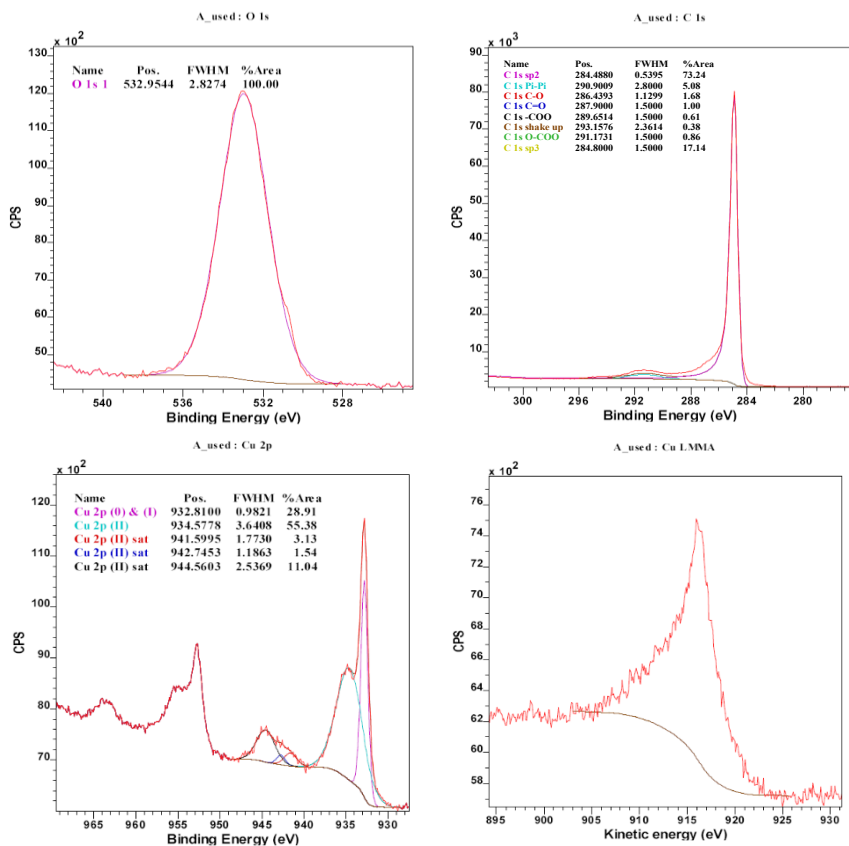


Figure S7. De-convoluted high resolution XPS C1s, O1s, Cu2p region spectra and Cu Auger LMM kinetic energy spectra of Material Ar.

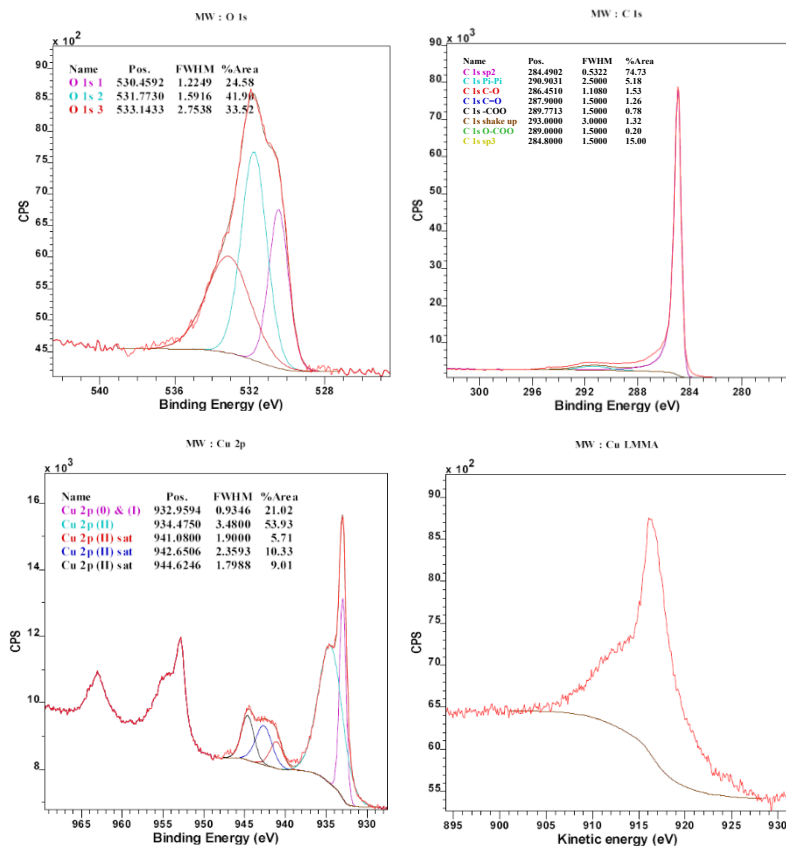


Figure S8. De-convoluted high resolution XPS C1s, O1s, Cu2p region spectra and Cu Auger LMM kinetic energy spectra of Material E_{MW} .

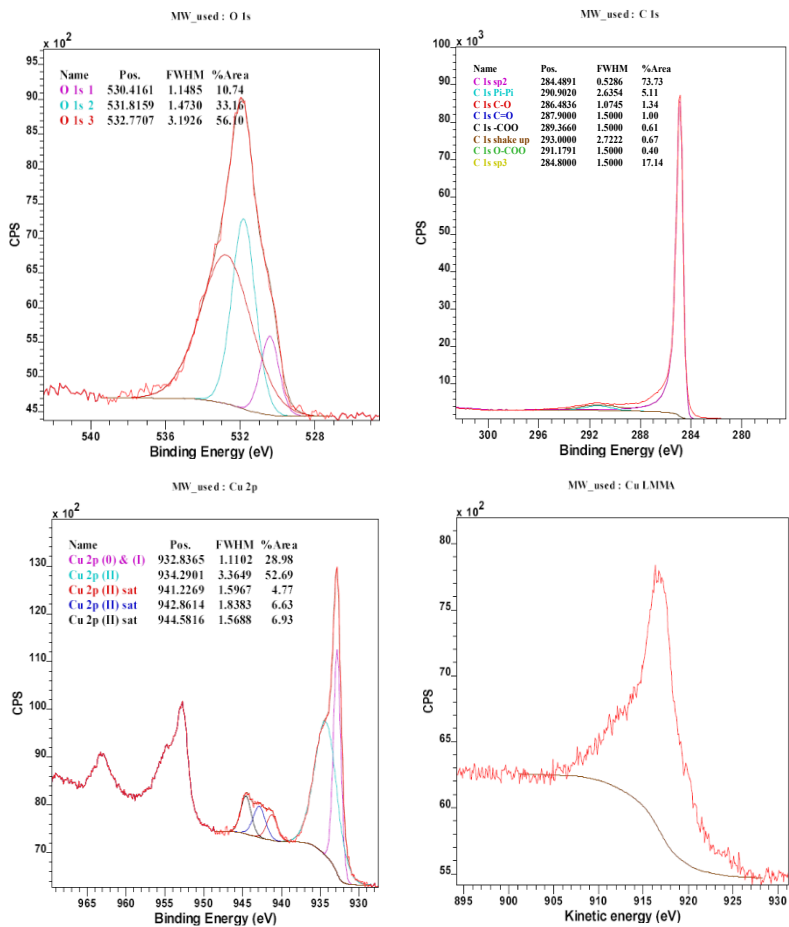


Figure S9. De-convoluted high resolution XPS C1s, O1s, Cu2p region spectra and Cu Auger LMM kinetic energy spectra of Material **E_{Mwr}**.

A.4. TEM images

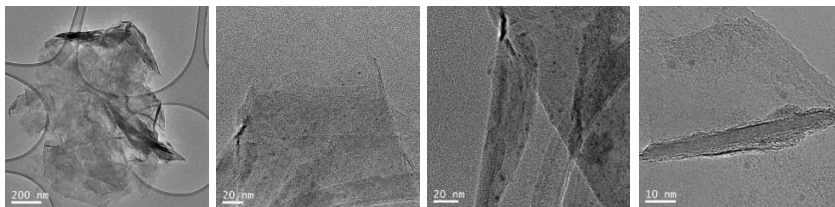


Figure S10. TEM images of material A.

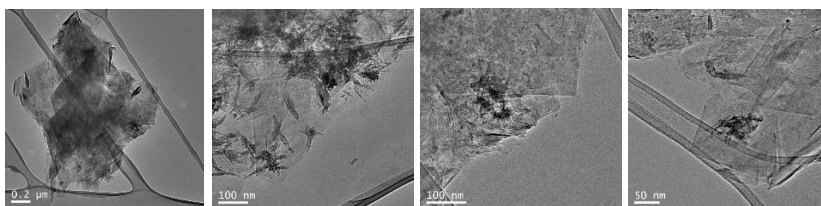


Figure S11. TEM images of Material Ar.

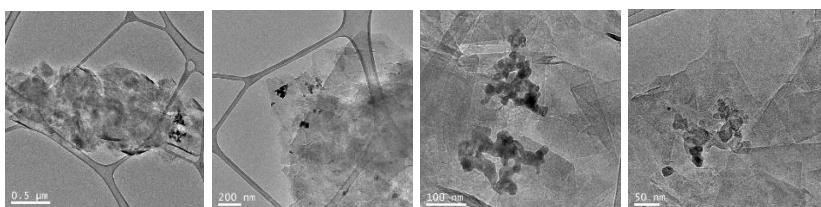


Figure S12. TEM images of material Emw.

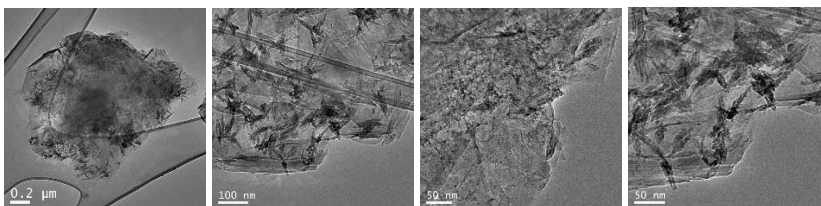
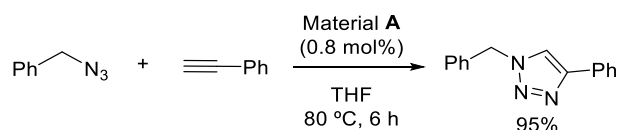


Figure S13. TEM images of material Emwr.

Part B. Additional information and experimental procedures of the borylation reactions

B.1. Experimental procedure for 1-benzyl-4-phenyl-1H-1,2,3-triazole synthesis



In a capped vial, material **A** (2.4 mg, 0.8 mol%) was suspended in THF (1 mL) and dispersed in an ultrasound bath during 5 min. Then, benzyl azide (0.43 mmol) and phenylacetylene (0.43 mmol) were added to the solution and heated at 80 °C for 6 h. Then, the catalyst is separated from the mixture by centrifugation at 7000 rpm, collecting the supernatant. Once separated, the catalyst is washed and resuspended with EtOAc, and separated by centrifugation collecting the supernatant. This process is repeated one more time. The solution is concentrated in vacuo and the residue was purified by flash chromatography (cyclo-hexane:ethyl acetate, 6:4) to afford the corresponding 1,2,3-triazole (96.1 mg, 95%) as a white solid. **¹H-RMN (CDCl₃, 300 MHz)** δ 7.77 (m, 2H), 7.65 (s, 1H), 7.32 (m, 8H), 5.53 (s, 2H). The spectroscopic data match with the described in the literature.¹²²

¹²² Ibtissen, J.; Meganem, F.; Girard, C. *Molecules*. **2009**, *14*, 528.

B.2. Experimental procedures for the alkyl halide borylation reaction

General considerations for the borylation procedure

The indicated mixture of reagents and solvent specified in each case are sonicated during 5 minutes. Although some reactions are performed in a glovebox, we demonstrated that the reactions work under Ar atmosphere using Schlenck techniques. In the case of aliphatic halides the reaction also works without an Ar atmosphere in most of the cases. The copper amount added to each experiment was calculated based on the %wt. Cu determined through TXRF for each material. After the corresponding reaction times, the catalyst is separated from the mixture by centrifugation at 7000 rpm, collecting the supernatant. Once separated, the catalyst was washed, resuspended in the indicated solvent, and separated by centrifugation collecting the supernatant. This process was repeated two more times. The collected organic phases are then washed with water. The combined organic phases were then dried over MgSO_4 , filtered, and concentrated at reduced pressure. All borylated compounds were purified by column chromatography using deactivated silica gel (Et_3N 5% w/w) and a cyclohexane:ethyl acetate mixture as eluent.

Borylation procedure for the alkyl halides (Conditions A)

In a vial, the catalyst (5 mol%), bis(pinacolato)diboron (95 mg, 0.38 mmol / 127 mg, 0.5 mmol, see table 2) and *t*-BuOLi (30 mg, 0.38 mmol) were added along with 1 mL of dry DMF, and the mixture was sonicated. Then the alkyl bromide (0.25 mmol) was added, and the mixture stirred vigorously at room temperature. Et_2O was used to rinse out the catalyst and the organic layers were washed 3 times to eliminate the DMF.

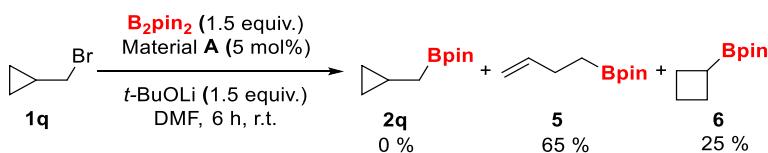
Borylation procedure for the aryl iodides (Conditions B)

In a screw-capped vial, the catalyst (2.5 mol%) was added and then placed into a glovebox. There, bis(pinacolato)diboron (159 mg, 0.63 mmol), *t*-BuOLi (30 mg, 0.38 mmol), the aryl iodide (0.25 mmol) and 1 mL of dry THF were added. Outside the glovebox, the vial with the mixture was then sonicated. The mixture was stirred vigorously at 60 °C for 24 h. After this time, the catalyst was washed and resuspended with EtOAc.

Borylation procedure for the aryl bromides (Conditions C)

In a screw-capped vial, the catalyst (5 mol%) was added and then placed into a glovebox. There, bis(pinacolato)diboron (159 mg, 0.63 mmol), MeONa (20.5 mg, 0.38 mmol), the aryl bromide (0.25 mmol) and 1 mL of dry DMA were added. Outside the glovebox, the vial with the mixture was then sonicated and the mixture is stirred vigorously at 60 °C for 6 h. After this time, the catalyst was washed and resuspended with EtOAc.

B.3. Additional mechanistic information



Scheme S1. Radical clock reaction.

The reaction was carried out following general procedure B. The isolated **5/6** products mixture were obtained by flash column chromatography purification of the crude using pentane : diethyl ether 20:1 as eluent.

According to the observed spectra of the mixture, we could identify the NMR signals of both open (**5**) and cycled products (**6**).¹²³ The difficulty to separate the two borylated products by conventional flash column chromatography led us to their isolation as a mixture. It is important to note that in both ¹H and ¹³C spectra appear important signals of different solvents such as pentane or diethyl ether. This is due to the impossibility of completely drying the products after the purification given the low boiling points of the products.

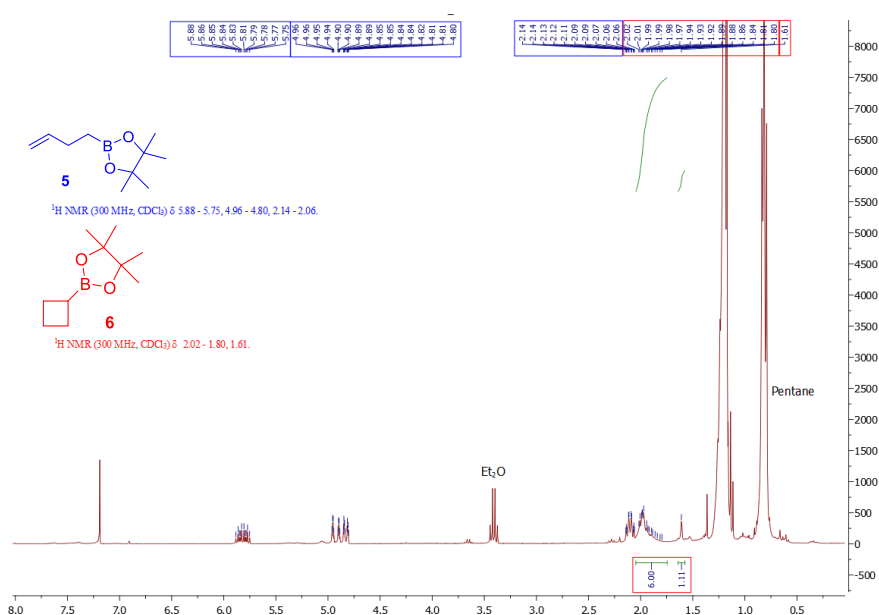


Figure S14. ¹H-NMR spectra of the pinacol boronic esters **5** and **6** mixture.

In the ¹H-NMR spectra (Figure S14), we could perfectly distinguish the NMR signals of the olefin present in the open product (**5**) at 6 and 5 ppm, as well as the allylic methylene signals at 2.2 ppm. Close to this multiplet, we could find a complex signal at 2 ppm that goes with a

¹²³ Zhou, X.-F.; Wu, Y.-D.; Dai, J.-J.; Li, Y.-J.; Huang, Y.; Xu, H.-J. *RSC Adv.* **2015**, *5*, 46672.

singlet at 1.6 ppm in a 6 to 1 ratio. These two multiplets match the described signals for the cyclobutyl boronic acid pinacol ester (**6**).

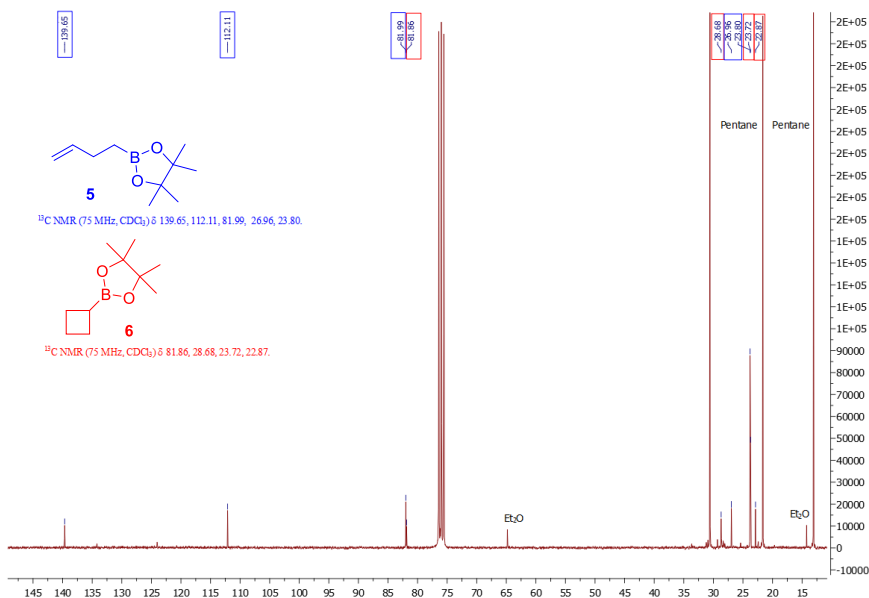
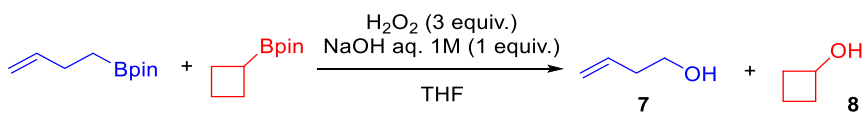


Figure S15. ^{13}C -NMR spectra of the pinacol boronic esters **5** and **6** mixture.

The ^{13}C -NMR spectra shows again the signals of both products matching the previously described spectroscopic data (Figure S15). The quadrupolar nature of the boron isotopes makes the signal of the carbon directly attached to the boron so broad that remains unseen in the spectra.



Scheme S2. Oxidation reaction of the pinacol boronic esters mixture

In order to ensure the existence of the cyclobutyl product, we carried out the oxidation of the mixture using the $\text{H}_2\text{O}_2/\text{NaOH}$ system (Scheme S3). After reaction completion, we could detect in the ^1H -NMR

spectra of the mixture a quintuplet at 4 ppm that could belong to the CH attached to the alcohol in the oxidized product **8** (Figure S16). The comparison between this signal and the described for the cyclobutanol revealed that they have the same multiplicity and chemical shift.

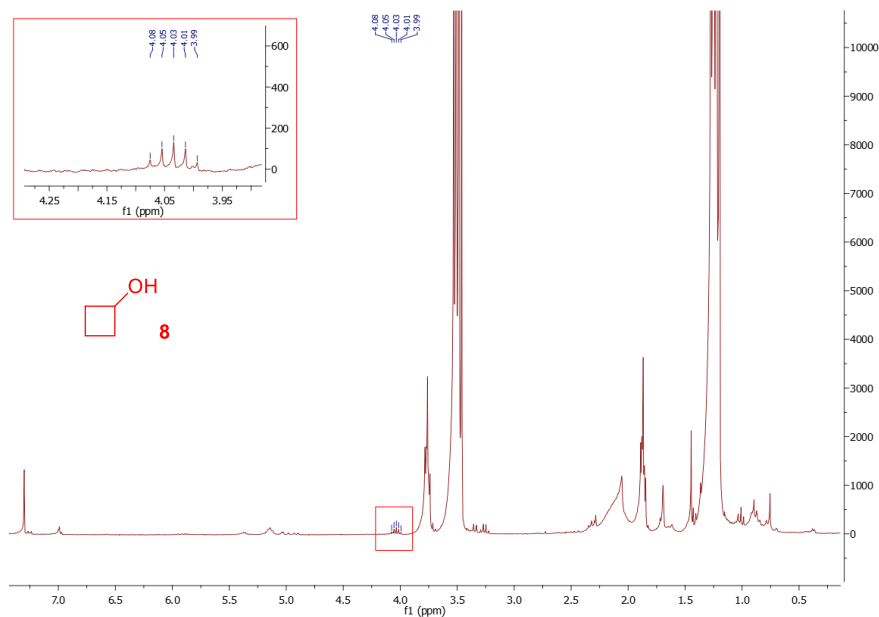
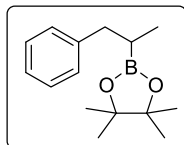


Figure S16. ^1H -NMR spectra of the pinacol boronic ester oxidation.

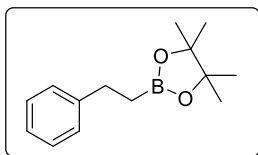
B.4. Characterization of aliphatic compounds

4,4,5,5-Tetramethyl-2-(1-phenylpropan-2-yl)-1,3,2-dioxaborolane

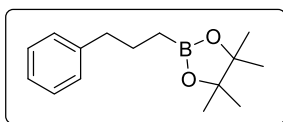
(2a)^{99a}



Prepared following general procedure A with no need of Ar atmosphere. The product was purified by column chromatography (cyclohexane:ethyl acetate 20:1) to get the product **2a** (55.4 mg, 90%) as a white solid. Spectroscopical data is in accordance with the literature. ^1H NMR (CDCl_3 , 300 MHz) δ 7.31 – 7.11 (m, 5H), 2.82 (dd, $J = 13.6, 7.5$ Hz, 1H), 2.56 (dd, $J = 13.6, 8.3$ Hz, 1H), 1.39 (m, 1H), 1.20 (d, $J = 3.1$ Hz, 12H), 0.98 (d, $J = 7.4$ Hz, 3H).

4,4,5,5-Tetramethyl-2-phenethyl-1,3,2-dioxaborolane (2b)^{98b}

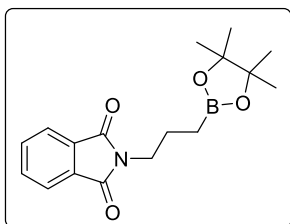
Prepared following general procedure A with no need of Ar atmosphere. The product was purified by column chromatography (cyclohexane:ethyl acetate 20:1) to get the product **2b** (52.3 mg, 90%) as a colorless oil. Spectroscopical data is in accordance with the literature. **¹H NMR (CDCl₃, 300 MHz)** δ 7.30-7.13 (m, 5H), 2.77 (t, J = 7.9 Hz, 2H), 1.24 (s, 12H), 1.16 (t, J = 7.9 Hz, 2H).

4,4,5,5-Tetramethyl-2-(3-phenylpropyl)-1,3,2-dioxaborolane (2c)¹²⁴

Prepared following general procedure A with no need of Ar atmosphere. The product was purified by column chromatography (cyclohexane:ethyl acetate 20:1) to get the product **2c** (56.6 mg, 92%) as a white solid. Spectroscopical data is in accordance with the literature. **¹H NMR (CDCl₃, 300 MHz, CDCl₃)** 7.32-7.26 (m, 2H), 7.23-7.13 (m, 3H), 2.63 (t, J = 7.8 Hz, 2H), 1.75 (p, J = 7.8 Hz, 2H), 1.26 (s, 12H), δ 0.85 (t, J = 7.9 Hz, 2H).

¹²⁴ Blakemore, P. R.; Burge, M. S. *J. Am. Chem. Soc.* **2011**, *129*, 3068.

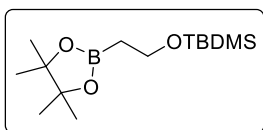
2-(3-(4,4,5,5-Tetramethyl-1,3,2-dioxaborolan-2-yl)propyl)-isoindoline-1,3-dione (2d)



Prepared following general procedure A under Ar atmosphere. The product was purified by column chromatography (cyclohexane:ethyl acetate 4:1) to get the product **2d** (50.4 mg, 64%) as a pale yellow oil. **¹H NMR**

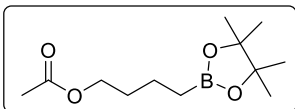
(CDCl₃, 300 MHz) δ 7.78-7.81 (m, 2H), 7.69-7.65 (m, 2H), 3.66 (t, J = 7 Hz, 2H), 1.77 (m, 2H), 1.19 (s, 12H), 0.79 (t, J = 8 Hz, 2H). **¹³C NMR (75 MHz, CDCl₃):** δ 168.8 (2 CO), 134.1 (2 CH), 132.6 (2 CH), 123.4 (2 CH), 83.5 (2 C), 40.2 (CH₂), 25.1 (4 CH₃), 23.5 (CH₂). **HRMS** (ES): calculated for C₁₇H₂₂BN₂O₄ (M⁺): 338.1537; found: 338.1543.

tert-Butyldimethyl(2-(4,4,5,5-tetramethyl-1,3,2-dioxaborolan-2-yl)ethoxy)silane (2e)

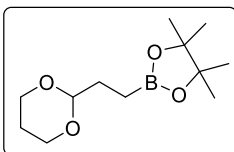


Prepared following general procedure A with no need of Ar atmosphere. The product was purified by column chromatography (cyclohexane:ethyl acetate 10:1) to get the product **2e** (60.8 mg, 85%) as a colorless oil. **¹H NMR**

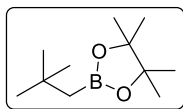
(CDCl₃, 300 MHz) δ 3.76 (t, J = 7.5 Hz, 2H), 1.23 (s, 12H), 1.10 (t, J = 7.6 Hz, 2H), 0.87 (s, 9H), 0.03 (s, 6H). **¹³C NMR (75 MHz, CDCl₃):** δ 83.4 (2 C), 60.3 (CH₂), 26.3 (3 CH₃), 25.2 (4 CH₃), 18.7 (C), -4.8 (2 CH₃). **HRMS** (ES): calculated for C₁₄H₃₁BO₃Si (M⁺): 309.2031; found: 309.2036.

4-(4,4,5,5-Tetramethyl-1,3,2-dioxaborolan-2-yl)butyl acetate (2f)

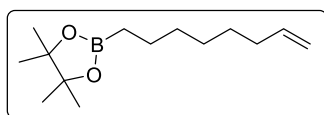
Prepared following general procedure A with no need of Ar atmosphere. The product was purified by column chromatography (cyclohexane:ethyl acetate 4:1) to get the product **2f** (52.7 mg, 87%) as a colorless oil. **¹H NMR (CDCl₃, 300 MHz)** δ 4.02 (t, J = 6.5 Hz, 2H), 3.00 (s, 3H), 1.60 (m, 2H) 1.45 (m, 2H), 1.22 (s, 12H), 0.77 (t, J = 7.7 Hz, 2H). **¹³C NMR (CDCl₃, 75 MHz)** δ 171.5 (CO), 83.3 (2 C), 64.8 (CH₂), 31.5 (CH₂), 25.1 (4 CH₃), 21.4 (CH₃), 20.8 (CH₂). **HRMS (ES)**: calculated for C₁₂H₂₃BO₄ (M⁺): 265.1584; found: 265.1579.

2-(2-(1,3-Dioxan-2-yl)ethyl)-4,4,5,5-tetramethyl-1,3,2-dioxaborolane (2g)^{99a}

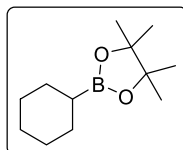
Prepared following general procedure A with no need of Ar atmosphere. The product was purified by column chromatography (cyclohexane:ethyl acetate 3:1) to get the product **2g** (54.5 mg, 90%) as a pale yellow oil. Spectroscopical data is in accordance with the literature. **¹H NMR (CDCl₃, 300 MHz)** δ 4.48 (t, J = 5.1 Hz, 1H), 4.09 (ddd, J = 11.7, 5.0, 1.2 Hz, 2H), 3.74 (td, J = 12.4, 2.5 Hz, 2H), 2.16 – 1.98 (m, 1H), 1.73 (td, J = 7.7, 5.2 Hz, 2H), 1.30 (m, 1H), 1.24 (s, 12H), 0.83 (t, J = 7.7 Hz, 2H).

4,4,5,5-Tetramethyl-2-neopentyl-1,3,2-dioxaborolane (2h)¹²⁵

Prepared following general procedure A with no need of Ar atmosphere. The product was purified by column chromatography (pentane:diethyl ether 50:1) to get the product **2h** (37.1 mg, 75%) as a colorless oil. Spectroscopical data is in accordance with the literature. **¹H NMR (CDCl₃, 300 MHz)** δ 1.25 (s, 12H), 0.99 (s, 9H), 0.81 (s, 2H). **¹³C NMR (75 MHz, CDCl₃)** δ 83.2 (2 C), 27.3 (3 CH₃), 25.2 (4 CH₃), 25.2 (C).

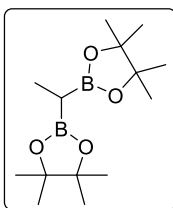
4,4,5,5-Tetramethyl-2-(oct-7-en-1-yl)-1,3,2-dioxaborolane (2i)

Prepared following general procedure A with no need of Ar atmosphere. The product was purified by column chromatography (cyclohexane:ethyl acetate 50:1) to get the product **2i** (29.8 mg, 50%) as a colorless oil. **¹H NMR (CDCl₃, 300 MHz)** δ 5.80 (ddt, $J = 16.9, 10.1, 6.7$ Hz, 1H), 5.04 – 4.86 (m, 2H), 2.02 (q, $J = 6.9$ Hz, 2H), 1.41 - 1.28 (m, 8H), 1.25 (s, 12H), 0.76 (t, $J = 7.6$ Hz, 2H). **¹³C NMR (75 MHz, CDCl₃)**: δ 139.6 (CH), 114.4 (CH), 83.2 (2 C), 34.2 (CH₂), 32.6 (CH₂), 29.3 (CH₂), 29.2 (CH₂) 25.2 (4 CH₃), 24.3 (CH₂). **HRMS (ES)**: calculated for C₁₄H₂₇BO₂ (M⁺, dimer): 499.4110; found: 499.4121.

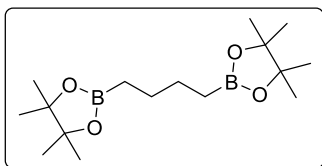
2-Cyclohexyl-4,4,5,5-tetramethyl-1,3,2-dioxaborolane (2j)^{99a}

Prepared following general procedure A with no need of Ar atmosphere. The product was purified by column chromatography (pentane:diethyl ether 50:1) to get the product **2j** (31.0 mg, 59%) as a colorless oil. Spectroscopical data is in accordance with the literature. **¹H NMR (CDCl₃, 300 MHz)** δ 1.70-1.52 (m, 4H), 1.38-1.23 (m, 6H), 1.22 (s, 12H), 1.02-0.90 (m, 1H).

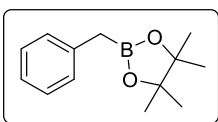
¹²⁵ Wang, D.; Mück-Lichtenfeld, C.; Studer, A. *J. Am. Chem. Soc.* **2019**, *141*, 14126.

2,2'-(Ethane-1,1-diyl)bis(4,4,5,5-tetramethyl-1,3,2-dioxaborolane)**(2k)**^{99a}

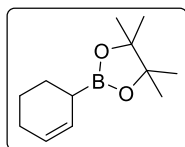
Prepared following general procedure A with no need of Ar atmosphere. The product was purified by column chromatography (cyclohexane:ethyl acetate 10:1) to get the product **2k** (42.3 mg, 60%) as a pale yellow oil. Spectroscopical data is in accordance with the literature. **¹H NMR (CDCl₃, 300 MHz)** δ 1.21 (s, 24H), 1.03 (d, J = 7.1 Hz, 3H), 0.71 (q, J = 6.9 Hz, 1H).

1,4-Bis(4,4,5,5-tetramethyl-1,3,2-dioxaborolan-2-yl)butane (2l)

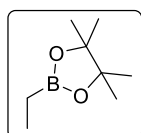
Prepared following general procedure A with no need of Ar atmosphere. The product was purified by column chromatography (cyclohexane:ethyl acetate 50:1) to get the product **2l** (59.7 mg, 77%) as a white solid. **¹H NMR (CDCl₃, 300 MHz)** δ 1.44-1.35 (m, 4H), 1.22 (s, 24H), 0.78-0.70 (m, 4H). **¹³C NMR (75 MHz, CDCl₃)**: δ 83.6 (4 C), 27.7 (2 CH₂), 25.6 (8 CH₃). **HRMS (ES)**: calculated for C₁₆H₃₂B₂O₄ (M⁺): 333.2385; found: 333.2395.

2-Benzyl-4,4,5,5-tetramethyl-1,3,2-dioxaborolane (2m)^{99a}

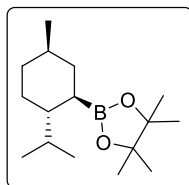
Prepared following general procedure A with no need of Ar atmosphere. The product was purified by column chromatography (cyclohexane:ethyl acetate 20:1) to get the product **2m** (44.1 mg, 81%) as a colorless oil. Spectroscopical data is in accordance with the literature. **¹H NMR (CDCl₃, 300 MHz)** δ 7.09-7.23 (m, 5H), 2.29 (s, 2H), 1.29 (s, 12H).

2-(Cyclohex-2-en-1-yl)-4,4,5,5-tetramethyl-1,3,2-dioxaborolane**(2n)**^{98b}

Prepared following general procedure A under Ar atmosphere. The product was purified by column chromatography (cyclohexane:ethyl acetate 50:1) to get the product **2n** (38.0 mg, 73%) as a colorless oil. Spectroscopical data is in accordance with the literature. ¹H NMR (CDCl₃, 300 MHz) δ 5.74 – 5.64 (m, 2H), 1.99 (m, 2H), 1.55 – 1.80 (m, 5H), 1.25 (s, 2H).

2-Ethyl-4,4,5,5-tetramethyl-1,3,2-dioxaborolane (2o)¹²⁶

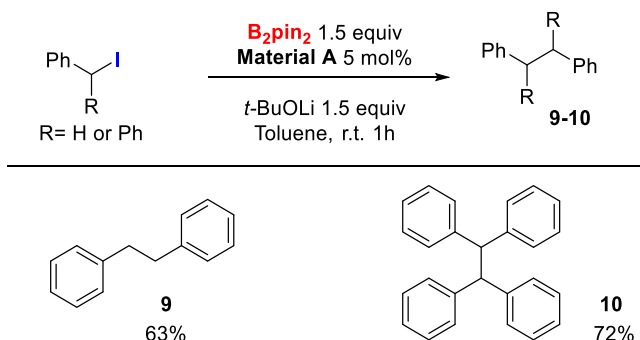
Prepared following general procedure A (starting from 10 mmol of bromoethane) with no need of Ar atmosphere. The product was purified by column chromatography (petroleum ether:diethyl ether 50:1) to get the product **2o** (1.322 g, 85%) as a colorless oil. Spectroscopical data is in accordance with the literature. ¹H NMR (CDCl₃, 300 MHz) δ 1.23 (s, 12H), 0.93 (t, *J* = 7.6 Hz, 3H), 0.74 (m, 2H).

2-((1R,2R,5R)-2-Isopropyl-5-methylcyclohexyl)-4,4,5,5-tetramethyl-1,3,2-dioxaborolane (2p)^{99a}

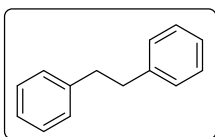
Prepared following general procedure A with no need of Ar atmosphere. The product was purified by column chromatography (cyclohexane:ethyl acetate 20:1) to get the product **2p** (39.8 mg, 60%) as a white solid. Spectroscopical data is in accordance with the literature. ¹H NMR (CDCl₃, 300 MHz) δ 0.77 (d, *J* = 7 Hz, 2H), 0.84 (d, *J* = 6.5 Hz, 2H), 0.88-1.02 (m, 7H), 1.20-1.35 (m, 14H), 1.55-1.75 (m, 4H).

¹²⁶ Cook, A. K.; Schimler, S. D.; Matzger, A. J.; Sandford, M. S. *Science*. **2016**, *351*, 1421.

B.5. Selective formation of the benzylic homocoupled products



1,2-Diphenylethane (9)¹²⁷

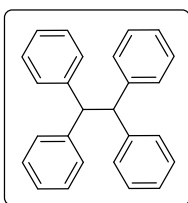


Prepared following general procedure A using toluene as solvent with no need of Ar atmosphere.

The product was purified by column chromatography (cyclohexane) to get the product **9** (28.7 mg, 63%) as a colorless oil. Spectroscopical data is in accordance with the literature.

¹H NMR (CDCl₃, 300 MHz) δ 2.93 (s, 4H), 7.15-7.30 (m, 10H).

1,1,2,2-Tetraphenylethane (10)¹²⁸



Prepared following general procedure A using toluene as solvent with no need of Ar atmosphere.

The product was purified by column chromatography (cyclohexane) to get the product **10** (60.2 mg, 72%) as a colorless oil. Spectroscopical

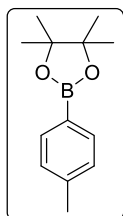
data is in accordance with the literature. **¹H NMR (CDCl₃, 300 MHz)** δ 4.77 (s, 2H), 6.93-7.02 (m, 4H), 7.07-7.11 (m, 8H), 7.14-7.17 (m, 8H).

¹²⁷ Black, P. J.; Edwards, M. G.; Williams, J. M. *Eur. J. Org. Chem.* **2006**, 19, 4367.

¹²⁸ Miura, M.; Nomura, M.; Satoh, T.; Kawasaki, S.; Wakui, H. *J. Am. Chem. Soc.* **2004**, 126, 8658.

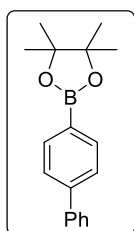
B.6. Characterization of aromatic compounds

4,4,5,5-Tetramethyl-2-(p-tolyl)-1,3,2-dioxaborolane (4a)^{98a}



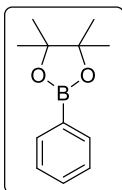
Prepared following general procedures B or C (starting from the aryl iodide or bromide, respectively). The product was purified by column chromatography (cyclohexane:ethyl acetate 20:1) to get the product **4a** (37.0 mg, 68%) as a pale yellow oil. Spectroscopical data in accordance with the literature. ¹H NMR (CDCl₃, 300 MHz) δ 7.73 (d, *J* = 7.6 Hz, 2H), 7.21 (d, *J* = 7.5 Hz, 2H), 2.38 (s, 3H), 1.36 (s, 12H).

2-([1,1'-Biphenyl]-4-yl)-4,4,5,5-tetramethyl-1,3,2-dioxaborolane (4b)¹²⁹

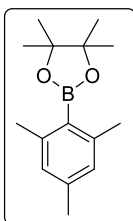


Prepared following general procedure C (starting from the aryl bromide). The product was purified by column chromatography (cyclohexane:ethyl acetate 20:1) to get the product **4b** (39.2 mg, 56%) as a white solid. Spectroscopical data in accordance with the literature. ¹H NMR (CDCl₃, 300 MHz) δ 7.92 (d, *J* = 8.2 Hz, 2H), 7.68 – 7.61 (m, 4H), 7.51 – 7.43 (m, 2H), 7.42 – 7.34 (m, 1H), 1.39 (s, 12H).

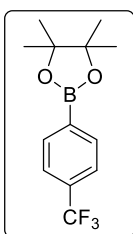
¹²⁹ Ji, S.; Qin, S.; Yin, C.; Luo, L.; Hua, Z. *Org. Lett.* **2022**, *24*, 64.

4,4,5,5-Tetramethyl-2-phenyl-1,3,2-dioxaborolane (4c)¹³⁰

Prepared following general procedures B or C (starting from the aryl iodide or bromide, respectively). The product was purified by column chromatography (cyclohexane:ethyl acetate 30:1) to get the product **4c** (34.1 mg, 67%) as a pale yellow liquid. Spectroscopical data in accordance with the literature. **¹H NMR (CDCl₃, 300 MHz)** δ 7.84 (d, J = 6.4 Hz, 2H), 7.51-7.45 (m, 1H), 7.41-7.36 (m, 2H), 1.37 (s, 12H).

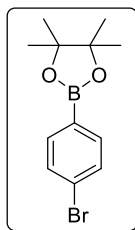
2-Mesityl-4,4,5,5-tetramethyl-1,3,2-dioxaborolane (4d)^{98a}

Prepared following general procedure B (starting from the aryl iodide). The product was purified by column chromatography (cyclohexane:ethyl acetate 50:1) to get the product **4d** (30.2 mg, 49%) as a pale yellow oil. Spectroscopical data in accordance with the literature. **¹H NMR (CDCl₃, 300 MHz)** δ 6.79 (s, 2H), 2.38 (s, 6H), 2.25 (s, 3H), 1.39 (s, 12H).

4,4,5,5-Tetramethyl-2-(4-(trifluoromethyl)phenyl)-1,3,2-dioxaborolane (4e)^{98a}

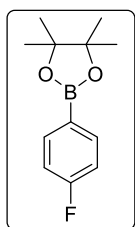
Prepared Following general procedure B or C (starting from the aryl iodide or bromide, respectively). The product was purified by column chromatography (cyclohexane:ethyl acetate 20:1) to get the product **4e** (47.6 mg, 70%) as a white solid. Spectroscopical data in accordance with the literature. **¹H NMR (CDCl₃, 300 MHz)** δ 7.93 (d, J = 7.8 Hz, 2H), 7.63 (d, J = 7.8 Hz, 2H), 1.37 (s, 12H).

¹³⁰ Zhu, W.; Ma, D. *Org. Lett.* **2008**, *8*, 261.

2-(4-Bromophenyl)-4,4,5,5-tetramethyl-1,3,2-dioxaborolane (4f)^{98a}

Prepared following general procedure B (starting from the aryl iodide).. The product was purified by column chromatography (cyclohexane:ethyl acetate 20:1) to get the product **4f** (53.0mg, 75%) as a pale yellow oil. Spectroscopical data in accordance with the literature. ¹H

NMR (CDCl₃, 300 MHz) δ 7.67 (d, J = 7.9 Hz, 2H), 7.51 (d, J = 7.9 Hz, 2H), 1.34 (s, 12H).

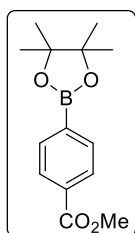
2-(4-Fluorophenyl)-4,4,5,5-tetramethyl-1,3,2-dioxaborolane (4g)¹³¹

Prepared following general procedure B (starting from the aryl iodide). The product was purified by column chromatography (cyclohexane:ethyl acetate 20:1) to get the product **4g** (41.1 mg, 74%) as a pale yellow oil. Spectroscopical data in accordance with the literature. ¹H

NMR (CDCl₃, 300 MHz) δ 7.87-7.81 (m, 2H), 7.13-7.05 (m, 2H), 1.38 (s, 12H).

Methyl-4-(4,4,5,5-tetramethyl-1,3,2-dioxaborolan-2-yl)benzoate

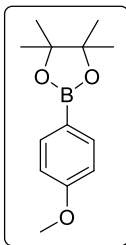
(4h)^{98a}



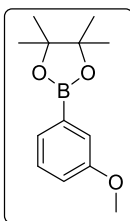
Prepared following general procedure B (starting from the aryl iodide). The product was purified by column chromatography (cyclohexane:ethyl acetate 10:1) to get the product **4h** (40.0 mg, 61%) as a pale yellow oil. Spectroscopical data in accordance with the literature. ¹H

NMR (CDCl₃, 300 MHz) δ 8.02 (d, J = 8.3 Hz, 2H), 7.87 (d, J = 8.3 Hz, 2H), 3.92 (s, 3H), 1.36 (s, 12H).

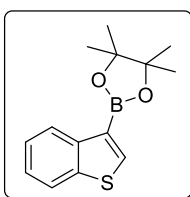
¹³¹ Zhu, W.; Ma, D. *Org. Lett.* **2008**, *8*, 261.

2-(4-Methoxyphenyl)-4,4,5,5-tetramethyl-1,3,2-dioxaborolane (4i)^{98a}

Prepared following general procedure B or C (starting from the aryl iodide or bromide, respectively). The product was purified by column chromatography (cyclohexane:ethyl acetate 20:1) to get the product **4i** (45.1 mg, 77%) as a pale yellow oil. Spectroscopical data in accordance with the literature. **¹H NMR (CDCl₃, 300 MHz)** δ 7.78-7.74 (m, 2H), 6.92-6.88 (m, 2H), 3.84 (s, 3H), 1.34 (s, 12H).

2-(3-Methoxyphenyl)-4,4,5,5-tetramethyl-1,3,2-dioxaborolane (4j)¹³⁰

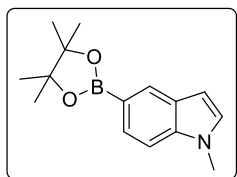
Prepared following general procedure B (starting from the aryl iodide). The product was purified by column chromatography (cyclohexane:ethyl acetate 20:1) to get the product **4j** (38.0 mg, 65%) as a pale yellow oil. Spectroscopical data in accordance with the literature. **¹H NMR (CDCl₃, 300 MHz)** δ 7.42 (d, $J = 7.2$ Hz, 1H), 7.38-7.25 (m, 2H), 7.06-6.99 (m, 1H), 3.85 (s, 3H), 1.36 (s, 12H).

2-(Benzo[b]thiophen-3-yl)-4,4,5,5-tetramethyl-1,3,2-dioxaborolane (4k)¹³²

Prepared following general procedure C (starting from the aryl bromide). The product was purified by column chromatography (cyclohexane:ethyl acetate 20:1) to get the product **4k** (19.5 mg, 30%) as a white solid. Spectroscopical data in accordance with the literature. **¹H NMR (CDCl₃, 300 MHz)** δ 8.42 – 8.36 (m, 1H), 8.09 (s, 1H), 7.92-7.88 (m, 1H), 7.45 – 7.31 (m, 2H), 1.40 (s, 12H).

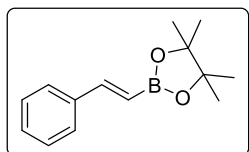
¹³² Nakagawa, H.; Kawai, S.; Nakashima, T.; Kawai, T. *Org. Lett.* **2009**, *11*, 1475.

1-Methyl-5-(4,4,5,5-tetramethyl-1,3,2-dioxaborolan-2-yl)-1H-indole
(**4l**)²¹²



Prepared following general procedure C (starting from the aryl bromide). The product was purified by column chromatography (cyclohexane:ethyl acetate 20:1) to get the product **4l** (27.0 mg, 42%) as a white solid. Spectroscopical data in accordance with the literature. **¹H NMR (CDCl₃, 300 MHz)** δ 8.17 (s, 1H), 7.68 (dd, J = 8.3, 1.0 Hz, 1H), 7.33 (d, J = 8.3 Hz, 1H), 7.05 (d, J = 3.1 Hz, 1H), 6.51 (dd, J = 3.1, 0.8 Hz, 1H), 3.80 (s, 3H), 1.38 (s, 12H).

(E)-4,4,5,5-Tetramethyl-2-styryl-1,3,2-dioxaborolane (**4m**)¹¹³

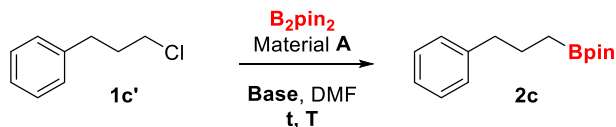


Prepared following general procedure C (starting from the vinyl bromide). The product was purified by column chromatography (cyclohexane:ethyl acetate 50:1) to get the product **4m** (38.0 mg, 66%) as a colorless oil. Spectroscopical data in accordance with the literature. **¹H NMR (CDCl₃, 300 MHz)** δ 7.57 – 7.51 (m, 2H), 7.45 (d, J = 18.6 Hz, 1H), 7.42 – 7.25 (m, 3H), 6.22 (d, J = 18.4 Hz, 1H), 1.36 (s, 12H).

Annex

1. Additional optimization tables of Chapter 1

Table A1. Aliphatic chloride borylation optimization.



Entry	Catalyst (%)	B_2pin_2 (equiv.)	Base (equiv.)	t (h)	T ($^{\circ}C$)	Conv ^a (%)
1	5	1.5	tBuOLi (1.5)	72	t.a.	40
2	5	1.5	tBuOK (1.5)	72	t.a.	25
3	5	1.5	MeOK (1.5)	72	t.a.	12
4	5	1.5	tBuOLi (1.5)	72	60	36
5	10	2	tBuOLi (2)	120	60	10
6	10	2	tBuOLi (2)	72	110	0
7	10	2	CS_2CO_3 (2)	72	110	0
8	10	2	CsF (2)	72	110	0
9 ^b	10	2	tBuOLi (2)	48	t.a.	0

^aConversions determined by 1H -NMR as starting material disappearance.

^bReaction performed under white light LED irradiation, toluene used as solvent.

**Part II. Diboron reagents in C-S bond
formation, deoxygenation of N-O bonds,
and C=N bond activation**

1. Introduction

Diboron reagents, and specially bis(pinacolato)diboron (B_2pin_2), have been widely used as stable, green, and cheap reagents in borylation reactions. As depicted in the introduction of the first part of this doctoral thesis, the main use of diboron compounds is the insertion of a boronic ester moiety in a variety of substrates due the facile interconversion of the products into many different functionalities.^{133,134} The introduction of the boron moiety usually needs the participation of a metal catalyst and a Lewis base to activate the B-B bond.¹³⁵

Diboron compounds have demonstrated their utility in a variety of transition metal-free organic transformations.¹³⁶ This second part of the doctoral thesis is focused on the use of diboron compounds in absence of metals to explore transformations that not only include borylation reactions.

In this sense, significant developments have been achieved in recent years using diboron reagents in combination with different Lewis bases. In this introduction, we will discuss the most representative precedents related to some aspects of our investigations which mostly deal with the use of pyridines to activate diboron compounds and promote different processes under very mild reaction conditions.

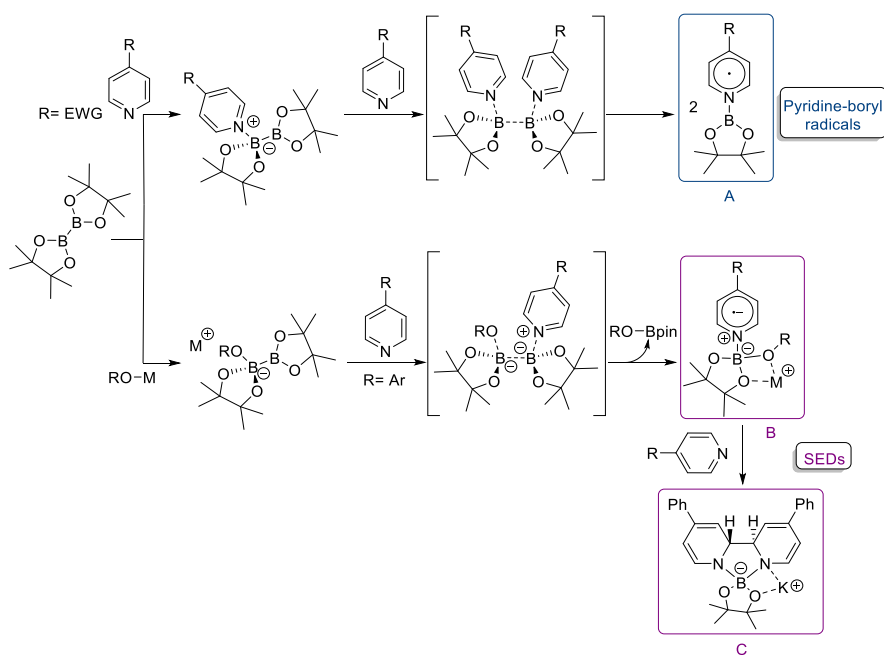
¹³³ Cid, J.; Gulyás, H.; Carbó, J. J.; Fernández, E. *Chem. Soc. Rev.* **2012**, *41*, 3558.

¹³⁴ Dewhurst, R. D.; Neeve, E. C.; Braunschweig, H.; Marder, T. B. *Chem. Commun.* **2015**, *51*, 9594.

¹³⁵ a) Wagner, A.; Kaifer, E.; Himmel, H.-J. *Chem. Commun.* **2012**, *48*, 5277. b) Sharmila, D.; Mondal, B.; Ramalakshmi, R.; Kundu, S.; Varghese, B.; Ghosh, S. *Chem. Eur. J.* **2015**, *21*, 5074.

¹³⁶ Neeve, E. C.; Geier, S. J.; Mkhaldid, I. A. J.; Westcott, S. A.; Marder, T. B. *Chem. Rev.* **2016**, *116*, 9091.

The reaction of a functionalized pyridine with a diboron compound can lead to different pyridine-boryl species.¹³⁷ When the reaction occurs in the absence of a base, it leads to the formation of pyridine-boryl radicals **A** (Scheme 1, above). However, different species are detected when a base alkoxide is also added to the mixture. These intermediates (**B**, **C**) have demonstrated a high tendency to give electrons and therefore are considered super electron donors (SED) (Scheme 1, below).



Scheme 1. Pyridine-boryl complexes formation.

The different nature of the formed species **A** and **B-C** implies a great impact in the reactions that these intermediates can promote and therefore they will be treated independently. It has been reported the use of pyridine-boryl radicals **A** as promoters of reductions, borylations, pyridine functionalization, or radical coupling reactions.

¹³⁷ Misal Castro, L. C.; Sultan, I.; Tsurugi, H.; Mashima, K. *Synthesis*. **2021**, 53, 3211.

On the other hand, super electron donors **B-C**, at the moment we started our investigations in the area, had a more limited scope of applications, being mainly reported as promoters of borylation reactions. All the advances related to these complexes will be summarized in the following section.

1.1. Pyridine-mediated B-B bond activation and application in Organic Synthesis

The history of these interesting and versatile intermediates started quite recently, having experienced a fast growth in terms of publications and applicability, and the advances in this area have been already collected in a review article.¹³⁷

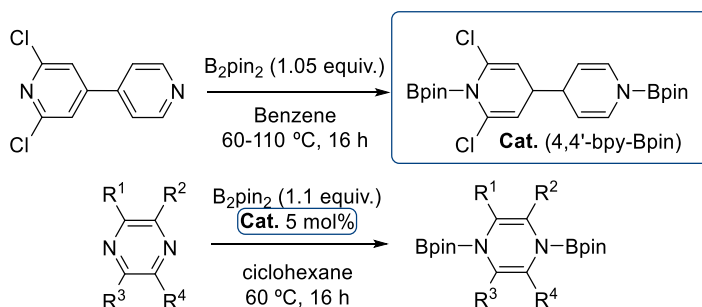
First, we will show the described processes promoted by the pyridine-boryl radicals (**A**), and then we will mention the progress in the use of boron-based SED (**B-C**).

One of the synthetic applications of the pyridine-boryl radicals deals with reduction of nitroderivatives. As the deoxygenating power of diboron reagents has determined the course of our investigations, we have included a small section to mention the described methods to cleave N-O bonds using diboron derivatives in the presence and in the absence of pyridines.

1.1.1. Synthetic Applications of Pyridine-Boryl Radicals

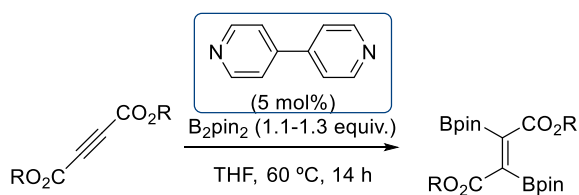
The first report dealing with B-B bond cleavage mediated by pyridines was published in 2015, when Suginome and coworkers described the first diboration of 4,4'-dipyridines using B_2pin_2 as

reducing agent (Scheme 2).¹³⁸ The dearomatized products (4,4'-bpy-Bpin) were able to catalyze the diboration of pyrazines through a process they called *oxidative boron transfer*. This publication did not include any study about the possible mechanism ruling the reaction, so the intermediates derived from these substrates were still unknown.



Scheme 2. Suginome's example of pyrazine borylation.

Years later, the same group reported the use of 4,4'-bipyridine as catalyst (5 mol%) and B_2pin_2 as boron source to perform the trans-diboration of acetylene dicarboxylates (Scheme 3).¹³⁹ In this publication the authors did include a mechanistic proposal discarding the presence of a radical pathway.



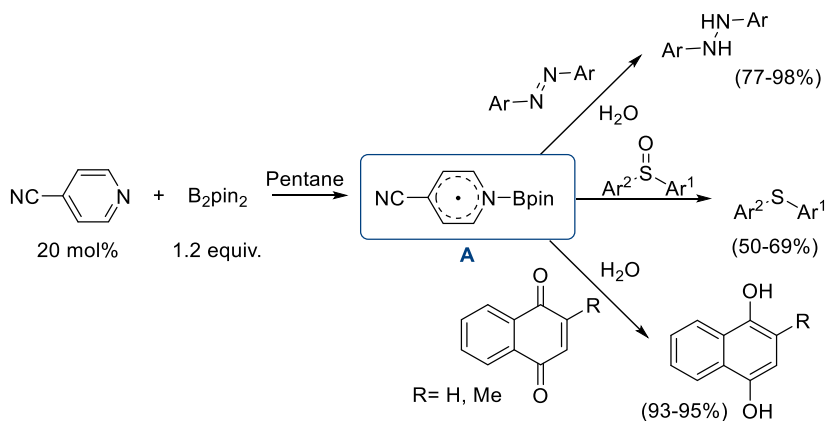
Scheme 3. Suginome's method for the trans-diboration of acetylene dicarboxylates.

A significant advance in this field is due to the works of Li's group. In 2016, they identified the formation of the radical intermediate **A**,

¹³⁸ Ohmura, T.; Morimasa, Y.; Suginome, M. *J. Am. Chem. Soc.* **2015**, *137*, 2852.

¹³⁹ Ohmura, T.; Morimasa, Y.; Suginome, M. *Chem. Lett.* **2017**, *46*, 1793.

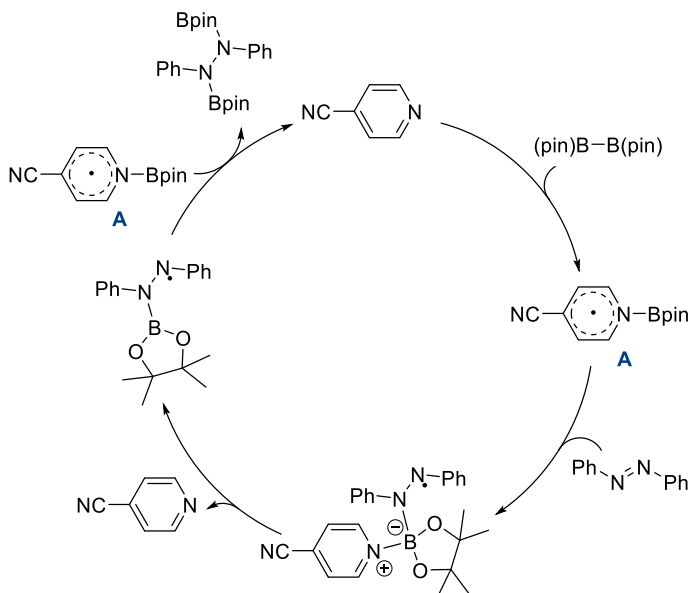
formed from the mixture of the 4-cyanopyridine and B_2pin_2 , as responsible of the efficient reduction of azocompounds, diaryl sulphoxides and quinones (Scheme 4).¹⁴⁰



Scheme 4. Li's method for the reduction of azocompounds, sulphoxides and quinones.

In their report, the authors included a plausible mechanistic cycle for the reduction of azobenzenes in which the *pyridine-boryl radical* intermediate **A** sequentially adds to the double bond to finally afford the bis-borylated product and the original 4-cyanopyridine (Scheme 5).

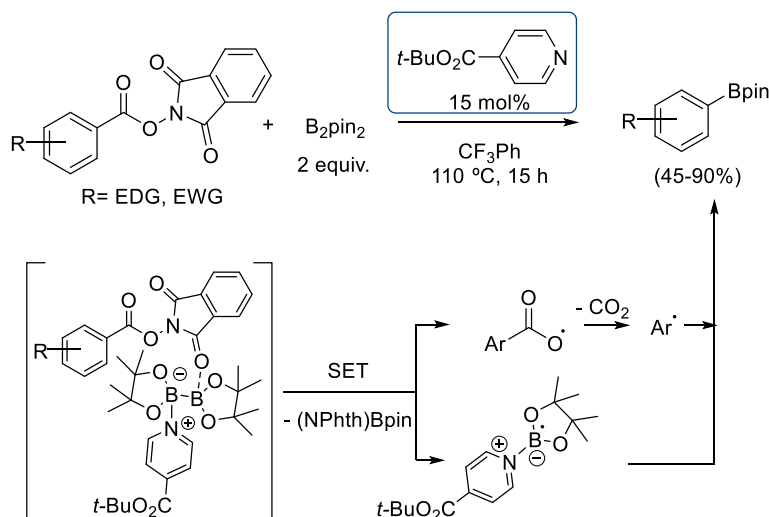
¹⁴⁰ Wang, G.; Zhang, H.; Zhao, J.; Li, W.; Cao, J.; Zhu, C.; Li, S. *Angew. Chem. Int. Ed.* **2016**, *55*, 5985.



Scheme 5. Li's proposed mechanism for the pyridine-boryl radical catalyzed reduction of azocompounds.

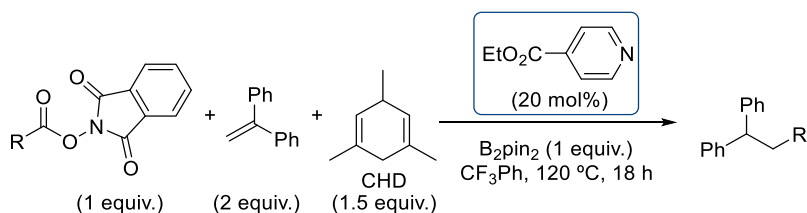
A very particular example of borylation under these base free conditions was published by the group of Fu in 2017.¹⁴¹ In their work, they developed a metal free variation of the previously reported metal catalyzed decarboxylative borylation of redox active esters (RAEs) (Scheme 6). An interesting feature of this metal-free procedure is also the use of an electron withdrawing group on the pyridine, in this case a 4-*tert*-butyl ester. In their report, authors postulate that the coordination of one of the oxygens of the phthalimide in the RAE to the B₂pin₂ facilitates the B-B bond cleavage. The following CO₂ extrusion leads to the consequent aryl radical formation, which reacts with the pyridine-boryl radical to afford the final borylated product.

¹⁴¹ Cheng, W. M.; Shang, R.; Zhao, B.; Xing, W. L.; Fu, Y. *Org. Lett.* **2017**, *19*, 4291.



Scheme 6. SED catalyzed RAE decarboxylative borylation described by Fu.

In 2018, Li described the pyridine-boryl promoted coupling of alkenes and redox active esters derived from aliphatic carboxylic acids (Scheme 7).¹⁴² They needed to add a stoichiometric amount of TME-1,4-CHD as an H-donor to efficiently promote the reaction. The authors suggested that an EWG at the C4 position of the pyridine catalyst was beneficial for the reaction.



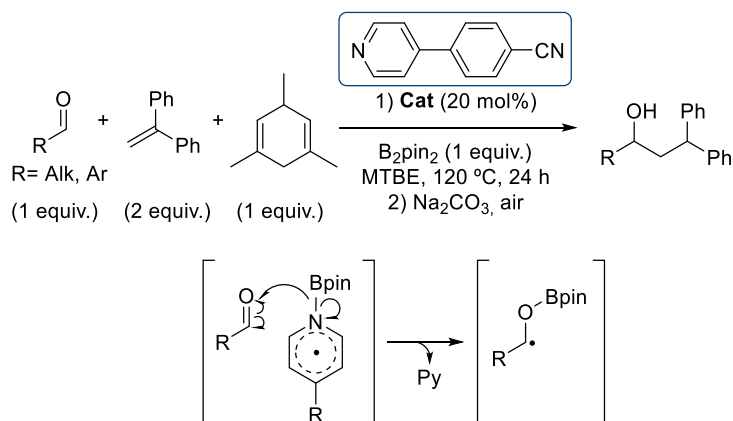
Scheme 7. Li's SED catalyzed coupling of alkenes with RAEs.

Also in 2018, Li and coworkers found the reaction conditions to promote the reductive coupling of aldehydes with alkenes (Scheme 8).¹⁴³ They proposed the addition of Bpin to the oxygen to afford the

¹⁴² Cao, J.; Wang, G.; Gao, L.; Yuan, D.; Xu, C.; Guo, X.; Li, S. *Chem. Commun.* **2018**, 54, 11534.

¹⁴³ Cao, J.; Wang, G.; Gao, L.; Xu, C.; Li, S. *Chem. Sci.* **2018**, 9, 3664.

formation of a C-O-Bpin carbonyl radical intermediate, which undergoes the radical coupling with alkenes. Through DFT calculations, they determined that the formation of the pyridine-boryl radical was favored by pyridines containing electron withdrawing groups at the C4 position. In this particular case, they used 4-(4-cyanophenyl)pyridine as catalyst.

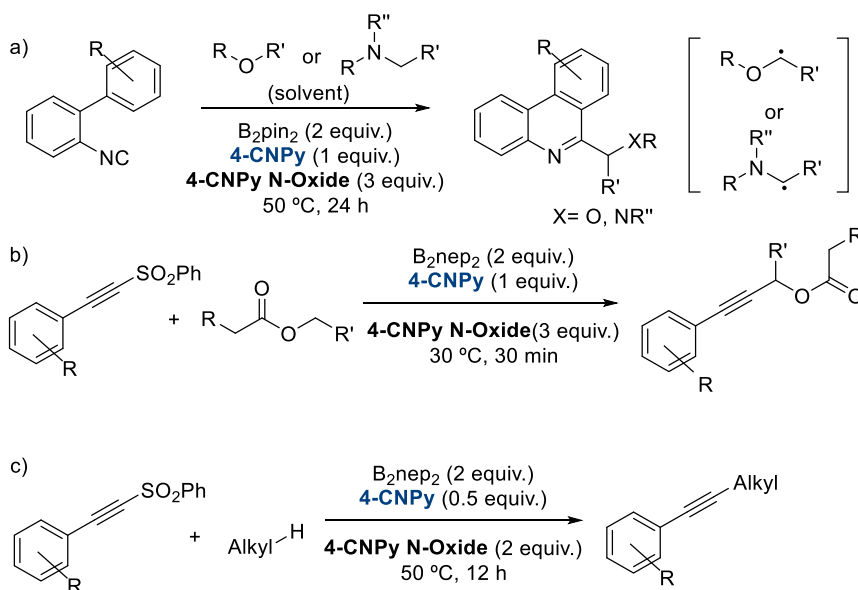


Scheme 8. Li's example of reductive coupling of aldehydes to alkenes.

The versatility of these pyridine-boryl radicals has also been exploited in C-H activation. In this field, the works of Tang and coworkers are of special importance. Throughout their publications, they have demonstrated that the combination of diboron species and a pyridine can lead to the hydrogen abstraction of different substrates. Within their first publication, they could get to the radical cyclization of aromatic isocyanates to afford phenanthridine derivatives (Scheme 9a).¹⁴⁴ Under the reaction conditions they obtained a series of products using different ethers and tertiary amines as substrates. Authors postulated that the pyridine-boryl intermediate is able to generate the radicals from the ethers and amines which later react with the

¹⁴⁴Guo, A.; Han, J-B.; Tang, X.-Y. *Org. Lett.* **2018**, *20*, 2351.

isocyanates. The role of the oxidant (4-cyanopyridine *N*-oxide) is double in this reaction, acting as a HBpin scavenger and rearomatizing the phenanthridine final product.



Scheme 9. Tang's works in C-H activation using SEDs.

Later, they found out that the use of alkyne sulphones as radical acceptors leads to the coupling of ethyl acetates (Scheme 9b)¹⁴⁵ and alkanes (Scheme 9c)¹⁴⁶ under similar conditions to the previously reported.

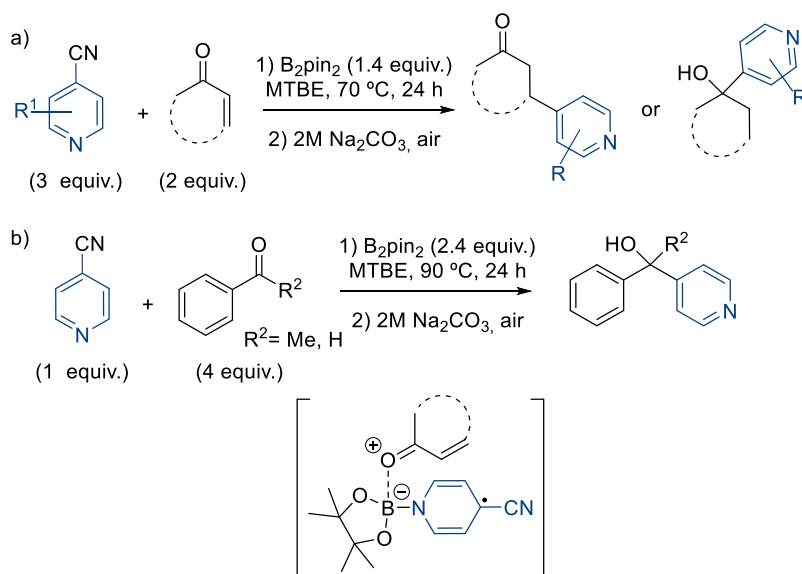
As may be expected, some groups have taken advantage of the reactivity of the pyridine-boryl radical to functionalize pyridines. In this area, the first example found in the literature was published by Li's group in 2017.¹⁴⁷ Herein, they described the addition of enones and ketones to 4-cyanopyridines in presence of B₂pin₂ (Scheme 10a and

¹⁴⁵ Guo, A.; Han, J.-B.; Zhu, L.; Wei, Y.; Tang, X.-Y. *Org. Lett.* **2019**, *21*, 2927.

¹⁴⁶ Han, J.-B.; San, H.H.; Guo, A.; Wang, L.; Tang, X. Y. *Adv. Synth. Cat.* **2021**, *363*, 2366.

¹⁴⁷ Wang, G.; Cao, J.; Gao, L.; Chen, W.; Huang, W.; Cheng, X.; Li, S. *J. Am. Chem. Soc.* **2017**, *139*, 3904.

10b). Through DFT calculations they proposed that the oxygen of the ketone coordinates one of the boron atoms and facilitates the dissociation of the diboron in the radical intermediate (a similar behavior to the observed in the decarboxylative borylation of RAEs, see scheme 6). The method provides the 1,4-addition to the enones with moderate to good yields, although in some cases along with the 1,2 adduct. The elimination of the NC-Bpin restores the aromaticity of the pyridine ring.

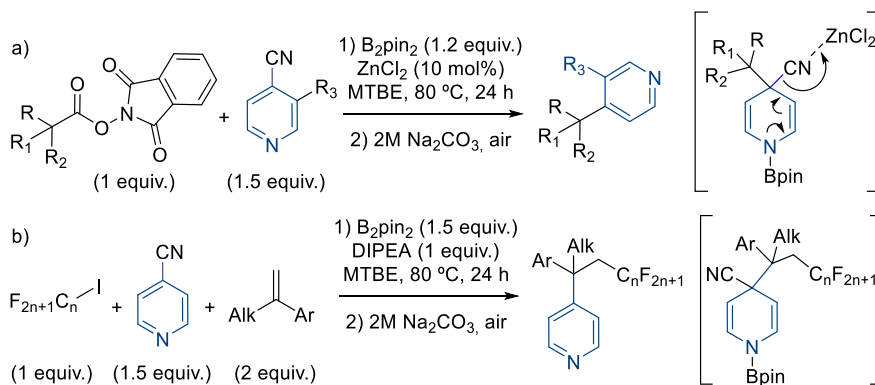


Scheme 10. Li's works in 4-cyanopyridine functionalization with carbonyl compounds

Years later, Li and coworkers could extrapolate this methodology to the decarboxylative coupling of RAEs with 4-cyanopyridines (Scheme 11a).¹⁴⁸ In this case, they avoided the undesired coupling reaction by the C2 position of the pyridine with the addition of a Lewis acid ($ZnCl_2$), which coordinates to the CN group, favoring the nitrile dissociation and

¹⁴⁸ Gao, L.; Wang, G.; Cao, J.; Chen, H.; Gu, Y.; Liu, X.; Cheng, X.; Ma, J.; Li, S. *ACS Catal.* **2019**, *9*, 10142.

the restoration of the aromaticity. The same year, they also published the introduction of perfluoroalkylated moieties and pyridines on alkenes via functionalization of 4-cyanopyridines (Scheme 11b).¹⁴⁹

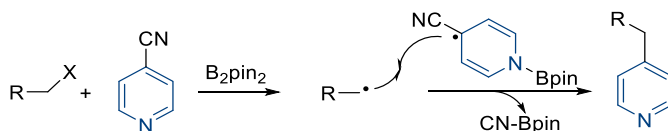


Scheme 11. Li's works in the 4-cyanopyridine functionalization.

The mechanism of this reaction follows a similar pathway than the previous, where the generation of the alkyl radical of the iodide by the pyridine-boryl intermediate is followed by its addition to the alkane. The new radical reacts with the pyridine-boryl intermediate to afford the final product.

As can be observed, the basis of this chemistry resides on the formation of the radicals in different substrates by the pyridine-boryl radical intermediate generated in situ, which attach to another molecule of pyridine-boryl radical to finally afford the C4-substituted pyridines (Scheme 12).

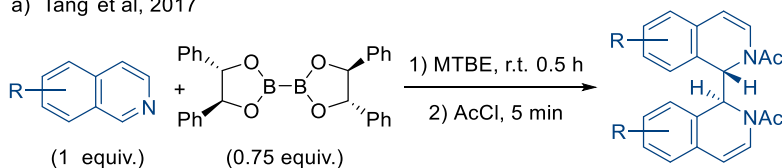
¹⁴⁹ Cao, J.; Wang, G.; Gao, L. Chen, H.; Liu, X.; Cheng, X.; Li, S. *Chem. Sci.* **2019**, *10*, 2767.



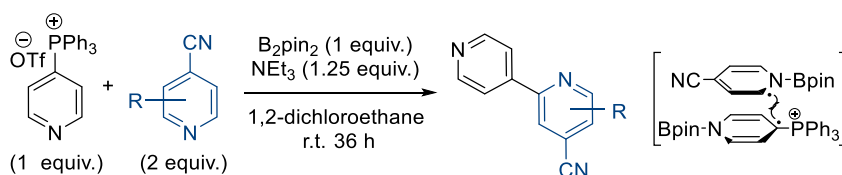
Scheme 12. Li's mechanistic proposal for the 4-cyanopyridines functionalization.

In parallel to Li's investigations, other groups developed several methods to obtain substituted pyridines and isoquinolines through the utilization of pyridine-boryl complexes. For example, in 2017 the group of Tang reported a highly diastereo and enantioselective reductive coupling of isoquinolines.¹⁵⁰ Through this novel method, they could obtain chiral substituted bisoquinolines with very good enantiomeric excesses and under mild conditions (Scheme 13a). The key to this selective process resides on the utilization of a chiral diboron reagent.

a) Tang et al, 2017



b) McNally et al, 2019



Scheme 13. Pyridine-boryl complexes promoted pyridine functionalization methods.

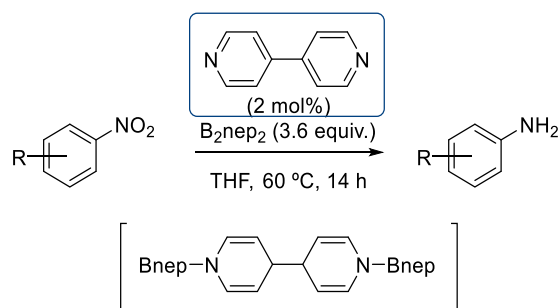
Years later, McNally and coworkers developed a pyridine-pyridine cross-coupling method using pyridine phosphonium salts and 4-

¹⁵⁰ Chen, D.; Xu, G.; Zhou, Q.; Chung, L. W.; Tang, W. *J. Am. Chem. Soc.* **2017**, *139*, 9767.

cyanopyridines as substrates (Scheme 13b).¹⁵¹ The use of the phosphonium salt as radical precursor allowed them to obtain the 2,4'-bipyridines in a regioselective fashion through a radical-radical coupling.

1.1.2. Diboron derivatives in deoxygenation of N-O bonds.

Although pyridine functionalization reactions constitute one of the main studied topics using pyridine-boryl radicals, the versatility of these substrates go even further. As introduced in Li's first work,¹⁴⁰ pyridine-boryl radicals can also be employed in reduction reactions. A good example of the utilization of these substrates as reducing systems was published in 2019 by Suginome and coworkers.¹⁵² Herein, they demonstrated that the addition of only a 2 mol% of 4,4'-bipyridine was enough to afford the reduction of a wide variety of nitroarenes to the corresponding anilines with very good yields (Scheme 14).



Scheme 14. Suginome's pyridine-boryl radical promoted reduction of nitroarenes.

¹⁵¹ Koniarczyk, J. L.; Greenwood, J. W.; Alegre-Requena, J. V.; Paton, R. S.; McNally, A. *Angew. Chem. Int. Ed.* **2019**, *58*, 14882.

¹⁵² Hosoya, H.; Misal Castro, L. C.; Sultan, I.; Nakajima, Y.; Ohmura, T.; Sato, K.; Tsurugi, H.; Suginome, M.; Mashima, K. *Org. Lett.* **2019**, *21*, 9812.

In this report, they made a great effort to identify the reaction intermediates, proposing a bis-boryl-pyridine intermediate and getting to the conclusion that the deoxygenation of the nitro group is favored by the formation of the nepB-O-Bnep product. Nevertheless, recent studies based on Suginome's work revealed that the intermediate involved in the reaction could be a pyridine-boryl radical with only one Bnep fragment attached to the bipyridine instead of two (figure 1).¹⁵³

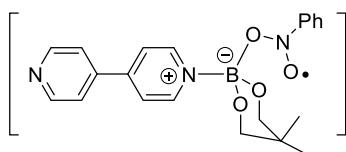


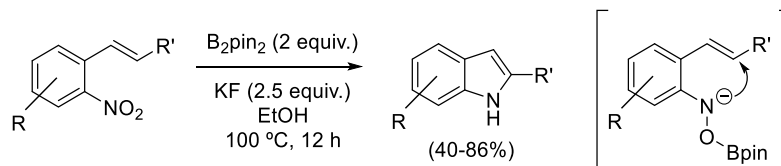
Figure 1. Jiao's proposed intermediate for the reduction of nitroarenes.

It is important to remark that diboron reagents have also been used to reduce nitro derivatives without the need of pyridine catalysts. Such is the case of the group of Song, which in 2016 reported the diboron mediated deoxygenation of *o*-nitrostyrenes to afford indoles (Scheme 15a).¹⁵⁴ Herein, authors postulate that a first deoxygenation of the nitro group by the B₂pin₂ leads to the nitrosyl anion, which in the presence of the vicinal alkene affords the final indole derivative through a 6-electron-5-atom electrocyclicization.

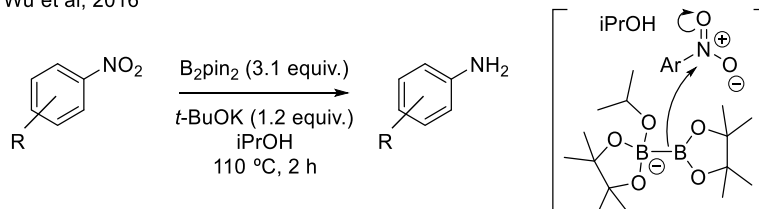
¹⁵³ Qi, J.-Q.; Jiao, L. *J. Org. Chem.* **2020**, *85*, 13877.

¹⁵⁴ Yang, K.; Zhou, F.; Kuang, Z.; Gao, G.; Driver, T. G.; Song, Q. *Org. Lett.* **2016**, *18*, 4088.

a) Song et al, 2016



b) Wu et al, 2016

**Scheme 15.** Diboron mediated reductions of nitroarenes.

The same year Wu and coworkers described the reduction of nitroaromatic compounds to the corresponding anilines using B₂pin₂ and *t*-BuOK in isopropanol.¹⁵⁵ They remark the crucial role of the base activating the diboron reagent through a boron-ate complex, as no reactivity is observed in the absence of the alkoxide. (Scheme 15b)

Due to the interest generated by these methods using diborons as reducing agents under metal free conditions, another research groups developed variations such as the reduction of nitroaromatics with B₂(OH)₄ in water,¹⁵⁶ or the DNA-compatible reduction protocol of nitroarenes and nitroalkanes using also B₂(OH)₄.¹⁵⁷

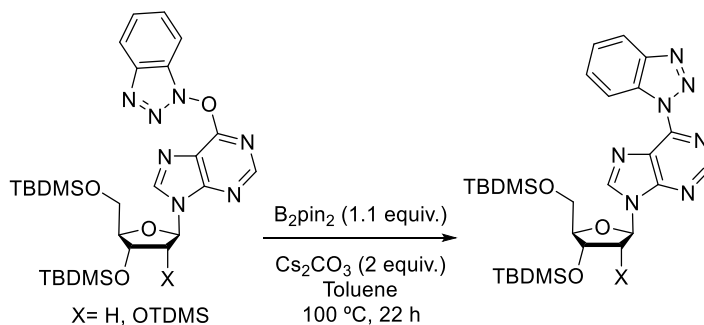
Interestingly, diboron compounds have also been described as effective reagents to break N-O bonds in other functional groups different from nitroderivatives. In 2008, Lakshman and coworkers reported the effective deoxygenation of inosine derivatives promoted

¹⁵⁵ Lu, H.; Geng, Z.; Li, J.; Zou, D.; Wu, Y.; Wu, Y. *Org. Lett.* **2016**, *18*, 2774.

¹⁵⁶ Chen, D.; Zhou, Y.; Zhou, H.; Liu, S.; Liu, Q.; Zhang, K.; Uozumi, Y. *Synlett.* **2018**, *29*, 1765.

¹⁵⁷ Du, H.-C.; Simmons, N.; Faver, J. C.; Yu, Z.; Palaniappan, M.; Riehle, K.; Matzuk, M. M. *Org. Lett.* **2019**, *21*, 2194.

by B_2pin_2 (Scheme 16).¹⁵⁸ They observed that the addition of 1.1 equivalents of B_2pin_2 in presence of Cs_2CO_3 led to the rearrangement of the N-O-C bond to afford a new N-C bond.

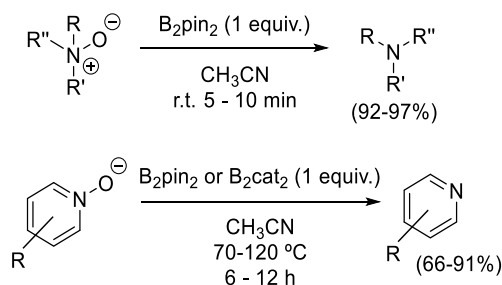


Scheme 16. Lakshman's first approach to the N-O bond reduction using B_2pin_2 .

This unexpected oxygen cleavage led the group of Lakshman to continue studying the reactivity of diboron compounds in the N-O reduction. As a result, three years later they reported the reduction of amines and pyridine *N*-oxides by diboron reagents in the absence of any additive (Scheme 17).¹⁵⁹ They pointed out that the reduction of pyridine *N*-oxides turns to be more difficult and need harsher reaction conditions. In some cases, they even needed to use a stronger Lewis acidic diboron compound (B_2cat_2) to afford the reaction. Being especially reluctant those pyridines with EWG such as a nitro group.

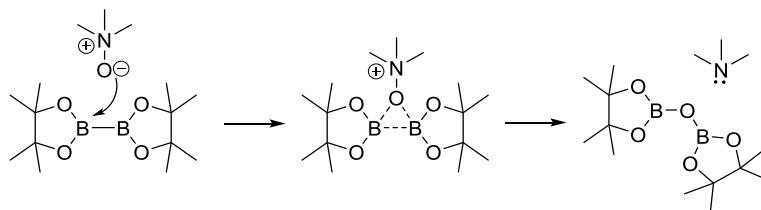
¹⁵⁸ Bae, S.; Lakshman L. K. *J. Org. Chem.* **2008**, *73*, 1311.

¹⁵⁹ Kokatla, H. P.; Thomson, P. F.; Bae, S.; Doddi, V. R.; Lakshman, M. K. *J. Org. Chem.* **2011**, *76*, 7842.



Scheme 17. Lakshman's diboron promoted reduction of pyridine and amine *N*-Oxides.

When they followed the reaction through ^{11}B -NMR experiments they detected the formation of pinB-O-Bpin. With this information they proposed a plausible mechanism in which the oxygen of the *N*-oxide reacts with the diboron compound followed by the liberation of the amine (Scheme 18).



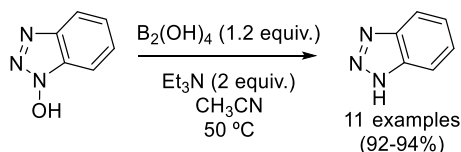
Scheme 18. Proposed mechanism for the B_2pin_2 mediated *N*-oxide reduction.

The simple and mild reaction conditions found by Lakshman for the reduction of *N*-oxides caught the attention of researchers at that time.¹⁶⁰ For example, the group of Bertozzi studied in 2016 the bioorthogonal application of this reaction in cells, finding biocompatible conditions.¹⁶¹ Moreover, this protocol was found later by the same group to be effective in the dehydroxylation of 1-hydroxy-

¹⁶⁰ Londregan, A. T.; Piotrowski, D. W.; Xiao, J. *Synlett*. **2013**, 24, 2695.

¹⁶¹ Kim, J.; Bertozzi, C. R. *Angew. Chem. Int. Ed.* **2015**, 54, 15777.

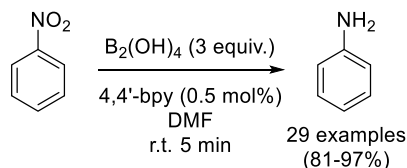
1-*H*-benzotriazoles using either B_2pin_2 or $B_2(OH)_4$ to access benzotriazoles (Scheme 19).¹⁶²



Scheme 19. Lakshman reduction of hydroxybenzotriazoles.

Other functional groups have also been reduced using diboron compounds. For example, B_2cat_2 have been used to reduce sulfoxides to sulfides,¹⁶³ and B_2pin_2 under visible-light promoted hydrogenation of azobenzenes to hydrazobenzenes.¹⁶⁴

A final example of the use of dirobon reagents as reductants was recently published by Han and coworkers.¹⁶⁵ In their report, they developed a chemoselective method for the reduction of nitroaromatics into anilines using $B_2(OH)_4$ and 4,4'-bipyridine as organocatalyst (Scheme 20). Through this methodology, authors demonstrated that the addition of the bipyridine enhances the reducing power of the diboron species. Although the mechanism is unclear, they discarded the presence of radical intermediates.



Scheme 20. Han's reduction of nitroarenes with $B_2(OH)_4$ and 4,4'-bpy.

¹⁶² Gurram, V.; Akula, H. K.; Garlapati, R.; Pottabathini, N.; Lakshman, M. K. *Adv. Synth. Catal.* **2015**, 357, 451.

¹⁶³ Takahashi, F.; Nori, K.; Yorimitsu, H. *Eur. J. Org. Chem.* **2020**, 3009.

¹⁶⁴ Song, M.; Zhou, H.; Wang, G.; Ma, B.; Jiang, Y.; Yang, J.; Huo, C.; Wang, X. *J. Org. Chem.* **2021**, 86, 4804

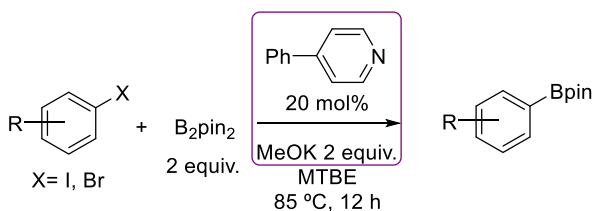
¹⁶⁵ Jang, M.; Lim, T.; Park, B. Y.; Han, M. S. *J. Org. Chem.* **2022**, 87, 910.

These reports remark the potential of diboron reagents as reducing agents in metal free protocols. At the same time, the variability of substrates reported suggests that diboron compounds could also act as reductants of other unexplored functional groups.

1.1.3. Super Electron Donors based on pyridine-boryl complexes

As mentioned in this introduction, SET processes are present in a wide variety of transformations. The term of organic super electron donor (SED) could be applied to those highly reactive organic species with strong reducing power. The use of these species has gained considerable attention as a more sustainable and tunable alternative to the use of metal-based reagents.

SEDs derived from pyridine-boryl complexes were described by Jiao and coworkers in the context of metal free conditions to efficiently borylate aromatic iodides and bromides by the addition of B_2pin_2 , 4-phenyl pyridine and KOMe (Scheme 21).¹⁶⁶



Scheme 21. Jiao's procedure for the aromatic halide borylation.

In the publication, the authors propose the formation of an aryl radical intermediate, formed from a SET process between the aryl halide and a "persistent radical" resulting from the mixture of the diboron, pyridine and base. Although the radical nature of the mechanism involved in the reaction was ensured by radical trapping

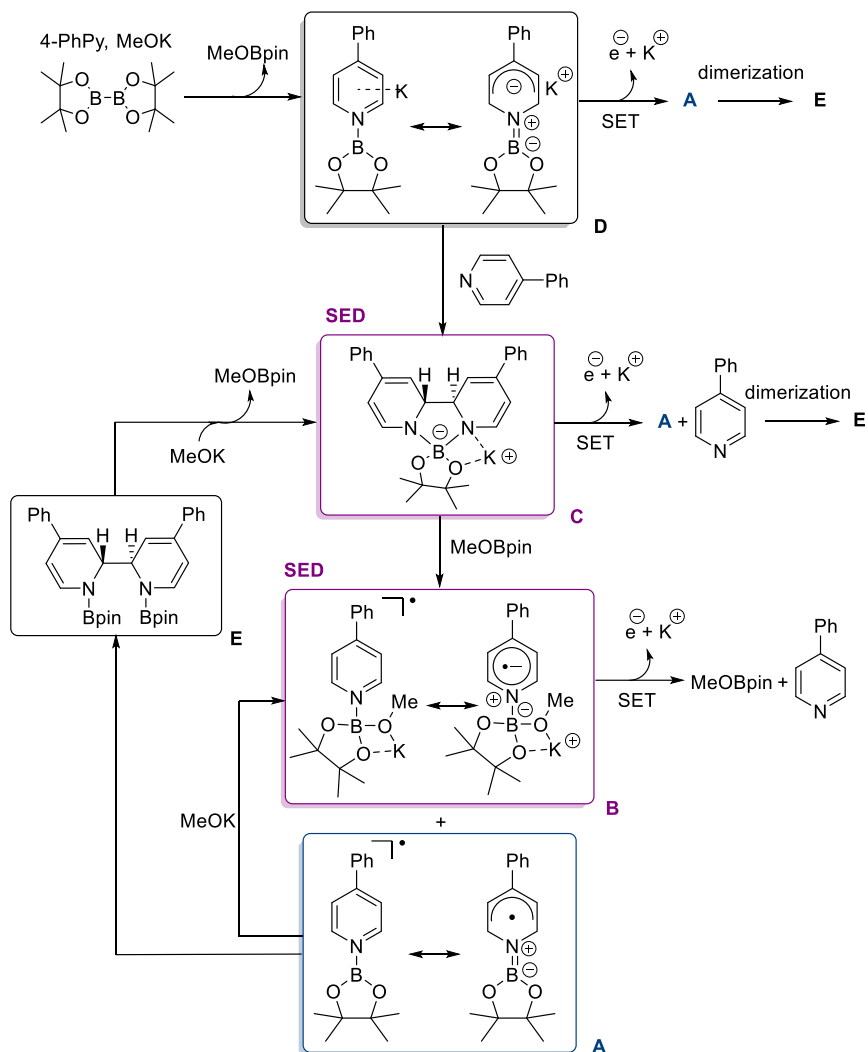
¹⁶⁶ Zhang, L.; Jiao, L. *J. Am. Chem. Soc.* **2017**, *139*, 607.

and EPR experiments, the structure of the intermediates responsible of the processes was not so clear.

Conscious of the potential of this methodology, Jiao and coworkers performed a deep study about the nature of the intermediate species involved in the borylation reaction. As a result, in 2018 they published a detailed analysis supported by theoretical calculations and experimental facts where they identified intermediates **B** and **C** as the intermediates able to act as super electron donors.¹⁶⁷ In this publication, they included an extensive mechanistic study which is summarize in Scheme 22.

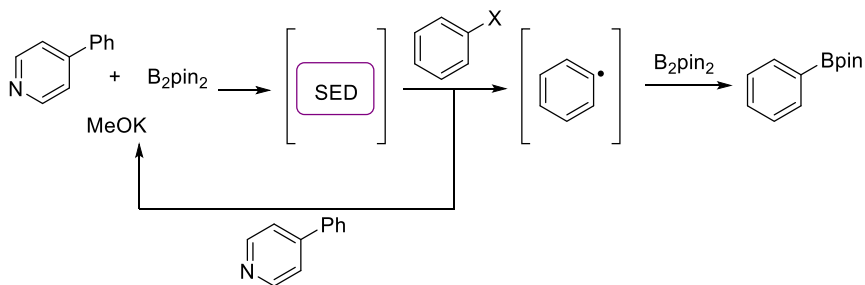
As can be observed in the mechanism, the formation of the SED intermediates implies the participation of the three components: diboron, pyridine and base, unlike pyridine-boryl radicals catalyzed processes where the absence of base leads the reactions through other mechanisms. In this publication, authors carried out the cyclic voltammetry of the reaction mixture and they got a reduction potential value of -1.1 V vs Fc^{+/0}, supporting the theory about the SED nature of these species. Thus, the role of the SED intermediates in the borylation reaction is the generation of the aryl radical.

¹⁶⁷ Zhang, L.; Jiao, L. *Chem. Sci.* **2018**, *9*, 2711.



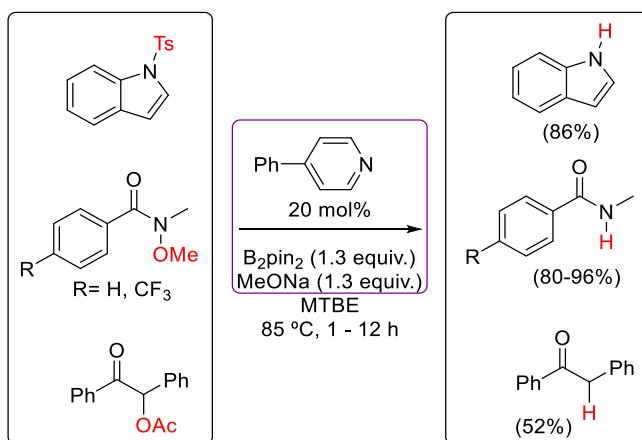
Scheme 22. SED intermediates and mechanism proposed by Jiao.

However, the introduction of the pinacol boronic ester moiety step is attributed to the B_2pin_2 as borylating agent and not to any of the pyridine-boryl complex intermediates (Scheme 23).



Scheme 23. Mechanism proposed for Jiao's super electron donor catalyzed borylation reaction.

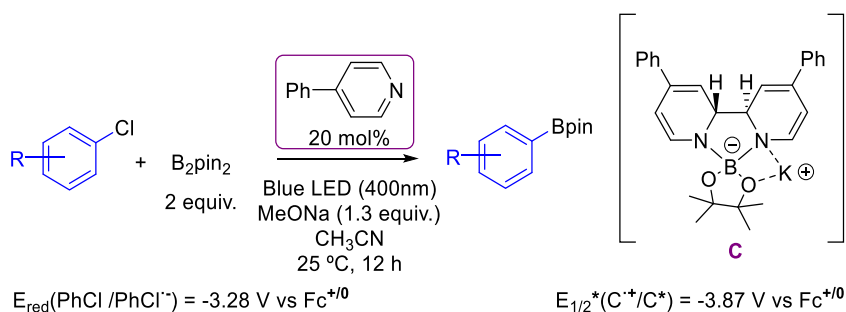
As a proof of the reducing power of these super electron donors, they also employed their optimized borylation conditions to the reductive cleavage of different substrates (Scheme 24).



Scheme 24. Jiao's reduction reactions using super electron donors.

Understanding the mechanism gave Jiao's group the opportunity to extend this chemistry to the borylation of other substrates, such as the borylation of more challenging aromatic chlorides (Scheme 25).¹⁶⁸

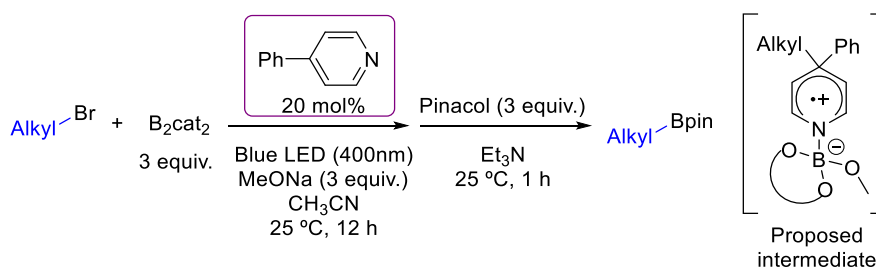
¹⁶⁸ Zhang, L.; Jiao, L. *J. Am. Chem. Soc.* **2019**, *141*, 9124.



Scheme 25. Jiao's borylation of aryl chlorides using super electron donors.

Having established the ability of SED's to borylate aromatic bromides, Jiao studied the oxidation potential of the SED intermediates under photoexcitation. As a result, he found that using visible light the SED mixture was able to efficiently generate the aryl radical and then borylate a wide range of aliphatic chlorides with good yields.

The same year, Jiao's group also developed the borylation of aliphatic halides under similar conditions than the previous aryl chlorides. However, to afford this transformation they needed to employ a more reactive diboron species such as B_2cat_2 as well as the use of light as promoter of the electron transfer step (Scheme 26).¹⁶⁹



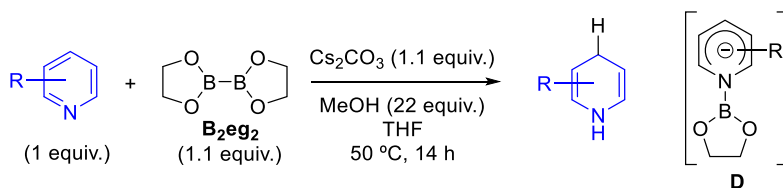
Scheme 26. Jiao's borylation of aliphatic halides using super electron donors.

In this case, the reaction mechanism is quite different than the aromatic halides. Authors propose that after the generation of the alkyl

¹⁶⁹ Zhang, L.; Wu, Z. Q.; Jiao, L. *Angew. Chem. Int. Ed.* **2019**, *58*, 1.

radical by the SED mixture, this radical incorporates to intermediate **B** (proposed intermediate) in a similar manner as described in the pyridine functionalization reactions (see Scheme 11). Nevertheless, with a phenyl substituent instead of a CN in the C4 position of the pyridine, is the alkyl radical who exits this intermediate to later react with the B_2cat_2 instead of the phenyl group.

All the information gathered by Jiao about these pyridine-boryl derived SEDs allowed him to also identify the anionic species **D** (see Scheme 21), through which he accomplished the preparation of 1,4-dihydropyridines.¹⁷⁰ The evolution through intermediate **D** is favored by the use of a low hindered diboron reagent (B_2eg_2), an inorganic base, and MeOH as proton source (Scheme 27).

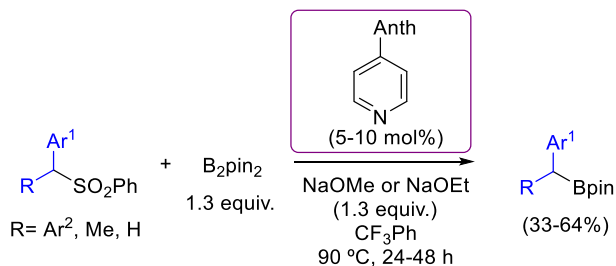


Scheme 27. Jiao's dihydropyridines synthesis.

The potential of the pyridine boryl complexes strategy developed by Jiao was also exploited by other authors to introduce boron containing moieties in different substrates. A recent publication where this methodology proves to be useful in other borylation reactions was reported by Crudden and coworkers in 2019.¹⁷¹ In this case, authors demonstrated that the use of a catalytic amount of 4-anthracylpyridine along with NaOMe or NaOEt, and B_2pin_2 , leads to the desulfonative borylation of benzyl sulfones (Scheme 28).

¹⁷⁰ Yang, H.; Zhang, L.; Zhou, F. Y.; Jiao, L. *Chem. Sci.* **2020**, *11*, 742.

¹⁷¹ Maekawa, Y.; Ariki, Z. T.; Nambo, M.; Crudden, C. M. *Org. Biomol. Chem.*, **2019**, *17*, 7300.



Scheme 28. Crudden's SED catalyzed desulfonative borylation.

As described in Jiao's borylation examples, the desulfonation step is also triggered by a SET reaction promoted by the SED pyridine-boryl complex. Next, authors proposed that the benzyl radical reacts with a MeOBpin molecule generated throughout the process to afford the borylated product.

Although the utilization of the pyridine-boryl complexes as super electron donors proves to be an efficient and modern strategy, it is still in its infancy. As can be seen, their utilization has been mainly limited to the borylation reaction of different substrates.

Nevertheless, we consider the area of this type of SED has a great potential. Many fundamental organic transformations, mainly redox reactions and those that imply radical intermediates, take place through a single-electron transfer (SET) process.¹⁷² Thus, the development of versatile electron donors, able to promote SET processes in an efficient and general way, as well as compatible with a variety of functional groups, is a topic of great interest.

Proof of the potential of the pyridine-boryl derived SEDs promoting SET processes is the existence of other organic molecules previously

¹⁷² Chatgililoglu, C.; Studer, A. *Encyclopedia of Radicals in Chemistry, Biology and Materials*, ed.; Wiley, New York, 2012.

described employed in alternative transformations. In fact, the first family of organic compounds considered as SED was described by Murphy's group in 2005.¹⁷³ They are based on neutral organic structures mainly composed by nitrogenated groups, which show a strong reducing character. Within his original publication, Murphy employed TDAE (1,1,2,2-tetra-(dimethylamine)ethene) as promoter of the intramolecular radical cyclization reaction of aromatic iodides with olefins, demonstrating the potential of these species in radical processes. The ability of these neutral organic electron donors to give electrons is based first on the aromatization energy residing in the radical cation, which partially restores the aromaticity of the molecule. And second, on the stabilization of the cation by the adjacent nitrogen atoms (figure 2).

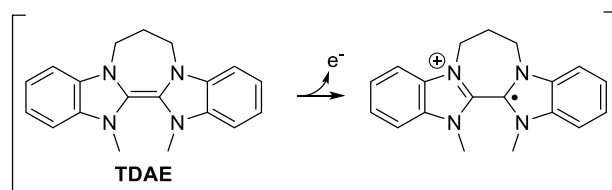


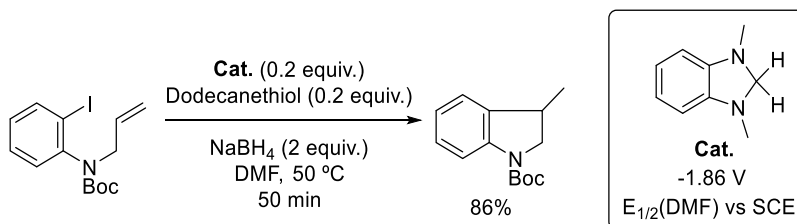
Figure 2. Stabilization of the radical cation intermediate in the TDAE structure.

Over the following years, Murphy's group kept studying the reactivity of these organic electron donors and found new applications, mainly as catalysts in dehalogenative couplings.¹⁷⁴ Recently, they published a "next-gen" neutral organic SED that can be used in catalytic

¹⁷³ Mahesh, M.; Thomson, D. W.; Zhou, S. Z.; Khan, T. A.; Murphy, J. A. *Angew. Chem. Int. Ed.* **2005**, *44*, 1356.

¹⁷⁴ a) Murphy, J. A.; Zhou, S.; Thomson, D. W.; Schoenebeck, F.; Mahesh, M.; Park, S. R.; Tuttle, T.; Berlouis, L. E. A. *Angew. Chem. Int. Ed.* **2007**, *46*, 5178. b) Zhou, S.; Anderson, G. M.; Mondal, B.; Doni, E.; Ironmonger, V.; Kranz, M.; Tuttle, T.; Murphy, J. A. *Chem. Sci.* **2014**, *5*, 476. c) Murphy, J. A. *J. Org. Chem.* **2014**, *79*, 3731. d) Balharm, J. P.; Coulthard, G.; Kane, R. G.; Delgado, N.; John, M. P.; Murphy, J. A. *Angew. Chem. Int. Ed.* **2016**, *55*, 4492.

amount in a previously reported intramolecular radical cyclization reaction (Scheme 29).¹⁷⁵



Scheme 29. Murphy's example of SED catalyzed radical reaction.

The main limitation of the utilization of this super electron donor as catalyst resides in the need of an external reductant addition (NaBH_4) to regenerate the catalyst. The specific reaction conditions found to employ this electron donors in catalytic fashion have limited their use in different reactions until date. However, despite the narrow range of application of the neutral organic SEDs, the reduction potential (showed in figure 2) point out that super electron donors could be employed in a wider type of reactions.

Organic Super Electron Donors

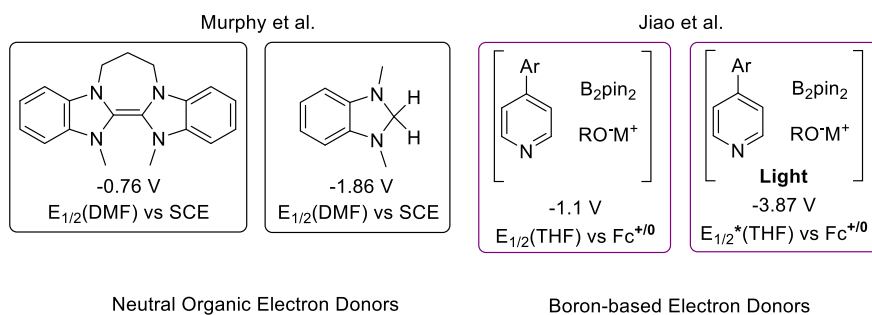


Figure 3. Different organic Super Electron Donors.

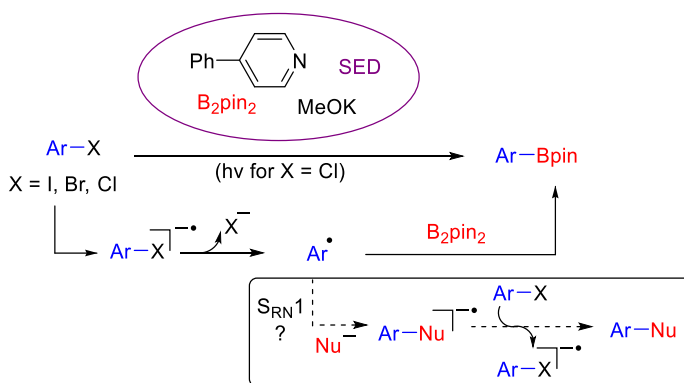
¹⁷⁵ Rohrbach, S.; Shah, R. S.; Tuttle, T.; Murphy, J. A. *Angew. Chem. Int. Ed.* **2019**, *58*, 11454.

2. Objectives

From the outset of our investigations, our goal was to expand the utility of Super Electron Donors (SEDs) derived from pyridine-boryl complexes to other reactions that not necessarily involve borylations. They present significant advantages as they are generated in situ from readily available reagents. In this sense, their general use in a reaction different from a borylation would be a significant advance in this field.

Chapter 2. Coupling of Thiols and Aromatic Halides Catalyzed by Pyridine-boryl Super Electron Donors

According to the background presented in the previous section, and given the outstanding ability found for the super electron donors derived from the pyridine-boryl complexes to afford aryl radicals, we envisioned that their employment in a different transformation apart from the borylation through a $S_{RN}1$ mechanism would be of interest (Scheme 30).



Scheme 30. Application of the SED promoted aryl radical formation to other reactions.

In this context, a useful reaction such as the C-S coupling of aryl thiolates as nucleophiles and aryl halides would be a very interesting

contribution. The development of this method would provide not only another application to the boron-based SEDs, but also it may provide a useful tool to form C-S bonds.

Therefore, our main objective for the **second chapter** will be checking the viability of the super electron donors strategy in the thiol-halide coupling reaction through a $S_{RN}1$ mechanism, finding a general method to obtain diaryl sulfides under metal free and mild conditions (Scheme 31).



Scheme 31. General approach for the SED catalyzed C-S coupling reaction.

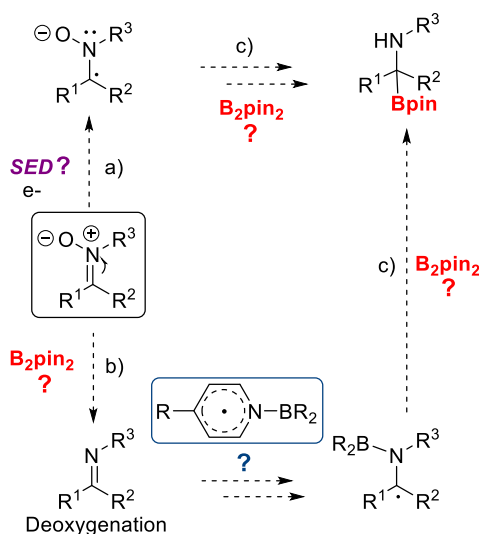
Chapter 3. Study of the Reactivity of Nitrones Using Different Diboron Containing Systems

Nitrones are very versatile, easy to prepare, and stable substrates, with a well-known ability to accept electrons and radicals. Therefore, we wondered if nitrones could be prone to react with diboron reagents, pyridine-boryl radicals or boron based SEDs to afford useful transformations. We initially considered nitrones as iminium subrogates susceptible of undergoing borylation through different possible approaches to provide chemically and biologically useful α -aminoboronic acid derivatives. Nevertheless, we recognize it is difficult to predict the evolution of nitrones when treated with these reagents (Scheme 32). A priori, several options could be possible.

a) Nitrones could accept the electron from the SED (B-C) and the corresponding anion radical strategically trapped.

b) Although the reduction of nitrones using diboron reagents has not been reported, we cannot discard this process as it is described the ability of the diboron reagents to afford the deoxygenation of several substrates such as amine and pyridine *N*-oxides. Moreover, pyridine-boryl radicals have also been described as efficient reducing agents for nitroarenes among others.

c) In a similar way to the reaction shown in scheme 8, the reaction of nitrones or the resulting imines with the pyridine-boryl radicals (C) could provide radicals which could evolve towards α -aminoboronates in the presence of an excess of diboron reagent or being trapped with an electrophile.



Scheme 32. Possible evolution of nitrones when treated with diboron containing systems.

Therefore, the main objective of the **third chapter** will be the thorough evaluation of the reactivity of nitrones with diboron reagents, including pyridine-boryl radicals, and super electron donors. This systematic study would allow us to assess the possibility to develop interesting transformations.

Part II. Chapter 2. Coupling of thiols and aromatic halides catalyzed by pyridine-boryl super electron donors

Chapter 2. Coupling of thiols and aromatic halides catalyzed by pyridine-boryl super electron donors

2.1. Introduction

As detailed in the general introduction of this second part of the thesis, super electron donors derived from the union of pyridine-boryl complexes and alkoxides exhibit a great potential to generate aryl radicals. However, the scarce applications reported using this strategy are focused on the borylation of the radical intermediates. In order to expand the scope of utilization of these interesting compounds, we decided to apply this strategy to the C-S bond formation. In the following lines, we will discuss the reasons of the interest of this transformation as well as the most relevant examples to prepare these products.

2.1.1. The interest of aromatic thioethers

To summarize the history of these products and their preparation, this section is focused on the synthesis of the thioether moiety through the coupling of aromatic halides and thiophenols in a chronological order, paying special attention on the modern methods described under metal free conditions.

The thioether formation reactions are important processes for the pharmaceutical and agrochemical industries since the C-S bond is widely encountered in many bioactive molecules.¹⁷⁶ Plenty of examples can be found in the literature where this functionality is present in

¹⁷⁶ Dunbar, K. L.; Scharf, D. H.; Litomska, A.; Hertweck, C. *Chem. Rev.* **2017**, *117*, 5521.

compounds for Alzheimer treatment, Parkinson's disease, HIV or cancer.^{177,178} Among the different sulfur containing functional groups, aromatic thioethers are very valuable fragments in drug development. Examples of commercial products containing this moiety are Thymitaq, Axitinib and Seroquel,^{179,180} as well as some organic materials and polymers (Figure 4).¹⁸¹ Moreover, these thioethers can also be used as key precursors in the synthesis of other relevant functional groups in chemistry such as sulphoxides, sulphones, sulphinilimines and sulphoximines.¹⁸²

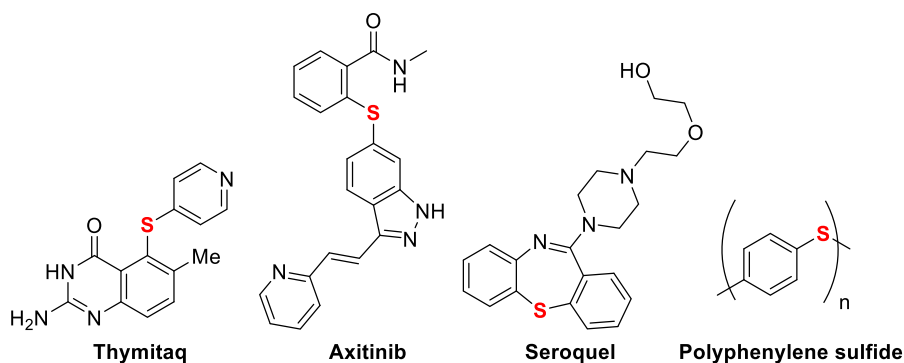


Figure 4. Important thiol containing drugs and polymers.

2.1.2. Methods to prepare diaryl thioethers

Due to their significant utility, aromatic thioether synthesis has been pursued by researchers since many years, being the direct coupling between an aromatic halide and a thiol the simplest way of

¹⁷⁷ Liu, G.; Huth, J. R.; Olejniczak, E. T.; Mendoza, R.; DeVries, P.; Leitz, S.; Reilly, E. B.; Okasinski, G. F.; Fesik, S. W.; von Geldern, T. W. *J. Med. Chem.* **2001**, *44*, 1202.

¹⁷⁸ Nielsen, S. F.; Nielsen, E. Ø.; Olsen, G. M.; Liljefors, T.; Peters, D. *J. Med. Chem.* **2000**, *43*, 2217.

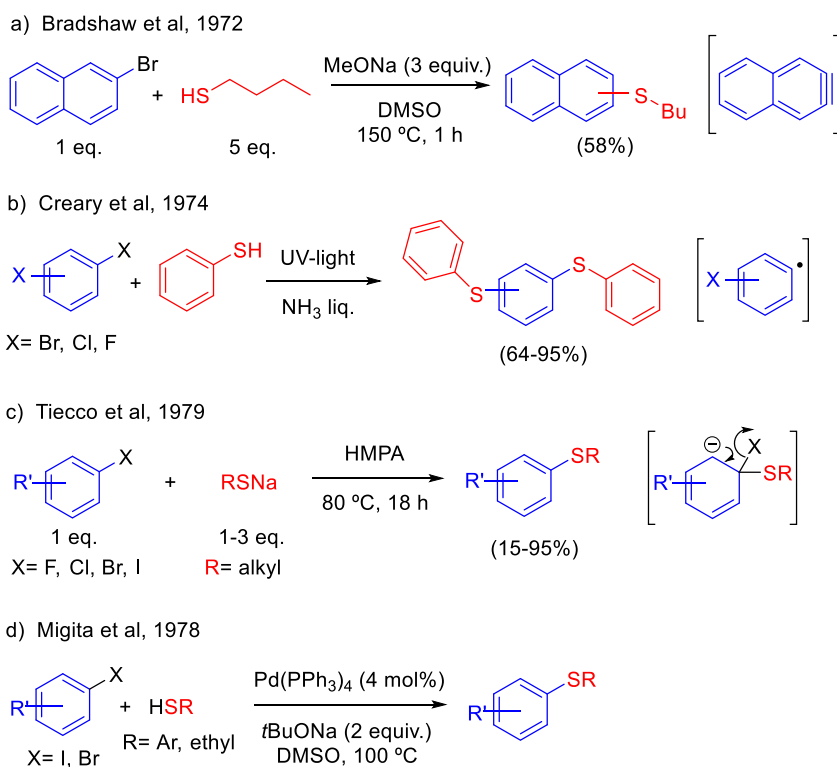
¹⁷⁹ Feng, M.; Tang, B.; Liang, S. H.; Jiang, X. *Curr Top Med Chem.* **2016**, *16*, 1200.

¹⁸⁰ Ilardi, E. A.; Vitaku, E.; Njardarson, J. T. *J. Med. Chem.* **2014**, *57*, 2832.

¹⁸¹ a) Iino, H.; Usui, T.; Hanna, J.-I. *Nat. Commun.*, **2015**, *6*, 6828. b) Boyd, D. A. *Angew. Chem., Int. Ed.* **2016**, *55*, 15486. c) Heine, N. B.; Studer, A. *Macrom. Rapid Commun.* **2016**, *37*, 1494.

¹⁸² *Advances in Sulfur Chemistry, Vol. 2* (Ed.: C. M. Rayner), JAI Press, Greenwich, CT, **2000**.

preparation. The first method involving the coupling of an aryl halide and a thiol was described by Bradshaw's group back in 1972 (Scheme 33a).¹⁸³ Herein, they proposed the use of an alkoxide as promoter of the coupling reaction between butylmercaptane and 2-bromonaphthalene through a benzyne intermediate, which leads to the regioisomer mixture.



Scheme 33. Initial methodologies in the C-S bond formation.

Two years later, a significative example was described by Creary and coworkers.¹⁸⁴ In their report, they could get to the complete disubstitution of aromatic dihalides with aryl thiols using UV light in liquid ammonia as solvent (Scheme 33b). The main feature of this

¹⁸³ Bradshaw, J. S.; Chen, E. Y.; Hales, R. H.; South, J. A. *J. Org. Chem.* **1972**, *37*, 2051.

¹⁸⁴ Bunnett, J. F.; Creary, X. *J. Org. Chem.* **1974**, *39*, 3173.

method was the regioselective substitution of the halides thanks to the formation of the corresponding aryl radicals, becoming the first example in the literature of a $S_{RN}1$ process applied to this transformation. However, this method was limited by its very harsh conditions, leading to a very poor functional group tolerance. Another remarkable example among the early reports was published by Tiecco and coworkers in 1979. In this publication they described the metal free coupling of alkyl thiolates with a variety of aryl halides in HMPA (hexamthylphosphoramidate) (Scheme 33c).¹⁸⁵ Years later, the same group demonstrated that this procedure worked with less toxic solvents such as DMF and DMA.¹⁸⁶ Although these first preparation procedures were described using metal free conditions, the publication of Migita's work in 1978 was crucial in the development of methods to prepare aryl thioether.¹⁸⁷ In their report, they demonstrated that the addition of a catalytic amount of a palladium(0) complex facilitates the formation of aryl thioethers from aryl halides and aryl or alkyl thiols, with a good functional group tolerance (Scheme 33d). Thanks to this publication, over the following years many research groups developed different metal catalyzed methods to obtain these products,¹⁸⁸ using

¹⁸⁵ Cogioli, P.; Maiolo, F.; Testaferri, L.; Tingoli, M.; Tiecco, M. *J. Org. Chem.* **1979**, *44*, 2642.

¹⁸⁶ Tiecco, M.; Testaferri, L.; Tingoli, M.; Chianelli, D.; Montanucci, M. *J. Org. Chem.* **1983**, *48*, 4289.

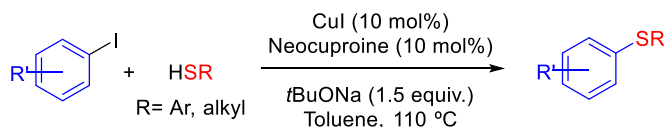
¹⁸⁷ Kosugi, M.; Shimizu, T.; Migita, T. *Chem Lett.* **1978**, 13.

¹⁸⁸ For a selection of reviews about transition metal catalyzed thioether formation see: a) Wendeborn, S.; Berteina, S.; Brill, W. K.-D.; De Mesmaeker, A. *Synlett*, **1998**, 671. b) Kondo, T.; Mitsudo, T. *Chem. Rev.* **2000**, *100*, 3205. c) Beletskaya, I. P.; Ananikov, V. P. *Chem. Rev.* **2011**, *111*, 1596. d) Lee, C-F; Basha, R. S.; Badsara, S. S. *Top. Curr. Chem.* **2018**, *376*(3), 1-45.

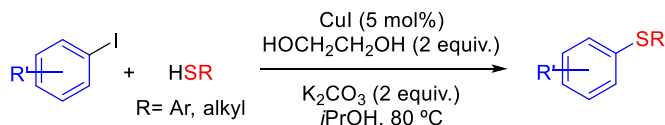
not only palladium catalysts but also other transition metals like nickel or platinum.^{189,190}

More recently in 2002, the groups of Buchwald and Venkataraman studied in parallel the use of much economic copper catalysts to obtain aromatic thioethers (Scheme 34a and 34b).^{191,192}

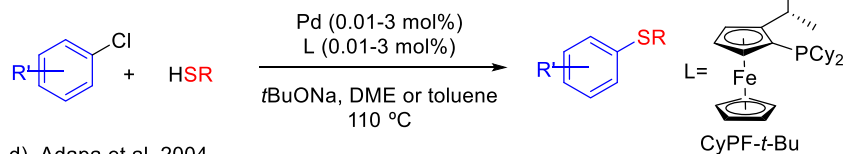
a) Buchwald et al, 2002



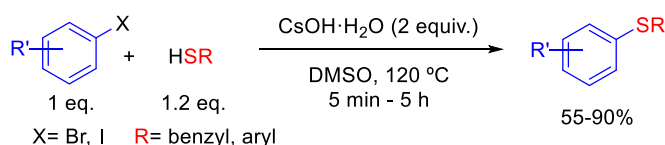
b) Venkataraman et al, 2002



c) Hartwig et al, 2006



d) Adapa et al, 2004



Scheme 34. Early 2000's methodologies in the C-S bond formation.

In their reports, authors described the use of copper iodide, a ligand, and a base, also at high temperatures, to couple aryl and alkyl thiols with aryl iodides. Later, an interesting input to this field was carried

¹⁸⁹ Takagi, K. *Chem. Lett.* **1987**, 2221.

¹⁹⁰ Page, P. C. B.; Klair, S. S.; Brown, M. P.; Harding, M. M.; Smith, C. S.; Maginn, S. J.; Mulley, S. *Tetrahedron Lett.* **1988**, 29, 4477.

¹⁹¹ Bates C. G.; Gujadhur R. K.; Venkataraman D. *Org. Lett.* **2002**, 4, 2803.

¹⁹² Kwong, F. Y.; Buchwald, S. L. *Org. Lett.* **2002**, 4, 3518.

out by the group of Hartwig in 2006.¹⁹³ In this example, the authors were able to develop an efficient (TON > 100) and general Pd(0) catalytic system. This method offered a great functional group tolerance and afforded the coupling reaction with halides, triflates and tosylates with good yields (Scheme 34c). A final remarkable example of this decade was published in 2004 by the group of Adapa. Herein, authors described the use of CsOH·H₂O as promoter of the coupling reaction between aromatic iodides and bromides with thiophenols under metal free conditions (Scheme 34d).¹⁹⁴ Although with a limited scope of the reaction and the use of high temperatures, they got to the products in relatively short reaction times.

Since Hartwig's and Buchwald's works, the scientific production around the C-S bond creation has experienced a great growth.¹⁹⁵

Moreover, the recent development of light driven reactions has also rendered interesting methods in C-S bond formation that, in many cases, imply thiyl radicals (RS·).¹⁹⁶ Some of these recent reports dealing with C-S bond formation under photocatalytic conditions are

¹⁹³ Fernández, M. A.; Shen, Q.; Hartwig, J. F. *J. Am. Chem. Soc.* **2006**, *128*, 2180.

¹⁹⁴ Varala, R.; Ramu, E.; Alam, M. M.; Adapa, S. R. *Chem. Lett.* **2004**, *33*, 1614.

¹⁹⁵ For selected examples see: a) Zhang, Y.; Ngeow, K. C.; Ying, J. Y. *Org. Lett.* **2007**, *9*, 3495. b) Shayah, M.; Organ, M. G. *Chem. Eur. J.* **2011**, *17*, 11719. c) Bastug, G.; Nolan, S. P. *J. Org. Chem.* **2013**, *78*, 9303. d) Venkanna, G. T.; Arman, H. D.; Tonzetich, Z. J. *ACS Catal.* **2014**, *4*, 2941. e) Scattolin, T.; Senol, E.; Yin, G.; Guo, Q.; Schoenebeck, F. *Angew. Chem. Int. Ed.* **2018**, *57*, 12425. f) Liu, D.; Ma, H. X.; Fang, P.; Mei, T.S. *Angew. Chem., Int. Ed.* **2019**, *58*, 5033. g) Panigrahi, R.; Sahu, S. K.; Behera, P. K.; Panda, S.; Rout, L. *Chem. Eur. J.* **2020**, *26*, 620. h) Bie, F.; Liu, X.; Cao, H.; Shi, Y.; Zhou, T.; Szostak, M.; Liu, C. *Org. Lett.* **2021**, *23*, 8098. i) Isshiki, R.; Kurosawa, M. B.; Muto, K.; Yamaguchi, J. *J. Am. Chem. Soc.* **2021**, *143*, 10333.

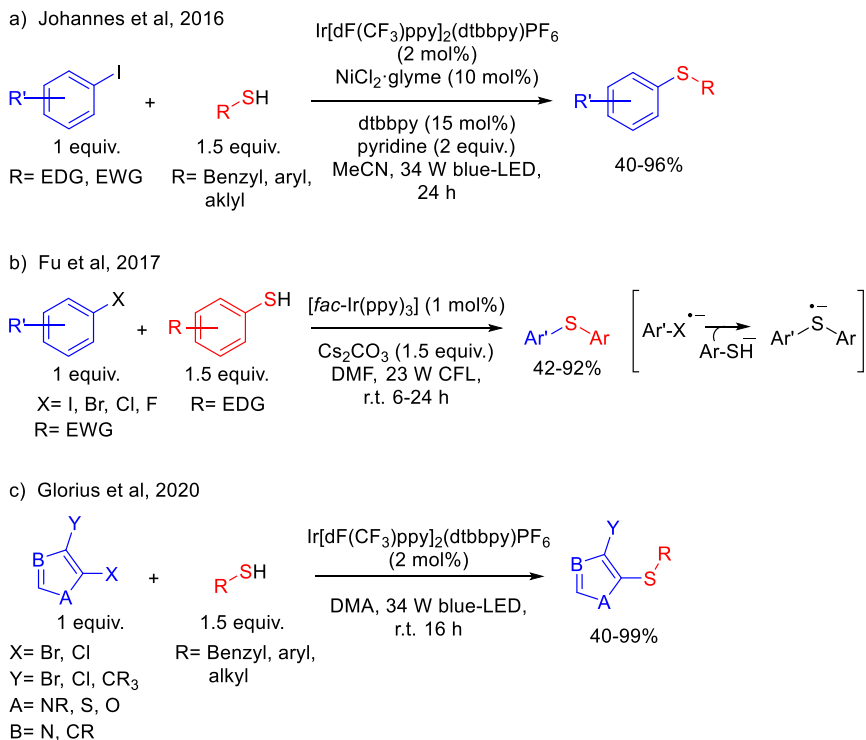
¹⁹⁶ For selected examples of photocatalyzed thioether formation see: a) Wang, X.; Cuny, G. D.; Noël, T. *Angew. Chem., Int. Ed.* **2013**, *52*, 7860. b) Jouffroy, M.; Kelly, C. B.; Molander, G. A. *Org. Lett.* **2016**, *18*, 876. c) Cavedon, C.; Seeberger, P. H.; Pieber, B. *Eur. J. Org. Chem.* **2019**, *1*, d) Guo, W.; Tao, K.; Tan, W.; Zhao, M.; Zheng, L.; Fan, X. *Org. Chem. Front.*, **2019**, *6*, 2048. e) Talukder, M. M.; Miller, J. T.; Cue, J. M. O.; Udumulle, C. M.; Bhadrans, A.; Biewer, M. C.; Stefan, M. C. *Organometallics*. **2021**, *40*, 83. f) Qin, Y.; Sun, R.; Gianoulis, N. P.; Nocera, D. G. *J. Am. Chem. Soc.* **2021**, *143*, 2005.

summarized in scheme 35. The first method where thiyl radicals were employed for their cross-coupling with iodoarenes was published by Johannes and coworkers in 2016 (Scheme 35a).¹⁹⁷ In their report, authors described the use of a dual catalytic system consisting of a nickel catalyst along with an iridium photocatalyst to efficiently couple benzyl and alkyl thiols with aryl halides.

A year later, the group of Fu developed a method using again an iridium photocatalyst to obtain diaryl thioethers through a thiyl intermediate (Scheme 35b).¹⁹⁸ Nevertheless, in this case authors focused on the coupling of aryl bromides and chlorides, which were elusive for Johannes's method. Also in this publication, they could get to the coupled products with no need of using a nickel cocatalyst, however, no benzylic or aliphatic thiols were used as coupling partners of the reaction. Although in their proposed mechanism authors included the formation of a thiyl radical as a consequence of the Ir(III) complex reduction, they pointed at the thiolate as the nucleophile of the radical nucleophilic substitution reaction with the aromatic radical anion.

¹⁹⁷ Oderinde, M. S.; Frenette, M.; Robbins, D. W.; Aquila, B.; Johannes, J. W. *J. Am. Chem. Soc.* **2016**, *138*, 1760.

¹⁹⁸ Jiang, M.; Li, H.; Yang, H.; Fu, H. *Angew. Chem., Int. Ed.* **2017**, *56*, 874.



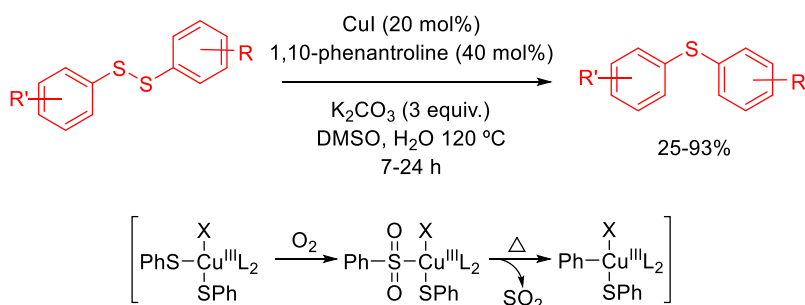
Scheme 35. Photocatalyzed C-S bond formation methods.

A final example related to photocatalyzed coupling methods was reported by the group of Glorius in 2020 (Scheme 35c).¹⁹⁹ Herein, they could couple a great variety of heteroaromatic bromides and chlorides with alkyl, benzyl and aryl thiols through a photocatalyzed process using an iridium catalyst. In their report, they proposed the homolytic aromatic substitution of the halides with thiyl radicals as the most plausible mechanism, sustained by competitive experiments and DFT studies.

As shown, an easy way to obtain aromatic thioethers from commercially available sources is the coupling of thiols with halides.

¹⁹⁹ Sandfort, F.; Knecht, T.; Pinkert, T.; Daniliuc, C. G.; Glorius, F. *J. Am. Chem. Soc.* **2020**, *142*, 6913.

Nevertheless, since the first works described by Bradshaw, many different methods have been published using different starting materials, like the employment of disulfides.^{200,201,202} A remarkable publication dealing with the use of these substrates was recently published by the group of Wang.²⁰³ In their work, they could get to a wide variety of diaryl sulfides and selenides, using a copper catalyst in DMSO, in the presence of K₂CO₃ as base (Scheme 36).



Scheme 36. Wang's copper catalyzed dechalcogenization of diaryl disulfides.

The authors propose the elimination of one of the sulfur atoms of the disulfide from the thermal elimination of a SO₂ molecule. This SO₂ moiety is previously formed by the oxidation of the thioether attached to the Cu(III) intermediate. The main drawback of this method resides in the need of previously synthesizing the symmetric or asymmetric disulfides.

²⁰⁰ Kumar, A.; Bhakuni, B. S.; Prasad, C. D.; Kumar, S.; Kumar, S. *Tetrahedron*. **2013**, *69*, 5383.

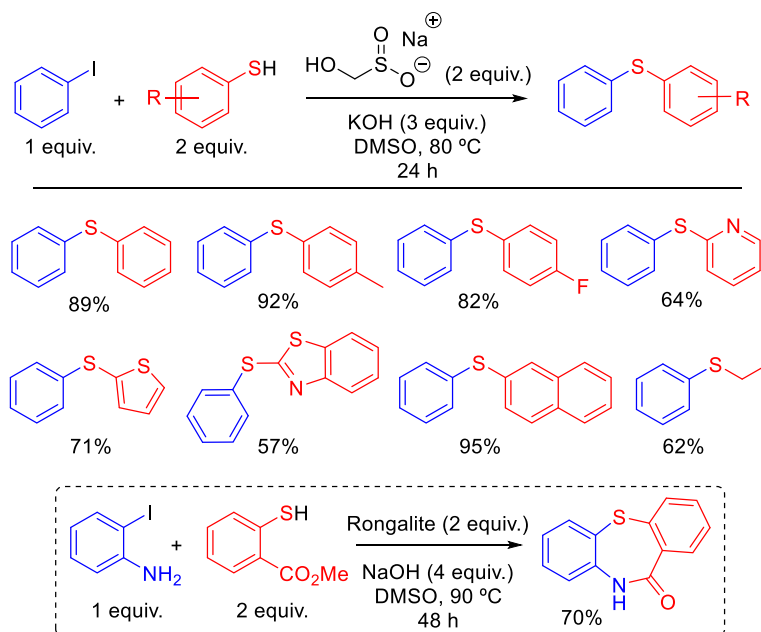
²⁰¹ Czyz, M. L.; Weragoda, G. K.; Monaghan, R.; Connell, T. U.; Brzozowski, M.; Scully, A. D.; Burton, J.; Lupton, D. W.; Polyzos, A. *Org. Biomol. Chem.*, **2018**, *16*, 1543.

²⁰² Landarani-Isfahani, A.; Mohammadpoor-Baltork, I.; Mirkhani, V.; Moghadam, M.; Tangestaninejad, S.; Rudbari, H. A. *RSC Adv.* **2020**, *10*, 21198.

²⁰³ Wang, Y.; Deng, J.; Chen, J.; Cao, F.; Hou, Y.; Yang, Y.; Deng, X.; Yang, J.; Wu, L.; Shao, X.; Shi, T.; Wang, Z. *ACS Catal.* **2020**, *10*, 2707.

Therefore, the generation of the diaryl thioether scaffold has been extensively studied over the years using very distinct strategies.²⁰⁴ Among all these methodologies previously reported we could highlight two recent publications due to the simplicity and versatility of the methods therein described.

One of the latest publications describing a metal free coupling of aryl halides and thiols was carried out by Wang and coworkers in 2019.²⁰⁵ Herein, they demonstrated that rongalite (sodium hydroxymethyl-sulfinate) could be used as radical promoter of the reaction (Scheme 37).

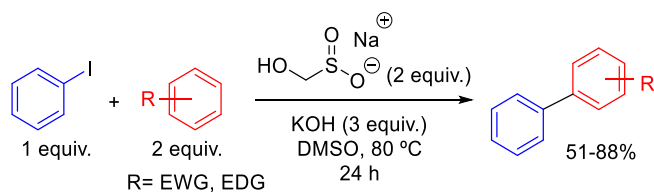


Scheme 37. Rongalite promoted radical coupling of aryl halides and thiols.

²⁰⁴ a) Fernández-Salas, J. A.; Pulis, A. P.; Procter, D. J. *Chem. Commun.*, **2016**, 52, 12364. b) Janhsen, B.; Daniliuc, C. G.; Studer, A. *Chem. Sci.* **2017**, 8, 3547. c) Xiong, B.; Xu, S.; Liu, Y.; Tang, K. W.; Wong, W. Y. *J. Org. Chem.* **2021**, 86, 1516.

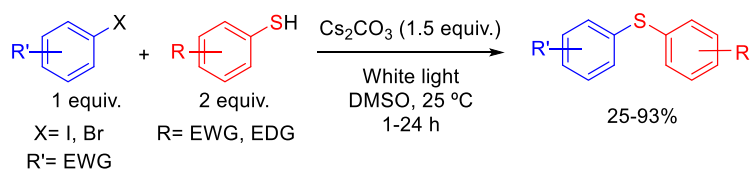
²⁰⁵ Yu, F.; Mao, R.; Yu, M.; Gu, X.; Wang, Y. *J. Org. Chem.* **2019**, 84, 9946.

Although the concept of the radical coupling present in this work is interesting, the narrow scope of the reaction could suggest a poor functional group tolerance maybe due to the harsh conditions employed. However, the ability of rongalite as electron donor proved to be also useful in the homolytic aromatic substitution of different arenes and heteroarenes, although with no regioselectivity (Scheme 38).



Scheme 38. Rongalite promoted radical coupling of aryl halides and arenes.

Finally, one of the most valued methods to get to the formation of these C-S bonds was described in 2017 by Miyake and coworkers.²⁰⁶ In their publication they achieved the coupling of aryl iodides and bromides with thiophenols promoted by white light in presence of cesium carbonate and DMSO (Scheme 39).

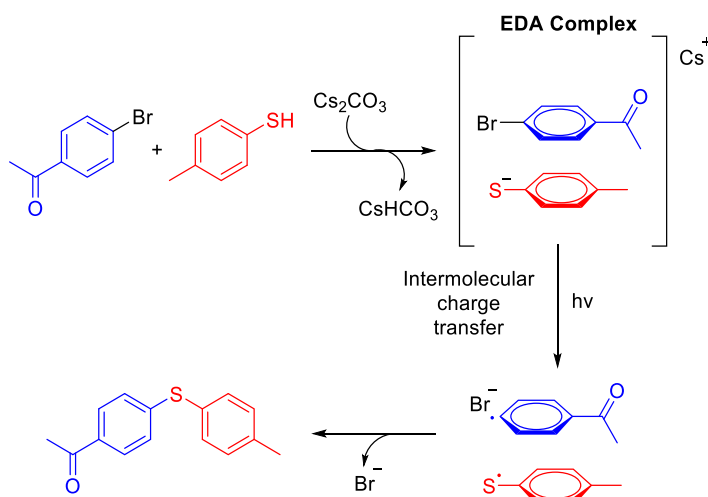


Scheme 39. Miyake's approach to aromatic thioethers.

With these reaction conditions, Miyake's group was able to synthesize diarylthioethers with good yields in absence of transition metal catalysts or the use of UV-light. This method allows the use of a wide variety of thiols and halides as starting materials, including heteroarenes in both fragments. Nevertheless, it is limited to aryl

²⁰⁶ Liu, B.; Lim, C. H.; Miyake G. M. *J. Am. Chem. Soc.* **2017**, *139*, 13616.

halides wearing EWG groups. The reason of these specific conditions is based on the mechanism ruling the reaction, which goes through an electron-donor-acceptor (EDA) complex (Scheme 40).^{207,208} In this EDA complex, the presence of light promotes the intermolecular charge transfer from the thiolate to the aromatic halide, generating a sulfur centered (thiyl) radical along with an aromatic radical. Finally, these two radicals collapse giving the desired aromatic thioether.



Scheme 40. Miyake's mechanistic proposal.

Despite of this limitation, Miyake's method represented not only a simple procedure to get to these interesting products, but also it was the first application of the EDA methodology to the C-S bond coupling.

²⁰⁷ Yuan, Y. Q.; Majumder, S.; Yang, M.; Guo, S. *Tetrahedron Lett.* **2020**, 61, 151506.

²⁰⁸ For a selection of reactions via EDA complex see: a) Arceo, E.; Jurberg, I. D.; Álvarez-Fernández, A.; Melchiorre, P. *Nat. Chem.* **2013**, 5, 750. b) Nappi, M.; Melchiorre, P. *Angew. Chem. Int. Ed.* **2014**, 53, 4921. c) Arceo, E.; Bahamonde, A.; Bergonzini, G.; Melchiorre, P. *Chem. Sci.* **2014**, 5, 2438. d) Tobisu, M.; Furukawa, T.; Chatani, N. *Chem. Lett.* **2013**, 42, 1203. e) Dohi, T.; Ito, M.; Yamaoka, N.; Morimoto, K. Fujioka, H.; Kita, Y. *Angew. Chem. Int. Ed.* **2010**, 49, 3334. f) Berionni, G.; Bertelle, P. A.; Marrot, J.; Goumont, R. *J. Am. Chem. Soc.* 2009, 131, 18224. g) Gotoh, T.; Padias, A. B.; Hall, J. H. *J. Am. Chem. Soc.* **1991**, 113, 1308. h) Crisenza, G. E. M.; Mazzarella, D.; Melchiorre, P. *J. Am. Chem. Soc.* **2020**, 142, 5461. i) Choudhuri, K.; Pramanik, M.; Mal, P. *J. Org. Chem.* **2020**, 85, 11997. k) McClain, E. J.; Monos, T. M.; Mori, M.; Beatty, J. W.; Stephenson, C. R. *J. ACS Catal.* **2020**, 10, 12636.

As could be expected, it made a great impact, and over the following years his publication gathered a great number of citations related to C-S bond formation reactions through metal free radical processes.²⁰⁹

With these precedents we reckoned that the use of diboron based super-electron-donors would provide a mild and complementary option to the existing methods to prepare thioethers. The discovery of these diboron-based SEDs is very recent and their synthetic potential is underdeveloped. They present significant advantages as they are generated in situ from readily available reagents. In this sense, their use in a reaction different from a borylation and particularly like **C-S** bond formation through a reaction of a **S_{RN}1** mechanism is a significant advance in both fields, the synthetic utility of pyridine-boryl complexes and a useful method in C-S bond formation.

²⁰⁹ a) Asadpour, M.; Azizzade, M.; Ghasemi, M.; Rajai-Daryasarei, S.; Jafarpour, F. *Synthesis* **2019**, *51*, A-H. b) Yang, M.; Cao, T.; Xu, T.; Liao, S. *Org. Lett.* **2019**, *21*, 8673. c) Blank, L.; Fagnoni, M.; Protti, S.; Rueping, M. *Synthesis* **2019**, *51*, 1243.

2.2. Results and discussion

According to Jiao's investigations, diboron-based SEDs have demonstrated to work efficiently in the borylation of aromatic halides. Thus, it is expected that one of the major difficulties when developing this method was to inhibit the borylation of the aryl radical intermediate.

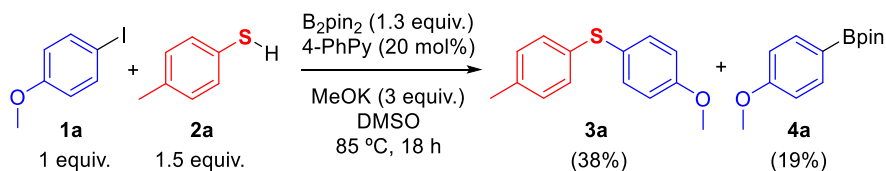
Additionally, we decided to test the C-S coupling reaction using 4-iodoanisole and 4-toluenethiol as model substrates because the combination of these two starting materials represents one of the mentioned limitations reported by Miyake's method.²⁰⁶

2.2.1. Optimization of the reaction

To begin our study of the reaction, we first tried conditions similar to those employed by Jiao for the borylation of aryl iodides (B_2pin_2 , MeOK, 85 °C)¹⁶⁶ but switching the solvent to DMSO. Although pyridine-boryl complexes can reduce sulfoxides to sulfides,¹⁴⁰ we decided to try DMSO as solvent at high concentration, as it is known to favor $S_{RN}1$ processes.^{210,211} We carried out the coupling reaction in presence of 4-phenylpyridine (4-PhPy) as catalyst, B_2pin_2 as boron source and MeOK as base. Under these conditions, we expected to generate the SED intermediates that catalyze the radical coupling reaction. The role of the base is double in these first attempts, forming the SED intermediate, and deprotonating the thiol. When we ran the reaction at 85 °C during 18 h we got the desired aromatic thioether **3a** with a 38% isolated yield (Scheme 41).

²¹⁰ D. A. Caminos, M. Puiatti, J. I. Bardagí and A. B. Peñéñory, *RSC Adv.*, **2017**, 7, 31148.

²¹¹ S. Rohe, G. Revol, T. Marmin, D. Barriault and L. Barriault, *J. Org. Chem.*, **2020**, 85, 2806.



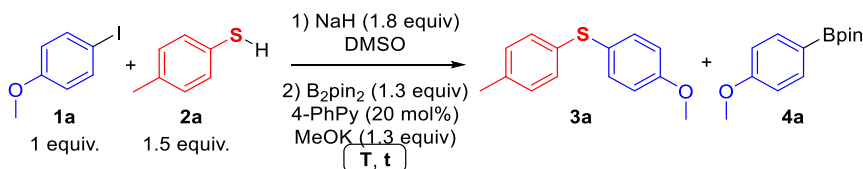
Scheme 41. First attempt for the SED catalyzed C-S coupling reaction.

Under these conditions the thioether **3a** was obtained along with the expected borylated product **4a** in a 2:1 ratio. Moreover, although the halide starting material is completely consumed under these conditions, the yield calculated by NMR of products **3a** and **4a** does not correlate to the 100% conversion, so there must be other competitive processes. We suspected that the low yield obtained could come from a protodehalogenation side reaction of the aromatic halide.²¹² The resulting anisole generated in this reaction could have passed unnoticed due to its volatility, losing it during the work up. On the other hand, the formation of this same product could also come from a protodeboronation event, which is known to occur under basic media at high temperatures.²¹³

Encouraged by the promising result obtained in the first attempt, we tried to focus on avoiding the borylation, as well as the possible protodehalogenation and/or protodeboronation side reactions. We evaluated the base needed for the deprotonation of the thiol by performing the reaction in a two-step one-pot reaction in which first we formed the thiolate using a small excess of NaH. Next, with the addition of the iodide along with the rest of the reagents, we obtained the coupled product **3a** with a 50% yield, minimizing the borylated product formation to a 6:1 ratio (Table 1, entry 1).

²¹² Niu, Y. J.; Siu, G. H.; Zheng, H. X.; Shan, X. H.; Tie, L.; Fu, J. L.; Qu, J. P.; Kang, Y. B. *J. Org. Chem.* **2019**, *84*, 10805.

²¹³ Kuang, Z.; Yang, K.; Zhou, Y.; Song, Q. *Chem. Commun.* **2020**, *56*, 6469.

Table 1. Time and temperature optimization performing the anion.

Entry	T (°C)	t (h)	Ratio 3a/4a	Conv (%) ^a	Yield 3a (%) ^b
1	85	18	6:1	100	50
2	50	15min	1:0	47	38
3	50	1	1:0	100	66
4	25	2.5	1:0	33	32
5	25	24	1:0	100	80 (68) ^c

^aConversions measured with ¹H-NMR compared to the remaining starting material. ^bYields measured by ¹H-NMR using nitromethane as internal standard. ^cYield in parentheses measured as isolated yield.

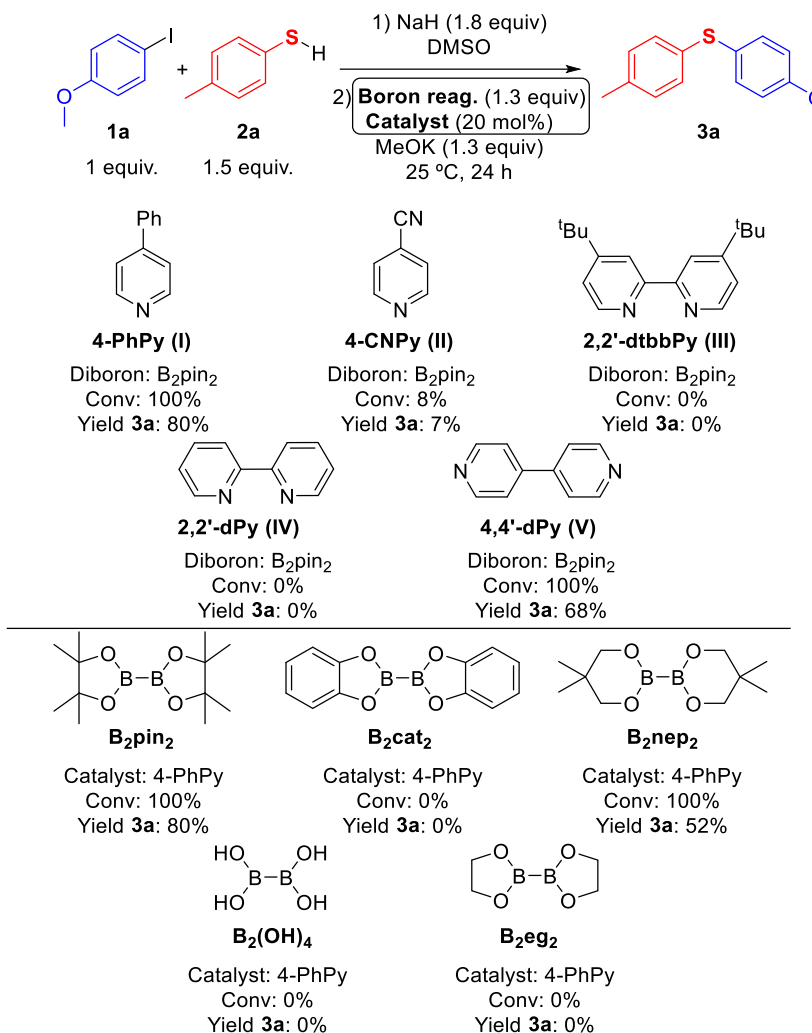
Then, we evaluated the effect of the temperature in the reaction outcome. We decreased the temperature to 50 °C and we noticed that the difference between the conversion of the starting material and the yield of **3a** was lower this time, narrowing the gap to only a 9% of possible anisole byproduct (entry 2). Moreover, at this temperature the presence of the borylated product **4a** reduced to zero. The increase of the reaction time to 1 hour led to full conversion of the iodide and a 66% yield of **3a** (entry 3). Considering the apparent secondary role of the temperature in the reaction, we carried out the reaction at room temperature. After 2.5 hours we observed almost no difference between conversion and yield (entry 4), and after 24 hours we obtained full conversion and 80% yield of product **3a** detected by NMR (entry 5). However, this yield dropped to a 68% when we isolated the product.

After optimizing the reaction time and temperature, we moved to evaluate the impact of the ratio of the different reagents in the reaction.

However, increasing the pyridine loading, the base amount, or the thiol ratio led to lower or very similar results (for more details see experimental section).

After identifying the optimal conditions with the initial reagents, we moved to study the effect of changing the pyridine catalyst and the boron source to the reaction (Scheme 42). The yields shown were calculated by ^1H NMR using an internal standard.

First, we tried the utilization of the 4-cyanopyridine (**II**), used by Li and coworkers in their first pyridine-boryl radicals' publication (see scheme 4).¹⁴⁰ In our case, the employment of pyridine **II** led to a very low product yield around 8%. Such a difference between the utilization of this 4-cyanopyridine (**II**) and the model 4-phenylpyridine (**I**) means that the electronic properties of the catalyst play a key role in the reaction. The catalytic activity of differently substituted dipyrindines was also tested. 4,4'-di-tert-butyl-2,2'-dipyridine (**III**) and 2,2'-dipyridine (**IV**) were not able to provide compound **3a**. When using 4,4'-dipyridine (**V**) as catalyst we obtained the desired product **3a** with good yield, although with a slightly lower yield compared to the model pyridine **I**.



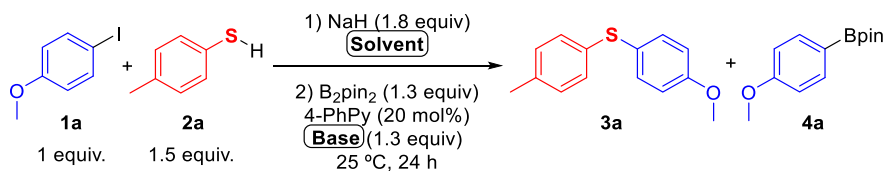
Scheme 42. Pyridine catalyst and boron source screening.

Regarding to the utilization of different boron sources in the C-S coupling reaction, we first switched from the initial B_2pin_2 to the more reactive B_2cat_2 . The higher reactivity of B_2cat_2 is explained by its enhanced Lewis acidity, derived from the less available electron pair of the oxygen atoms, which are shared with the aromatic ring. The use of B_2cat_2 in this SEDs formation have been introduced by Jiao in his latest publications.^{168,169} However, this diboron reagent proved to be ineffective for our purpose, observing no product formation. Then, we

checked the viability of the reaction in presence of other typical diboron sources such as the B_2nep_2 and the $B_2(OH)_4$. Tetrahydroxydiboron ($B_2(OH)_4$) demonstrated to be inadequate in our system, however, using the B_2nep_2 we observed full conversion of the starting material but only a 50% isolated yield of the desired thioether. Finally, we considered using the less hindered B_2eg_2 . This compound was employed by the group of Jiao in their pyridine reduction method (see Scheme 26),¹⁷⁰ but in our case we did not detect any product. This behavior could be explained by the reduction of the pyridine promoted by the B_2eg_2 , affording the corresponding dihydropyridine.

Finally, we moved to optimize the solvent and base used in the reaction (Table 2). Although the screening was wider, herein are depicted the most relevant results (for more details see experimental section).

Table 2. Solvent and base screening.



Entry	Solvent	Base	Ratio 3a/4a	Conv ^a (%)	Yield ^b 3 ^a (%)
1	DMSO	MeOK	1/0	100	89 (68)
2	CH ₃ CN	MeOK	n.d.	0	-
3	MTBE	MeOK	n.d.	0	-
4	DMF	MeOK	2/1	70	30
5	DMA	MeOK	1/0	100	66
6	DMSO	MeONa	1/0	80	68
7	DMSO	MeOLi	4/1	88	59
8	DMSO	C ₂ CO ₃ MeOK	4/1	88	50

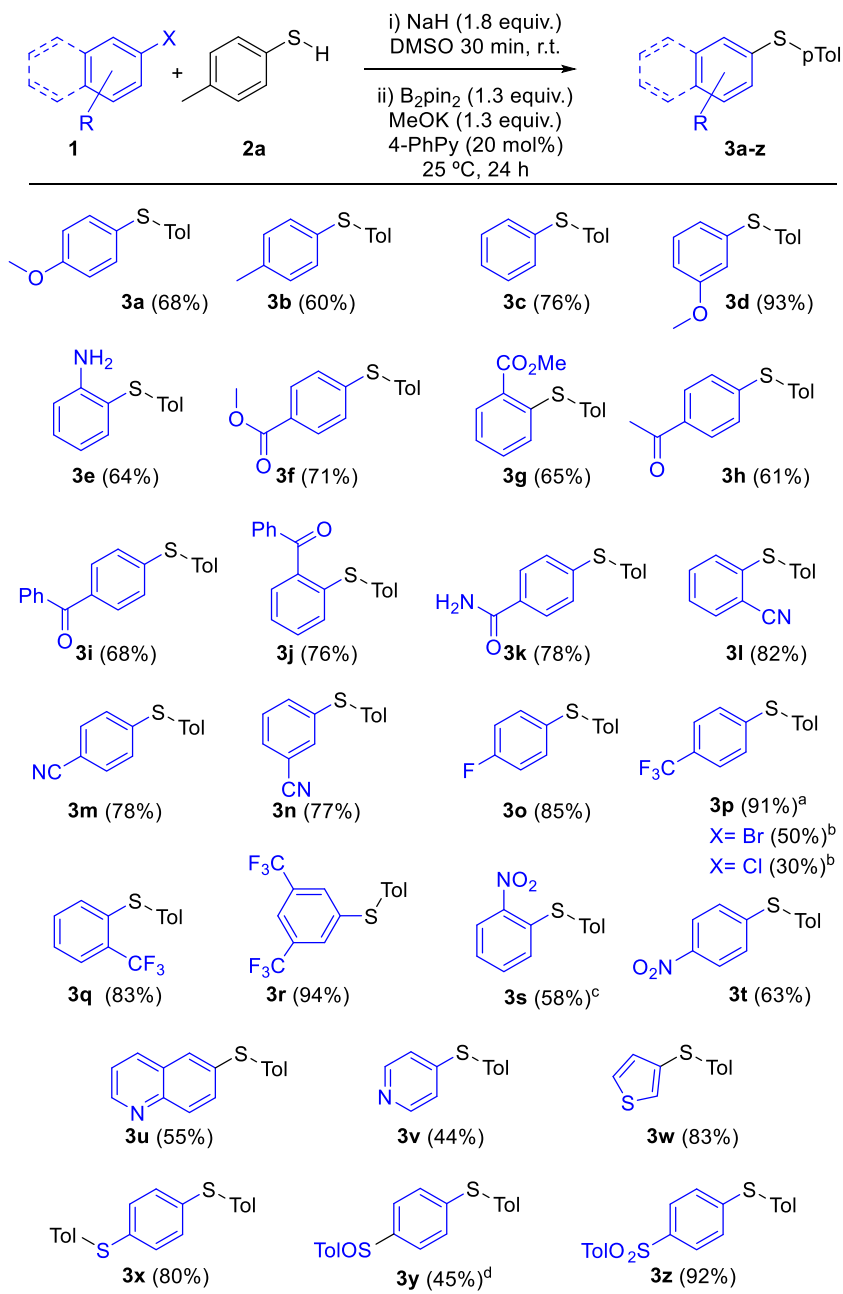
^aConversions measured with ¹H-NMR compared to the remaining starting material. ^bYields measured by ¹H-NMR using nitromethane as internal standard.

The use of commonly employed solvents in pyridine-boryl radicals involving reactions like CH₃CN or MTBE gave no product **3a** (entries 2, 3).^{166,168} Polar aprotic solvents such as DMF or DMA (entries 4-5) provided **3a** but in lower yield than using DMSO. At this point we hypothesized that maybe DMSO elimination during workup was counterproductive to the product yield. In order to reduce this drawback, we tried some solvent mixtures, but none of them gave better results.

Regarding the base screening, we focused on methyl alkoxides due to their previous utilization in SED promoted reactions. We analyzed the counterion influence, observing that the smaller the alkali ion, the lower the reaction yield (entries 6-7). Attempts varying the base in the thiol deprotonation step led to worse yield results (entry 8).

2.2.2. Substrate scope

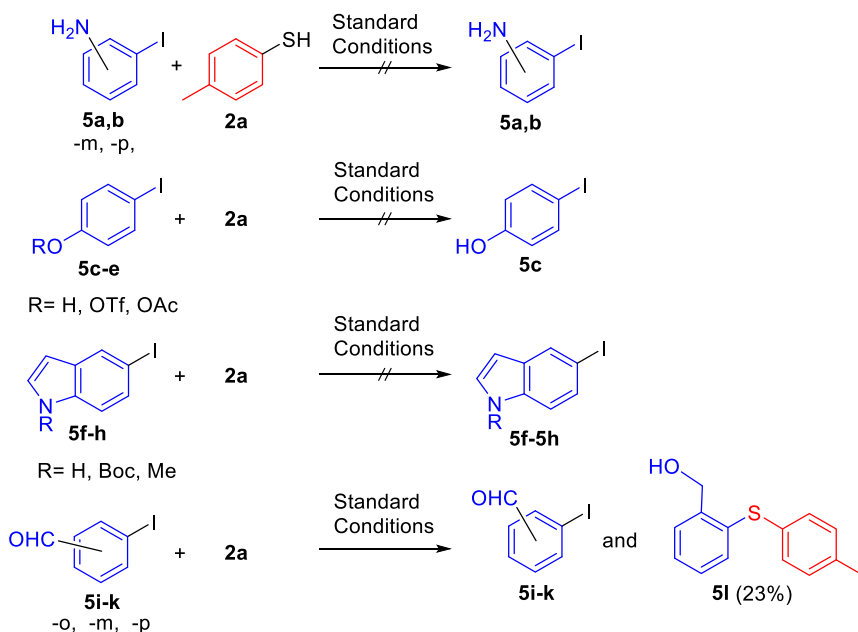
Once set the optimal conditions of our radical coupling reaction, we moved to study the scope of the transformation. First, we tested a great number of aromatic halides (**1a-z**), finding a broad functional group tolerance at different positions (Table 3). The reaction works well with iodobenzene (**3b**) and 4-iodotoluene (**3c**), as well as with electron donating groups in different positions (**3d**, **3e**). The reaction also tolerates the presence of methyl esters (**3f**, **3g**), amides (**3k**), and even the presence of ketones (**3h-j**), which could have been prone to reduction under the SED conditions. Other EWG are compatible too, such as nitrile (**3l-n**), fluorine (**3o**) or CF₃ moieties (**3p-r**).

Table 3. Scope of halides.

*X=I unless otherwise stated. ^a Gram-scale experiment in 93 % yield. ^b Aryl bromide and chloride were used in each case. ^c Obtained along with a 33% of **3e**. ^d Obtained along with a 16% **3x**.*

We also demonstrated in the preparation of compound **3p** (R=CF₃) that the method is compatible with the use of bromides and chlorides although with lower yields. This same example was also prepared in gram scale with no yield drop. Strong EWG groups like NO₂ were compatible as well (**3s**, **3t**). The method is even compatible with heteroaromatic substrates (**3u**, **3v**, **3w**), including pyridines, which are often susceptible of functionalization as shown in the antecedents.^{147,148,149,170} The reducing character of the pyridine-boryl intermediates can be observed in the partial reduction of the nitro (**3s**) and the sulfoxide (**3y**) examples. In these examples we obtained the coupled product along with the reduced and coupled product (**3e** and **3x** respectively).

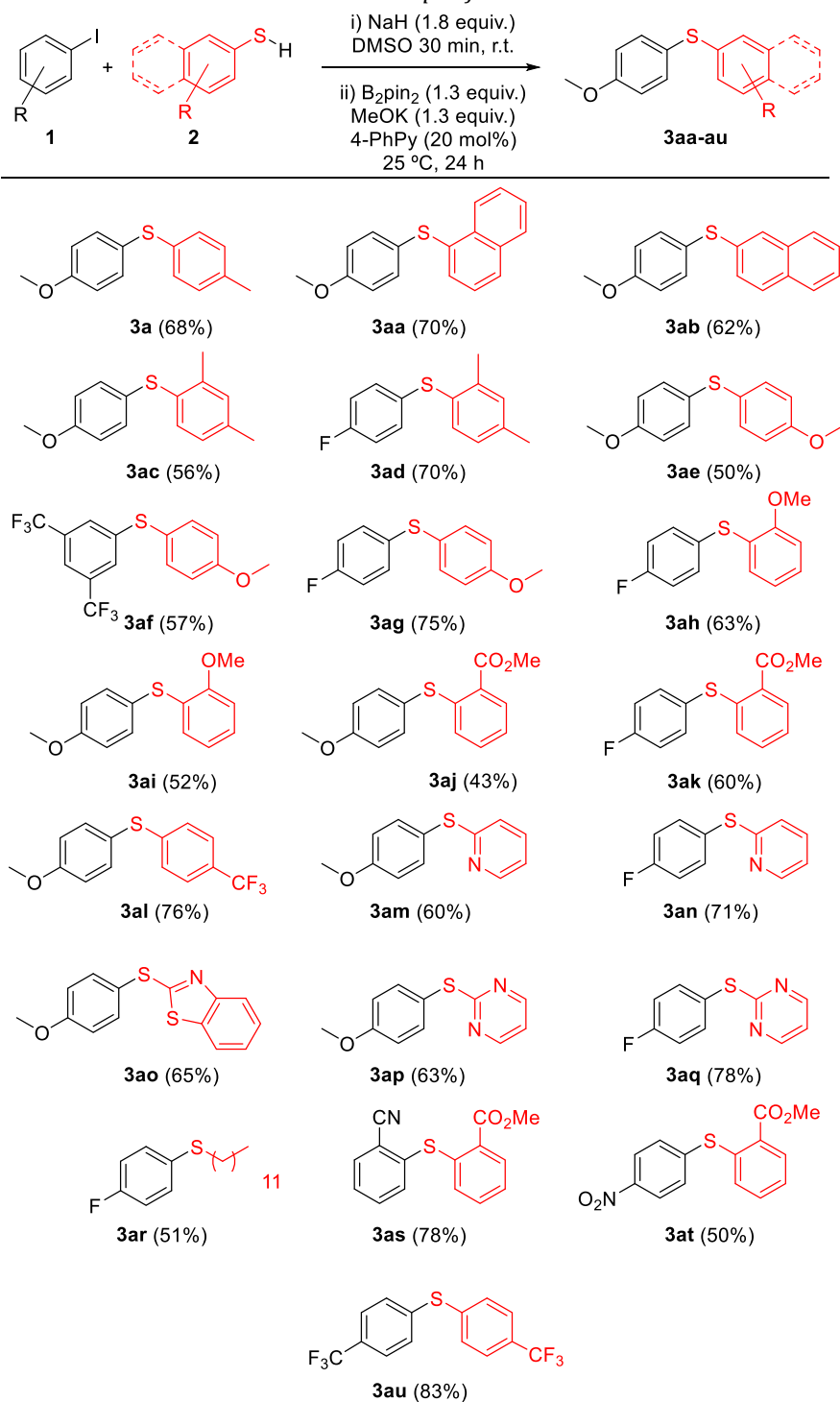
As shown in scheme 43, throughout the study of substrate scope we found some examples where the method proved to be ineffective.



Scheme 43. Troublesome examples.

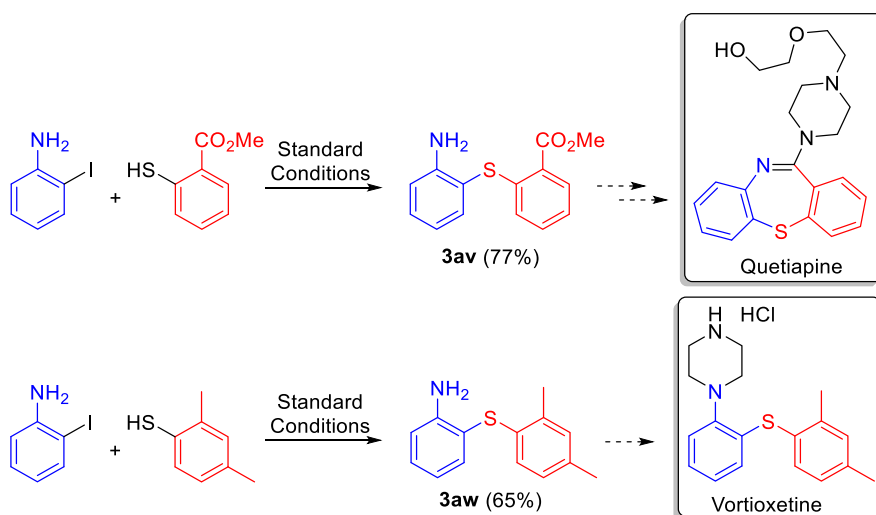
Surprisingly, meta and para substituted amines (**5a-b**) were not tolerated under the reaction conditions, obtaining the starting materials unaltered. This behavior is intriguing considering the moderate yield observed for the ortho regioisomer **3e** (Table 3). The use of differently hydroxy derived groups (**5c-e**) led in all cases to the alcohol (**5c**) recovery. The same behavior was observed when we used indole derivatives, obtaining the unprotected substrate when using the Boc protected indole (**5g**), or the starting material when we employed the methylated indole (**5h**). These results were not surprising because anilines and indoles have been already pointed out in the literature as problematic substrates in SED mediated processes.¹⁶⁸ Another struggling group of substrates found for this method are the benzaldehyde derivatives. In this case, we found a similar behavior as when we used amines. For meta and para substrates (**5j-k**) we observed no reaction, but in the case of the ortho substituted aldehyde (**5i**), we detected a 23% yield of the coupled and reduced product **5l**. This result along with the partial reduction of the nitro group in product **3s**, made us think of the existence of a possible intramolecular electron transfer from the aryl radical intermediate to the group in ortho position.

Next, we moved to check the viability of the method when using different substitution in the thiol ring (Table 4).

Table 4. Scope of thiols.

We were delighted to find that the reaction worked for aromatic thiols wearing both EDG and EWG. The reaction showed again a very good functional group tolerance, even expanding the scope of heterocycles to pyrimidines (**3ap-3aq**) and benzothiazoles (**3ao**) as well as pyridines (**3am-3an**). Moreover, we demonstrated that the reaction affords the coupling of aryl iodides with aliphatic thiols (**3ar**). Finally, the coupling reaction between electron-deficient counterparts turned out to be also compatible with the method. We obtained the thioether products bearing highly EWG in both ends of the molecules such as nitrile (**3as**), nitro (**3at**), and CF_3 (**3au**). Consequently, the method overcomes one of the main drawbacks of the previously reported EDA method,²⁰⁶ which was not suitable for the use of electron rich iodides.

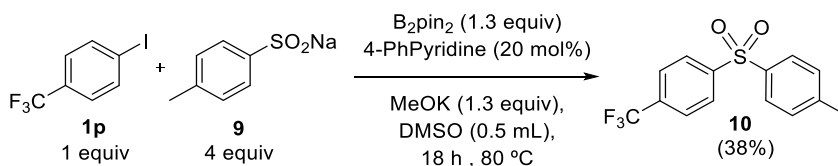
As a proof of the utility of the method, we also tested the coupling reaction in the synthesis of key intermediates of two different drugs (Scheme 44).



Scheme 44. Application of our method to the synthesis of drug intermediates.

Under the standard conditions, we could isolate with good yields of products **3av** and **3aw**, which after several steps would lead to the formation of Quetiapine²¹⁴ and Vortioxetine²¹⁵ respectively.

As a proof of the possibilities that the method could offer, and due to the notable results obtained in the C-S bond formation reaction coupling aromatic thiols and halides, we wondered if this protocol could be applied to other nucleophiles apart from thiols. To this end, we carried out the coupling reaction of **1p** with sodium toluenesulfonate **9** employing the standard conditions at 80 °C (Scheme 45). We could isolate sulfone **10** with an unoptimized 38% yield after 18 h. This result shows the potential of using this SED system.



Scheme 45. *S_{RN}1* reaction using sodium toluenesulfonate as substrate.

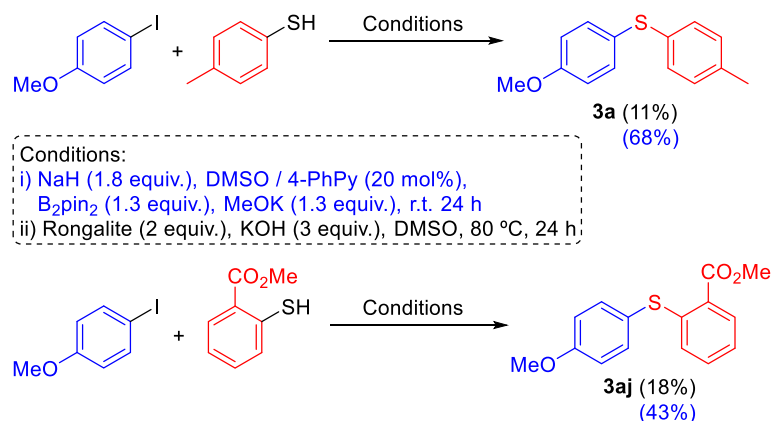
2.2.3. Comparative study with previously reported methods

According to this broad substrate scope, we have demonstrated that the method surpasses previously reported metal free methodologies in terms of functional group tolerance and mild reaction conditions. Apart from Miyake's work, another good example to carry out a comparative study is the rongalite promoted thioether formation. Although rongalite demonstrated a great versatility promoting different radical processes from aryl iodides, in their publication, the

²¹⁴ Panda, N.; Jena, A. K.; Mohapatra, S. *Appl. Catal. A*, **2012**, *433*, 258.

²¹⁵ Boros, Z.; Nagy, L.; Kátai, K.; Köhegyi, I.; Ling, I.; Nagy, T.; Iványi, Z.; Oláh, M.; Ruzsics, G.; Temesi, O.; Volk, B. *J. Flow Chem.* **2019**, *9*, 101.

authors only performed the C-S coupling reaction using iodobenzene and a small group of thiols. Therefore, in order to compare our method with this previously reported radical coupling, we carried out the coupling reaction using the conditions described using rongalite as promoter.²⁰⁵ To this end, we tested the reaction using two different coupling partners that we successfully coupled in our scope (Scheme 46).



Scheme 46. Comparison of the rongalite method results versus SED method.

Using 2 equiv. of rongalite as promoter and 3 equiv. of KOH as base in DMSO at 80 °C, we obtained the model thioether product **3a** with an 11% yield, a poorer result than the 68% yield obtained when we carried out the reaction under our conditions (in blue). Moreover, we also tested the rongalite method in the formation of one of our most challenging substrates (**3aj**), and again our method seemed to demonstrate a better performance versus the use of rongalite. However, although authors do not mention any treatment prior to its utilization, the possible hydration of rongalite could be affecting its performance in our hands as radical promoter of the reaction.

2.2.4. Catalytic version of the method

At this point, due to the remarkable results obtained we wondered if we could perform the reaction adding a catalytic amount of B_2pin_2 and MeOK. Developing a catalytic version of the SED promoted C-S coupling would boost the interest of the reaction. To check this hypothesis, we carried out a set of experiments adding 0.5 and 0.2 equivalents of B_2pin_2 and MeOK, using aryl iodides and thiols with different substitution (Table 5).

Table 5. Catalytic version of the SED promoted C-S coupling reaction.

R₁, R₂ Isolated yields (%)

B ₂ pin ₂ , MeOK (equiv.)	OMe, CH ₃ (3a)	H, CH ₃ (3c)	CF ₃ , CH ₃ (3p)	CF ₃ , CF ₃ (3aw)
1,3	68	76	91	83
0,5	44	75	86	77
0,2	-	53	79	51

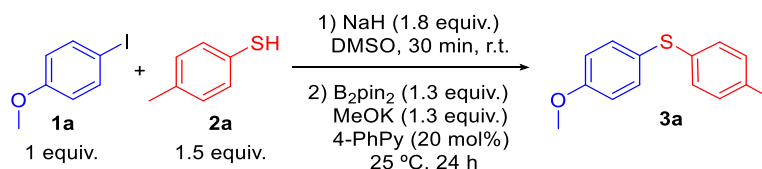
To our delight, when we performed the reaction adding 0.5 equivalents of the boron source and base, we obtained the desired thioethers with almost no erosion of the yield in most cases. As can be seen in table 5, only when we employed iodoanisole, the yield of **3a** dropped from a 68% to a 44%, meaning a strong dependence of the electronic properties in the reactivity of the haloarene. The recovery of iodoanisole starting material in the reaction crude suggests that a longer reaction time could lead to higher yield. On the other hand, using different haloarenes like **3c**, **3p**, and **3aw**, we observed a remarkable performance under catalytic conditions, obtaining almost the same results as when we added 1.3 equivalents of B_2pin_2 and MeOK.

Moreover, the equivalents could be lowered to 0.2, obtaining the corresponding products with still good yields.

2.2.5. Control experiments and mechanistic insights

According to the radical anion nature of the SED intermediates implicated in the reaction as well as the precedents employing these species, we considered that a radical mechanism could be ruling the coupling reaction. In order to ensure the hypothesis of a $S_{RN}1$ pathway and to understand better the role of the different reagents in the reaction, we carried out a set of control experiments and mechanistic assays (Table 6).

Table 6. Control experiments and mechanistic assays.



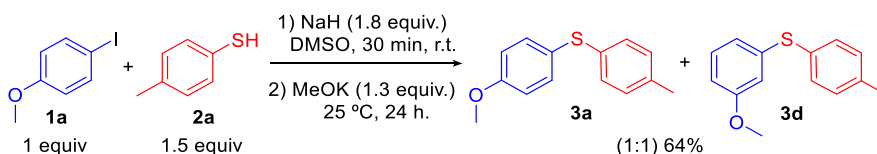
Entry	Base	Additive	Conv ^a (%)	Yield ^b (%)
1	MeOK (1.3)	-	100	80
2	MeOK (1.3)	In dark	100	75
3	-	-	0	-

^aConversions measured with 1H -NMR compared to the remaining starting material. ^bYields measured by 1H -NMR using nitromethane as internal standard.

First, we observed that under strict absence of light the reaction worked as well, obtaining product **3a** with a 75% yield (entry 2), very similar to what we obtained under the standard conditions (entry 1). This result discards in some extent any possible photoinduced process participating in the reaction. Next, the reaction in absence of MeOK reflected the major role of the alkoxide base in the reaction mechanism,

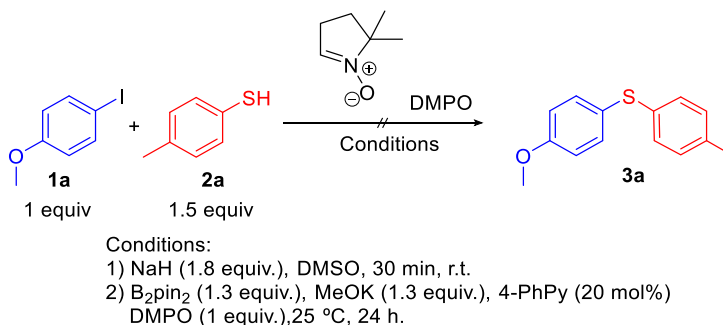
leading to full recovery of the starting materials after the reaction time (entry 3). This result points out that the reaction is really catalysed by a SED species where the three components (B_2pin_2 , MeOK and pyridine) participate, and not a pyridine-boryl radical catalysed process where the alkoxide is not part of the reactive intermediate.

This hypothesis is reinforced by the result obtained when we carried out the reaction with no addition of B_2pin_2 and pyridine (Scheme 47). In this case, we obtained the regioisomer mixture of *para* (**3a**) and *meta* (**3d**) products in a 1:1 ratio. It is clear then, that in this case the reaction is likely going through a benzyne intermediate, which could react with the thiolate with both ends of the triple bond indistinctly.



Scheme 47. Base promoted coupling reaction.

Additionally, we performed the model reaction between **1a** and **2a** in presence of 1 equiv. of 5,5-dimethyl-1-pyrroline *N*-oxide (DMPO) as electron trap (Scheme 48).

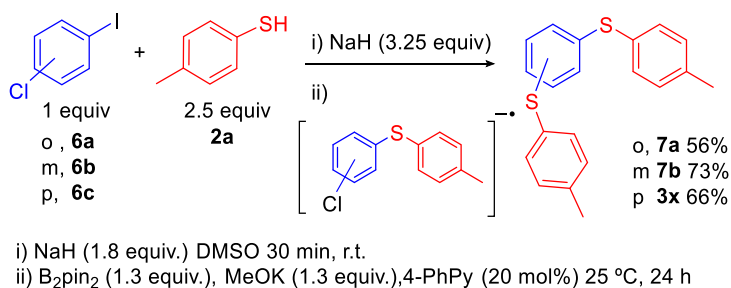


Scheme 48. Model reaction in presence of a radical trap.

As expected, we observed full inhibition of the coupling reaction. This result could support the theory of a radical process involved in the reaction mechanism. However, we could not isolate any intermediate in the complex mixture to confirm this hypothesis. As mentioned in the objectives, this reaction made us identify the potential interesting and unexplored reactivity of nitrones with diboron reagents in the presence and absence of pyridine derivatives and/or bases. Moreover, this result drove us to ask ourselves about the convenience of using nitrones as radical probes when using diboron reagents. The investigation of this reactivity will be the aim of the second chapter of the second part of the present thesis.

Although we were not able to deduce the evolution of DMPO in presence of the SED mixture, this reaction led us to reinforce the idea of the interest of analysing the behavior of nitrones in the presence of diboron reagents:

A final set of experiments that support the theory of a radical process involved in the reaction is showed in scheme 49. In this case, we carried out the reaction under the standard conditions using chloro-iodo-benzenes as substrates in *ortho*, *meta*, and *para* relative positions.

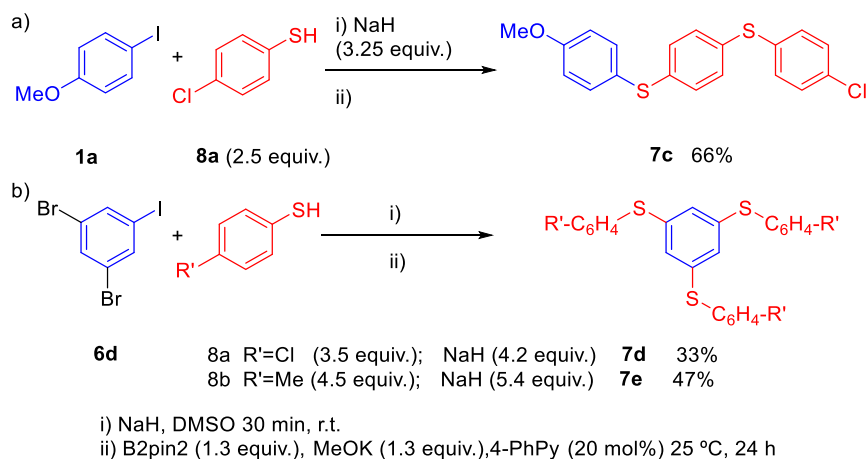


Scheme 49. Double C-S coupling of chloro-iodo-arenes.

Surprisingly, we got to the double C-S coupling products with moderate to good yields depending on the position of the halogens. These results contrast with the obtained when we used a single chloride as precursor of the aryl radical (**3p**), where the reaction afforded only a 30% yield of the product. Such a difference in reactivity could be explained by a second intramolecular electron transfer of the resulting radical anion intermediate **A** once the iodide has reacted.

Moved by the easy preparation of dicoupled products through an intramolecular electron transfer, we decided to study the reaction using different polyhalogenated substrates. Moreover, the preparation of multifunctionalized products would widen the interest of the method, since they are only accesible through metal catalysed methods employing disulfides as substrates.^{202,216} Under the standard conditions using 4-chlorobenzenethiol **8a** as substrate, we could get to bis-sulfide **7c** and **7d** in good yields (Scheme 50a). The products bearing a chlorine moiety on their structure, could be further functionalized to get to more complex compounds or even lead to polymeric materials.

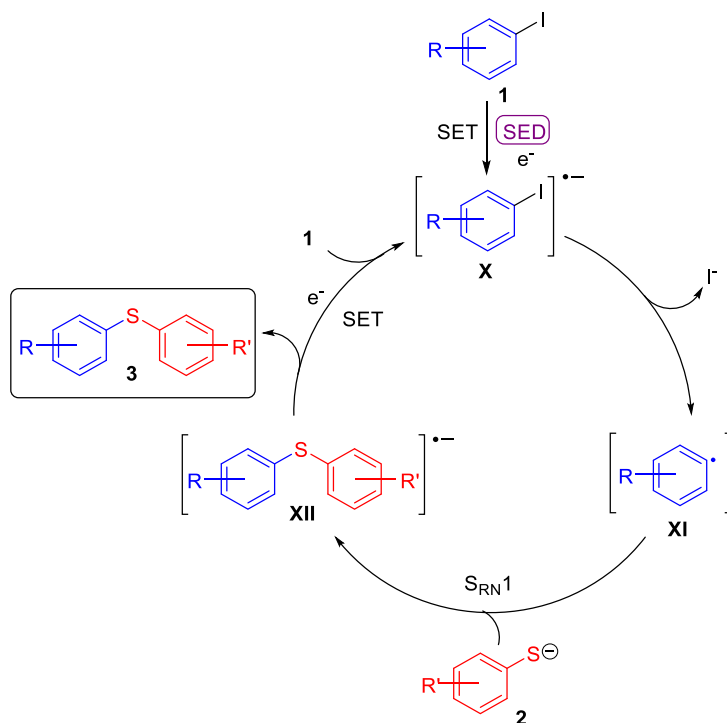
²¹⁶ Liu, Y.; Wang, H.; Zhang, J.; Wan, J. P.; Wen, C. *RSC Adv.* **2014**, *4*, 19472.



Scheme 50. Multifunctionalized products formation.

In addition, using aryl trihalide **6d** as substrate we could obtain the corresponding tricoupled products **7d** and **7e** with remarkable yields after three C-S bond formation reactions (Scheme 50b).

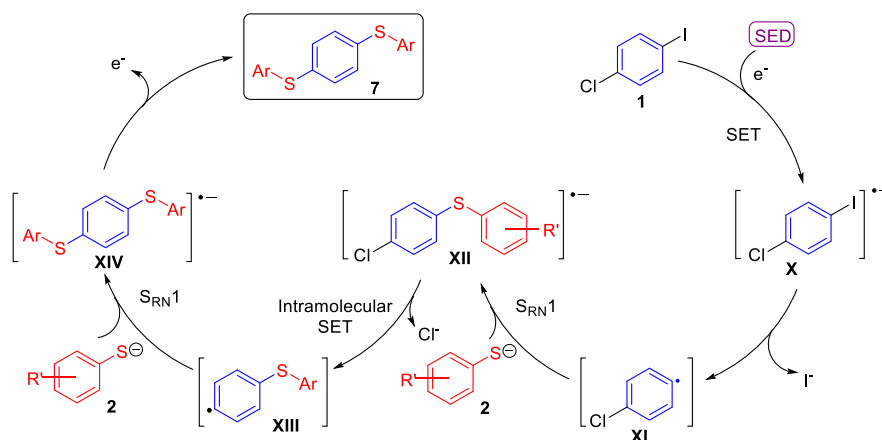
With all the information gathered thanks to the control and mechanistic experiments, we could get to a mechanistic proposal for the SED catalysed C-S coupling reaction (Scheme 51). For the sake of clarity, the mechanistic proposal for the polyhalogenated substrates will be described in a different scheme.



Scheme 51. Proposed catalytic cycle for the coupling reaction.

The catalytic cycle for the C-S coupling could start by the SET reaction between the aromatic halide and the super electron donor to afford the radical anion intermediate **X**. Based on the experiment in absence of MeOK, we could assume that the catalytic active species is formed by B₂pin₂, MeOK and 4-phenylpyridine (SED). The radical anion intermediate **X**, by the elimination of iodide, leads to the formation of the aryl radical **XI**. Next, the previously formed thiolate reacts with the radical through a S_{RN}1 reaction to get to the intermediate **XII**. Finally, this radical anion intermediate provides the thioether final product **3**. Along with this product, intermediate **XII** could give an electron to the halide starting material **1** by a single electron transfer step, making the process catalytic.

On the other hand, if there is a chloride in the iodide molecule, the reaction should follow the same pathway as the previous until the formation of **XII** (Scheme 52). Then, the subsequent elimination of the chloride would be favored by an intramolecular SET reaction in intermediate **XII**, affording the radical intermediate **XIII**. Next, the addition of another thiolate molecule **2** to this radical leads to intermediate **XIV**, which finally affords the dicoupled product **7**.

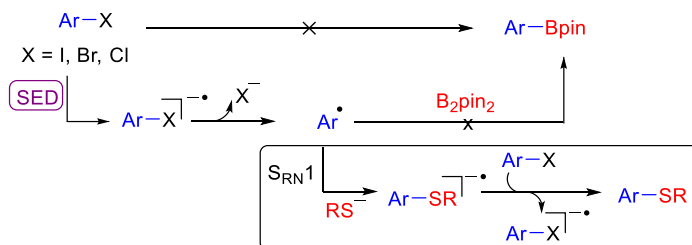


Scheme 52. Mechanistic proposal for the dicoupled products formation.

In the case of using a chloride substituent in the thiol and not in the iodoarene, the reaction mechanism should proceed in a similar manner.

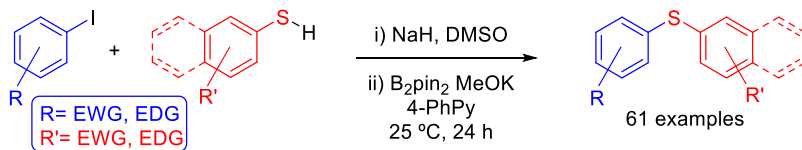
2.3. Conclusions

In summary, we have proven that pyridine–boryl complexes can be used as SEDs to selectively thiolate aromatic halides versus potential competitive reactions such as borylation or pyridine functionalization (Scheme 53).



Scheme 53. SED catalyzed C-S coupling reaction selectivity.

We have developed a mild, straightforward, and scalable protocol that allows C–S coupling. The experimental results point out to a $S_{RN}1$ mechanism, and it is general for a wide variety of substrates including the, in some cases reluctant, aryl halides with EDGs (Scheme 54).



Scheme 54. SED catalyzed C-S coupling.

The potential value of this transformation has been proven by preparation of some drug intermediates and bis- and tris-functionalized sulfides. Therefore, it constitutes a complementary strategy to other described methods for C–S bond formation. The method also allows the use of catalytic B_2pin_2 and MeOK, and open access to explore new synthetic transformations.

**Part II. Chapter 3. Study of the
reactivity of nitrones using different di-
boron containing systems**

Chapter 3. Study of the reactivity of nitrones using different diboron containing systems

3.1. Introduction

The present chapter summarizes the systematic evaluation of the reactivity of nitrones with different diboron compounds under various reaction conditions. Through this study we should be able to understand the behavior of these carbonyl derivatives, the products that they can afford, and therefore, their potential transformations. In this introduction, that will be divided in three sections, we will discuss some aspects that will provide context to our results. The first part will briefly introduce the nitron motif and its reactivity, followed by the main methods of nitron deoxygenation, and finally some reactions of nitrones that imply radical intermediates.

3.1.1. The nitron functionality

Nitrones are compounds of great utility in organic synthesis, mainly due to their versatility as well as the wide range of nitrogenated compounds that they can be transformed into.²¹⁷ Nitrones are also free radical trapping agents that reduce damage in some biological systems^{218,219} and thus are very attractive potential therapeutic agents.²²⁰

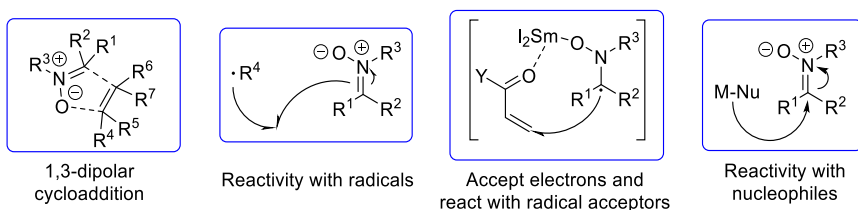
²¹⁷ Grigoriev, I. A. *Nitrile Oxides, Nitrones and Nitronates in Organic Synthesis: Novel Strategies in Synthesis*, ed. H. Feuer, Wiley, New Jersey, 2nd edn, 2008, pp. 129–434.

²¹⁸ Carney, J. M.; Floyd, R. A. *J. Mol. Neurosci.* **1991**, *3*, 47.

²¹⁹ Thomas, C. E.; Ohlweiler, D. F.; Carr, A. A.; Nieduzak, T. R.; Hay, D. A.; Adams, G.; Vaz, R.; Bernotas, R. C. *J. Biol. Chem.* **1996**, *271*, 3097.

²²⁰ Floyd, R. A.; Kopke, R. D.; Choi, C-H.; Foster, S. B.; Doblaz, S.; Towner, R. A. *Free Radic. Biol. Med.* **2008**, *45*, 1361.

The versatility exhibited by nitrones resides in the electrophilicity of the double C-N bond, which participates in 1,3-dipolar additions to afford biologically valuable nitrogen-containing heterocycles.²²¹ However, although they are commonly employed as dipoles in cycloadditions, they can participate also in a broad scope of transformations including reactions with radicals, they can accept electrons and react with electron acceptors. In addition, nitrones are electrophiles able to react with a variety of nucleophiles (Scheme 55).^{222,223,224}



Scheme 55. Nitrones reactivity.

Furthermore, nitrones are substrates especially useful in comparison to their corresponding imine derivatives due to their easy handling, stability, and commercial availability.²²⁵ Moreover, the configurational stability of the nitrone moiety makes easy the diastereoselective and enantioselective addition reactions to these substrates.²²⁶ Another possible transformation of nitrones is the reduction to imines and amines. We will summarize below some aspects related with the reactivity of nitrones that we consider important to contextualize our results in this section.

²²¹ Berthet, M.; Cheviet, T.; Dujardin, J.; Parrot, I.; Martinez, J. *Chem. Rev.* **2016**, *116*, 15235.

²²² Yang, Y-S.; Shen, Z-L.; Loh, T-P. *Org. Lett.* **2009**, *11*, 1209.

²²³ Masson, G.; Cividino, P.; Py, S.; Vallée, Y. *Angew. Chem. Int. Ed.* **2003**, *42*, 2265.

²²⁴ Tejero, T.; Merchan, F. L.; Franco, S.; Merino, P. *Synlett.* **2000**, 442.

²²⁵ Murahashi, S.; Imada, Y. *Chem. Rev.* **2019**, *119*, 4684.

²²⁶ Lombardo, M.; Trombini, C.; *Synthesis*, **2000**, 759.

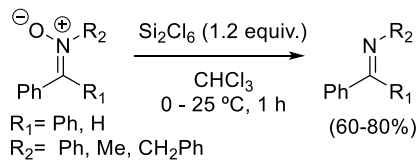
3.1.2. Deoxygenation of nitrones

The reduction of nitrones to afford imines is described by using metals or different organic reagents, but normally these methods are limited by harsh procedures, side reactions or lack of selectivity.²²⁵

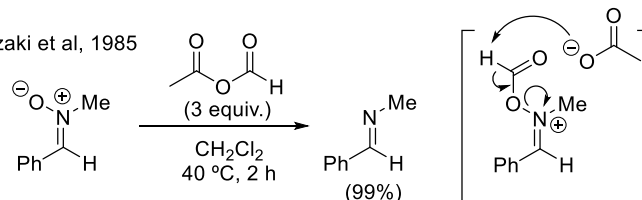
In the 70's decade silanes were known as good deoxygenating agents in the reduction of phosphine oxides and sulfides, amine *N*-oxides, or aryl nitrocompounds due to the great affinity of silicon to oxygen. In 1978 Hortmann and coworkers extended the use of Si₂Cl₆ to the deoxygenation of nitrones (Scheme 56a).²²⁷ Although the scope was limited to 4 examples, this method required relatively mild conditions and afforded the corresponding imines avoiding the further reduction of the double C-N bond.

²²⁷ Koo, J-Y.; Yu, C-C.; Hortmann, A. G. *J. Org. Chem.* **1978**, *43*, 2289.

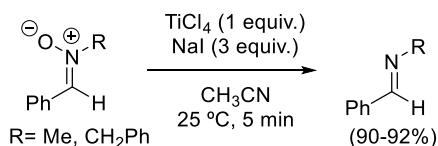
a) Hortmann et al, 1978



b) Okazaki et al, 1985



c) Balicki et al, 1990



Scheme 56. Early reports of the reduction of nitrones to imines.

Another report of selective nitronium deoxygenation was published in 1985 by Okazaki's group. Herein, they developed the deoxygenation of tertiary amines *N*-oxides with acetic formic anhydride.²²⁸ Apart from these oxides, they demonstrated that the method could be applied to other substrates such as nitrones (Scheme 56b). However, they reported the use of *N*-methyl nitrones, but *N*-aryl nitrones gave complex mixtures under their conditions.

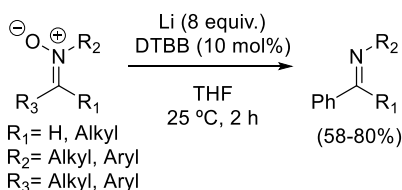
A final example of the early reduction of nitrones to imines was reported by Balicki and coworkers, when they employed a TiCl_4/NaI system for the mild reduction of the *N*-O bond (Scheme 56c).²²⁹ Under these conditions the reaction proceeded in a very short time, but the scope was limited to 2 examples.

²²⁸ Tokitoh, N.; Okazaki, R. *Chem. Lett.* **1985**, *14*, 1517.

²²⁹ R. Balicki, *Chem. Ber.*, **1990**, *123*, 647.

These early methods set the basis of the selective reduction of nitrones to imines, and the following years different approaches have been published regarding the use of different promoters such as metal salts,²³⁰ silanes,²³¹ or under photoinduced conditions.²³²

Among the more recently described methodologies we could highlight the work by Yus and coworkers in 2001.²³³ In their report, they described the use of a lithium/DTBB system as reductant of a variety of aliphatic and aromatic nitrones (Scheme 57). However, the use of excess lithium powder limits the functional group tolerance despite the efficient reduction of the nitrono moiety.



Scheme 57. Yus's procedure for the nitrono deoxygenation reaction.

Some other reports have been published until date regarding the selective deoxygenation of nitrones to imines,²³⁴ or their reduction to amines.²³⁵ Nevertheless, they are based on the use of metals as reducing agents that are usually expensive and/or not chemoselective.

²³⁰ a) Konwar, D.; Boruah, R. C.; Sandhu, J. S. *Synthesis*, **1990**, 337. b) Ilankumaran, P.; Chandrasekaran, S. *Tetrahedron Lett.* **1995**, *36*, 4881. c) Somasundaram, N.; Srinivasan, C. *Tetrahedron Lett.* **1998**, *39*, 3547. d) Jeevandram, A.; Cartwright, C.; Ling, Y. C. *Synth. Commun.* **2000**, *30*, 3153.

²³¹ Hwu, J. R.; Tseng, W. N.; Patel, H. V.; Wong, F. F.; Horng, D.-N.; Liaw, B. R.; Lin, L. C. *J. Org. Chem.* **1999**, *64*, 2211.

²³² Kawamura, Y.; Iwano, Y.; Shimizu, Y. *Chem. Lett.* **1994**, *23*, 707.

²³³ Radivoy, F.; Alonso, G.; Yus, M. *Synthesis*, **2001**, *3*, 427.

²³⁴ a) Ilias, M.; Barman, D. C.; Prajapati, D.; Sandhu, J. S. *Tetrahedron Lett.* **2002**, *43*, 1877. b) Saini, A.; Kumar, S.; Sandhu, J. S. *Synlett.* **2006**, *17*, 395. c) Singh, S. K.; Reddy, M. S.; Mangle, M.; Ganesh, K. R. *Tetrahedron.* **2007**, *63*, 126.

²³⁵ Rodrigo, E.; Waldvogel, S. R. *Chem. Sci.* **2019**, *10*, 2044.

Therefore, the development of an alternative method using mild and metal free conditions to afford imines would be of interest.

3.1.3. Nitrones in Reactions Involving Radicals

As depicted in the first part of the chapter introduction, nitrones can react with a wide variety of nucleophiles, unsaturated compounds, and also with radicals. The double C-N bond has demonstrated to be a good radical acceptor, and nitrones have been employed since long time ago as free-radical traps. Therefore, as mentioned, nitrones are also interesting from a biological point of view and extensively studied for the treatment of human diseases.²³⁶ In addition, thanks to the configurational stability of the nitron structure, the radical addition to chiral nitrones gives the C-C bond formation with high stereocontrol.

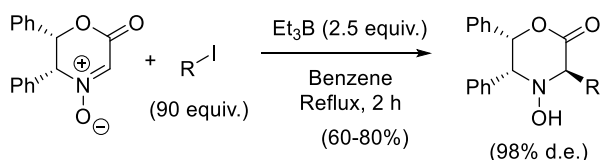
Scheme 58a shows one diastereoselective example of the utilization of nitrones as radical acceptors in C-C bond formation.²³⁷ Herein, authors use of Et₃B as radical initiator in the radical addition of alkyl iodides to chiral glyoxylic nitrones to obtain the coupled products with high diastereomeric excesses, which after a few steps lead to the enantiopure amino acids.

²³⁶ a) Janzen, E. G.; Nutter, D. E.; Davis, E. R.; Blackburn, B. J., Poyer, J. L.; McCay, P. B. *Can. J. Chem.* **1978**, *56*, 2237. b) R. A. Floyd. *Adv. Pharmacol.* **1996**, *38*, 361. c) Marco-Contelles, J. J. *Med. Chem.* **2020**, *63*, 13413. d) Cancela, S.; Canclini, L.; Mourglia-Ettlin, G.; Hernández, P.; Merlino, A.; *Eur. J. Pharmacol.* **2020**, *871*, 172926.

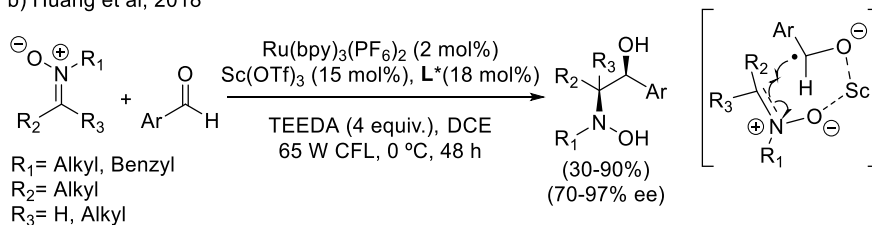
²³⁷ Ueda, M.; Miyabe, H.; Teramachi, M.; Miyata, O.; Naito, T. *Chem. Commun.* **2003**, 426.

Reactions with radicals

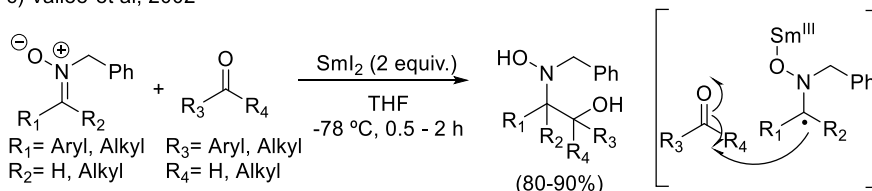
a) Naito et al, 2003



b) Huang et al, 2018

**Nitrones in SET processes**

c) Vallée et al, 2002

**Scheme 58.** Seminal reports of nitrones in radical reactions.

Nitrones have also been employed in radical addition reactions under photocatalytic conditions. Through the utilization of light as promoter, researchers have developed new reactions such as the C-C bond formation between nitrones and tertiary amines through C-H functionalization,²³⁸ or the iridium photocatalyzed reductive fluoroalkylation of nitrones.²³⁹ An interesting example in this field was published by the group of Huang in 2018.²⁴⁰ In this report, authors got to the enantioselective synthesis of vicinal hydroxyamino alcohols

²³⁸ Itoh, K.; Kato, R.; Kinugawa, D.; Kamiya, H.; Kudo, R.; Hasegawa, M.; Fujii, H.; Suga, H. *Org. Biomol. Chem.* **2015**, *13*, 8919.

²³⁹ Supranovich, V. I.; Levin, V. V.; Struchkova, M. I.; Dilma, A. D. *Org. Lett.* **2018**, *20*, 840.

²⁴⁰ Ye, C-X.; Melcamu, Y. Y.; Li, H-H.; Cheng, J-T.; Zhang, T-T.; Ruan, Y-P.; Zheng, X.; Lu, X.; Huang, P-Q. *Nat. Commun.* **2018**, *9*, 410.

through the reductive cross-coupling of nitrones with aldehydes (Scheme 58b). The use of a ruthenium photocatalyst and a coreductant (*N,N,N',N'*-tetrathylethylenediamine/TEEDA) ensure the radical coupling between the nitrones and the aromatic aldehydes. However, it is the combination of the rare earth Lewis acid and the *N,N'*-dioxide chiral ligand the key of the asymmetrical radical process to afford the enantiopure products.

A remarkable example of the utilization of nitrones in SET processes was published by the group of Vallée in 2002.²⁴¹ In their publication, they demonstrated that the addition of an equimolecular amount of SmI₂ induces the cross-coupling of nitrones with aldehydes and ketones (Scheme 58c). The reaction of the samarium with the nitronone generates a radical intermediate which adds to the carbonyl.

This same principle was applied later by the same group to the addition of nitrones to α,β -unsaturated esters,²²³ and by other groups to different carbonyl derivatives.²⁴²

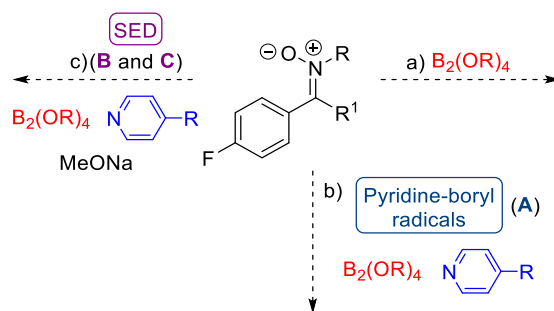
According to these precedents, nitrones could easily participate in radical processes either accepting electrons or radicals. Then, it made us wonder if nitrones could be good candidates to react with super electron donors (**B**, **C**) and pyridine-boryl radicals (**A**).

²⁴¹ Masson, G.; Py, S.; Vallée, Y. *Angew. Chem. Int. Ed.* **2002**, *41*, 1772.

²⁴² a) Riber, D.; Skrydstrup, T. *Org. Lett.* **2003**, *5*, 229. b) Zhong, Y-W.; Xu, M-H.; Lin, G-Q. *Org. Lett.* **2004**, *6*, 3953. c) Burchak, O. N.; Philouze, C.; Chavant, P. Y.; Py, S. *Org. Lett.* **2008**, *10*, 3021. d) Gilles, P.; Py, S. *Org. Lett.* **2012**, *14*, 1042. e) Xu, C-P.; Huang, Huang, P-Q.; Py, S. *Org. Lett.* **2012**, *14*, 2034. f) Pirkhod'ko, A.; Walter, O.; Zevaco, T. A.; Garcia-Rodriguez, J.; Mouhtady, O.; Py, S. *Eur. J. Org. Chem.* **2012**, 3742.

Moreover, given the ability of diboron compounds to reduce N-O bonds on different substrates, the deoxygenation of nitrones in presence of diborons could be feasible.

Therefore, in this chapter we present a preliminary systematic evaluation of the reactivity of nitrones in presence of diboron compounds, pyridine-boryl radicals, and super electron donors separately (Scheme 59).



Scheme 59. Systematic analysis of the reactivity of nitrones and diboron containing systems.

3.2. Results and discussion

The previously reported methods in the literature point out that diboron compounds can deoxygenate amine *N*-oxides on their own,¹⁵⁹ and pyridine *N*-oxides and nitrocompounds in the presence of bases¹⁵⁵ and pyridines¹⁵¹ as additives. However, there are no reports studying this reaction with nitrones. Thus, we started our study of the reactivity of nitrones testing their behavior first with the sole addition of diboronic esters, and then with different additives.

3.2.1. Reactivity of nitrones with diboron reagents

As we suspected, some preliminary results revealed us that the treatment of nitrones with diboron compounds afforded the corresponding imine derivative. As the reduction of nitrones to imines is not a trivial transformation as well as unexplored using diboron compounds, we decided to investigate the reaction in more detail.

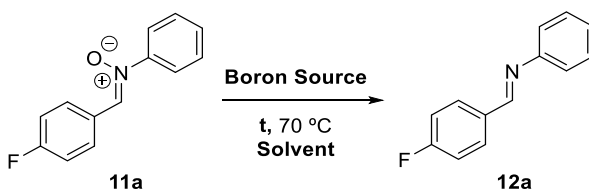
Optimization of the deoxygenation reaction

To start our study, we chose nitrone **11a** as model substrate. We decided to use deuterated solvents and determine the yield by ¹H-NMR using an internal standard in order to minimize the manipulation of the imine as they are substrates prone to hydrolysis. Most significative results are collected in table 7.

When we treated nitrone **11a** with 1 equivalent of B₂pin₂ in DMSO at 70 °C we obtained the corresponding imine with a remarkable 87% NMR yield (entry 1). The use of B₂nep₂ provided almost the same result (entry 2). Using long reaction times, and other solvents such as acetonitrile, methanol or benzene gave similar results (entries 3-5).

The imine **12a** could be isolated after a simple filtration through a short path of silica gel in a 79% yield after only 2 h of reaction (entry 6).

Table 7. Optimization of the deoxygenation reaction.



Entry	B ₂ R ₂ (equiv.)	t (h)	Solvent	Conv. (%) ^a	Yield (%) ^b
1	B ₂ pin ₂ (1)	18	DMSO- <i>d</i>	87	n.d.
2	B ₂ nep ₂ (1)	18	DMSO- <i>d</i>	89	n.d.
3	B ₂ nep ₂ (1)	18	CD ₃ CN	90	n.d.
4	B ₂ nep ₂ (1)	18	MeOD	87	n.d.
5	B ₂ nep ₂ (1)	18	C ₆ D ₆	91	72
6	B ₂ nep ₂ (1)	2	C ₆ D ₆	88	79
7	B ₂ nep ₂ (1.2)	2	C ₆ D ₆	92	n.d.
8	B ₂ nep ₂ (1.2)	2	CH ₃ CN	n.d.	40
9	B ₂ nep ₂ (1.2)	2	Dioxane	n.d.	25
10	B ₂ nep ₂ (1.2)	2	MTBE	n.d.	75
11	B ₂ nep ₂ (1.2)	2	DMSO- <i>d</i>	14	n.d.
12	B ₂ nep ₂ (1.2)	2	EtOAc	n.d.	78
13	B ₂ nep ₂ (1.2)	2	THF	n.d.	25
14	B ₂ nep ₂ (1.2)	2	CDCl ₃	85	n.d.
15	B ₂ nep ₂ (1.2)	2	MeOH	n.d.	93
16	B ₂ nep ₂ (1.2)	2	Toluene	n.d.	95
17	B₂nep₂ (1.2)	2	C₆H₅CF₃	n.d.	99
18 ^c	B ₂ nep ₂ (1.2)	2	C ₆ H ₅ CF ₃	n.d.	17
19	B ₂ pin ₂ (1.2)	2	C ₆ H ₅ CF ₃	n.d.	48
20	B ₂ cat ₂ (1.2)	2	C ₆ H ₅ CF ₃	n.d.	84

^aYields measured by ¹H-NMR using nitromethane as internal standard. ^bIsolated yields. ^c25°C.

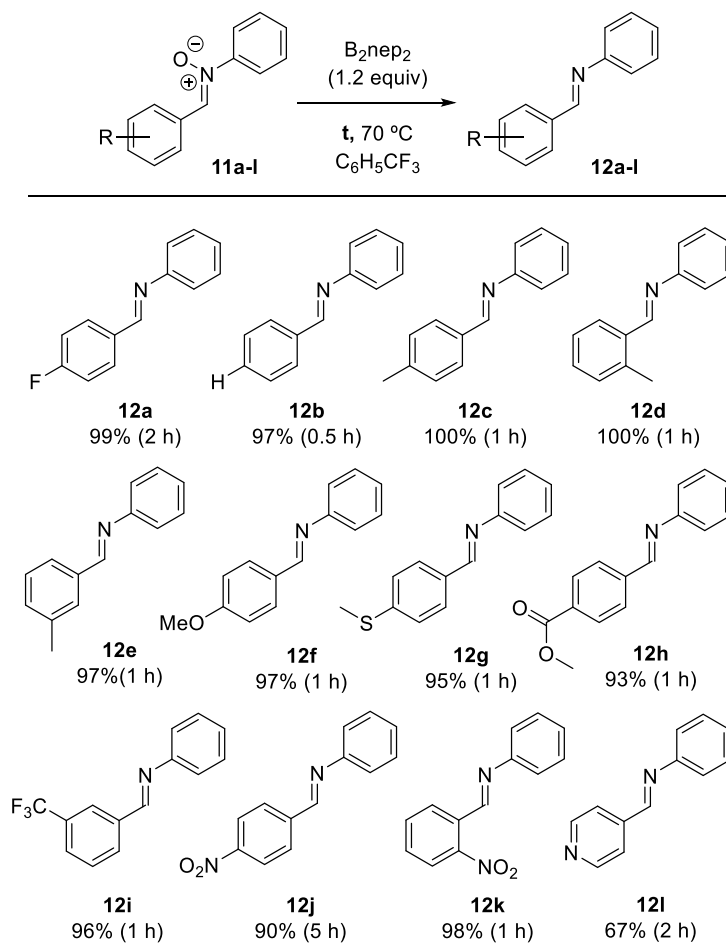
Increasing the diboron reagent amount to 1.2 equivalents provided the deoxygenated product **12a** with a slightly better yield (entry 7). Under these conditions, we tested a large number of non-polar, polar protic and polar aprotic solvents (entries 8-17), and we found that trifluorotoluene was the optimal one. After 2 h we could successfully isolate imine **12a** with almost quantitative yield (entry 17). We reasoned that the yield dropped in the more polar solvents probably

due to the higher content in water than in the non-polar that favors the hydrolysis of the imine. On the other hand, the reaction temperature turned to be crucial, as when we performed the reaction at room temperature, we obtained the desired product with only a 17% yield (entry 18).

Finally, we tested the influence of the diboron nature under the optimized conditions. The use of B₂pin₂ and B₂cat₂ (entries 19-20) could not improve the result obtained when using B₂nep₂ (entry 17).

Substrate scope of the deoxygenation reaction

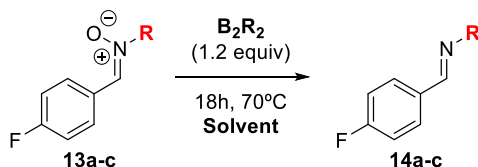
Once optimized the reaction conditions, we moved to study the scope of the deoxygenation reaction (Table 8). The reaction tolerates a good number of aromatic rings bearing different functional groups. Electron-neutral substrates such as **12b**, or different electron-rich aromatic rings wearing methyl (**12c**, **12d**, **12e**), methoxy (**12f**), or thiomethyl (**12g**) groups are converted to the corresponding imines with excellent yields and in short reaction times.

Table 8. Diboron promoted nitrene deoxygenation substrate scope.

The method is also applicable to electron-deficient substrates such as esters (**12h**), or trifluoromethyl groups (**12i**). Under these conditions, nitro groups remain unchanged, and the corresponding imines are obtained with similar results (**12j**, **12k**). This is not a surprising result since, according to the literature, nitroaromatics need the addition of an additive like pyridine to afford their reduction to anilines.¹⁵¹ Finally, pyridine substituted nitrones work as well under the reaction conditions (**12l**).

As a part of the substrate scope, we also tested the influence of the N-substituent in the reactivity of the nitrones and different diboron sources (Table 9).

Table 9. Nitrogen substitution study.

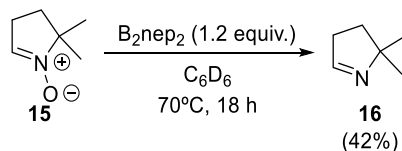


Entry	R	B ₂ R ₂	Solvent	Prod.	Yield (%) ^a
1	<i>t</i> -Bu	B ₂ nep ₂	C ₆ H ₅ CF ₃	14a	26
2	<i>t</i> -Bu	B ₂ eg ₂	C ₆ H ₅ CF ₃	14a	16
3	<i>t</i> -Bu	B ₂ cat ₂	C ₆ H ₅ CF ₃	14a	30
4	<i>t</i> -Bu	B ₂ pin ₂	C ₆ H ₅ CF ₃	14a	n.d.
5	Me	B ₂ nep ₂	C ₆ D ₆	14b	46 ^b
6	Benzyl	B ₂ nep ₂	C ₆ H ₅ CF ₃	14c	85

^aIsolated yields. ^bYields measured by ¹H-NMR using nitromethane as internal standard.

Notably, the utilization of nitrones with aliphatic substituents in the nitrogen has a dramatic effect in the product yield. In the case of using a *tert*-butyl group, imine **14a** was isolated with a 26% yield when using B₂nep₂ as boron source (entry 1). The utilization of other diboron reagents such as B₂eg₂ and B₂cat₂ conducted to similar results (entries 2 and 3). B₂pin₂ is not able to reduce the *tert*-butyl nitronium derivative, probably due to the steric hinderance of both reagents (entry 4). Using a methyl group leads to the formation of imine **14b** with only a 46% NMR yield (entry 5). This imine undergoes decomposition during chromatography. Imine **14c** bearing a benzyl group was successfully obtained with 85% isolated yield under the standard conditions (entry 6).

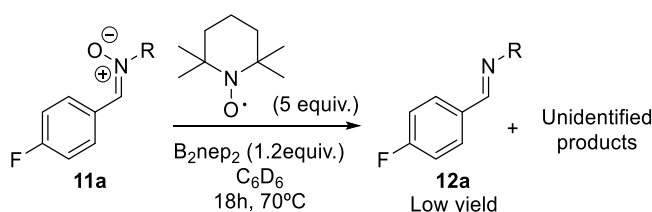
Finally, we checked the behavior of the cyclic nitron **15** in the deoxygenation reaction. Under the optimized conditions, we observed a clean conversion of the nitron to imine **16** with a 42% NMR yield (Scheme 60).



Scheme 60. *DMPO deoxygenation reaction.*

As described in the previous chapter, this nitron in the presence of the SED combination gave a complex reaction mixture. The result of scheme 60 clearly put on doubt the use of *DMPO* as a radical probe in the presence of diboron reagents.

At this point, we decided to study the reaction outcome if we added a typical radical inhibitor such as TEMPO under the standard conditions (Scheme 61). As expected, the model reactions and the different variations that we tested led to the low conversion of nitron **11a** towards imine **12a**, as well as a complex mixture containing TEMPO derived products.

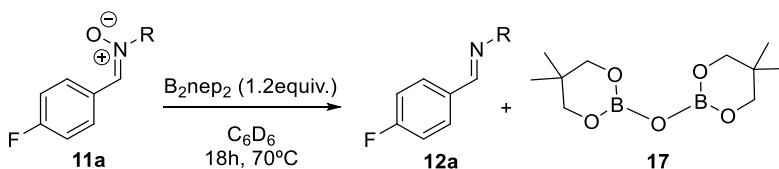


Scheme 61. *Nitron deoxygenation reaction in presence of TEMPO.*

This result could suggest a radical mechanism. Nevertheless, the experiments and theoretical studies depicted below point out a different mechanism.

Mechanistic insights into the nitrono deoxygenation

Next, we moved to study the mechanism ruling the reduction process. Combining ^{11}B -NMR, ^{13}C -NMR and mass spectra analysis of the products formed under the standard reaction conditions, we could identify compound **17** as byproduct (Scheme 62).



Scheme 62. Study of the B_2nep_2 evolution in the deoxygenation reaction.

In collaboration with Professor Inés Alonso from our department, we calculated the energy profiles of the reaction in presence of either B_2nep_2 or B_2pin_2 (Figure 5). According to the profile, it seems evident that the formation of two B-O bonds is the driving force of the reaction.²⁴³ After coordination of the diboron reagent to the nitrono, the calculation is consistent with a concerted mechanism in which the B-O bonds formation is simultaneous to the rupture of the N-O bond.

On the other hand, the difference in the energy barrier of the transition states when using B_2nep_2 or B_2pin_2 is approximately only 3 Kcal. This small difference does not match with the experimental observation, where B_2pin_2 proves to be much less reactive than B_2nep_2 .

²⁴³ Carter, C. A. G.; John, K. D.; Mann, G.; Martin, R. L.; Cameron, T. M.; Baker, R. T.; Bishop, K. L.; Broene, R. D.; Westcott, S. A. *Group 13 Chemistry: From Fundamentals to Applications* Ed.; P. J. Shapiro, D. A. Atwood, American Chemical Society, Washington DC, 2002; pp 70-87.

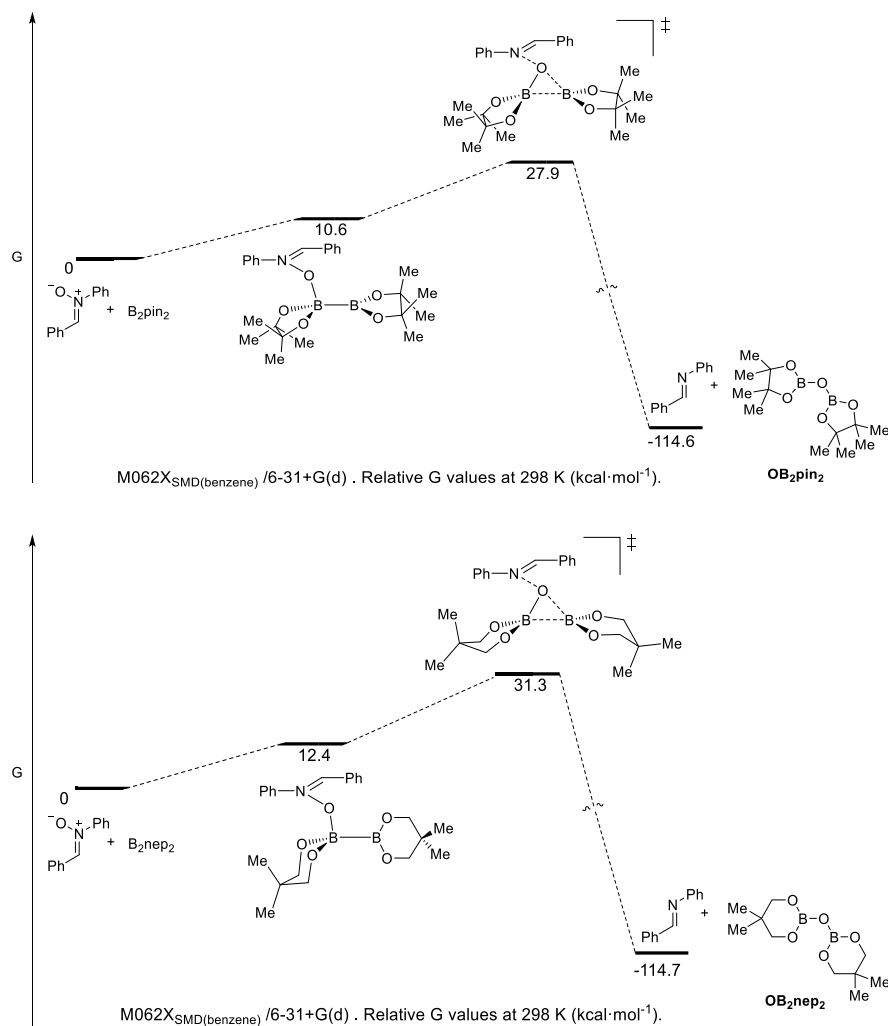
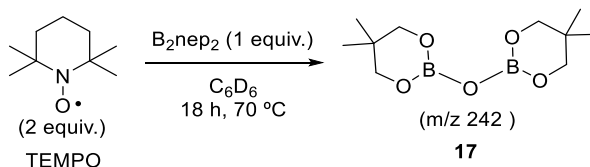


Figure 5. Energy profiles of the nitrono deoxygenation using *B*₂*nep*₂ and *B*₂*pin*₂.

Hence, the calculations seem to rule out the radical mechanism pointed out by the previous experiment using TEMPO (Scheme 61), and we suspected that TEMPO could also react with diboron reagents. In fact, when TEMPO was treated with *B*₂*nep*₂ and we follow the reaction by GC-MS we could detect two peaks at 6.16 and 8.99 min

being the latter associated to a m/z 242, which correspond to compound **17** (scheme 63).



Scheme 63. TEMPO control experiment.

This result also suggests that TEMPO could not be the most appropriate radical trap in reactions that use diboron reagents. Decomposition of TEMPO in presence of diboron reagents under certain conditions has already been pointed out in the literature.¹⁰⁴ Although more thorough studies must be performed, TEMPO could inhibit the reactions by just consuming the diboron reagent undergoing deoxygenation.

3.2.2. Reactivity of nitrones and diboron reagents in the presence of alkoxides

According to previously mentioned antecedents, we also considered of interest to evaluate the role of an alkoxide as additive in the reduction of nitrones. To this end, we calculated the energies of the possible transition states responsible for the deoxygenation of nitrones with diboron reagents in presence of MeOK as additive (Figure 6). According to the calculations, the reactions should be clearly faster in the presence of an alkoxide either using B_2pin_2 or B_2nep_2 (compare a and b, c and d). In parentheses are shown the difference of energies regarding the previous intermediate to the transition state.

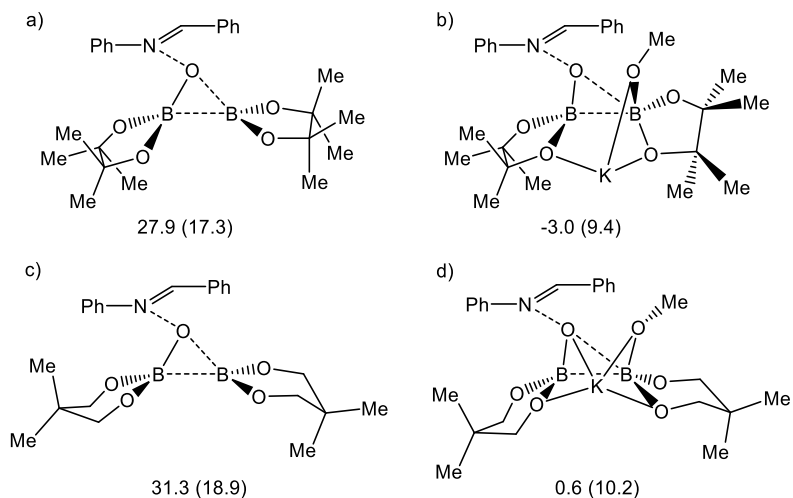


Figure 6. Energy of the intermediates in the deoxygenation ($\text{kcal}\cdot\text{mol}^{-1}$).

These calculations agree with the previous observation reported by Wu and coworkers,¹⁵⁵ when they determined that the reduction of the more challenging nitroaromatics to the corresponding anilines needed the addition of a base along with B_2pin_2 to work.

With these premises in hand, we carried out a set of experiments using different deuterated solvents and base equivalents of MeOK to assess the effect on the reactivity of diboron compounds towards nitroene deoxygenation (Figure 7). Nevertheless, as can be observed in the graph, although the results do not seem to follow a clear tendency, the presence of the alkoxide do slow down the deoxygenation reaction.

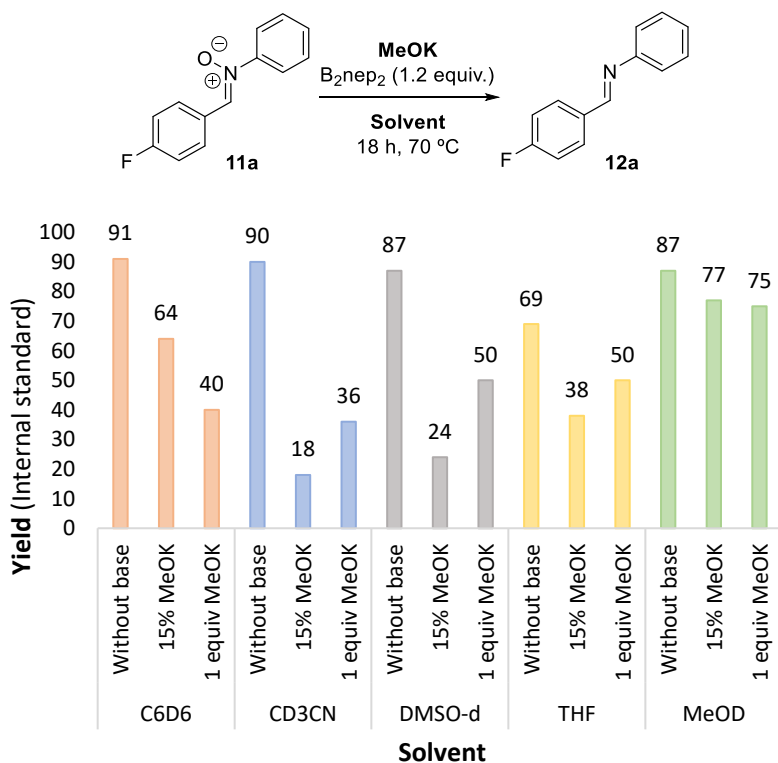


Figure 7. Nitron reactivity in presence of base-activated diborons.

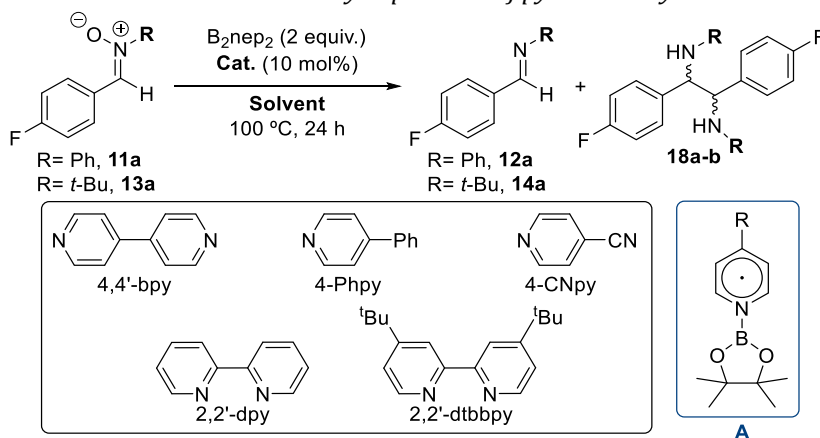
We hypothesize that these apparent anarchical experimental results could be a consequence of several factors such as the base solubility and the stability of the diboron reagent. The poor solubility of the base in non-polar solvents could inhibit its participation in the reaction. B₂nep₂ is a more labile diboron compound that could undergo exchange of alcohols in the presence of MeOK more easily than the bulkier B₂pin₂.

However, these results contrast with recent studies in our laboratory, where different nitrogenated compounds such as nitrosamines and hydrazines also showed a better performance towards the reduction reaction using the diboron-base mix compared to the diboron sole addition.

2.2.3. Reactivity of nitrones in presence of pyridine-boryl radicals

The activation of diboron compounds is not limited to the addition of an alkoxide to the mixture. As demonstrated in previous reports, the addition of a pyridine,¹⁵² enhance the reactivity of diborons to afford new transformations through the formation of pyridine-boryl radicals (Species **A**). Therefore, we tested the influence of the addition of different pyridine derivatives in the reaction of B₂nep₂ and nitrones **11** and **13** (Table 10).

Table 10. Nitronne reactivity in presence of pyridine-boryl radicals.



Entry	R	Solvent	Catalyst	Prod.	Ratio (12a/18)	Yield 18 (%) ^a
1	Ph	CF ₃ Ph	4,4'-bpy	18a	21/79	65
2	Ph	CH ₃ CN	4,4'-bpy	18a	0/100	80 ^b
3	Ph	CH ₃ CN	4-Phpy	18a	0/100	50
4	Ph	CH ₃ CN	4-CNpy	18a	82/18	15
5	Ph	CH ₃ CN	2,2'-bpy	18a	100/0	n.d.
6	Ph	CH ₃ CN	2,2'-dtbbpy	18a	100/0	n.d.
7	<i>t</i> -Bu	CH ₃ CN	4,4'-bpy	18b	10/90	67 ^b

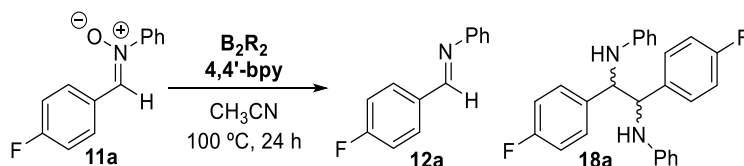
^aYield determined by ¹H RMN using nitromethane as internal standard. ^bIsolated yield.

As can be observed, using catalytic 4,4'-bipyridine in trifluorotoluene at 100 °C we obtained the corresponding imine **12a** along with

diamine **18a** in a 65% NMR yield (entry 1). This diamine could be the result of the homocoupling of two radical intermediates. Among the variety of solvents that we tested, CH₃CN turned to be the optimal, obtaining the diamine **18a** as a diastereomeric mixture with an 80% isolated yield. The utilization of different pyridines as catalysts of the reaction led in all cases to lower yields of the diamine **18a** product (entries 3-6). Finally, we checked if this homocoupling reaction was also affected by the nitrogen substitution of the nitrone as did the deoxygenation. In this case, we observed a similar behavior, being the *tert*-butyl substituted nitrone less reactive though, with a 67% isolated yield (entry 7).

Next, we moved to determine the effect of the equivalents of the reagents in the diamine formation reaction outcome (Table 11).

Table 11. Optimization of the pyridine and diboron equivalents.



Entry	4,4'-bpy (%)	B ₂ R ₂ (equiv.)	Ratio (12/18) ^a	Yield (%)
1	(10%)	B ₂ nep ₂ (2)	(0/100)	80 ^c 18a
2	(10%)	B ₂ nep ₂ (1)	(100/0)	58 ^b 12a
3	(10%)	B ₂ nep ₂ (3)	(0/100)	57 ^c 18a
4	(10%)	B ₂ pin ₂ (2)	(91/9)	68 ^b 12a
5	(5%)	B ₂ nep ₂ (2)	(0/100)	72 ^c 18a
6	(15%)	B ₂ nep ₂ (2)	(0/100)	58 ^c 18a
7	(20%)	B ₂ nep ₂ (2)	(0/100)	57 ^c 18a

^aDetermined by ¹H RMN using nitromethane as internal standard. ^bCalculated by ¹H-NMR using nitromethane as internal standard. ^cIsolated yield.

As depicted in the table, the variation of the B₂nep₂ amount to 1 equivalent led to the full inhibition of the diamine formation (entry 2),

and the increase to 3 equivalents turned to be counterproductive to the diamine yield (entry 3). The utilization of B_2pin_2 afforded the imine/diamine mixture with imine **12a** as major product (entry 4). When we lowered the pyridine amount to a 5 mol% we obtained a good 72% yield of **18a** (entry 5), which decreased when we increased the amount to 15 and 20 mol% (entries 6 and 7).

Additional control experiments were carried out, and we determined that water traces diminish the reaction yield (probably due to imine hydrolysis), and the reaction seems to be not affected by the presence /absence of light.

The tendency of nitrones to be reduced in the presence of diboron reagents and the formation of diamine **18a**, made us suspect that the diamine was the result of the coupling of two imine derivatives. In fact, the result showed in table 12 confirmed this hypothesis. When we performed the reaction using imines **12a** and **14a** as substrates, both imines with Ph and *t*-Bu substituents evolved towards the diamine formation, being the yield higher with the phenyl derivative (entries 1 and 3) than with the *t*-Bu substituent (entry 2). The use of just 1 equivalent of B_2nep_2 also seemed to be beneficial for the process (compare entries 1 with 3 and 2 with 4).

Table 12. Diamine formation from the imine.

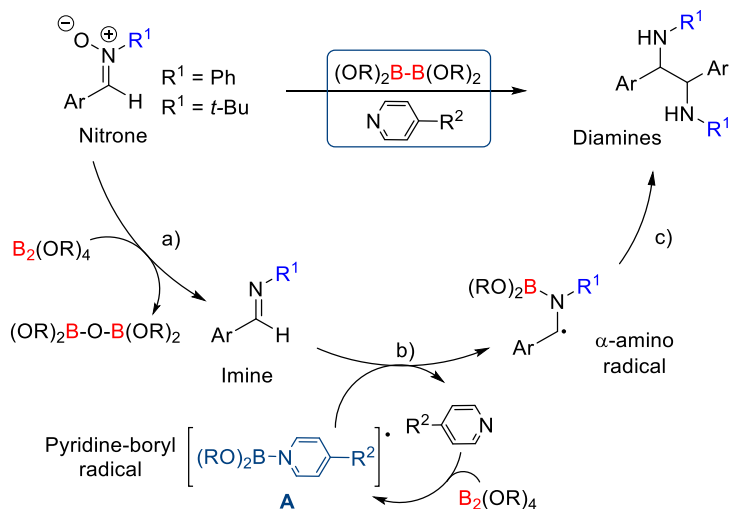
$\text{R} = \text{Ph}, \mathbf{12a}$
 $\text{R} = t\text{-Bu}, \mathbf{14a}$

Entry	R	B ₂ nep ₂ (equiv.)	Conv. ^a (%)	Yield ^b (%)
1	Ph	2	100	54%
2	^t Bu	2	29	-
3	Ph	1	100	73%
4	^t Bu	1	100	40%

^aDetermined by ¹H-RMN. ^bYield determined by ¹H-NMR using nitromethane as internal standard.

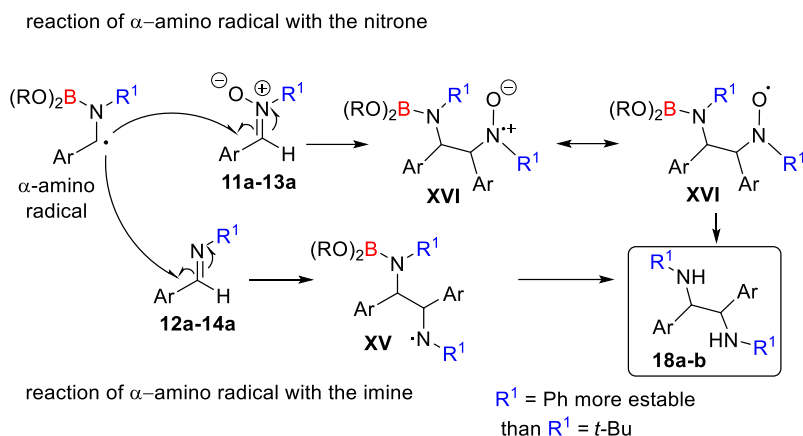
Interestingly, the yields of diamines starting from the imines were lower than when starting from the corresponding nitrones, especially in the case of the *t*-Butyl substituent.

Although we need to perform more experiments, with the existing data we proposed the following preliminary mechanism (Scheme 64). We have proven that nitrones undergo reduction to form the corresponding imine in the presence of a diboron reagent, along with the formation of the species (OR)₂B-O-B(OR)₂ (step a). Once some imine is formed, the pyridine-boryl radical **A** would react with it, forming the α-amino radical (step b). Subsequently, the α-amino radical would react with itself to form the corresponding diamines (step c).



Scheme 64. Diamine formation mechanistic proposal.

The α -amino radical could also react with the corresponding imine and/or nitron (Scheme 65). The coupling of the α -amino radical with imines **12** or **14** would provide a radical intermediate **XV**, which would be more stable in the case of R=Ph than when R= *t*-Bu. The reaction of the α -amino radical with nitrones would provide the stable nitroxil radical **XVI**, which after deoxygenation would evolve towards diamine **18**. The existence of these alternative pathways could explain the fact that the diamines **18** are obtained in higher yields starting from nitrones instead of imines (compare Tables 9 and 11) and the higher yield obtained with the phenyl derivatives.

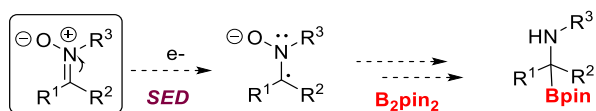


Scheme 65. Diamine **18** possible formation pathways from α -amino radical.

The formation of diamines is an interesting subject to exploit in the future.²⁴⁴ Moreover, the trapping of the α -amino radical with other substrates opens new synthetic possibilities.

3.2.4. Reactivity of nitrones in presence of super electron donors

Finally, we moved to study the reactivity of the model nitron **11a** under super electron donor conditions. We were interested in the treatment of nitrones with the SED mixture in order to capture the radical intermediate with B_2pin_2 to provide α -aminoboronates (Scheme 66).²⁴⁵



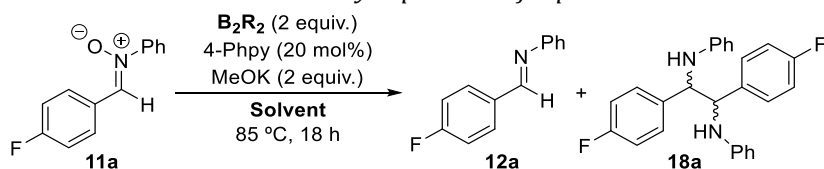
Scheme 66. α -aminoboronates formation proposal.

²⁴⁴ Zhou, M.; Li, K.; Chen, D.; Xu, R.; Xu, G.; Tang, W. *J. Am. Chem. Soc.* **2020**, *142*, 10337.

²⁴⁵ a) Ohmura, T.; Awano, T.; Sugimoto, M. *J. Am. Chem. Soc.*, **2010**, *132*, 13191. b) Ohmura, T.; Awano, T.; Sugimoto, M. *J. Am. Chem. Soc.*, **2011**, *133*, 20738.

To this end, we added to the diboron reagent and 4-phenylpyridine and MeOK as alkoxide base to the nitron. Nevertheless, as can be observed in table 13, the generation of the super electron donor using different solvents provides the reduction of the nitron and the formation of the diamine. The yields obtained when using the base are lower than when using conditions of table 10. Under the standard SED conditions using 4-Phpy and MeOK, diamine **18a** yield drops to a 59% (entry 1). The use of CH₃CN and MTBE as solvents lead to similar results (entries 2-3).

Table 13. Nitron reactivity in presence of super electron donors.



Entry	Solvent	Ratio ^a (12a/18a)	Yield 18a (%) ^a
1	CF ₃ Ph	34:66	59
2	CH ₃ CN	24:76	56
3	MTBE	0:100	63

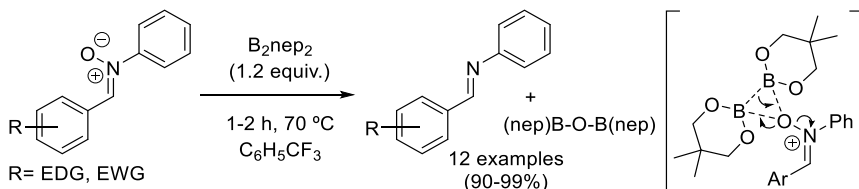
^aDetermined by ¹H RMN using nitromethane as internal standard.

Therefore, the preliminary attempts of utilization of diboron-derived SEDs with nitrones neither brings new transformations, nor represents any advantage in the reduction of nitrones or in the formation of diamines.

3.3. Conclusions

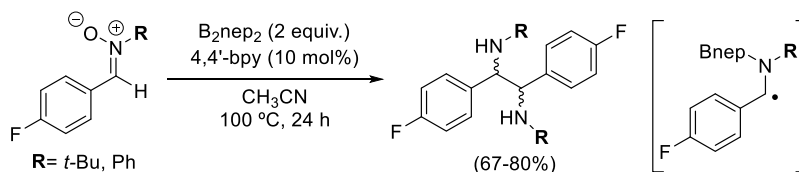
In conclusion, the reactivity of nitrones has been studied in the presence of diboron reagents, as well as in presence of catalytic pyridine derivatives, with and without MeONa.

We have found that nitrones react with diboron reagents to form the corresponding imines in high yields, representing a complementary mild and cheap method to the previously reported procedures to attain imines from nitrones (Scheme 67). We proved that the deoxygenation occurs via formation of a $(OR)_2B-O-B(OR)_2$ species which makes the process thermodynamically favoured. The process, which according to theoretical calculations occurs through a concerted mechanism, seems to be very sensitive to steric hindrance around the nitrono substituent and around the diboron reagent.



Scheme 67. Diboron promoted nitrono reduction to imines.

When nitrones are treated with diboron reagents in the presence of catalytic amounts of substituted pyridines, they evolve towards the formation of diamines, which can be obtained in high yields (Scheme 68). The pyridine-boryl radicals could promote the formation of an α -amino radical intermediate from the substituted imine which undergoes dimerization to provide the corresponding diamines.



Scheme 68. Pyridine-boryl radical promoted diamine formation.

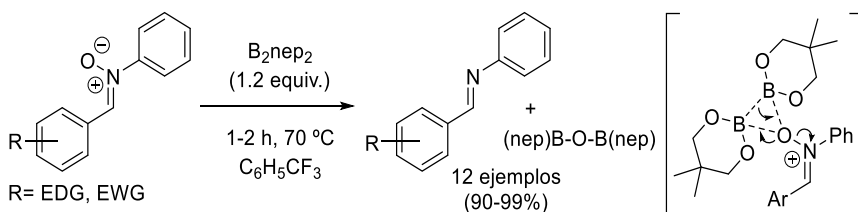
This transformation opens access to a powerful strategy to provide amine containing compounds via reaction of the α -amino radical intermediate with radical acceptors or even radical cyclization. These processes are currently being explored in our laboratory.

Although it is described that nitrones could evolve to form aminoxyl radical via single electron transfer (SET), the use of super electron donors derived from diboron reagents in the presence of catalytic amounts of pyridines and MeONa evolve towards deoxygenation. This process seems to be more favoured due to the oxophilic nature of boron and the stability of the B-O-B bonds.

3.3. Conclusiones

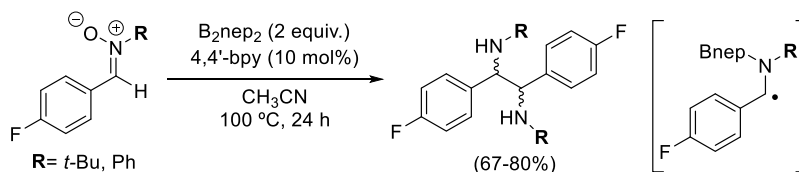
En conclusión, hemos estudiado la reactividad de las nitronas en presencia de reactivos de diboro, así como en presencia de reactivos de diboro activados por diferentes piridinas en cantidades catalíticas, con y sin MeONa.

Hemos encontrado que las nitronas reaccionan con ésteres diborónicos para dar las correspondientes iminas con elevados rendimientos. De esta manera, el método representa una alternativa suave y barata con respecto a los procedimientos previamente publicados para preparar iminas a partir de nitronas (esquema 67). Hemos demostrado que la desoxigenación ocurre vía formación de una especie $(OR)_2B-O-B(OR)_2$ termodinámicamente favorecida. El proceso parece ser bastante sensible al impedimento estérico del sustituyente de la nitrona, así como del reactivo de boro utilizado.



Esquema 67. Reducción de nitronas a iminas promovida por ésteres borónicos.

Cuando las nitronas se trataron con reactivos de diboro en presencia de cantidades catalíticas de diferentes piridinas sustituidas, éstas evolucionaron a la formación de diaminas con altos rendimientos (esquema 68). Los radicales boril-piridina pueden promover la formación de un α -amino radical a partir de la imina sustituida, el cual da la dimerización que proporciona las correspondientes diaminas.



Esquema 68. Formación de diaminas promovida por radicales boril-piridina.

Esta transformación da acceso a una potente estrategia para llegar a compuestos con aminas vía reacción del radical α -amina intermedio con electrófilos, o incluso mediante ciclación radicalica. Estos procesos están siendo actualmente estudiados en nuestro laboratorio.

Aunque está descrito que las nitronas pueden evolucionar para dar radicales aminoxilo vía procesos "single electron transfer" (SET), el uso de súper electrón donadores derivados de diboros en presencia de piridinas en cantidad catalítica y MeONa lleva a la desoxigenación de las nitronas. Este proceso parece estar más favorecido debido a la naturaleza oxofílica del boro y a la estabilidad de los enlaces B-O-B.

Part II. Chapter 2. Experimental Section

A. General methods and materials

Nuclear Magnetic Resonance (NMR)

Monodimensional and bidimensional NMR spectra were acquired at 25 °C on a Bruker AC-300 spectrometer using CDCl₃ as the solvent, running at 300 and 75 MHz for ¹H and ¹³C, respectively. Chemical shifts (δ) are reported in ppm relative to residual solvent signals (CDCl₃, 7.26 ppm for ¹H NMR, and 77.0 ppm for ¹³C NMR). In all ¹H NMR spectra, multiplicity is indicated as follows: br (broad signal), s (singlet), d (doublet), t (triplet), q (quartet), quint (quintet), sex (sextet), sep (septet), non (nonet) or m (multiplet). Coupling constant values (in Hertz) and number of protons for each signal are also indicated.

Chromatography

For thin layer chromatography (TLC) Supelco silica gel plates with fluorescence indicator 254 nm were used and compounds were visualized by irradiation with UV light and/or by treatment with a solution of KMnO₄ (1.5 g), K₂CO₃ (10 g), and 10% NaOH (1.25 mL) in H₂O (200 mL) or a solution of phosphomolybdic acid (12 g), in EtOH (250 mL) followed by heating. For specific boronic ester visualization, TLC were treated with a solution of (NH₄)₆Mo₇O₂₄ · 4H₂O (2.5 g), Ce(NH₄)₄(SO₄)₄ · 2H₂O (1 g), H₂SO₄ (10 mL) in H₂O (90 mL) followed by strong heating. Flash column chromatography (FCC) was performed using Merck Millipore 60 Å, 40-63 μm silica gel and compressed air.

Mass spectrometry

Mass spectra (MS) and High Resolution Mass Spectra (HRMS) were obtained in a *VG AutoSpec Spectrometer* in positive electrospray ionisation (ESI) or electron impact ionisation (EI). Obtained data are expressed in mass/charge (m/z) units. Values between parentheses

indicate relative intensities with regard to the base peak.

Miscellaneous

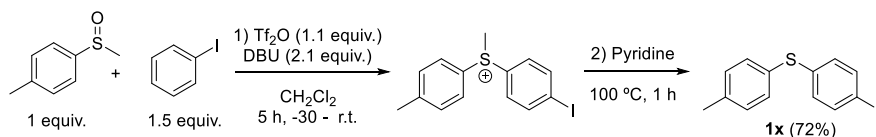
c-Hexane and AcOEt were supplied by *Carlo Erba* and were used without previous purification. All the other reactants were purchased from *Aldrich*, *Fluorochem* or *Alfa Aesar* and were also used without any previous treatment, except otherwise indicated.

All described synthesized products and their spectroscopic data are consistent with the references indicated next to the name of each compound.

Dry solvents were deoxygenated before used following the freeze-pump-thaw procedure.

B. Experimental section of Chapter 2

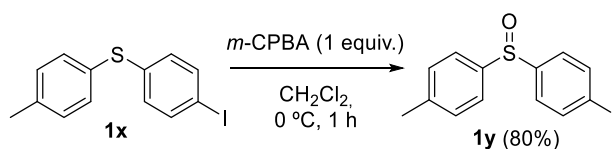
Synthesis of the (4-iodophenyl)(*p*-tolyl)sulfane (**1x**)²⁴⁶



(4-Iodophenyl)(*p*-tolyl)sulfane (**1x**) was prepared following the procedure described in the literature.²⁴⁷ Methyl *p*-tolyl sulfoxide (154 mg, 1 mmol) was dissolved in CH_2Cl_2 (5 mL) in an oven-dried sealed vial and the solution was cooled to -30°C . Tf_2O (310 mg, 1.1 mmol) was then added dropwise, followed by the iodobenzene (306 mg, 1.5 mmol). After 15 minutes at -30°C , the reaction was stirred at r.t. for 1.5 h. Then, DBU was added and the mixture was stirred for another 4 h. The solution was quenched with H_2O (10 mL) and the aqueous layer was extracted with CH_2Cl_2 (3 x 10 mL). The combined organic layers were dried over MgSO_4 and concentrated at reduced pressure. The crude oil was then dissolved in pyridine (5 mL) and stirred at 100°C for 1 h. The solution was concentrated under vacuo and the resulting crude was purified by flash column chromatography using a cyclohexane:toluene 100:1 mixture as eluent. The spectroscopical data were in accordance with the literature. **$^1\text{H NMR}$ (300 MHz, CDCl_3)** δ 7.56 (d, $J = 8.4$ Hz, 2H), 7.33 (d, $J = 8.1$ Hz, 2H), 7.17 (d, $J = 8.3$ Hz, 2H), 6.96 (d, $J = 8.5$ Hz, 2H), 2.37 (s, 3H).

²⁴⁶ Bhowmik, A.; Yadav, M.; Fernandes, R. S. *Org. Biomol. Chem.* **2020**, *18*, 2447.

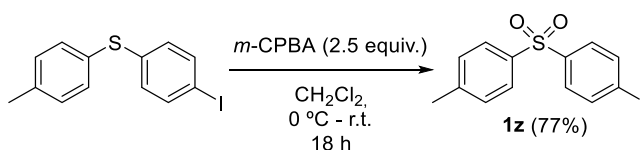
²⁴⁷ Fernández-Salas, J. A.; Pulis, A. P.; Procter, D. J. *Chem. Commun.* **2016**, *52*, 12364.

Synthesis of the 1-iodo-4-(*p*-tolylsulfinyl)benzene (**1y**)²⁴⁸

To a solution of aryl iodide **1x** (80 mg, 0.25 mmol) in CH₂Cl₂ (1.25 mL) a solution of *m*-CPBA (43.2 mg, 0.25 mmol) in CH₂Cl₂ (1.25 mL) was added dropwise at 0 °C. The mixture was stirred at the same temperature for 1 h and then quenched with saturated aqueous NaHCO₃. The mixture was extracted with CH₂Cl₂ (3 x 5 mL) and the combined organic layers were dried over MgSO₄, filtered, and concentrated at reduced pressure. The resulting crude was purified by flash chromatography using a cyclohexane : ethyl acetate 20:1 mixture as eluent. The spectroscopical data were in accordance with the literature. ¹H NMR (300 MHz, CDCl₃) δ 7.79 (d, *J* = 8.5 Hz, 2H), 7.51 (d, *J* = 8.2 Hz, 2H), 7.35 (d, *J* = 8.6 Hz, 2H), 7.27 (d, *J* = 8.4 Hz, 2H), 2.37 (s, 3H).

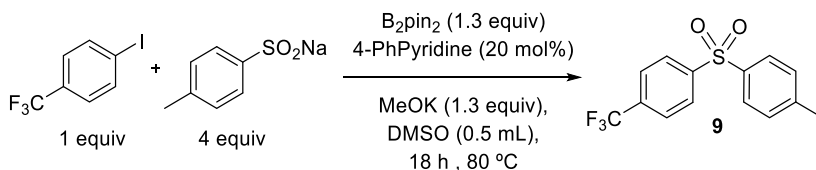
²⁴⁸ Chen, D-L.; Sun, Y.; Chen, M.; Li, X.; Zhang, L.; Huang, X.; Bai, Y.; Luo, F.; Peng, B. *Org. Lett.* **2019**, *21*, 3986.

Synthesis of the 1-iodo-4-tosylbenzene (**1z**)²⁴⁹



To a solution of aryl iodide **1x** (158 mg, 0.5 mmol) in CH₂Cl₂ (2.5 mL) a solution of *m*-CPBA (259 mg, 1.5 mmol) in CH₂Cl₂ (2.5 mL) was added dropwise at 0 °C. The mixture was stirred at room temperature for 18 h and then quenched with saturated aqueous NaHCO₃. The mixture was extracted with CH₂Cl₂ (3 x 10 mL) and the combined organic layers were dried over MgSO₄, filtered, and concentrated at reduced pressure. The resulting crude was purified by flash chromatography using a cyclohexane : ethyl acetate 20:1 mixture as eluent. The spectroscopical data were in accordance with the literature. ¹H NMR (300 MHz, CDCl₃) δ 7.84 (d, *J* = 8.6 Hz, 2H), 7.80 (d, *J* = 8.4 Hz, 2H), 7.62 (d, *J* = 8.6 Hz, 2H), 7.30 (d, *J* = 8.1 Hz, 2H), 2.39 (s, 3H).

Preliminary attempt of the C-S coupling using sulfinate



In a nitrogen filled glovebox at ambient temperature, sodium *p*-toluenesulfinate (1 mmol) was added to a screw capped vial and diluted in 0.8 mL of dry and deoxygenated DMSO. Then, B₂pin₂ (0.325 mmol, 82.6 mg), 4-phenylpyridine (0.05 mmol, 7.8 mg), MeOK (0.325

²⁴⁹ Wu, X.; Wang, Y. *New J. Chem.* **2018**, *42*, 10953.

mmol, 22.3 mg), and -iodo-4-(trifluoromethyl)benzene (0.25 mmol) were sequentially added to the solution. The vial was then sealed with a Teflon cap, and the mixture was stirred at 80°C for 24 h.

After this time, the reaction was diluted with 10 mL EtOAc and the solution was washed with H₂O, the organic phase was then dried over Na₂SO₄, filtered, and concentrated under reduced pressure. The crude was finally purified by flash column chromatography using a cHex: EtOAc mixture as eluent (20:1 to 9:1) to afford the sulfone **9** (30 mg, 38 %). Spectroscopic data were in accordance with the literature. ¹H NMR (300 MHz, CDCl₃) δ 8.06 (d, *J* = 8.2 Hz, 2H), 7.85 (d, *J* = 8.3 Hz, 2H), 7.76 (d, *J* = 8.3 Hz, 2H), 7.34 (d, *J* = 8.1 Hz, 2H), 2.42 (s, 3H).

General procedures for the C-S coupling reaction

For convenience, most of the reactions have been performed in the glovebox. Nevertheless, we have demonstrated in several cases that the method can be translated to a Schlenk line with no significant drop in the yield.

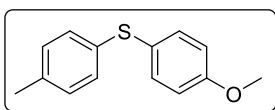
Procedure in the glovebox

In a nitrogen filled glovebox at ambient temperature, the corresponding thiol (0.375 mmol) was added to a screw capped vial and diluted in 0.5 mL of dry and deoxygenated DMSO. Then, NaH (0.45 mmol, 10.8 mg) is added observing gas evolution, and the mixture is stirred at room temperature for 30 minutes. After complete deprotonation of the thiol; B₂pin₂ (0.325 mmol, 82.6 mg), 4-phenylpyridine (0.05 mmol, 7.8 mg), MeOK (0.325 mmol, 22.3 mg), and the corresponding iodide (0.25 mmol) were sequentially added to the thiolate solution. The vial was then sealed with a Teflon cap, and the mixture was stirred at room temperature for 24 h.

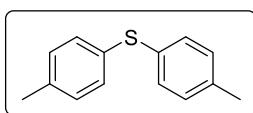
After this time, the reaction was diluted with 10 mL EtOAc and DMSO was eliminated following two different techniques specified in each case. In **method A** the solution was washed with H₂O, the organic phase was then dried over Na₂SO₄, filtered, and concentrated under reduced pressure. In **method B** (for compounds partially soluble in water **3e**, **3k**, **3s**, **3ar**, **3as**) the solution was filtered through a short pad of silica. The pad is then washed with a 10:1 *c*Hex : EtOAc mixture, and the filtrate is concentrated in vacuo. Once eliminated the DMSO, the crude was finally purified by flash column chromatography using a *c*Hex : EtOAc mixture as eluent to afford the desired diaryl thioether.

Procedure outside the glovebox

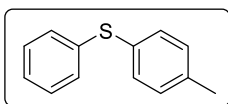
In a screw capped vial, the corresponding thiol (0.375 mmol) is added along with NaH (0.45 mmol, 10.8 mg), and the vial is evacuated and backfilled with argon 3 times. Then, the mixture of solids is diluted with 0.5 mL of dry and deoxygenated DMSO, and the solution is stirred for 30 min at room temperature (gas evolution observed). After complete deprotonation of the thiol, B₂pin₂ (0.325 mmol, 82.6 mg), 4-phenylpyridine (0.05 mmol, 7.8 mg), MeOK (0.325 mmol, 22.3 mg), and the corresponding iodide (0.25 mmol) were sequentially added as solids to the thiolate solution under Ar positive pressure. The vial is then sealed with a Teflon cap, and the mixture was purged with argon for 5 minutes. After this, the mixture was stirred at room temperature for 24 h. After this time, the reaction is diluted with 10 mL EtOAc and the solution is treated according to either method A or B.

(4-Methoxyphenyl)(*p*-tolyl)sulfane (3a)²⁰⁶

Synthesized according to general procedure, method A using either the combination of 4-iodoanisole and 4-methyl benzenethiol or 4-iodotoluene and 4-methoxybenzenethiol. The product was purified by column chromatography (cyclohexane:ethyl acetate 100:1) to get the product **3a** (39.1 mg, 68%). Spectroscopical data were in accordance with the literature.¹H NMR (300 MHz, CDCl₃) δ 7.37 (d, *J* = 8.7 Hz, 1H), 7.10 (dd, *J* = 20.8, 8.1 Hz, 2H), 6.87 (d, *J* = 8.7 Hz, 1H), 3.81 (s, 2H), 2.31 (s, 2H).

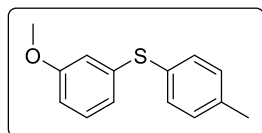
Di-*p*-tolylsulfane (3b)²⁵⁰

Synthesized according to general procedure, method A. The product was purified by column chromatography (cyclohexane:toluene 100:1) to get the product **3b** (32.1 mg, 60%). Spectroscopical data were in accordance with the literature.¹H NMR (300 MHz, CDCl₃) δ 7.29 (d, *J* = 8.0 Hz, 4H), 7.16 (d, *J* = 8.0 Hz, 4H), 2.38 (s, 6H).

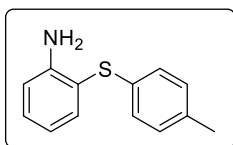
Phenyl(*p*-tolyl)sulfane (3c)¹⁹³

Synthesized according to general procedure, method A. The product was purified by column chromatography (cyclohexane) to get the product **3c** (38 mg, 76%). Spectroscopical data were in accordance with the literature.¹H NMR (300 MHz, CDCl₃) δ 7.38 – 7.08 (m, 9H), 2.37 (s, 3H).

²⁵⁰ Ke, F.; Qu, Y.; Jiang, Z.; Li, Z.; Wu, D.; Zhou, X. *Org. Lett.* **2011**, *13*, 454.

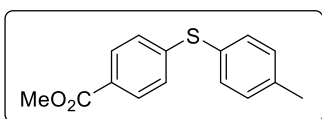
(3-Methoxyphenyl)(*p*-tolyl)sulfane (3d)²⁰³

Synthesized according to general procedure, method A. The product was purified by column chromatography (cyclohexane:ethyl acetate 100:1) to get the product **3d** (53.4 mg, 93%). Spectroscopical data were in accordance with the literature.¹**H NMR (300 MHz, CDCl₃)** δ 7.33 (d, J = 8.1 Hz, 2H), 7.22 – 7.11 (m, 3H), 6.83 (d, J = 8.3 Hz, 1H), 6.80 (t, J = 1.9 Hz, 1H), 6.73 (dd, J = 8.2, 2.5 Hz, 1H), 3.75 (s, 3H), 2.35 (s, 3H).

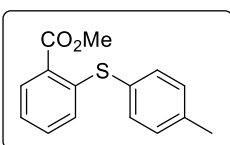
2-(*p*-Tolylthio)aniline (3e)²⁵¹

Synthesized according to general procedure, method B. The product was purified by column chromatography (cyclohexane:ethyl acetate 100:1) to get the product **3e** (33 mg, 64%). Spectroscopical data were in accordance with the literature.¹**H NMR (300 MHz, CDCl₃)** δ 7.45 (dt, J = 9.4, 4.7 Hz, 1H), 7.26 – 7.18 (m, 1H), 7.08 – 7.00 (m, 4H), 6.83 – 6.70 (m, 2H), 4.28 (s br, 2H), 2.29 (s, 3H).

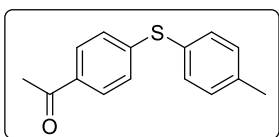
²⁵¹ Panova, Y. S.; Kashin, A. S.; Vorobev, M. G.; Degtyareva, E. S.; Ananikov, V. P. *ACS Catal.* **2016**, *6*, 3637.

Methyl 4-(*p*-tolylthio)benzoate (**3f**)²⁰⁶

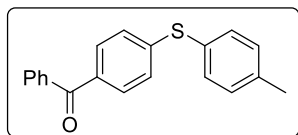
Synthesized according to general procedure, method A. The product was purified by column chromatography (cyclohexane:ethyl acetate 100:1) to get the product **3f** (46 mg, 71%). Spectroscopical data were in accordance with the literature. ¹H NMR (300 MHz, CDCl₃) δ 7.87 (d, *J* = 8.6 Hz, 2H), 7.41 (d, *J* = 8.1 Hz, 2H), 7.22 (d, *J* = 7.9 Hz, 2H), 7.15 (d, *J* = 8.6 Hz, 2H), 3.88 (s, 3H), 2.39 (s, 3H).

Methyl 2-(*p*-tolylthio)benzoate (**3g**)²⁰³

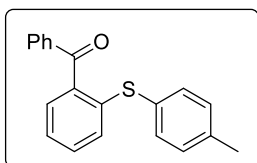
Synthesized according to general procedure, method A. The product was purified by column chromatography (cyclohexane:ethyl acetate 50:1) to get the product **3g** (37.6 mg, 65%). Spectroscopical data were in accordance with the literature. ¹H NMR (300 MHz, CDCl₃) δ 7.98 (dd, *J* = 7.8, 1.5 Hz, 1H), 7.46 (d, *J* = 8.0 Hz, 2H), 7.23 (m, 3H), 7.10 (t, *J* = 7.5 Hz, 1H), 6.80 (d, *J* = 8.2 Hz, 1H), 3.96 (s, 3H), 2.41 (s, 3H).

1-(4-(*p*-Tolylthio)phenyl)ethan-1-one (**3h**)²⁰³

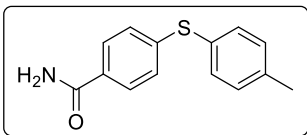
Synthesized according to general procedure, method A. The product was purified by column chromatography (cyclohexane:ethyl acetate 20:1) to get the product **3h** (37 mg, 62%). Spectroscopical data were in accordance with the literature. ¹H NMR (300 MHz, CDCl₃) δ 7.80 (d, *J* = 8.6 Hz, 2H), 7.41 (d, *J* = 8.1 Hz, 2H), 7.22 (d, *J* = 7.9 Hz, 2H), 7.15 (d, *J* = 8.7 Hz, 2H), 2.54 (s, 3H), 2.40 (s, 3H).

Phenyl(4-(*p*-tolylthio)phenyl)methanone (3i)²⁰⁶

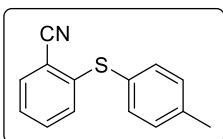
Synthesized according to general procedure, method A. The product was purified by column chromatography (cyclohexane:ethyl acetate 100:1) to get the product **3i** (52 mg, 68%). Spectroscopical data were in accordance with the literature. ¹H NMR (300 MHz, CDCl₃) δ 7.81 – 7.72 (m, 2H), 7.72 – 7.64 (m, 2H), 7.63 – 7.53 (m, 1H), 7.53 – 7.40 (m, 4H), 7.32 – 7.14 (m, 4H), 2.40 (s, 3H).

Phenyl(2-(*p*-tolylthio)phenyl)methanone (3j)

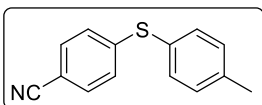
Synthesized according to general procedure, method A. The product was purified by column chromatography (cyclohexane:ethyl acetate 100:1) to get the product **3j** (57.7 mg, 76%) as a yellow oil. ¹H NMR (300 MHz, CDCl₃) δ 7.82 (d, *J* = 7.3 Hz, 2H), 7.58 (t, *J* = 7.3 Hz, 1H), 7.51 – 7.38 (m, 3H), 7.36 – 7.07 (m, 7H), 2.34 (s, 3H). ¹³C NMR (75 MHz, CDCl₃) δ 196.8 (CO), 138.9 (C), 138.7 (2C), 137.8 (C), 133.9 (CH), 133.4 (CH), 131.2 (CH), 130.8 (C), 130.7 (CH), 130.5 (CH), 130.5 (CH), 130.0 (CH), 128.7 (CH), 125.7 (CH), 21.5 (CH₃). HRMS (EI⁺) Calcd for C₂₀H₁₆OS [M]⁺ 304.0922, Found 304.0928.

4-(*p*-Tolylthio)benzamide (3k)²⁵²

Synthesized according to general procedure, method B. The product was purified by column chromatography (cyclohexane:ethyl acetate 4:1) to get the product **3k** (45.8 mg, 75%). Spectroscopical data were in accordance with the literature. ¹H NMR (300 MHz, CDCl₃) δ 7.66 (d, *J* = 8.6 Hz, 2H), 7.39 (d, *J* = 8.1 Hz, 2H), 7.20 (m, 4H), 6.01 (br s, 2H), 2.39 (s, 3H).

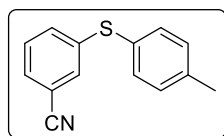
2-(*p*-Tolylthio)benzonitrile (3l)²⁰⁶

Synthesized according to general procedure, method A. The product was purified by column chromatography (cyclohexane:ethyl acetate 100:1) to get the product **3l** (46 mg, 82%). Spectroscopical data were in accordance with the literature. ¹H NMR (300 MHz, CDCl₃) δ 7.61 (d, *J* = 7.7 Hz, 1H), 7.46 – 7.30 (m, 3H), 7.30 – 7.16 (m, 3H), 7.03 (d, *J* = 8.1 Hz, 1H), 2.39 (s, 3H).

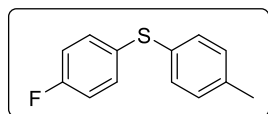
4-(*p*-Tolylthio)benzonitrile (3m)²⁰³

Synthesized according to general procedure, method A. The product was purified by column chromatography (cyclohexane:ethyl acetate 10:1) to get the product **3m** (44 mg, 78%). Spectroscopical data were in accordance with the literature. ¹H NMR (300 MHz, CDCl₃) δ 7.45 (d, *J* = 8.7 Hz, 2H), 7.41 (d, *J* = 8.2 Hz, 2H), 7.25 (d, *J* = 8.0 Hz, 2H), 7.12 (d, *J* = 8.6 Hz, 2H), 2.41 (s, 3H).

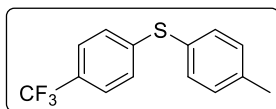
²⁵² Gendre, F.; Yang, M.; Diaz, P. *Org. Lett.* **2005**, *7*, 2719.

3-(*p*-Tolylthio)benzonitrile (**3n**)²⁵³

Synthesized according to general procedure, method A. The product was purified by column chromatography (cyclohexane:ethyl acetate 10:1) to get the product **3n** (43 mg, 77%). Spectroscopical data were in accordance with the literature. ¹H NMR (300 MHz, CDCl₃) δ 7.44 – 7.27 (m, 6H), 7.22 (d, *J* = 7.9 Hz, 2H), 2.40 (s, 3H).

(4-Fluorophenyl)(*p*-tolyl)sulfane (**3o**)²⁵⁴

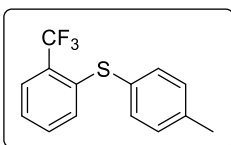
Synthesized according to general procedure, method A. The product was purified by column chromatography (cyclohexane:toluene 100:1) to get the product **3o** (46.2 mg, 85%). Spectroscopical data were in accordance with the literature. ¹H NMR (300 MHz, CDCl₃) δ 7.32 (m, 2H), 7.25 (d, *J* = 8.0 Hz, 2H), 7.13 (d, *J* = 7.9 Hz, 2H), 7.00 (m, 2H), 2.35 (s, 3H).

p-Tolyl(4-(trifluoromethyl)phenyl)sulfane (**3p**)²⁵⁴

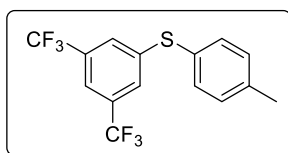
Synthesized according to general procedure, method A. The product was purified by column chromatography (cyclohexane:ethyl acetate 100:1) to get the product **3p** (61 mg, 91%). In the case of the gram-scale experiment, we started from 4 mmol (1088 mg) of iodide to get the product **3p** (1.005 g, 93%). Spectroscopical data were in accordance with the literature. ¹H NMR (300 MHz, CDCl₃) δ 7.45 (d, *J* = 8.3 Hz, 2H), 7.40 (d, *J* = 8.2 Hz, 2H), 7.21 (m, 4H), 2.39 (s, 3H).

²⁵³ Yoo, B. W.; Yu, B. R.; Yoon, C. M. *J. Sulfur. Chem.* **2015**, *36*, 358.

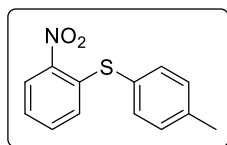
²⁵⁴ Timpa, S. D.; Pell, C. J.; Ozerov, O. V. *J. Am. Chem. Soc.* **2014**, *136*, 14772.

p-Tolyl(2-(trifluoromethyl)phenyl)sulfane (**3q**)²⁵⁵

Synthesized according to general procedure, method A. The product was purified by column chromatography (cyclohexane:ethyl acetate 100:1) to get the product **3q** (55.6 mg, 83%). Spectroscopical data were in accordance with the literature. **¹H NMR (300 MHz, CDCl₃)** δ 7.67 (d, *J* = 7.7 Hz, 1H), 7.38 (d, *J* = 8.1 Hz, 2H), 7.35 – 7.22 (m, 2H), 7.20 (d, *J* = 8.0 Hz, 2H), 7.11 (d, *J* = 7.9 Hz, 1H), 2.39 (s, 3H).

(3,5-Bis(trifluoromethyl)phenyl)(*p*-tolyl)sulfane (**3r**)²⁰⁶

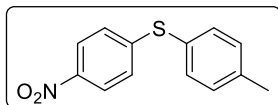
Synthesized according to general procedure, method A. The product was purified by column chromatography (cyclohexane) to get the product **3r** (79 mg, 94%). Spectroscopical data were in accordance with the literature. **¹H NMR (300 MHz, CDCl₃)** δ 7.65 (s, 1H), 7.57 (s, 2H), 7.46 (d, *J* = 8.1 Hz, 2H), 7.30 (d, *J* = 7.9 Hz, 2H), 2.46 (s, 3H).

(2-Nitrophenyl)(*p*-tolyl)sulfane (**3s**)²⁵⁶

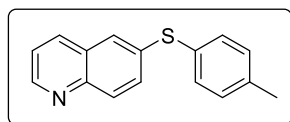
Synthesized according to general procedure, method B. The product was purified by column chromatography (cyclohexane:ethyl acetate 20:1) to get the product **3s** (35.5 mg, 58%). Spectroscopical data were in accordance with the literature. **¹H NMR (300 MHz, CDCl₃)** δ 8.24 (d, *J* = 8.2 Hz, 1H), 7.48 (d, *J* = 7.9 Hz, 2H), 7.39 – 7.25 (m, 3H), 7.21 (t, *J* = 7.7 Hz, 1H), 6.87 (d, *J* = 8.2 Hz, 1H), 2.45 (s, 3H).

²⁵⁵ Still, I. W. J.; Toste, F. D. *J. Org. Chem.* **1996**, *61*, 7677.

²⁵⁶ Zhang, X.; Lu, G.; Cai, C. *Green Chem.* **2016**, *18*, 5580.

(4-Nitrophenyl)(p-tolyl)sulfane (3t)²⁵⁷

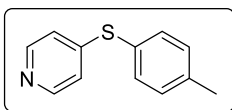
Synthesized according to general procedure, method B. The product was purified by column chromatography (cyclohexane:ethyl acetate 20:1) to get the product **3t** (38.6 mg, 63%). Spectroscopical data were in accordance with the literature. ¹H NMR (300 MHz, CDCl₃) δ 8.05 (d, J = 9.0 Hz, 2H), 7.44 (d, J = 8.1 Hz, 2H), 7.27 (d, J = 7.8 Hz, 2H), 7.14 (d, J = 9.0 Hz, 2H), 2.42 (s, 3H).

6-(p-Tolylthio)quinoline (3u)²⁵⁸

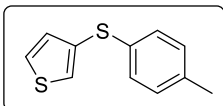
Synthesized according to general procedure, method A. The product was purified by column chromatography (cyclohexane:ethyl acetate 10:1) to get the product **3u** (32 mg, 55%). Spectroscopical data were in accordance with the literature. ¹H NMR (300 MHz, CDCl₃) δ 8.84 (dd, J = 4.2, 1.6 Hz, 1H), 8.12 – 7.88 (m, 2H), 7.69 – 7.48 (m, 2H), 7.48 – 7.30 (m, 3H), 7.19 (d, J = 8.2 Hz, 2H), 2.38 (s, 3H).

²⁵⁷ Zhao, J. N.; Kayumov, M.; Wang, D. Y.; Zhang, A. *Org. Lett.* **2019**, *21*, 7303.

²⁵⁸ Li, Y.; Bao, G.; Wu, X. F. *Chem. Sci.* **2020**, *11*, 2187.

4-(*p*-Tolylthio)pyridine (**3v**)²⁵⁹

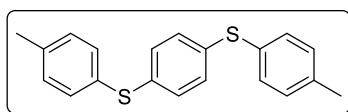
Synthesized according to general procedure, method A. The product was purified by column chromatography (cyclohexane:ethyl acetate 10:1) to get the product **3v** (22.2 mg, 44%). Spectroscopical data is in accordance with the literature. ¹H NMR (300 MHz, CDCl₃) 8.31 (d, *J* = 6.2 Hz, 2H), 7.44 (d, *J* = 8.1 Hz, 2H), 7.26 (d, *J* = 7.9 Hz, 2H), 6.91 (d, *J* = 6.2 Hz, 2H), 2.41 (s, 3H).

3-(*p*-Tolylthio)thiophene (**3w**)²⁶⁰

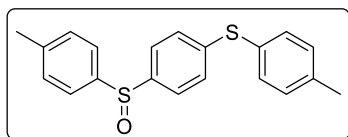
Synthesized according to general procedure, method A. The product was purified by column chromatography (cyclohexane) to get the product **3w** (42.4 mg, 83%). Spectroscopical data were in accordance with the literature. ¹H NMR (300 MHz, CDCl₃) δ 7.35 (dd, *J* = 4.9, 3.0 Hz, 1H), 7.30 (dd, *J* = 3.0, 1.2 Hz, 1H), 7.21 (d, *J* = 8.2 Hz, 2H), 7.11 (d, *J* = 8.1 Hz, 2H), 7.03 (dd, *J* = 5.0, 1.2 Hz, 1H), 2.33 (s, 3H).

²⁵⁹ Ishitobi, K.; Isshiki, R.; Asahara, K. K.; Lim, C.; Muto, K.; Yamaguchi, J. *Chem. Lett.* **2018**, *47*, 756.

²⁶⁰ Sugimura, Y.; Hazama, Y.; Nishiyama, Y.; Yano, T.; Shimizu, S.; Yoshida, S.; Hosoya, T. *Chem. Commun.* **2015**, *51*, 16613.

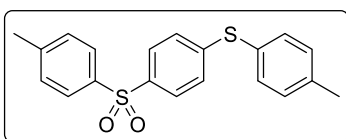
1,4-Bis(*p*-tolylthio)benzene (**3x**)²⁰²

Synthesized according to general procedure, method A starting from iodide **1x**, or from iodide **6c** and adding 2.5 equivalents of the thiol and 3.25 equivalents of NaH. The product was purified by column chromatography (cyclohexane:toluene 100:1) to get the product **3x** (32 mg, 80%). Spectroscopical data were in accordance with the literature. **¹H NMR (300 MHz, CDCl₃)** δ 7.29 (d, *J* = 8.2 Hz, 4H), 7.18 – 7.10 (m, 8H), 2.34 (s, 3H).

p-Tolyl(4-(*p*-tolylsulfinyl)phenyl)sulfane (**3y**)

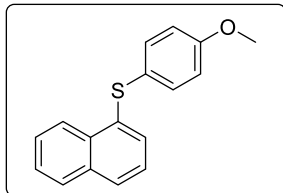
Synthesized according to general procedure, method A. The product was purified by column chromatography (cyclohexane:ethyl acetate 10:1) to get the product **3y** (20 mg, 45%). **¹H NMR (300 MHz, CDCl₃)** δ 7.49 (d, *J* = 8.2 Hz, 2H), 7.45 (d, *J* = 8.4 Hz, 2H), 7.35 (d, *J* = 8.1 Hz, 2H), 7.25 (d, *J* = 8.2 Hz, 2H), 7.18 (m, 4H), 2.37 (s, 6H). **¹³C NMR (75 MHz, CDCl₃)** δ 143.2 (C), 143.0 (C), 142.6 (C), 141.9 (C), 139.4 (C), 134.4 (CH), 130.7 (CH), 130.3 (CH), 128.7 (C), 128.3 (CH), 125.7 (CH), 125.2 (CH), 21.7 (CH₃), 21.5 (CH₃). **HRMS (EI⁺)** Calcd for C₂₀H₁₈OS₂ [M]⁺ 338.0799, Found 338.0810.

p-Tolyl(4-tosylphenyl)sulfane (**3z**)



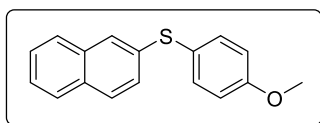
Synthesized according to general procedure, method A. The product was purified by column chromatography (cyclohexane:ethyl acetate 10:1) to get the product **3z** (41 mg, 92%). **¹H NMR (300 MHz, CDCl₃)** δ 7.78 (d, *J* = 8.3 Hz, 2H), 7.72 (d, *J* = 8.5 Hz, 2H), 7.38 (d, *J* = 8.1 Hz, 2H), 7.27 (d, *J* = 7.8 Hz, 2H), 7.22 (d, *J* = 8.0 Hz, 2H), 7.12 (d, *J* = 8.5 Hz, 2H), 2.39 (s, 6H). **¹³C NMR (75 MHz, CDCl₃)** δ 146.9 (C), 144.3 (C), 140.0 (C), 139.1 (C), 138.6 (C), 135.1 (CH), 130.9 (CH), 130.1 (CH), 128.1 (CH), 127.8 (CH), 127.3 (C), 127.0 (CH), 21.8 (CH₃), 21.6 (CH₃). **HRMS (EI⁺)** Calcd for C₂₀H₁₈O₂S₂ [M]⁺ 354.0748, Found 354.0763.

(4-Methoxyphenyl)(naphthalen-1-yl)sulfane (**3aa**)²⁶¹

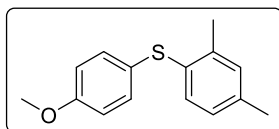


Synthesized according to general procedure, method A. The product was purified by column chromatography (cyclohexane:ethyl acetate 100:1) to get the product **3aa** (41 mg, 62%). Spectroscopical data were in accordance with the literature. **¹H NMR (300 MHz, CDCl₃)** δ 8.45 – 8.32 (m, 1H), 7.86 (m, 1H), 7.74 (dd, *J* = 6.6, 2.8 Hz, 1H), 7.57 – 7.49 (m, 2H), 7.41 – 7.30 (m, 4H), 6.87 (d, *J* = 8.6 Hz, 2H), 3.80 (s, 3H).

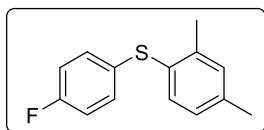
²⁶¹ Prasad, D. J. C.; Sekar G. *Org. Lett.* **2011**, *13*, 1008.

(4-Methoxyphenyl)(naphthalen-2-yl)sulfane (3ab)²⁰⁶

Synthesized according to general procedure, method A. The product was purified by column chromatography (cyclohexane:ethyl acetate 100:1) to get the product **3ab** (47 mg, 70%). Spectroscopical data were in accordance with the literature. ¹H NMR (300 MHz, CDCl₃) δ 7.72 (m, 3H), 7.60 (s, 1H), 7.52 – 7.34 (m, 4H), 7.30 (dd, *J* = 8.6, 1.8 Hz, 1H), 6.92 (d, *J* = 8.8 Hz, 2H), 3.84 (s, 3H).

(2,4-Dimethylphenyl)(4-methoxyphenyl)sulfane (3ac)²⁶²

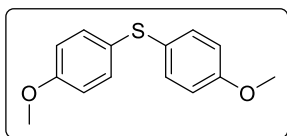
Synthesized according to general procedure, method A. The product was purified by column chromatography (cyclohexane:ethyl acetate 100:1) to get the product **3ac** (34 mg, 56%). Spectroscopical data were in accordance with the literature. ¹H NMR (300 MHz, CDCl₃) δ 7.26 (d, *J* = 8.6 Hz, 2H), 7.03 (m, 2H), 6.91 (m, 1H), 6.86 (d, *J* = 8.7 Hz, 2H), 3.81 (s, 3H), 2.35 (s, 3H), 2.30 (s, 3H).

(2,4-Dimethylphenyl)(4-fluorophenyl)sulfane (3ad)²⁶³

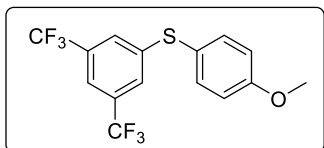
Synthesized according to general procedure, method A. The product was purified by column chromatography (cyclohexane:ethyl acetate 100:1) to get the product **3ad** (42.6 mg, 70%). Spectroscopical data were in accordance with the literature. ¹H NMR (300 MHz, CDCl₃) δ 7.25 – 7.12 (m, 3H), 7.09 (m, 1H), 7.02 – 6.93 (m, 3H), 2.34 (s, 3H), 2.33 (s, 3H).

²⁶² Xu, X. B.; Liu, J.; Zhang, J. J.; Wang, Y. W.; Peng, Y. *Org. Lett.* **2013**, *15*, 550.

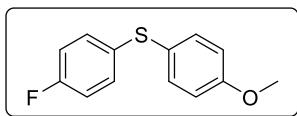
²⁶³ Malik, P.; Chakraborty, D. *Appl. Org. Chem.* **2012**, *26*, 557.

Bis(4-methoxyphenyl)sulfane (3ae)²⁰³

Synthesized according to general procedure, method A. The product was purified by column chromatography (cyclohexane:ethyl acetate 10:1) to get the product **3ae** (31 mg, 50%) as a 2.5:1 mixture with the *p*-methoxyphenyl disulfide. Spectroscopical data were in accordance with the literature. ¹H NMR (300 MHz, CDCl₃) δ 7.32 (d, *J* = 8.9 Hz, 4H), 6.88 (d, *J* = 8.8 Hz, 4H), 3.83 (s, 3H).

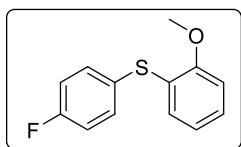
(3,5-Bis(trifluoromethyl)phenyl)(4-methoxyphenyl)sulfane (3af)²⁶⁴

Synthesized according to general procedure, method A. The product was purified by column chromatography (cyclohexane:ethyl acetate 100:1) to get the product **3af** (50 mg, 57%). Spectroscopical data were in accordance with the literature. ¹H NMR (300 MHz, CDCl₃) δ 7.65 (s, 1H), 7.57 (s, 2H), 7.46 (d, *J* = 8.1 Hz, 2H), 7.30 (d, *J* = 7.9 Hz, 2H), 2.46 (s, 3H).

(4-Fluorophenyl)(4-methoxyphenyl)sulfane (3ag)²⁰³

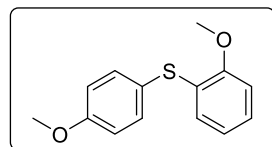
Synthesized according to general procedure, method A. The product was purified by column chromatography (cyclohexane:ethyl acetate 20:1) to get the product **3ag** (44 mg, 75%). Spectroscopical data were in accordance with the literature. ¹H NMR (300 MHz, CDCl₃) δ 7.46 – 7.31 (m, 2H), 7.31 – 7.12 (m, 2H), 7.07 – 6.78 (m, 4H), 3.81 (s, 3H).

²⁶⁴ Cheng, J. H.; Yi, C. L.; Liu, T. J.; Lee, C. F. *Chem. Commun.* **2012**, 48, 8440.

(4-Fluorophenyl)(2-methoxyphenyl)sulfane (3ah)²⁰³

Synthesized according to general procedure, method A. The product was purified by column chromatography (cyclohexane:ethyl acetate 20:1) to get the product **3ah** (37 mg, 63%).

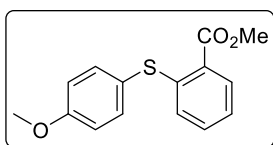
Spectroscopical data were in accordance with the literature. **¹H NMR (300 MHz, CDCl₃)** δ 7.42 (m, 2H), 7.26 (m, 1H), 7.14 – 6.98 (m, 3H), 6.91 (m, 2H), 3.92 (s, 3H).

(2-Methoxyphenyl)(4-methoxyphenyl)sulfane (3ai)²⁶⁵

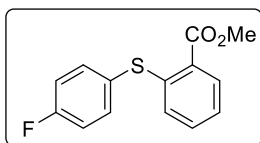
Synthesized according to general procedure, method A. The product was purified by column chromatography (cyclohexane:ethyl acetate 100:1) to get the product **3ai** (30.5 mg, 50%).

Spectroscopical data were in accordance with the literature. **¹H NMR (300 MHz, CDCl₃)** δ 7.44 (d, J = 8.7 Hz, 2H), 7.16 – 7.01 (m, 1H), 6.95 – 6.67 (m, 5H), 3.91 (s, 3H), 3.83 (s, 3H).

²⁶⁵ Park, N.; Park, K.; Jang, M.; Lee, S. *J. Org. Chem.* **2011**, 76, 4371.

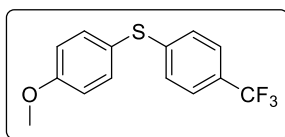
Methyl 2-((4-methoxyphenyl)thio)benzoate (3aj)²⁶⁶

Synthesized according to general procedure, method A. The product was purified by column chromatography (cyclohexane:ethyl acetate 4:1) to get the product **3aj** (30 mg, 43%). Spectroscopical data were in accordance with the literature. **¹H NMR (300 MHz, CDCl₃)** δ 7.98 (dd, $J = 7.8, 1.5$ Hz, 1H), 7.49 (d, $J = 8.8$ Hz, 2H), 7.26 – 7.18 (m, 1H), 7.12 – 7.05 (m, 1H), 6.97 (d, $J = 8.8$ Hz, 2H), 6.74 (dd, $J = 8.2, 1.0$ Hz, 1H), 3.96 (s, 3H), 3.86 (s, 3H).

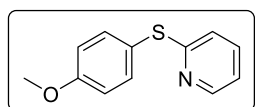
Methyl 2-((4-fluorophenyl)thio)benzoate (3ak)²⁰³

Synthesized according to general procedure, method A. The product was purified by column chromatography (cyclohexane:ethyl acetate 20:1) to get the product **3ak** (44 mg, 73%). Spectroscopical data were in accordance with the literature. **¹H NMR (300 MHz, CDCl₃)** δ 7.99 (dd, $J = 7.8, 1.6$ Hz, 1H), 7.60 – 7.50 (m, 2H), 7.30 – 7.20 (m, 1H), 7.20 – 7.07 (m, 3H), 6.75 (d, $J = 8.0$, 1H), 3.96 (s, 3H).

²⁶⁶ Sander, C.; Gendron, T.; Yiannaki, E.; Cybulska, K.; Kalber, T. L.; Lythgoe, M. F.; Arstad, E. *Sci. Rep.* **2015**, *5*, 9941.

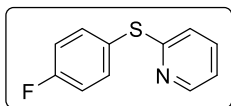
(4-Methoxyphenyl)(4-(trifluoromethyl)phenyl)sulfane (3al)²⁶⁷

Synthesized according to general procedure, method A. The product was purified by column chromatography (cyclohexane:ethyl acetate 20:1) to get the product **3al** (53 mg, 76%). Spectroscopical data were in accordance with the literature. ¹H NMR (300 MHz, CDCl₃) δ 7.50 (m, 4H), 7.18 (d, *J* = 8.6 Hz, 2H), 7.00 (d, *J* = 8.8 Hz, 2H), 3.90 (s, 3H).

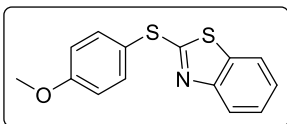
2-((4-Methoxyphenyl)thio)pyridine (3am)²⁶¹

Synthesized according to general procedure, method A. The product was purified by column chromatography (cyclohexane:ethyl acetate 20:1) to get the product **3am** (32 mg, 60%). Spectroscopical data were in accordance with the literature. ¹H NMR (300 MHz, CDCl₃) δ 8.44 – 8.35 (m, 2H), 7.53 (d, *J* = 8.9 Hz, 1H), 7.42 (td, *J* = 7.9, 1.9 Hz, 2H), 7.00 – 6.91 (m, 3H), 6.78 (d, *J* = 8.1 Hz, 1H), 3.84 (s, 3H).

²⁶⁷ Kibriya, G.; Mondal, S.; Hajra, A. *Org. Lett.* **2018**, *20*, 7740.

2-((4-Fluorophenyl)thio)pyridine (3an)²⁶⁸

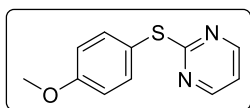
Synthesized according to general procedure, method A. The product was purified by column chromatography (cyclohexane:toluene 100:1) to get the product **3an** (43 mg, 79%). Spectroscopical data were in accordance with the literature. **¹H NMR (300 MHz, CDCl₃)** δ 8.41 (dd, *J* = 4.8, 0.9 Hz, 1H), 7.64 – 7.53 (m, 2H), 7.46 (td, *J* = 7.8, 1.9 Hz, 1H), 7.11 (m, 2H), 6.99 (ddd, *J* = 7.4, 4.9, 0.8 Hz, 1H), 6.87 (d, *J* = 8.1 Hz, 1H).

2-((4-Methoxyphenyl)thio)benzo[d]thiazole (3ao)²⁶⁹

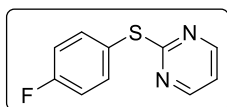
Synthesized according to general procedure, method A. The product was purified by column chromatography (cyclohexane:ethyl acetate 20:1) to get the product **3ao** (44 mg, 65%). Spectroscopical data were in accordance with the literature. **¹H NMR (300 MHz, CDCl₃)** δ 7.85 (d, *J* = 8.1 Hz, 1H), 7.64 (m, 3H), 7.38 (m, 1H), 7.24 (m, 1H), 7.00 (d, *J* = 8.4 Hz, 2H), 3.87 (s, 3H).

²⁶⁸ Platon, M.; Wijaya, N.; Rampazzi, V.; Cui, L.; Rousselin, Y.; Saeys, M.; Hierso, J. C. *Chem. Eur. J.* **2014**, *20*, 12584.

²⁶⁹ Ranjit, S.; Lee, R.; Heryadi, D.; Shen, C.; Wu, J.; Zhang, P.; Huang, K. W.; Liu, X. *J. Org. Chem.* **2011**, *76*, 8999.

2-((4-Methoxyphenyl)thio)pyrimidine (3ap)²⁷⁰

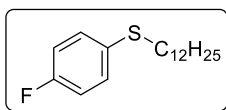
Synthesized according to general procedure, method A. The product was purified by column chromatography (cyclohexane:ethyl acetate 10:1) to get the product **3ap** (34.2 mg, 63%). Spectroscopical data were in accordance with the literature. ¹H NMR (300 MHz, CDCl₃) δ 8.47 (d, *J* = 4.8 Hz, 2H), 7.54 (d, *J* = 8.8 Hz, 2H), 7.00 – 6.91 (m, 3H), 3.84 (s, 3H).

2-((4-Fluorophenyl)thio)pyrimidine (3aq)²⁷¹

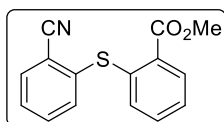
Synthesized according to general procedure, method A. The product was purified by column chromatography (cyclohexane:ethyl acetate 20:1) to get the product **3aq** (40 mg, 78%). Spectroscopical data were in accordance with the literature. ¹H NMR (300 MHz, CDCl₃) δ 8.49 (d, *J* = 4.8 Hz, 2H), 7.66 – 7.52 (m, 2H), 7.13 (m, 2H), 6.98 (t, *J* = 4.9 Hz, 1H).

²⁷⁰ Yonova, I. N.; Osborne, C. A.; Morrissette, N. S.; Jarvo, E. R. *J. Org. Chem.* **2014**, *79*, 1947.

²⁷¹ Morofuji, T.; Shimizu, A.; Yoshida, J. *Chem. Eur. J.* **2015**, *21*, 3211.

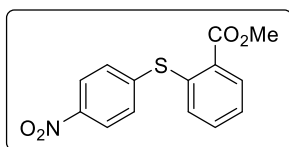
Dodecyl(4-fluorophenyl)sulfane (3ar)²⁷²

Synthesized according to general procedure, method A. The product was purified by column chromatography (cyclohexane:ethyl acetate 100:1) to get the product **3ar** (37 mg, 51%). Spectroscopical data were in accordance with the literature. **¹H NMR (300 MHz, CDCl₃)** δ 7.40 – 7.27 (m, 2H), 7.06 – 6.91 (m, 2H), 2.90 – 2.81 (m, 2H), 1.76 – 1.51 (m, 3H), 1.52 – 1.16 (m, 22H), 0.88 (t, *J* = 6.7 Hz, 3H).

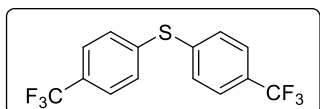
Methyl 2-((2-cyanophenyl)thio)benzoate (3as)

Synthesized according to general procedure, method A. The product was purified by column chromatography (cyclohexane:ethyl acetate 10:1) to get the product **3as** (52 mg, 78%). **¹H NMR (300 MHz, CDCl₃)** δ 8.01 (d, *J* = 7.7, 1H), 7.78 (d, *J* = 7.3 Hz, 1H), 7.68 – 7.55 (m, 2H), 7.55 – 7.43 (m, 1H), 7.40 – 7.18 (m, 2H), 6.82 (d, *J* = 8.0 Hz, 1H), 3.95 (s, 3H). **¹³C NMR (75 MHz, CDCl₃)** δ 166.9 (CO), 139.6 (C), 138.3 (C), 136.1 (CH), 134.6 (CH), 133.6 (CH), 132.8 (CH), 131.5 (CH), 129.2 (CH), 128.9 (C), 128.9 (CH), 126.1 (CH), 118.4 (C), 117.0 (CN), 52.6 (CH₃). **HRMS (EI⁺)** Calcd for C₁₅H₁₁NO₂S [M]⁺ 269.0510, Found 269.0504.

²⁷² Cheng, J. H.; Ramesh, C.; Kao, H. L.; Wang, Y. J.; Chan, C. C.; Lee, C. F. *J. Org. Chem.* **2012**, *77*, 10369.

Methyl 2-((4-nitrophenyl)thio)benzoate (3at)²⁷³

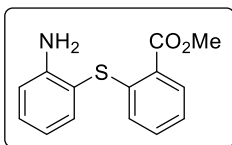
Synthesized according to general procedure, method A. The product was purified by column chromatography (cyclohexane:ethyl acetate 20:1) to get the product **3at** (35 mg, 50%). Spectroscopic data were in accordance with the literature. ¹H NMR (300 MHz, CDCl₃) δ 8.18 (d, *J* = 8.7 Hz, 2H), 7.98 (d, *J* = 7.5 Hz, 1H), 7.50 (d, *J* = 8.7 Hz, 2H), 7.39 (m, 2H), 7.21 (d, *J* = 7.8 Hz, 1H), 3.92 (s, 3H).

Bis(4-(trifluoromethyl)phenyl)sulfane (3au)²⁷⁴

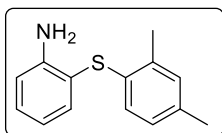
Synthesized according to general procedure, method A. The product was purified by column chromatography (cyclohexane:ethyl acetate 100:1) to get the product **3au** (66 mg, 83%). Spectroscopic data were in accordance with the literature. ¹H NMR (300 MHz, CDCl₃) δ 7.59 (d, *J* = 8.2 Hz, 4H), 7.45 (d, *J* = 8.2 Hz, 4H).

²⁷³ Ali, A.; Wang, J.; Nathans, R. S.; Cao, H.; Sharova, N.; Stevenson, M.; Rana, T. M. *ChemMedChem.* **2012**, *7*, 1217.

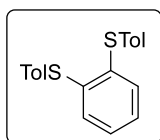
²⁷⁴ Mitamura, K.; Yatabe, T.; Yamamoto, K.; Yabe, T.; Suzuki, K.; Yamaguchi, K. *Chem. Commun.* **2021**, *57*, 3749.

Methyl 2-((2-aminophenyl)thio)benzoate (**3av**)²¹⁴

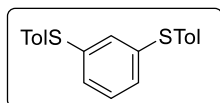
Synthesized according to general procedure, method B. The product was purified by column chromatography (cyclohexane:ethyl acetate 20:1) to get the product **3av** (56.3 mg, 77%). Spectroscopical data were in accordance with the literature. **¹H NMR (300 MHz, CDCl₃)** δ 8.02 (dd, *J* = 7.8, 1.6 Hz, 1H), 7.46 (dd, *J* = 7.6, 1.5 Hz, 1H), 7.34 – 7.22 (m, 2H), 7.13 (t, *J* = 7.8 Hz, 1H), 6.90 – 6.71 (m, 3H), 3.97 (s, 3H), 3.80 (br, 2H).

2-((2,4-Dimethylphenyl)thio)aniline (**3aw**)²¹⁵

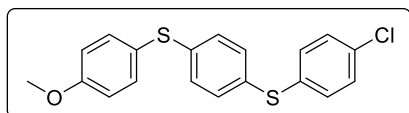
Synthesized according to general procedure, method B. The product was purified by column chromatography (cyclohexane:ethyl acetate 50:1) to get the product **3aw** (35 mg, 65%). Spectroscopical data were in accordance with the literature. **¹H NMR (300 MHz, CDCl₃)** δ 7.38 (dd, *J* = 7.7, 1.5 Hz, 1H), 7.29 – 7.19 (m, 1H), 7.02 (s, 1H), 6.90 – 6.65 (m, 4H), 4.14 (br, 2H), 2.41 (s, 3H), 2.28 (s, 3H).

1,2-Bis(*p*-tolylthio)benzene (**7a**)²⁶⁰

Synthesized according to general procedure, method A, but adding 2.5 equivalents of the thiol and 3.25 equivalents of NaH. The product was purified by column chromatography (cyclohexane) to get the product **7a** (30 mg, 50%). Spectroscopical data were in accordance with the literature. **¹H NMR (300 MHz, CDCl₃)** δ 7.36 (d, *J* = 8.1 Hz, 4H), 7.21 (d, *J* = 8.0 Hz, 4H), 7.11 (s, 4H), 2.41 (s, 6H).

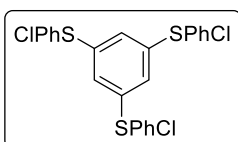
1,3-Bis(*p*-tolylthio)benzene (**7b**)²¹⁶

Synthesized according to general procedure, method A, but adding 2.5 equivalents of the thiol and 3.25 equivalents of NaH. The product was purified by column chromatography (cyclohexane) to get the product **7b** (44 mg, 73%). Spectroscopical data were in accordance with the literature. ¹H NMR (300 MHz, CDCl₃) δ 7.29 (d, *J* = 8.0 Hz, 4H), 7.15 – 7.08 (m, 6H), 7.06 – 6.97 (m, 2H), 2.36 (s, 6H).

(4-Chlorophenyl)(4-((4-methoxyphenyl)thio)phenyl)sulfane (**7c**)

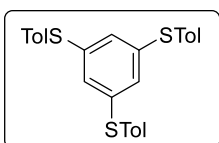
Synthesized according to general procedure, method A, but adding 2.5 equivalents of the thiol and 3.25 equivalents of NaH. The product was purified by column chromatography (cyclohexane:ethyl acetate 20:1) to get the product **7c** (59 mg, 66%). ¹H NMR (300 MHz, CDCl₃) δ 7.52 – 7.41 (m, 2H), 7.35 – 7.18 (m, 6H), 7.11 (d, *J* = 7.4 Hz, 2H), 6.96 (d, *J* = 7.7 Hz, 2H), 3.87 (s, 3H). ¹³C NMR (75 MHz, CDCl₃) δ 160.4 (CH₃), 139.3 (C) 136.1 (2 CH), 134.5 (C), 132.4 (2 CH), 132.0 (C), 131.8 (2 CH), 129.6 (C), 129.5 (2 CH), 128.6 (2 CH), 123.4 (C), 115.4 (2CH). HRMS (EI⁺) Calcd for C₁₉H₁₅ClOS₂ [M]⁺ 358.0253, Found 358.0262.

1,3,5-Tris((4-chlorophenyl)thio)benzene (7d)



Synthesized according to general procedure, method A, but adding 3.5 equivalents of the thiol and 4.2 equivalents of NaH. The product was purified by column chromatography (cyclohexane:toluene 100:1) to get the product **7d** (30 mg, 33%). $^1\text{H NMR}$ (300 MHz, CDCl_3) δ 7.33 – 7.27 (m, 12H), 6.83 (s, 3H). $^{13}\text{C NMR}$ (75 MHz, CDCl_3) δ 139.5 (C), 134.9 (C), 134.5 (CH), 131.8 (C), 129.9 (CH), 127.0 (CH). HRMS (MALDI+) Calcd for $\text{C}_{24}\text{H}_{15}\text{Cl}_3\text{S}_3$ $[\text{M}]^+$ 503.9401, Found 503.9383.

1,3,5-Tris(*p*-tolylthio)benzene (7e)²⁷⁵

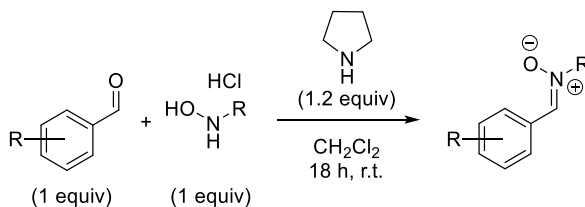


Synthesized according to general procedure, method A, but adding 4.5 equivalents of the thiol and 5.4 equivalents of NaH. The product was purified by column chromatography (cyclohexane:toluene 100:1) to get the product **7e** (41 mg, 47%). Spectroscopical data were in accordance with the literature. $^1\text{H NMR}$ (300 MHz, CDCl_3) δ 7.28 (d, $J = 8.1$ Hz, 6H), 7.14 (d, $J = 8.0$ Hz, 6H), 6.79 (s, 3H), 2.40 (s, 9H).

²⁷⁵ Arisawa, M.; Suzuki, T.; Ishikawa, T.; Yamaguchi, M. *J. Am. Chem. Soc.* **2008**, *130*, 12215.

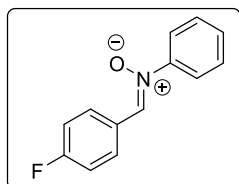
**Part II. Chapter 3. Experimental
Section**

Nitrone synthesis²⁷⁶



To an equimolecular mixture of the corresponding aldehyde (1 mmol) and hydroxylamine (1 mmol) in CH_2Cl_2 (2 mL), pyrrolidine (1.2 mmol) was added, and the mixture is stirred at room temperature. After the corresponding reaction time, the crude is filtered through a short pad of silica gel with EtOAc and concentrated at reduced pressure. The final nitrones are purified by FCC using a cHex : Ethyl acetate 4:1 mixture as eluent unless otherwise stated.

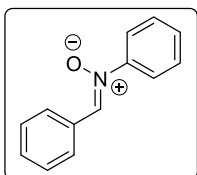
(Z)-1-(4-Fluorophenyl)-N-phenylmethanimine oxide (11a)²⁷⁷



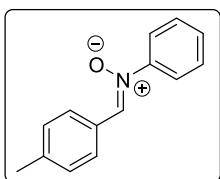
Reaction was performed following the general procedure of nitrone synthesis. Spectroscopic data were in accordance with the literature. ^1H NMR (300 MHz, CDCl_3) δ 8.45 (m, 2H), 7.92 (s, 1H), 7.82 – 7.71 (m, 2H), 7.54 – 7.45 (m, 3H), 7.17 (t, $J = 8.7$ Hz, 2H).

²⁷⁶ Morales, S.; Guijarro, F. G.; Alonso, I.; García-Ruano, J. L.; Cid, M. B. *ACS Catal.* **2016**, *6*, 84.

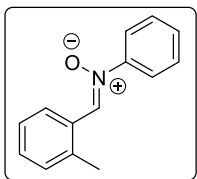
²⁷⁷ Zhou, S.; Liu, X.; Hu, W.; Ke, Z.; Xu, X. *J. Am. Chem. Soc.* **2021**, *143*, 14703.

(Z)-N,1-Diphenylmethanimine oxide (11b)²⁷⁸

Reaction was performed following the general procedure of nitron synthesis. Spectroscopic data were in accordance with the literature. ¹H NMR (300 MHz, CDCl₃) δ 8.41 (m, 2H), 7.94 (s, 1H), 7.83 – 7.74 (m, 2H), 7.58 – 7.43 (m, 6H).

(Z)-N-Phenyl-1-(p-tolyl)methanimine oxide (11c)²⁷⁹

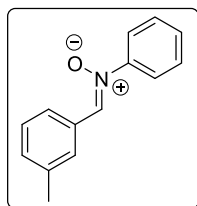
Reaction was performed following the general procedure of nitron synthesis. Spectroscopic data were in accordance with the literature. ¹H NMR (300 MHz, CDCl₃) δ 8.31 (d, *J* = 8.2 Hz, 2H), 7.90 (s, 1H), 7.83 – 7.75 (m, 2H), 7.55 – 7.43 (m, 3H), 7.30 (d, *J* = 8.1 Hz, 1H), 2.43 (s, 3H).

(Z)-N-Phenyl-1-(o-tolyl)methanimine oxide (11d)

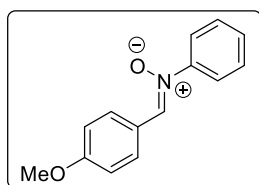
Reaction was performed following the general procedure of nitron synthesis. ¹H NMR (300 MHz, CDCl₃) δ 9.43 – 9.33 (m, 1H), 8.08 (s, 1H), 7.84 – 7.73 (m, 2H), 7.50 (m, 3H), 7.43 – 7.32 (m, 2H), 7.31 – 7.23 (m, 1H), 2.46 (s, 3H). ¹³C NMR (75 MHz, CDCl₃) δ 149.8 (CN), 137.0 (C), 131.9 (C), 130.8 (CH), 130.4 (CH), 129.9 (CH), 129.3 (CH), 129.1 (C), 128.0 (CH), 126.5 (CH), 122.0 (CH), 20.0 (CH₃).

²⁷⁸ Mukherjee, A.; Dateer, R. B.; Chaudhuri, R.; Bhunia, S.; Karad, S. N.; Liu, R-S. *J. Am. Chem. Soc.* **2011**, *133*, 15372.

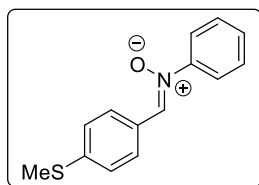
²⁷⁹ Ren, X.; Lu, J.; Wang, M.; Guo, M.; Li, H.; Pan, X.; Li, L.; Munyentwali, A.; Yang, Q. *ACS Catal.* **2020**, *10*, 13701.

(Z)-N-Phenyl-1-(m-tolyl)methanimine oxide (11e)²⁸⁰

Reaction was performed following the general procedure of nitron synthesis. Spectroscopic data were in accordance with the literature. **¹H NMR (300 MHz, CDCl₃)** δ 8.34 (s, 1H), 8.13 (d, *J* = 7.9 Hz, 1H), 7.90 (s, 1H), 7.83 – 7.74 (m, 2H), 7.57 – 7.44 (m, 3H), 7.39 (m, 1H), 7.31 (d, *J* = 7.5 Hz, 1H), 2.44 (s, 3H).

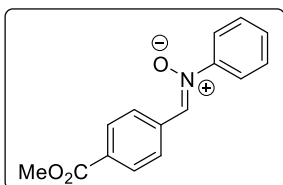
(Z)-1-(4-Methoxyphenyl)-N-phenylmethanimine oxide (11f)²⁷⁷

Reaction was performed following the general procedure of nitron synthesis. Spectroscopic data were in accordance with the literature. **¹H NMR (300 MHz, CDCl₃)** δ 8.42 (d, *J* = 9.0 Hz, 2H), 7.87 (s, 1H), 7.83 – 7.74 (m, 2H), 7.55 – 7.42 (m, 3H), 7.02 (d, *J* = 9.0 Hz, 2H), 3.90 (s, 3H).

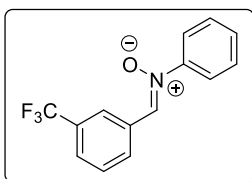
(Z)-1-(4-(Methylthio)phenyl)-N-phenylmethanimine oxide (11g)

Reaction was performed following the general procedure of nitron synthesis. Spectroscopic data were in accordance with the literature. **¹H NMR (300 MHz, CDCl₃)** δ 8.34 (d, *J* = 8.7 Hz, 2H), 7.89 (s, 1H), 7.84 – 7.72 (m, 2H), 7.48 (m, 3H), 7.32 (d, *J* = 8.6 Hz, 2H), 2.55 (s, 3H). **¹³C NMR (75 MHz, CDCl₃)** δ 148.8 (CN), 142.6 (C), 133.9 (C), 129.7 (CH), 129.2 (CH), 129.0 (CH), 127.1 (C), 125.2 (CH), 121.5 (CH), 14.8 (CH₃).

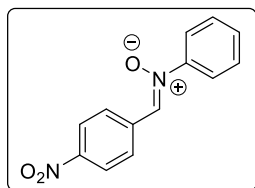
²⁸⁰ Kong, L.; Han, X.; Liu S.; Zou, Y.; Lan, Y.; Li, X. *Angew. Chem. Int. Ed.* **2020**, *59*, 7188.

(Z)-1-(4-(Methoxycarbonyl)phenyl)-N-phenylmethanimineoxide**(11h)**²⁸⁰

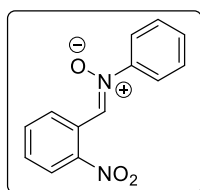
Reaction was performed following the general procedure of nitron synthesis. Spectroscopic data were in accordance with the literature. **¹H NMR (300 MHz, CDCl₃)** δ 8.46 (d, J = 8.4 Hz, 2H), 8.15 (d, J = 8.6 Hz, 2H), 8.01 (s, 1H), 7.84 – 7.75 (m, 2H), 7.55 – 7.47 (m, 3H), 3.96 (s, 3H).

(Z)-N-Phenyl-1-(3-(trifluoromethyl)phenyl)methanimine oxide (11i)

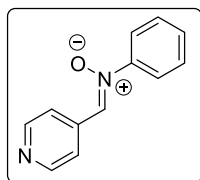
Reaction was performed following the general procedure of nitron synthesis. Spectroscopic data were in accordance with the literature. **¹H NMR (300 MHz, CDCl₃)** 8.72 (s, 1H), 8.60 (d, J = 7.9 Hz, 1H), 8.02 (s, 1H), 7.86 – 7.75 (m, 2H), 7.73 (d, J = 7.8 Hz, 1H), 7.62 (m, 1H), 7.52 (m, 3H). **¹³C NMR (75 MHz, CDCl₃)** δ 148.8 (CN), 132.9 (C), 131.6 (C), 131.3 (CH), 130.8 (C), 130.2 (CH), 129.2 (CH), 129.1 (CH), 127.0 (CH), 125.4 (CH), 121.6 (CH). **HRMS (EI⁺)** Calcd for C₁₄H₁₀F₃N [M]⁺ 304.0922, Found 304.0928.

(Z)-1-(4-Nitrophenyl)-N-phenylmethanimine oxide (11j)²⁸¹

Reaction was performed following the general procedure of nitron synthesis. Spectroscopic data were in accordance with the literature. ¹H NMR (300 MHz, CDCl₃) δ 8.57 (d, *J* = 9.0 Hz, 2H), 8.33 (d, *J* = 9.0 Hz, 2H), 8.08 (s, 1H), 7.80 (m, 2H), 7.58 – 7.48 (m, 3H).

(Z)-1-(2-Nitrophenyl)-N-phenylmethanimine oxide (11k)²⁸¹

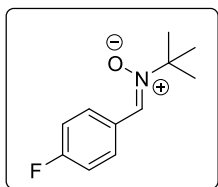
Reaction was performed following the general procedure of nitron synthesis. Spectroscopic data were in accordance with the literature. ¹H NMR (300 MHz, CDCl₃) δ 9.41 (d, *J* = 8.1 Hz, 1H), 8.61 (s, 1H), 8.10 (d, *J* = 8.2 Hz, 1H), 7.87 – 7.72 (m, 3H), 7.63 – 7.48 (m, 4H). ¹³C NMR (75 MHz, CDCl₃) δ 149.0 (CN), 147.4 (C), 133.3 (CH), 130.4 (CH), 130.3 (CH), 129.3 (CH), 129.1 (CH), 128.2 (C), 124.8 (CH), 124.4 (C), 121.6 (CH).

(Z)-N-Phenyl-1-(pyridin-4-yl)methanimine oxide (11l)²⁸²

Reaction was performed following the general procedure of nitron synthesis. Spectroscopic data were in accordance with the literature. ¹H NMR (300 MHz, CDCl₃) δ 8.77 (d, *J* = 4.7 Hz, 2H), 8.17 (d, *J* = 4.8 Hz, 2H), 7.96 (s, 1H), 7.84 – 7.74 (m, 2H), 7.53 (m, 3H).

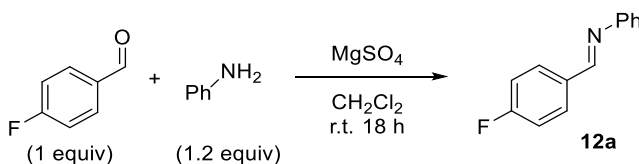
²⁸¹ Martinez-Pardo, P.; Blay, G.; Escrivá-Palomo, A.; Sanz-Marco, A.; Vila, C.; Pedro, J. R. *Org. Lett.* **2019**, *21*, 4063.

²⁸² Parisotto, S.; Boggio, P.; Prandi, C.; Venturello, P.; Deagostino, A. *Tetrahedron Lett.* **2015**, *56*, 5791.

(Z)-N-tert-butyl-1-(4-fluorophenyl)methanimine oxide (13a)

1.61 (s, 9H).

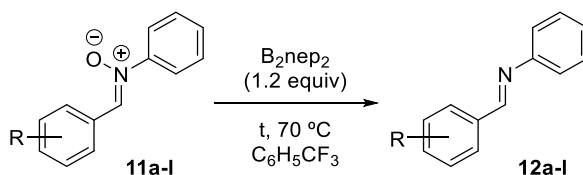
Reaction was performed following the general procedure of nitron synthesis with a reaction time of 5 h. **¹H NMR (300 MHz, CDCl₃)** δ 8.33 (dd, *J* = 8.9, 5.6 Hz, 2H), 7.54 (s, 1H), 7.10 (t, *J* = 8.8 Hz, 2H),

Imine synthesis²⁸³

In a sealed vial CH₂Cl₂ (3 mL) and MgSO₄ /mol. sieves 4 Å (~100 mg) were added and allowed to stir for 5 minutes at r.t. To the vial was added the corresponding aldehyde (3 mmol) and aniline (3 mmol) or amine (3.6 mmol). The vial was sealed and purged with nitrogen for 10 minutes. The reaction mixture was allowed to stir under a balloon of nitrogen for 18 hours. After this time, the mixture was filtered through a pad of cotton wool washing with CH₂Cl₂. The filtrate was concentrated at reduced pressure to give the imine products. The crude products were pure enough without further purification. The spectroscopic data is in accordance with the literature.²⁸³ **¹H NMR (300 MHz, CDCl₃)** δ 8.42 (s, 1H), 7.91 (m, 2H), 7.40 (t, *J* = 7.6 Hz, 2H), 7.26 – 7.11 (m, 5H).

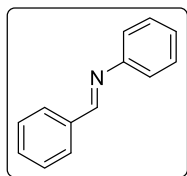
²⁸³ Leitch, J. A.; Rogova, T.; Duarte, F.; Dixon D. J. *Angew. Chem. Int. Ed.* **2020**, *59*, 4121.

Deoxygenation reaction



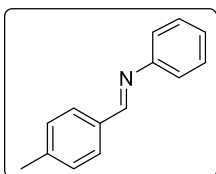
A vial was charged with nitronium (0.10 mmol) and B_2nep_2 (0.12 mmol). Then, it was sealed with a Teflon cap and was connected to an argon-vacuum line and backfilled with argon. Anhydrous solvent (0.5 mL) was added, and the mixture was stirred for the indicated time and temperature. The resulting solution was filtered through a short pad with silica deactivated with triethylamine with a mixture of Hexane: EtOAc (20:1) to obtain the final imine.

(E)-N,1-Diphenylmethanimine (12b)²⁸⁴

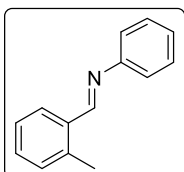


Reaction was performed following the general procedure of nitronium reduction (17.6 mg, 97%). Spectroscopical data were in accordance with the literature. $^1\text{H NMR}$ (300 MHz, CDCl_3) δ 8.48 (s, 1H), 7.93 (m, 2H), 7.57 – 7.46 (m, 3H), 7.42 (m, 2H), 7.30 – 7.17 (m, 3H).

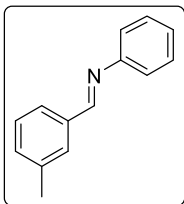
²⁸⁴ Jangir, R.; Ansari, M.; Kaleeswaran, D.; Rajaraman, G.; Palaniandavar, M.; Murugavel, R. *ACS Catal.* **2019**, *9*, 10940.

(E)-N-Phenyl-1-(p-tolyl)methanimine (12c)²⁸⁵

Reaction was performed following the general procedure of nitron reduction (19.5 mg, 99%). Spectroscopical data were in accordance with the literature. ¹H NMR (300 MHz, CDCl₃) δ 8.44 (s, 1H), 7.81 (d, *J* = 8.0 Hz, 2H), 7.48 – 7.35 (m, 2H), 7.35 – 7.20 (m, 5H), 2.44 (s, 3H).

(E)-N-Phenyl-1-(o-tolyl)methanimine (12d)²⁸⁶

Reaction was performed following the general procedure of nitron reduction (19.3 mg, 99%). ¹H NMR (300 MHz, CDCl₃) δ 8.80 (s, 1H), 8.12 (d, *J* = 7.6, 1H), 7.50 – 7.21 (m, 8H), 2.64 (s, 3H).

(E)-N-Phenyl-1-(m-tolyl)methanimine (12e)²⁸⁷

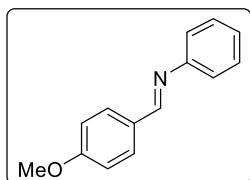
3H).

Reaction was performed following the general procedure of nitron reduction (18.9 mg, 97%). ¹H NMR (300 MHz, CDCl₃) δ 8.45 (s, 1H), 7.79 (s, 1H), 7.68 (d, *J* = 7.4 Hz, 1H), 7.46 – 7.19 (m, 7H), 2.45 (s,

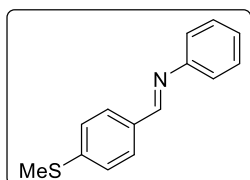
²⁸⁵ Tuyen, T. N.; Sin, K-S.; Kim, Y. P.; Park, H. *Arch. Pharm. Res.* **2005**, *28*, 1013.

²⁸⁶ Kim, H.; Kim, H. T.; Lee, J. H.; Hwang, H.; An, D. K. *RSC Adv.* **2020**, *10*, 34421.

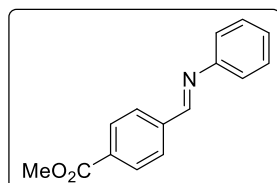
²⁸⁷ Lyu, H.; Quan, Y.; Cheng, B.; Xie, Z. *Chem. Commun.* **2021**, *57*, 7930.

(E)-1-(4-Methoxyphenyl)-N-phenylmethanimine (12f)²⁸⁸

Reaction was performed following the general procedure of nitron reduction (20.5 mg, 97%). Spectroscopical data were in accordance with the literature. ¹H NMR (300 MHz, CDCl₃) δ 8.40 (s, 1H), 7.87 (d, *J* = 8.8 Hz, 2H), 7.40 (m, 2H), 7.22 (m, 3H), 7.00 (d, *J* = 8.7 Hz, 2H), 3.89 (s, 3H).

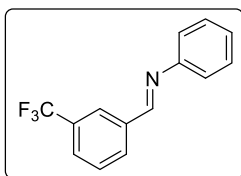
(E)-1-(4-(Methylthio)phenyl)-N-phenylmethanimine (12g)

Reaction was performed following the general procedure of nitron reduction (21.6 mg, 95%). ¹H NMR (300 MHz, CDCl₃) δ 8.41 (s, 1H), 7.82 (d, *J* = 8.3 Hz, 2H), 7.40 (m, 2H), 7.32 (d, *J* = 8.2 Hz, 2H), 7.24 (m, 3H), 2.55 (s, 3H). ¹³C NMR (75 MHz, CDCl₃) δ 159.6 (CN), 152.1 (C), 143.2 (C), 132.9 (C), 129.1 (CH), 129.1 (CH), 125.8 (CH), 125.7 (CH), 120.8 (CH), 15.1 (CH₃).

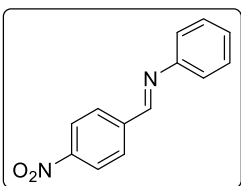
Methyl (E)-4-((phenylimino)methyl)benzoate (12h)

Reaction was performed following the general procedure of nitron reduction (22 mg, 93%). ¹H NMR (300 MHz, CDCl₃) δ 8.53 (s, 1H), 8.16 (d, *J* = 8.4 Hz, 2H), 7.99 (d, *J* = 8.3 Hz, 2H), 7.43 (m, 2H), 7.27 (m, 3H), 3.97 (s, 3H). ¹³C NMR (75 MHz, CDCl₃) δ 166.4 (CO), 158.9 (CN), 151.4 (C), 139.9 (C), 132.2 (C), 129.9 (CH), 129.1 (CH), 128.5 (CH), 126.4 (CH), 120.8 (CH), 52.4 (CH₃).

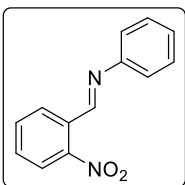
²⁸⁸ Kwon, M. S.; Kim, S.; Park, S.; Bosco, W.; Chidrala, R. K.; Park, J. *J. Org. Chem.* **2009**, *74*, 2877.

(E)-N-Phenyl-1-(3-(trifluoromethyl)phenyl)methanimine (12i)

Reaction was performed following the general procedure of nitro reduction (23.8 mg, 96%). **¹H NMR (300 MHz, CDCl₃)** δ 8.52 (s, 1H), 8.21 (s, 1H), 8.09 (d, *J* = 7.7 Hz, 1H), 7.75 (d, *J* = 7.8 Hz, 1H), 7.62 (t, *J* = 7.8 Hz, 1H), 7.44 (t, *J* = 7.7 Hz, 2H), 7.27 (m, 3H). **¹³C NMR (75 MHz, CDCl₃)** δ 158.4 (CN), 151.3 (C), 136.9 (C), 131.9 (CH), 131.9 (CH), 129.2 (CH), 129.2 (C), 127.7 (CH), 126.5 (CH), 125.4 (CH), 120.8 (CH).

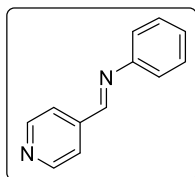
(E)-1-(4-Nitrophenyl)-N-phenylmethanimine (12j)²⁸⁹

Reaction was performed following the general procedure of nitro reduction (20.3 mg, 90%). Spectroscopical data were in accordance with the literature. **¹H NMR (300 MHz, CDCl₃)** δ 8.57 (s, 1H), 8.35 (d, *J* = 8.7 Hz, 2H), 8.10 (d, *J* = 8.7 Hz, 2H), 7.45 (t, *J* = 7.8 Hz, 2H), 7.29 (m, 3H).

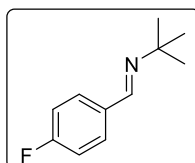
(E)-1-(2-Nitrophenyl)-N-phenylmethanimine (12k)

Reaction was performed following the general procedure of nitro reduction (22 mg, 98%). **¹H NMR (300 MHz, CDCl₃)** δ 8.96 (s, 1H), 8.33 (d, *J* = 7.7 Hz, 1H), 8.09 (d, *J* = 8.1 Hz, 1H), 7.76 (t, *J* = 7.4 Hz, 1H), 7.64 (t, *J* = 7.6 Hz, 1H), 7.50 – 7.38 (m, 2H), 7.35 – 7.24 (m, 3H). **¹³C NMR (75 MHz, CDCl₃)** δ 155.9 (CN), 151.1 (C), 133.6 (CH), 131.2 (CH), 131.1 (C), 129.8 (CH), 129.3 (CH), 126.9 (CH), 124.6 (CH), 121.2 (CH).

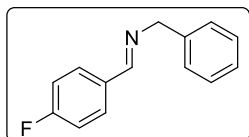
²⁸⁹ Torregrosa, R.; Pastor I. M.; Yus, M. *Tetrahedron*, **2005**, *61*, 11148.

(E)-N-Phenyl-1-(pyridin-4-yl)methanimine (12I)²⁹⁰

Reaction was performed following the general procedure of nitron reduction in dry MeOH (12.2 mg, 67%). Spectroscopical data were in accordance with the literature. ¹H NMR (300 MHz, CDCl₃) δ 8.81 (d, *J* = 6.0 Hz, 2H), 8.50 (s, 1H), 7.80 (d, *J* = 6.0 Hz, 2H), 7.47 (m, 2H), 7.37 – 7.24 (m, 3H).

(E)-N-Tert-butyl-1-(4-fluorophenyl)methanimine (14a)²⁹¹

Reaction was performed following the general procedure of nitron reduction (6 mg, 30%). Spectroscopical data were in accordance with the literature. ¹H NMR (300 MHz, CDCl₃) δ 8.24 (s, 1H), 7.81 – 7.68 (m, 2H), 7.08 (m, 2H), 1.30 (s, 9H).

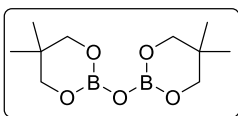
(E)-N-Benzyl-1-(4-fluorophenyl)methanimine (14c)²⁹²

Reaction was performed following the general procedure of nitron reduction (18.1 mg, 85%). Spectroscopical data were in accordance with the literature. ¹H NMR (300 MHz, CDCl₃) δ 8.37 (s, 1H), 7.85 – 7.75 (m, 2H), 7.42 – 7.27 (m, 5H), 7.17 – 7.06 (m, 2H), 4.83 (s, 2H).

²⁹⁰ Won, K. J.; Jinling, H.; Kazuya, Y.; Noritaka, M. *Chem. Lett.* **2009**, *38*, 920.

²⁹¹ Okamoto, S.; Arik, R.; Tsujioka, H.; Sudo, A. *J. Org. Chem.* **2017**, *82*, 9731.

²⁹² Dong, Z.; Lishe, G.; Fan, Y.; Huan, W.; Youge, P.; Jie, L.; Walsh, P. J. *Nat. Commun.* **2021**, *12*, 7060.

2,2'-oxybis(5,5-dimethyl-1,3,2-dioxaborinane) (17)²⁹³

Reaction was performed following the general procedure of nitrene reduction. Spectroscopical data were in accordance with the literature. ¹H

NMR (300 MHz, C₆D₆) δ 3.65 (s, 8H), 0.98 (s, 12H). **¹³C NMR (75 MHz, C₆D₆)** δ 73.1 (CH₂), 31.8 (C), 21.7 (CH₃). **¹¹B NMR (96 MHz, C₆D₆)** δ 17.5. **MS (EI⁺)** Calcd for C₁₀H₂₀B₂O₅ [M]⁺ 242.1497, Found 242.15.

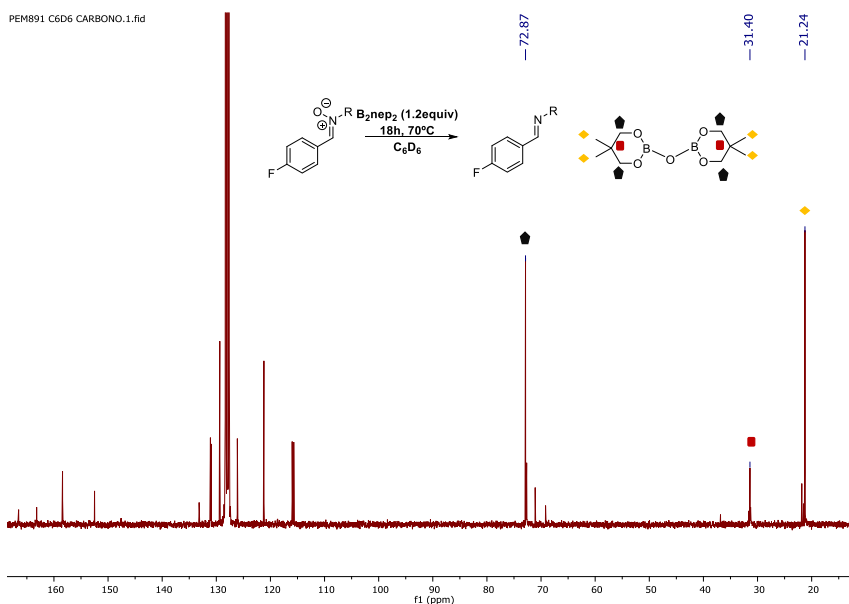
Additional experiments

Figure S1. ¹³C NMR characterization of the model deoxygenation reaction.

²⁹³ Peltier, J. L.; Soleihavou, M.; Martin, D.; Jazzar, R.; Bertrand, G. *J. Am. Chem. Soc.* **2020**, *142*, 16479.

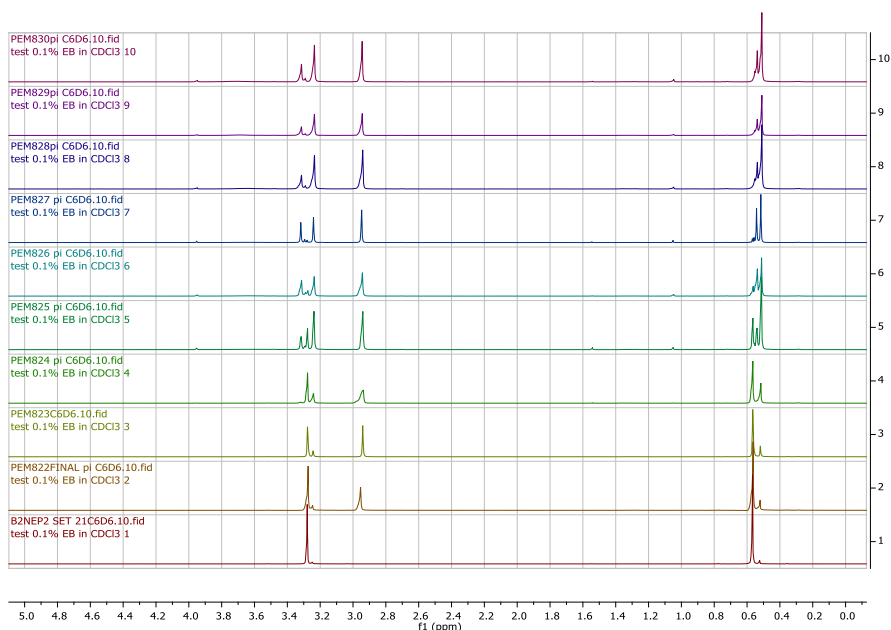
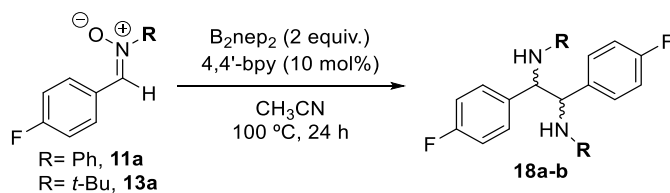
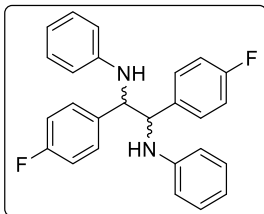


Figure S2. ^1H NMR B_2nep_2 reaction outcome over time.

Diamine synthesis



A vial was charged with nitron (0.10 mmol) and B_2nep_2 (0.2 mmol). Then, it was sealed with a Teflon cap and was connected to an argon-vacuum line and backfilled with argon. Anhydrous CH_3CN (0.5 mL) was added, and the mixture was stirred for 24 h at 100 °C. The resulting solution was filtered through a short pad with silica deactivated with triethylamine with a mixture of Hexane: EtOAc (4:1) to obtain the final diamine.

1,2-Bis(4-fluorophenyl)-*N1,N2*-diphenylethane-1,2-diamine (18a)

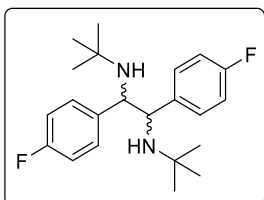
Reaction was performed following the general procedure of diamine synthesis (16 mg, 80%).

$^1\text{H RMN}$ (300 MHz, CDCl_3) δ 7.18 – 7.05 (m, 4H), 7.01 – 6.88 (m, 8H), 6.70 (m, 2H), 6.55 – 6.45 (m, 4H), 4.94 (s, 2H), 4.50 (s, 2H). **$^{13}\text{C RMN}$**

(75 MHz, CDCl_3) 163.9 (C), 163.7 (C), 146.7 (C), 146.1 (C), 135.5 (C), 133.7 (C), 129.3 (CH), 129.1 (CH), 129.0 (CH), 128.8 (CH), 118.4 (CH), 118.2 (CH), 115.5 (CH), 115.5 (CH), 114.1 (CH), 113.8 (CH), 63.6 (CH), 61.4 (CH).

N1,N2-Di-tert-butyl-1,2-bis(4-fluorophenyl)ethane-1,2-diamine

(18b)²⁹¹



Reaction was performed following the general procedure of diamine synthesis (12 mg, 67%).

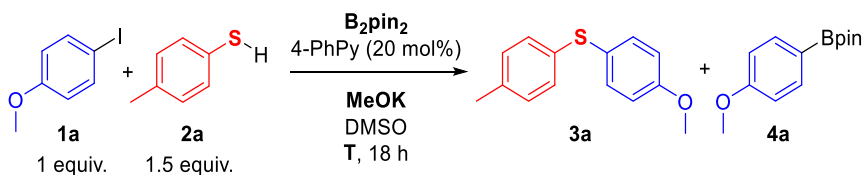
Spectroscopical data were in accordance with the literature. **$^1\text{H RMN}$ (300 MHz, CDCl_3)** δ 7.35 – 7.22 (m, 4H), 7.11 (m, 4H), 6.97 (m, 4H),

6.84 (t, $J = 8.5$ Hz, 4H), 3.65 (s, 2H), 3.61 (s, 2H), 1.50 (br, 4H), 0.83 (s, 18H), 0.72 (s, 18H).

Annex

1. Additional optimization tables of Chapter 2

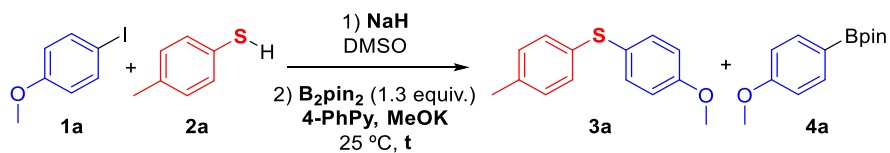
Table A2. First optimization experiments.



Entry	Boron Source	Base	T (°C)	Ratio 3a:4a	Conv (%) ^a	Yield 3a (%) ^b
1	B_2pin_2 (1.3)	MeOK (3)	85	2:1	100	(38%) ^c
2	B_2pin_2 (0.2)	MeOK (2.3)	85	1:0	20	Trace
3	B_2pin_2 (1.3)	MeOK (3)	50	2:1	100	40

^aConversions measured with 1H -NMR compared to the remaining starting material.

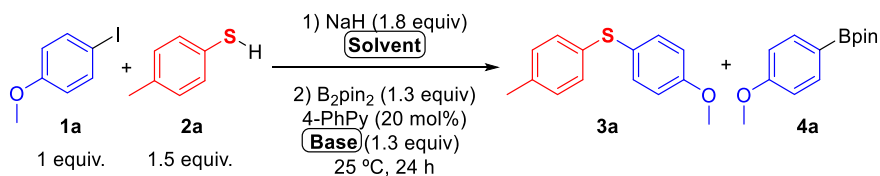
^bYields measured by 1H -NMR using Nitromethane as internal standard. ^cYield in parentheses measured as isolated yield.

Table A3. Reagents ratio optimization.

Entry	Ratio 1a:2a	Cat.	Base	Ratio 3a/4a	Conv (%) ^a	Yield ^b 3a(%)
1	1:1.5	4-PhPy (20%)	NaH (1.8) MeOK (1.3)	1:0	100	80
2	1:1.5	4-PhPy (30%)	NaH (1.8) MeOK(1.3)	1:0	100	84
3	1:1.5	4-PhPy (10%)	NaH (1.8) MeOK (1.3)	5:1	90	68
4	1:1	4-PhPy (20%)	NaH (1.8) MeOK (1.3)	4:1	100	74
5	1:2	4-PhPy (20%)	NaH (2.2) MeOK (1.3)	7:1	100	70
6	1:2	4-PhPy (20%)	NaH (2.2) MeOK (2.6)	n.d.	78	53
7	1:1.5	4-PhPy (20%)	NaH (1.8) MeOK (2.6)	n.d.	100	67

^aConversions measured with 1H -NMR compared to the remaining starting material.

^bYields measured by 1H -NMR using nitromethane as internal standard.

Table A4. Solvent and base screening.

Entry	Solvent	Base	Ratio 3a/4a	Conv ^a (%)	Yield ^b 3a (%)
1	DMSO	MeOK	1/0	100	89(68)
2	CF ₃ Tol	MeOK	1/0	6	-
3	CH ₃ CN	MeOK	n.d.	0	-
4	DMF	MeOK	2/1	70	30
5	DMA	MeOK	1/0	100	66
6 ^c	DMA	MeOK	4/1	64	40
7	THF	MeOK	1/0	32	-
8	HFIP	MeOK	n.d.	0	-
9	MTBE	MeOK	n.d.	0	0
10	MTBE:DMSO 2.5:1	MeOK	1/0	66	58
11	DMSO	MeONa	1/0	80	68
12 ^c	DMSO	MeONa	4/1	100	80
13	DMSO	MeOLi	4/1	88	59
14	DMSO	C ₂ CO ₃ MeOK	4/1	88	50

^aConversions measured with ¹H-NMR compared to the remaining starting material. ^bYields measured by ¹H-NMR using nitromethane as internal standard. ^c50 °C, 18 h. ^dNaH 1.5 equiv.

Ramírez-Jiménez, R.; **Franco, M.**; Rodrigo, E.; Sainz, R.; Ferritto, R.; Lamsabhi, A. M.; Aceña, J. L.; Cid, M. B. Unexpected Reactivity of Graphene Oxide with DBU and DMF. *J. Mater. Chem. A* **2018**, *6*, 12637.

De Angelis, S.; **Franco, M.**; Trimini, A.; González, A.; Sainz, R.; Degennaro, L.; Romanazzi, G.; Carlucci, C.; Petrelli, V.; De la Esperanza, A.; Goñi, A.; Ferritto, R.; Aceña, J. L.; Luisi, R.; Cid, M. B. A Study of Graphene-Based Copper Catalysts: Copper(I) Nanoplatelets for Batch and Continuous-Flow Applications. *Chem. Asian J.* **2019**, *14*, 3011.

Franco, M.; Sainz, R.; Lamsabhi, A. M.; Díaz, C.; Tortosa, M.; Cid, M. B. Evaluation of the Role of Graphene-Based Cu(I) Catalysts in Borylation Reactions. *Catal. Sci. Technol.* **2021**, *11*, 3501.

Franco, M.; Vargas, E. L.; Tortosa, M.; Cid, M. B. Coupling of Thiols and Aromatic Halides Promoted by Diboron Derived Super Electron Donors. *Chem. Commun.* **2021**, *57*, 11653.